MECHANISMS OF MELANOMA TUMOR PROGRESSION

EDITED BY: Vladimir Spiegelman and Vijayasaradhi Setaluri
PUBLISHED IN: Frontiers in Oncology

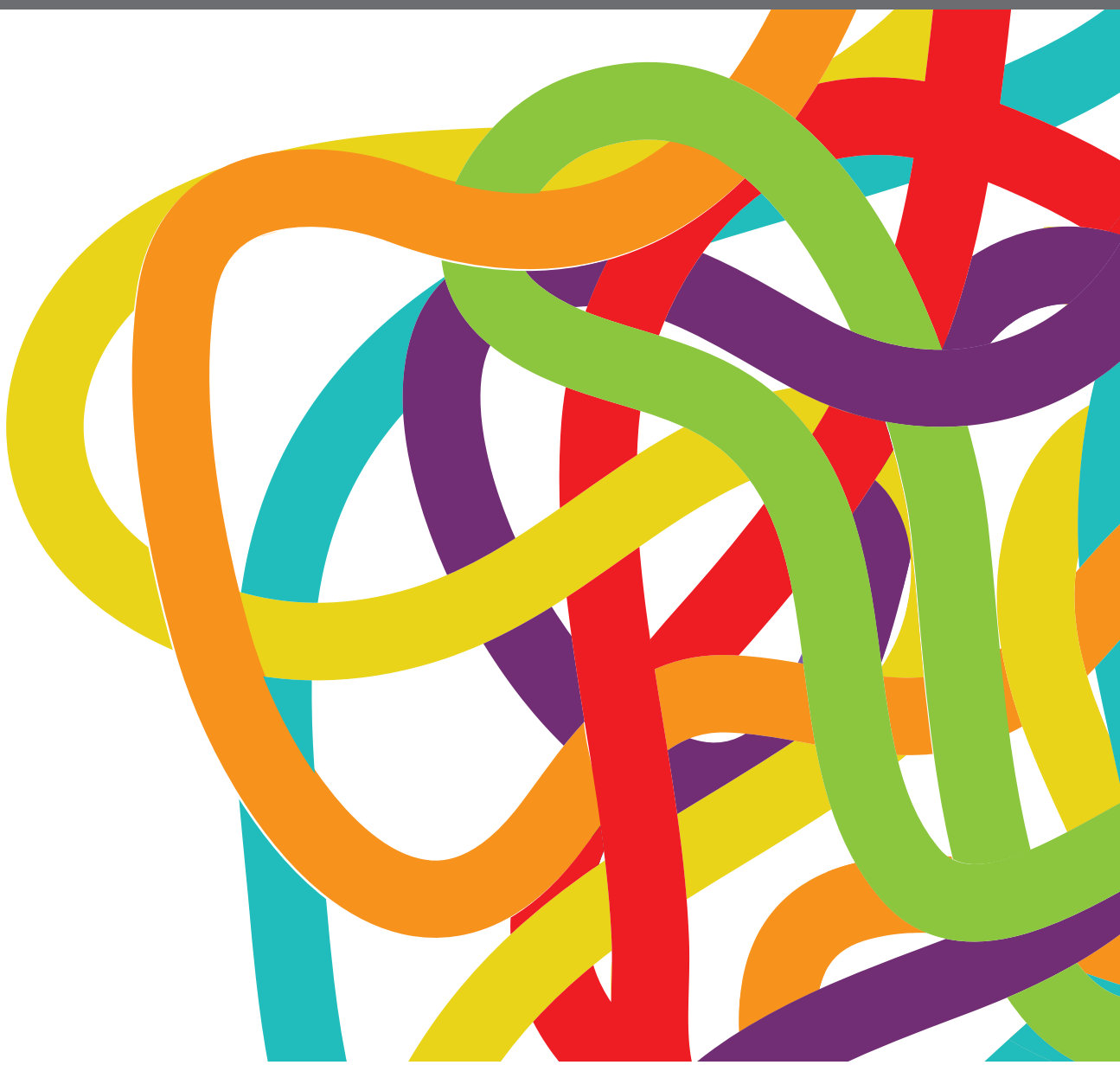

frontiers Research Topics

frontiers

ISSN 1664-8714
ISBN 978-2-88974-448-0
DOI 10.3389/978-2-88974-448-0

About Frontiers

Frontiers is more than just an open-access publisher of scholarly articles: it is a pioneering approach to the world of academia, radically improving the way scholarly research is managed. The grand vision of Frontiers is a world where all people have an equal opportunity to seek, share and generate knowledge. Frontiers provides immediate and permanent online open access to all its publications, but this alone is not enough to realize our grand goals.

Frontiers Journal Series

The Frontiers Journal Series is a multi-tier and interdisciplinary set of open-access, online journals, promising a paradigm shift from the current review, selection and dissemination processes in academic publishing. All Frontiers journals are driven by researchers for researchers; therefore, they constitute a service to the scholarly community. At the same time, the Frontiers Journal Series operates on a revolutionary invention, the tiered publishing system, initially addressing specific communities of scholars, and gradually climbing up to broader public understanding, thus serving the interests of the lay society, too.

Dedication to Quality

Each Frontiers article is a landmark of the highest quality, thanks to genuinely collaborative interactions between authors and review editors, who include some of the world's best academicians. Research must be certified by peers before entering a stream of knowledge that may eventually reach the public - and shape society; therefore, Frontiers only applies the most rigorous and unbiased reviews.
Frontiers revolutionizes research publishing by freely delivering the most outstanding research, evaluated with no bias from both the academic and social point of view. By applying the most advanced information technologies, Frontiers is catapulting scholarly publishing into a new generation.

What are Frontiers Research Topics?

Frontiers Research Topics are very popular trademarks of the Frontiers Journals Series: they are collections of at least ten articles, all centered on a particular subject. With their unique mix of varied contributions from Original Research to Review Articles, Frontiers Research Topics unify the most influential researchers, the latest key findings and historical advances in a hot research area! Find out more on how to host your own Frontiers Research Topic or contribute to one as an author by contacting the Frontiers Editorial Office: frontiersin.org/about/contact

MECHANISMS OF MELANOMA TUMOR PROGRESSION

Topic Editors:
Vladimir Spiegelman, Penn State Milton S. Hershey Medical Center, United States
Vijayasaradhi Setaluri, University of Wisconsin-Madison, United States

Citation: Spiegelman, V., Setaluri, V., eds. (2022). Mechanisms of Melanoma Tumor Progression. Lausanne: Frontiers Media SA. doi: 10.3389/978-2-88974-448-0

Table of Contents

frontiers in Oncology

ORIGINAL RESEARCH
published: 28 October 2020
doi: 10.3389/fonc.2020.579625

Tre2-Bub2-Cdc16 Family Proteins Based Nomogram Serve as a Promising Prognosis Predicting Model for Melanoma

Ling Tang[1,2,3], *Cong Peng*[3,4,5], *Su-Si Zhu*[1,2,3], *Zhe Zhou*[3,4,5], *Han Liu*[1,2], *Quan Cheng*[1,2,6*], *Xiang Chen*[3,4,5*] *and Xiao-Ping Chen*[1,2*]

[1] Department of Clinical Pharmacology, Xiangya Hospital, Central South University, Changsha, China, [2] Institute of Clinical Pharmacology, Central South University, Hunan Key Laboratory of Pharmacogenetics, Changsha, China, [3] Hunan Key Laboratory of Skin Cancer and Psoriasis, Xiangya Hospital, Central South University, Changsha, China, [4] Department of Dermatology, Xiangya Hospital, Central South University, Changsha, China, [5] Hunan Engineering Research Center of Skin Health and Disease, Xiangya Hospital, Central South University, Changsha, China, [6] Department of Neurosurgery, Xiangya Hospital, Central South University, Changsha, China

Tre2-Bub2-Cdc16 (TBC) proteins are conserved in eukaryotic organisms and function as negative feedback dominating the GAPs for Rab GTPases, while the function of TBC proteins in melanoma remains unclear. In this study, we observed the differential expression of 33 TBC genes in TCGA datasets classified by clinical features. Seven prognostic-associated TBC genes were identified by LASSO Cox regression analysis. Mutation analysis revealed distinctive frequency alteration in the seven prognostic-associated TBCs between cases with high and low scores. High-risk score and cluster 1 based on LASSO Cox regression and consensus clustering analysis were relevant to clinical features and unfavorable prognosis. GSVA analysis showed that prognostic-associated TBCs were related to metabolism and protein transport signaling pathway. Correlation analysis indicated the relationship between the prognostic-associated TBCs with RAB family members, invasion-related genes and immune cells. The prognostic nomogram model was well established to predict survival in melanoma. What's more, interference of one of the seven TBC proteins TBC1D7 was confirmed to inhibit the proliferation, migration and invasion of melanoma cells *in vitro*. In summary, we preliminarily investigated the impact of TBCs on melanoma through multiple bioinformatics analysis and experimental validation, which is helpful for clarifying the mechanism of melanoma and the development of anti-tumor drugs.

Keywords: melanoma, Tre2-Bub2-Cdc16, nomogram, prognostic, model

OPEN ACCESS

Edited by:
Vijayasaradhi Setaluri, University of Wisconsin-Madison, United States

Reviewed by:
Aurobind Vidyarthi, Yale University, United States
Pamela Bond Cassidy, Oregon Health and Science University, United States

***Correspondence:**
Xiao-Ping Chen
chenxiaoping@csu.edu.cn
Xiang Chen
chenxiangck@126.com
Quan Cheng
chengquan@csu.edu.cn

Specialty section:
This article was submitted to Skin Cancer, a section of the journal Frontiers in Oncology

Received: *03 July 2020*
Accepted: *05 October 2020*
Published: *28 October 2020*

Citation:
Tang L, Peng C, Zhu S-S, Zhou Z, Liu H, Cheng Q, Chen X and Chen X-P (2020) Tre2-Bub2-Cdc16 Family Proteins Based Nomogram Serve as a Promising Prognosis Predicting Model for Melanoma. Front. Oncol. 10:579625. doi: 10.3389/fonc.2020.579625

INTRODUCTION

Melanoma is the most aggressive skin tumor that accounts for 90% of the deaths caused by skin cancer (1). The incidence has been continuously rising over the past decades with about 232,100 new cases and 55,500 deaths annually. In 2012, the world standard incidence fluctuated from 0.2 in southeast Asia to 7.7 in America, 10.2 in EU and 13.8 in North America every 100,000 people years (2). Multiple risk factors have been known to be associated with risk for melanoma such as hair, heteromorphic nevus, family history, age, gender, and increased exposure to ultraviolet radiation (3, 4). At the early stage of tumor progression, surgical resection is the primary approach to convincing a good prognosis. Once it progresses to stages of metastasis, it's hard to cure owing to therapy resistance and recurrence in spite of the application of targeted therapy and immunotherapy (5, 6). There is an urgent need to clarify the complexity of pathogenesis during the progression and treatment of melanoma.

Proteins containing the Tre2-Bub2-Cdc16 (TBC) domain belong to the Rab-specific GTPase-activating proteins (GAPs) that are highly conserved in eukaryotic organisms (7). These proteins regulate the GAPs for Rab GTPases that control the production of cytokinesis through negative feedback mechanisms. The family includes 44 predicted proteins and regulates multiple cellular biological processes such as obesity, epilepsy, allergic dermatitis and cancer (8). Knowledge about the function of the TBC family is growing. For examples, TBC1D4 is an Akt substrate and participates in the transport of glucose transporter 4 (GLUT4) to the plasma membrane (9, 10). TBC1D3 (also referred to as PRC17) is overexpressed in prostate cancer and its overexpression promotes the growth of NIH3T3 cells (11). TBC1D7, the GAP for Rab17, can significantly promote the growth of lung cancer cells, and an obvious correlation between the expression of TBC1D7 and poor prognosis is observed (12). TBC1D16 is identified as a driver of melanoma and promotes the growth of melanoma cells (13). However, the function of TBC family proteins in melanoma is largely unknown.

In this study, we conducted a comprehensive analysis of 33 TBC family members and their possible roles in predicting disease prognosis in melanoma through bioinformatics tools and experimental validation. These data showed that seven prognostic-associated TBCs engaged in the progression of melanoma. A prognostic nomogram model based on the seven prognostic-associated TBCs was well established in predicting survival, providing novel insights into the diagnosis and therapies in melanoma.

MATERIALS AND METHODS

Datasets Analysis

The training set from the Cancer Genome Atlas (TCGA) database with clinical information and the validation set of the GEO database (GSE65904) for melanoma patients were downloaded, the clinical information of the patients was shown in the **Supplementary Table 1**.

Least Absolute Shrinkage and Selection Operator (LASSO) Cox Regression Analysis

The risk assessment model based on TBCs was constructed by LASSO Cox regression analysis. A total of 33 TBC members were introduced to count the coefficients of LASSO based on the highest value of lambda described previously (14). The formula of risk score was created based on its coefficients in multivariate cox regression analysis and the expression values of the seven prognostic-associated TBC genes. Melanoma patients in TCGA dataset were grouped into low-risk group and high-risk group based on the cut-off point of median risk score.

Alterations of Genes in Melanoma

To explore the genetic alterations in melanoma, melanoma samples were grouped into low-risk and high-risk groups based on the risk scores. The mutation frequency of the top 20 genes in the low- and high-risk groups were counted and displayed, the data of copy number variations and Human genome reference consortium h19 were downloaded from the TCGA and GISTIC 2.0, respectively (15). Mutation frequencies of the seven prognostic-associated TBCs identified in our study was also analyzed.

Consensus Clustering Analysis

Melanoma samples were divided into unique groups through consensus clustering analysis with the R language "Consensus Cluster Plus" as reported elsewhere (16). The number of clusters named K ranging from 2 to 10, and the supreme number of clusters was decided based on the cumulative distribution curves and consensus matrices (17). The difference in the expression of TBC genes and clinical traits between two clusters were displayed with heat map.

Survival Analysis

Melanoma samples from the TCGA dataset were divided into groups (high-risk and low-risk or cluster 1 and cluster 2) based on risk scores or clusters. The Kaplan-Meier curve was used to compare the overall survival (OS), progression-free interval (PFI), and disease-specific survival (DSS) between the groups. Additionally, distant-metastasis survival (DMS) and DSS in GEO (GSE65904) patients set were also analyzed.

Gene Set Variation Analysis (GSVA)

The R language "GSVA" was used to execute the functional enrichment analysis to clarify the unique signaling pathways of TBC families in melanoma, the cutoff value of $|\text{correlation coefficient}| > 0.5$ was defined (18). Gene Ontology (GO) and Kyoto Encyclopedia of Genes and Genomes (KEGG) pathway analysis were carried out with the help of the Molecular Signatures Database (MSigDB) (19). The correlation between TBCs and RABs family members that are involved in protein transport and key genes relevant to the hallmarks of cancer including invasion and epithelial-mesenchymal transition (EMT) was also investigated.

Prognostic Nomogram Construction

The prognostic model was established according to univariate and multivariate Cox regression analyses with $P < 0.05$. A nomogram was constructed using "RMS package" (20) to predict 5- and 10-year OS based on the results produced based on Cox regression analyses, and the prediction precision of the prognostic nomogram for OS was assessed by the calibration of the area under the curve (AUC).

Delineation of the Receiver Operating Curve (ROC)

ROC and AUC were used to observe the predicted performance of TBCs, risk scores and clustering in multiple clinical traits including 5- year OS, 10- year OS and subtypes.

Cell Lines and siRNA Transfection

Melanoma cells A375 and Sk-Mel-28 purchased from American Type Culture Collection (ATCC) which were cultured in Dulbecco's modified Eagle's medium (BI, Israel) with 10% fetal bovine serum (FBS) (BI, Israel) at 37°C in 5% CO2. 100nM siRNA purchased from RIBO Biotechnology was transfected into for 24–72 h using turbofect (Thermofisher, USA) according the manufacturer's instruction.

Quantitative Real-Time PCR

RNA was extracted from melanoma cells A375 and Sk-Mel-28 interfered with si-TBC1D7 and NC as control. cDNA was synthesized for real-time PCR adopting SYBR Green qPCR mix (CWBiotech, China). The primers are listed as following: TBC1D7-Forward: GAGTCCCATGCCAAGGTGATGATG; TBC1D7- Reverse: TGCGGAGATAGACTTCAGCCTGAG; GAPDH- Forward: CTTTGGTATCGTGGAAGGACTC; GAPDH- Reverse: AGTAGAGGCAGGGATGATGT.

Cell Proliferation

Melanoma cells 2.5×103 A375 and Sk-mel-28 interfered with si-TBC1D7 were seeded into 96 wells and cultured with complete medium for 24, 48, and 72 h. Cell proliferation was detected with CCK-8 kit according the manufacturer's instruction at 450 nM wavelength, the OD values were detected with microplate reader (BioTek).

Migration and Invasion

For migration, 1×10^4 melanoma cells were seeded into the upper chambers (Corning, USA) with 550ul medium containing 30% FBS put into the lower chambers and cultured for 24 h. Similarly, chambers with Matrigel (Corning, USA) embedded were used to detect invasion with the number of 5×10^4 cells. After culturing for 30 h, cells in the upper chambers were removed, transwell chambers fixed with 4% paraformaldehyde were stained with 0.5% crystal violet. five random fields of vision were captured and counted.

Statistical Analysis

All the analytic methods were carried out with the R package (version 3.5.3). Two-tailed Students' *t*-test was used to analyze the difference between two subgroups, while the comparison of multiple subgroups was assessed by a one-way ANOVA. The prognostic value based on risk scores and clinical traits was analyzed by univariate and multivariate Cox regression analysis. The algorithm of partition around medoids (PAM) was introduced into consensus clustering analysis. The clinical features' discrepancy between clusters was assessed by the Chi-squared test. Comparison of OS, PFI, DSS and DMS between subgroups (low-risk vs high-risk score, cluster 1 vs cluster 2) was carried out by Kaplan-Meier, and correlation analysis was determined by Spearman's rank correlation coefficient. $P< 0.05$ was regarded as statistical significance. The Schoenfeld test was used to evaluate the proportional hazards (PH) assumption.

RESULTS

Relationship Between the mRNA Expression of TBCs and Clinical Traits in Melanoma

The workflow designed for the study was displayed in **Figure 1**. A total of 33 TBC family members were shown in the TCGA dataset. mRNA expression levels of some of the TBCs genes were closely related to some clinical traits of melanoma such as tumor type, tumor status, age, gender and stage. Specially, we observed significantly increased mRNA expression level for 10 *TBC* genes (*TBC1D5*, *TBC1D19*, *TBC1D13*, *TBC1D24*, *TBC1D1*, *TBC1D16*, *TBC1D7*, *TBC1D14*, *TBC1D10C*, and *TBC1D22A*), and decreased mRNA expression level for 21 *TBC* genes (*TBCK*, *TBC1D30*, *TBC1D22B*, *TBC1D10A*, *TBC1D17*, *SGSM1*, *SGSM2*, *SGSM3*, *TBC1D3*, *TBC1D2*, *TBC1D2B*, *TBC1D20*, *TBC1D9B*, *TBC1D25*, *TBC1D21*, *TBC1D4*, *TBC1D12*, *TBC1D15*, *TBC1D23*, *TBC1D26*, and *TBC1D28*) in skin cutaneous melanoma (SKCM) compared with normal tissues (**Figure 2A**). The mRNA expression levels of 15 genes (*TBC1D10C, TBC1D22A, TBC1D4, TBC1D12, EV15, TBC1D15, TBC1D23, TBC1D8B, TBC1D19, TBCK, TBC1D5, TBC1D1, TBC1D30, TBC1D2B* and *SGSM1*) was increased in cases with metastasis as compared with those only with the primary focuses (**Figure 2B**). According to the clinical stage, differences in the mRNA expression of *TBC1D10C, TBC1D7, TBC1D4, TBC1D1, TBC1D9B*, and *TBC1D14* were also observed (**Figure 2C**). Furthermore, difference between patients stratified by neoplasm cancer status (with tumor vs tumor free) registered was also analyzed. We observed a higher mRNA expression of *TBC1D10C, TBC1D4, TBC1D12, TBCK, TBC1D5, TBC1D30* and a lower expression of *TBC1D24* in patients with tumor compared with tumor free patients (**Supplementary Figure 1A**). We also observed differential mRNA expression of *TBC1D10C, TBC1D19, TBC1D5, TBC1D12, EV15, TBC1D23, TBC1D17*, and *TBC1D7* in tumor tissue sites (**Supplementary Figure 1B**). Age seemed to have no effect on the mRNA expression of the majority of the TBC family members in melanoma except for *TBC1D4, TBC1D1, TBC1D25*, and *TBC1D10A* (**Supplementary Figure 1C**).

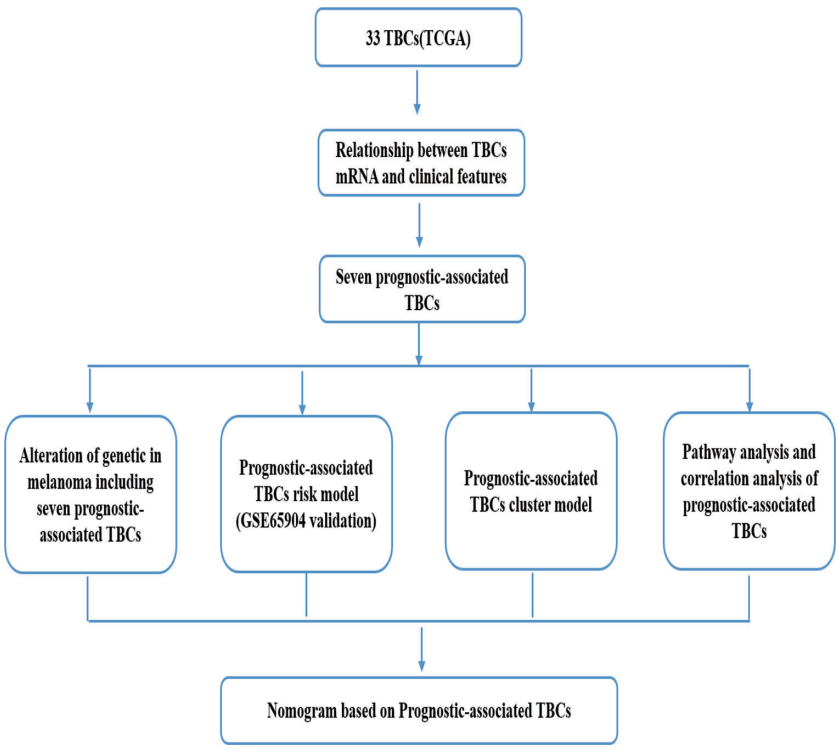

FIGURE 1 | A flowchart designed for the study.

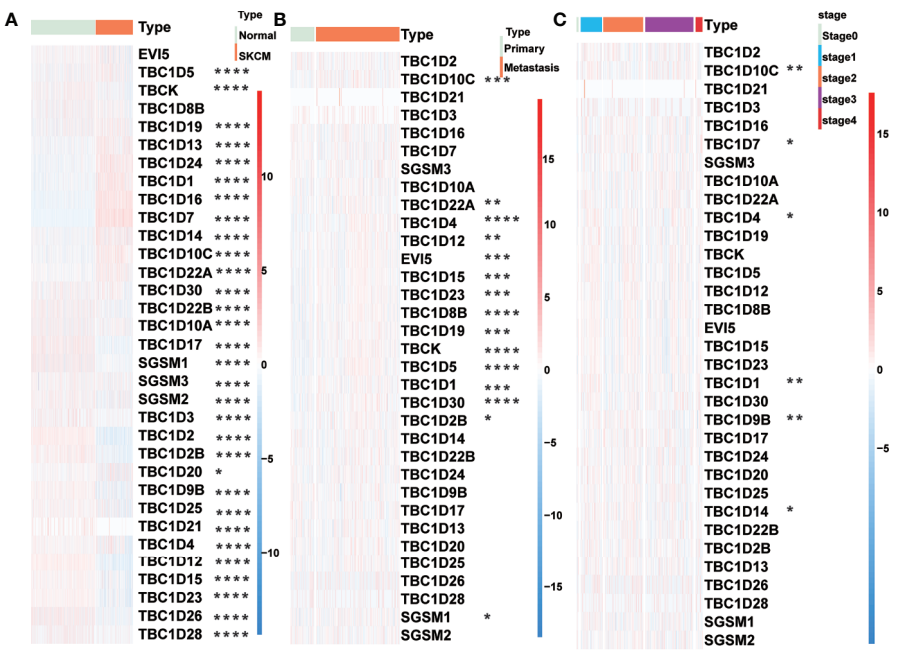

FIGURE 2 | Relationship between TBCs mRNA expression and clinical features in melanoma. The heat maps based on clustering analysis according to the subgroups exhibited the differential expression patterns of TBCs (Tumor type: Normal vs Tumor **(A)**, Tumor type: Primary vs Metastasis **(B)** and Tumor stage: stage0 vs stage1 vs stage2 vs stage3 vs stage4 **(C)**. *p < 0.05, **p < 0.01, ***p < 0.001, **** < 0.0001.

Identification of Seven Prognostic-Associated TBC Genes in Melanoma Based on LASSO Cox Regression Analysis and Somatic Mutations of These Genes in Melanoma

Univariate Cox regression analysis was performed to identify prognostic-associated TBCs genes with melanoma samples from the TCGA dataset. As shown in **Figures 3A–C**, 8 of the 33 *TBC* genes showed marked prognostic value ($p < 0.05$). The prognostic-associated genes were further analyzed with the LASSO Cox regression model and the minimum partial likelihood deviance after cross-validation was adopted to identify the optimal lambda value. Seven prognosis-associated *TBC* genes including *TBC1D13*, *TBC1D16*, *TBC1D7*, *TBC1D8B*, *TBC1D15*, *TBC1D19*, and *TBC1D10C* were identified (**Figures 3D–F**). Comparison of the transcription levels of the seven prognostic-associated TBC genes with the TCGA melanoma dataset showed that the relative mRNA expression of 5 gens (*TBC1D10C*, *TBC1D19*, *TBC1D16*, *TBC1D13* and *TBC1D7*) were significantly upregulated, 1 (*TBC1D15)* was significantly downregulated, while 1 (*TBC1D8B*) was comparable in the SKCM as compared with the normal tissues (**Supplementary Figure 2A**). Changes in protein expression levels of these 7 representative TBCs in melanoma with immunohistochemistry staining data based on the online Human Protein Atlas was also

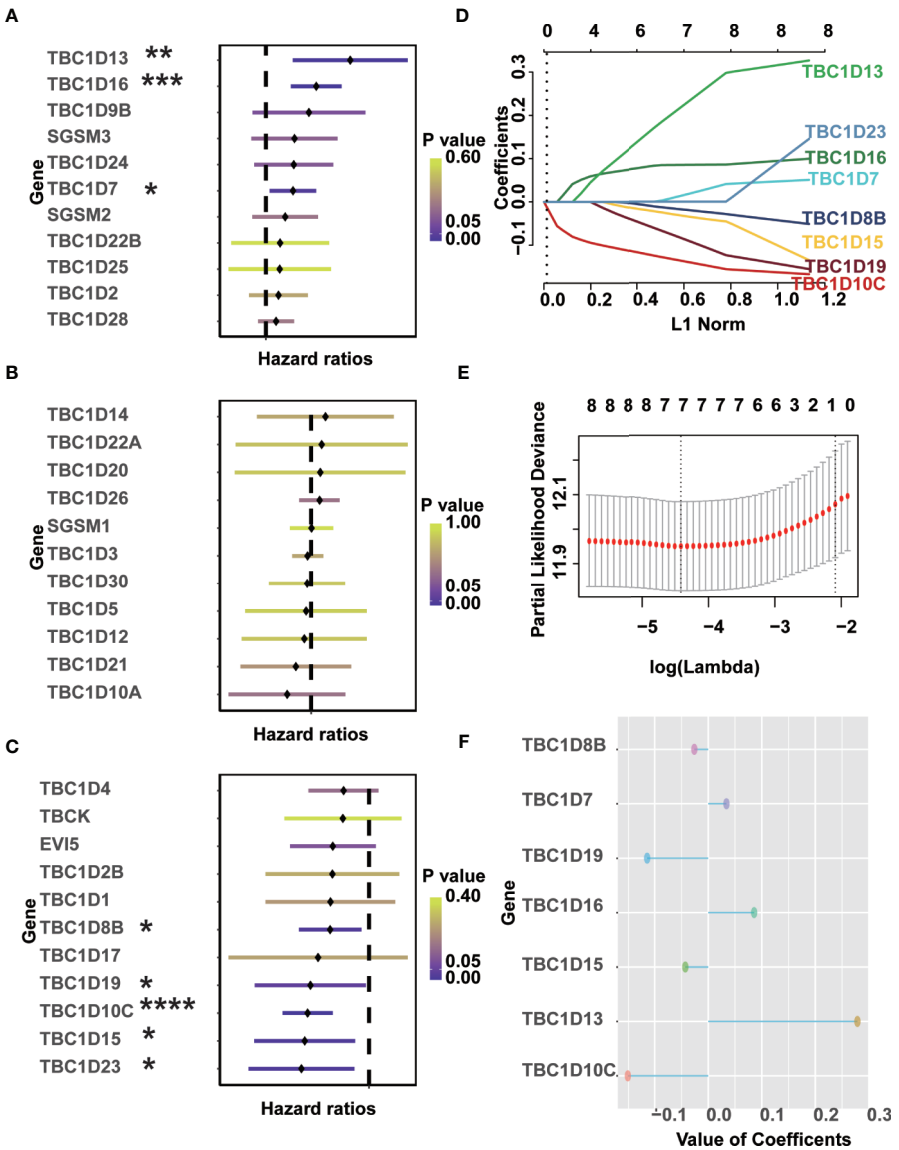

FIGURE 3 | Identification of prognostic-associated TBCs from TCGA. **(A–C)** Univariate Cox regression analyses were finished to screen prognostic-associated TBCs from TCGA. **(D–F)** LASSO coefficients of the seven prognostic-associated TBCs were calculated and displayed. *p < 0.05, **p < 0.01, ***p < 0.001, **** < 0.0001.

analyzed. As shown in **Supplementary Figures 3A–D**, protein expression of TBC1D10C, TBC1D19, TBC1D16, and TBC1D13 were increased significantly in melanoma tissues.

We further analyzed the occurrence of somatic mutations in the TBC genes and their influences on melanoma prognosis. Somatic mutations were observed in 212 (96.36%) and 198 (89.59%) of 221 samples in subgroups with low- and high-risk signature, respectively. Both groups shared mutations in 12 genes (TTN, MUC16, BRAF, DNAH5, ADGRV1, LPR1B, PCLO, RP1, MGAM, DNAH7, ANK3, and PKHD1L1). The frequency of the mutations in the low- and high-signature groups were 75 vs 69% for TTN, 73 vs 60% for MUC16, 54 vs 46% for BRAF, 46 vs 43% for PCLO, 39 vs 31% for ADGRV1, 39 vs 37% for LRP1B, 39 vs 29% for RP1, 37 vs 31% for MGAM, 37 vs 30% for DNAH7, 35 vs 30% for ANK3, 33 vs 32% for PKHD1L1, and the frequency of DNAH5 was identical in both groups (49%). We also observed mutations of CSMD2 (35%), DNAH8 (35%), MUC17 (35%), APOB (34%), DNAH9 (33%), and DSCAM (33%) in low signature group, and the mutation of HYDIN (32%), FAT4 (32%), FLG (31%), USH2A (29%), CSMD3 (29%), and THSD7B (29%) in the high signature group (**Figures 4A, B**). What's more, mutations in the seven prognostic-associated TBC genes were observed in 56 (11.99%) of the 467 TCGA samples, among which TBC1D8 showed the most frequent mutation with a frequency of 6%. It's worth noting that missense mutation was the most common type of mutation for these genes (**Figure 4C**).

Higher Seven Prognostic-Associated TBCs Risk Score Resulted in Worse Prognosis and Metastasis in Melanoma Patients

The seven prognostic-associated TBC genes screened out from the LASSO Cox regression analysis were fitted into a formula

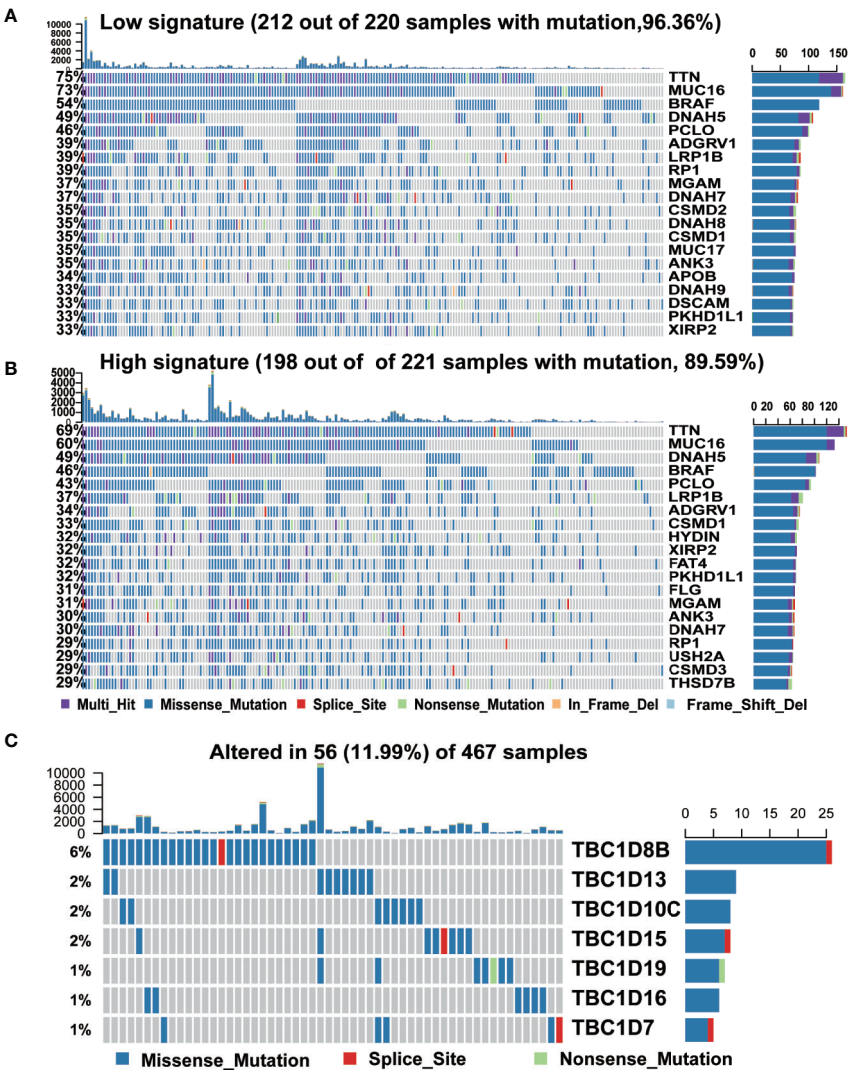

FIGURE 4 | The mutation frequency of top 20 genes and seven prognostic TBC genes in melanoma. **(A, B)**. Mutated oncogenes in melanoma were distributed into low and high risk-score subgroups. The mutation frequency of top 20 genes. **(C)**. Frequency of the seven prognostic TBC genes in total samples from the TCGA dataset.

based on gene expression level to calculate the risk score with the coefficient of each gene identified by multivariate Cox regression analysis. The risk score = −0.026×exp (TBC1D8B) + 0.034×exp (TBC1D7) − 0.114×exp (TBC1D19) + 0.086×exp (TBC1D16) − 0.043 × exp (TBC1D15) + 0.279×exp (TBC1D13) − 0.151×exp (TBC1D10C). The heat map exhibited the expression patterns of seven prognostic-associated TBC genes in TCGA dataset according to the risk scores (**Figure 5A**). Comparison of the risk scores among subgroups according to clinical characteristics were shown in **Figure 5B**. A higher mean risk score with Breslow depth value ≥3 compared with Breslow depth value <3 was observed (**Figure 5B**). According to melanoma Clark levels, the risk score of Clark level V was higher than that of the Clark level II and III, respectively (**Figure 5B**). Those died patients showed a significantly higher mean risk score than the alive patients. Patients with tumor also showed higher risk scores as compared with tumor-free patients (**Figure 5B**). Metastasis patients also showed higher risk scores than the primary patients, and the risk score was the highest in patient with distant metastasis (**Figure 5B**). Melanoma patients were grouped into low- and high-risk subgroups based on the median risk score. The high-risk patients showed poor outcomes in comparison with the low-risk patients in terms of OS, PFI, and DSS (**Figure 5C**). Patients were further divided into primary and metastasis melanoma based on the tumor type. In the primary patients, no difference in OS and DSS was observed between the high and low risk groups, except for a shorter PFI in high risk patients (**Supplementary Figure 4A**). However, in patients with metastasis, the high-risk subgroup showed remarkably poorer OS, PFI, and DSS (**Figure 5D**). Similarly, patients in the high-risk subgroup showed a shorter DMS and DSS than those in the low-risk subgroup in the validation GSE dataset (GSE65904) (**Supplementary Figure 4B**). These findings indicated that the TBCs-based diagnosis model is of excellence sensitivity.

Consensus Clustering Analysis of Melanoma Indicated Poor Prognosis in the Cluster With Higher Expression of the Prognostic-Associated TBC Genes

To explore the potential predictive value of TBC family members, melanoma samples were analyzed by consensus clustering analysis. The results from the cumulative distribution function (CDF) curves and consensus matrixes showed the best performance as the optimal number of clusters k was set at 2 (k=2) (**Figures 6A, B**). Principal component analysis also showed differential mRNA expression in TBC genes between the two clusters (**Figure 6C**). Clustering analysis based on the prognostic-associated TBC genes integrated with clinical traits showed that the cluster 1 was associated with tumor status (**Figure 6C**). Difference in mRNA expression of the prognostic-associated TBC genes between the two groups were also observed, specifically, a higher expression of TBC1D16, TBC1D7, TBC1D19, TBC1D8B, TBC1D15, and a lower expression of TBC1D10C was observed in cluster 1. Patients in cluster 1 showed obviously shorter OS and DSS for the TCGA melanoma dataset (**Figure 6E**), though no difference in PFI was observed (**Supplementary Figure 4C**). When stratified by primary and metastasis characteristics, no difference in OS and DSS between the clusters except for a shorter PFI in cluster 1 was observed for the primary patients (**Supplementary Figure 4E**). For the metastasis patients, cluster 1 showed obviously shorter OS and DSS (**Figure 6F**) but comparable PFI than cluster 2 (**Supplementary Figure 4D**).

Pathway Analysis and Correlation Analysis of the Seven Prognostic-Associated TBC Genes

GSVA analysis was conducted to investigate the possible biological functions of the TBC genes in melanoma. The top 10 signaling pathways with significant differences were selected from GO and KEGG analysis. Majority of these associated pathways are involved in the metabolism of signaling molecules such as purine metabolism, aminoacyl tRNA biosynthesis, glycosylphosphatidylinositol GPI anchor biosynthesis, oxidative phosphorylation, glycolysis and dicarboxylate. Some pathways were involved in transportation such as protein export, lysosome, aromatic amino acid transport, inner-mitochondrial membrane organization, protein transmembrane import into intracellular organelle. Also, pathways related to the regulation of apoptotic DNA fragmentation and negative regulation of cell cycle arrest were also observed (**Figure 7A**). Potential biological function analysis of the seven prognostic-associated *TBC* genes showed that *TBC1D16*, *TBC1D13* and *TBC1D7* were strongly correlated with pathways described above (**Supplementary Figures 5A, B**).

The main function of Rab proteins is to recruit effector molecules to promote the activation of downstream traffic events. Therefore, we analyzed the correlation of mRNA expression of the seven prognostic-associated TBC genes with 27 Rab family genes reported by literatures (**Figure 7B**). Strong correlations between the prognostic-associated TBCs and RAB genes were observed. Positive correlation between TBC1D18 and 10 Rab genes (RAB18, RAB12, RAB14, RAB33B, RAB11A, RAB2A, RAB8R, RAB10, RAB22A, and RAB6A) was observed. TBC1D15 also correlated with 10 Rab genes (RAB18, RAB12, RAB14, RAB33B, RAB11A, RAB2A, RAB8B, RAB10, RAB22A, and RAB6A). TBC1D19 correlated extensively with 10 of the Rab genes (RAB18, RAB12, RAB14, RAB33B, RAB11A, RAB2A, RAB8B, RAB10, RAB22A, and RAB6A).

Correlations between the 7 prognostic-associated TBC genes and invasion-related genes including BSG, EGFR, matrix metalloproteinases (MMP2, MMP7, MMP9, MMP14, MMP1, and MMP3) and EMT-related genes (TWIST1, VIM, CDH2, ACTA2, and ZEB1) were also analyzed. Specifically, TBC1D10C was correlated positively with MMP9, MMP7 and EGFR. TBC1D16 correlated positively with MMP14 and BSG. TBC1D13 was correlated positively with MMP2, MMP14, BSG and EGFR. TBC1D19 was correlated positively with MMP2, MMP14 and EGFR (**Figure 7C**). In addition, TBC1D8B, TBC1D10C, TBC1D15, TBC1D13, and TBC1D19 were correlated positively with TWIST1, VIM, CDH2, ACTA2, and ZEB1, respectively (**Figure 7D**).

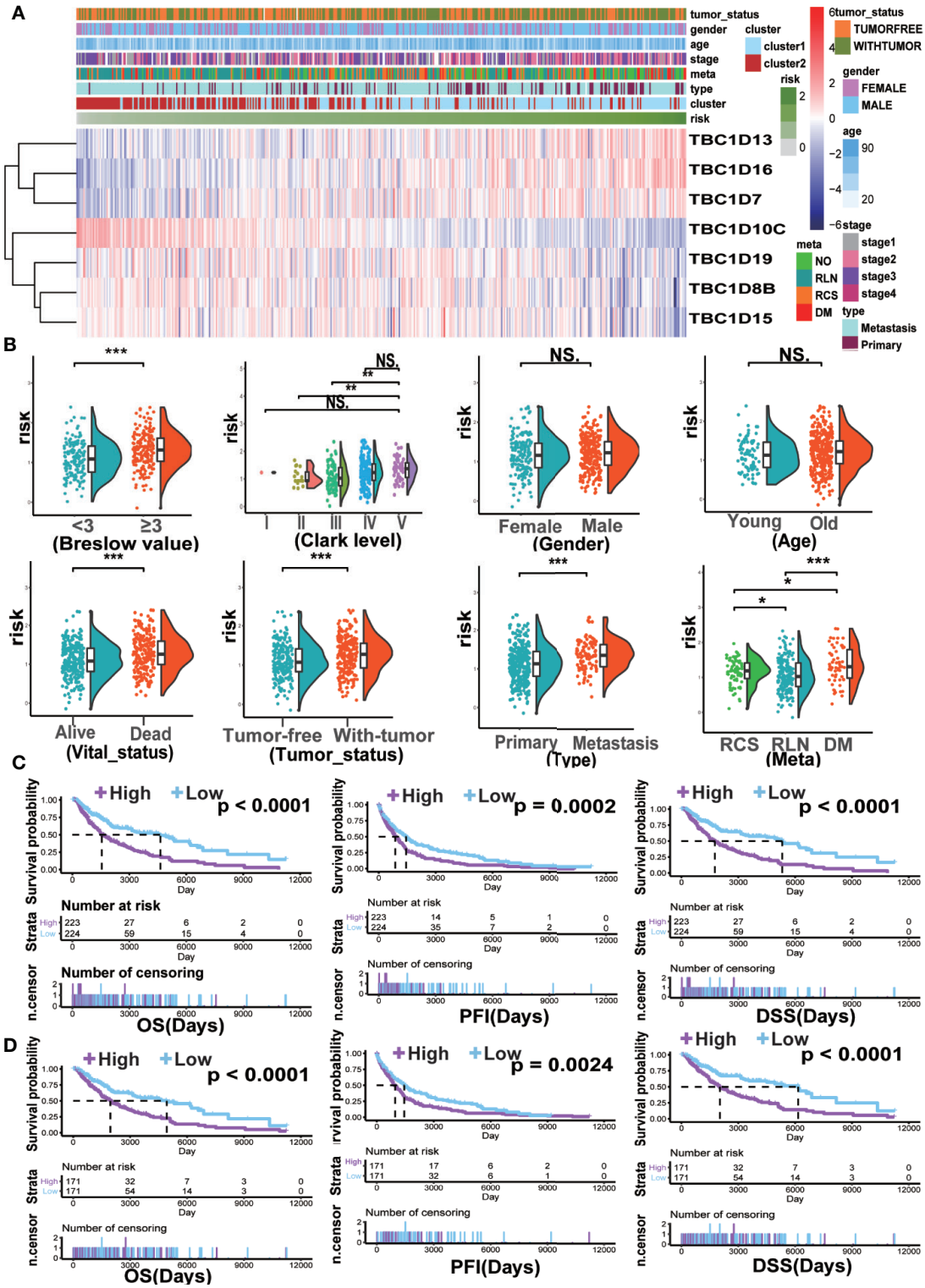

FIGURE 5 | The clinical characteristics and survival analysis based on risk score. **(A)** The risk score model of the seven prognostic-associated TBCs in melanoma was constructed based on the coefficient of LASSO. The distributions of clinical characteristics and the seven prognostic-associated TBCs expression based on the risk scores are showed with heat map. **(B)** The differences in risk score within various subgroups classified by clinical features including Breslow value, Clark level, Gender, Age, Vital status, Tumor status, Tumor type and Meta in the melanoma TCGA dataset. *p < 0.05, **p < 0.01, ***p < 0.001, NS. p > 0.05. Kaplan ± Meier survival analyses demonstrated the differences in OS, PFI and DSS based on risk scores (High vs Low) in tumor tissues **(C)** and Metastasis tissues **(D)** from TCGA.

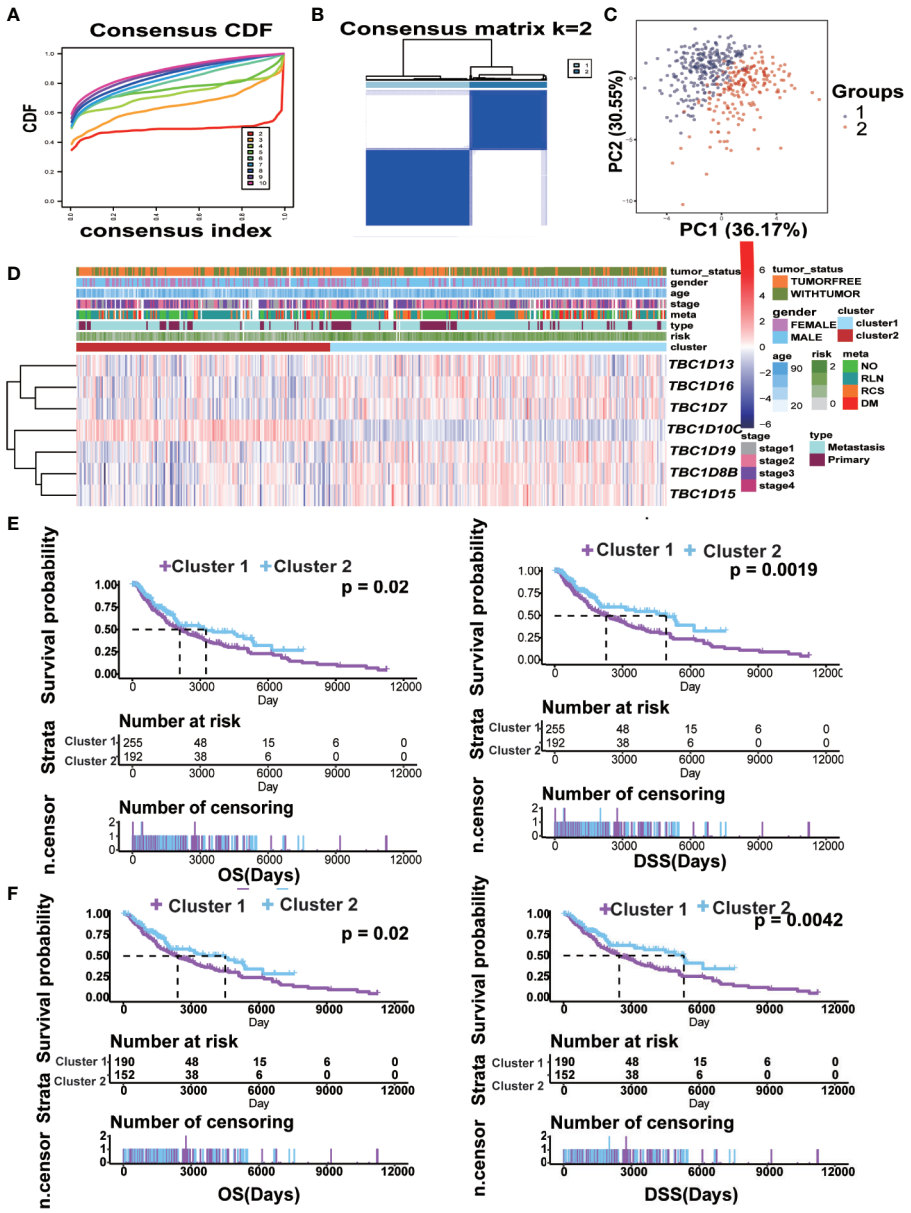

FIGURE 6 | Construction of cluster model and the clinical characteristics and survival analysis based on clusters. **(A)** Clustering by the consensus clustering algorithm with k= 2 to 10. The cumulative distribution function (CDF) plot of the TBCs mRNA expression in melanoma from TCGA. k=2 was defined as the optimal number. **(B)** Consensus matrix for 2 clusters. The dark blue rectangles show the samples assigned to the 2 clusters while the light blue lines represent the unassigned samples. **(C)** The distributions of clinical features and the seven prognostic associated TBCs expression according to the clusters (cluster 1 vs cluster 2) in TCGA are showed by heat maps. **(D)** Comparisons of risk score values between subgroups separated by clinicopathological characteristics. Kaplan ± Meier survival analyses demonstrated the differences in OS and DSS based on clusters (cluster 1 vs cluster 2) in tumor tissues **(E)** and Metastasis tissues **(F)** from TCGA.

Associations Between the Seven Prognostic-Associated TBC Genes With Immune Characteristics

To determine whether there was correlation between the seven prognosis-associated TBC genes and immune cells, a further analysis with immune cells including monocytic lineage, T cells, CD8 T cells, cytotoxic lymphocytes, NK cells, B lineage, myeloid dendritic cells, neutrophils, endothelial cells plus fibroblasts were analyzed. Differential expression profiles of immune cells in melanoma from the TCGA dataset was indicated by the heatmap (**Figure 8A**). Correlation between the seven prognostic-associated TBC genes with the immune cells was shown in **Figure 8B**. The results showed TBC1D8B, TBC1D10C, TBC1D15, and TBC1D19 were correlated with immune

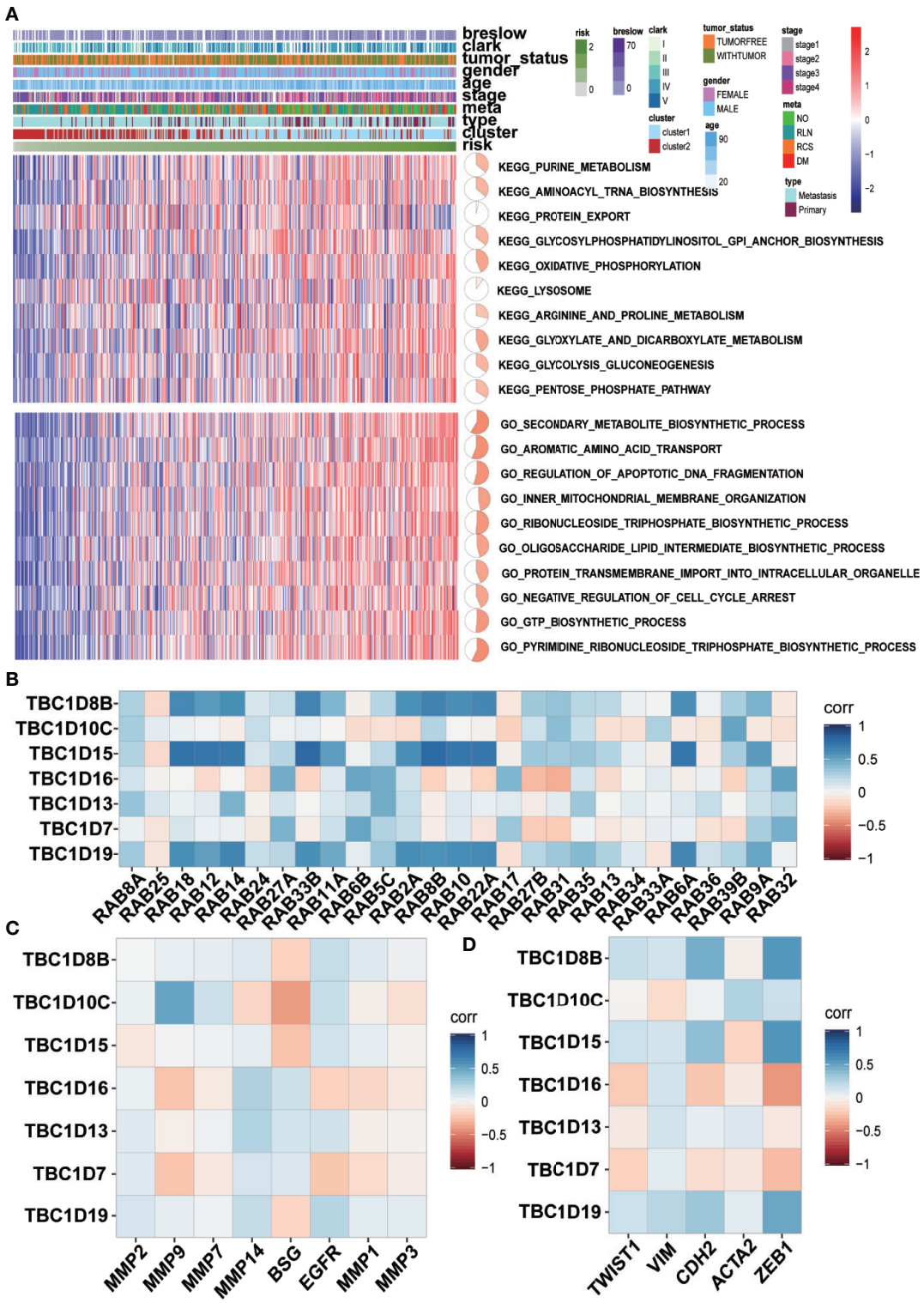

FIGURE 7 | GSVA analyses and correlation analysis. **(A)** GSVA analyses for the seven prognostic-associated TBCs. The distribution of risk scores, clinical characteristics and gene set enrichment of different pathways was displayed by heatmap. **(B)** Correlation analysis between the seven prognostic TBCs and several important RAB family **(C)** Correlation analysis between the seven prognostic TBCs and and invasion related genes (MMP2, MMP9, MMP7, MMP14, BSG, EGFR, MMP1, and MMP3). **(D)** Correlation analysis between the seven prognostic TBCs and EMT associated genes (TWIST1, VIM, CDH2, ACTA2, and ZEB1).

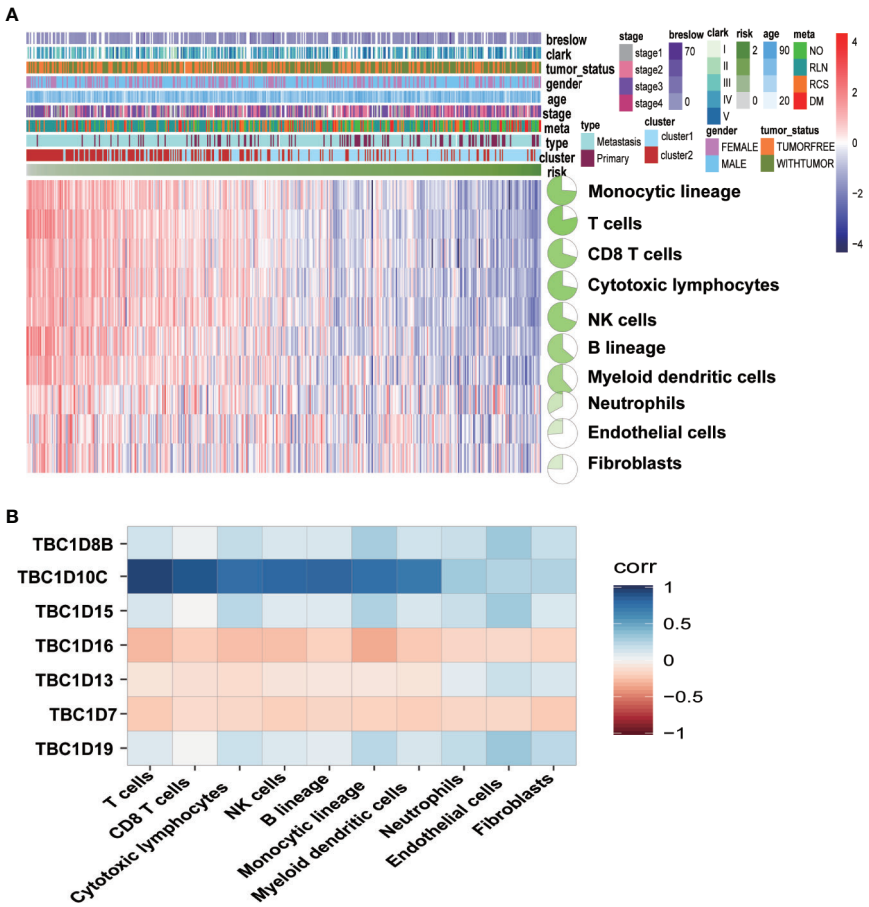

FIGURE 8 | Associations between the seven prognostic-associated TBC genes with immune characteristics. **(A)** The relationship of the distributions of clinical features and immune cells in TCGA is showed by heat maps. **(B)** Correlation analysis between the seven prognostic TBCs and immune cells.

signatures. Interestingly, TBC1D10C was found to be correlated with T cells, CD8 T cells, cytotoxic lymphocytes, NK cells, B lineage, monocytic lineage and myeloid dendritic cells. Only weak correlations between TBC1D16, TBC1D13, TBC1D7, and immune cells were observed.

Prognostic Nomogram Model Constructed Based on Age, Stage, Risk Score, and Primary Focus Predicted OS in Melanoma

Univariate and multivariate Cox analyses were used to assess the independent prognostic index associated with the clinical outcomes of patients. Results of multivariate Cox analysis showed that age (HR=1.02, P=0.0015), stage 2 (HR=1.76, P=0.0019), risk score (HR=2.43, P=7.42E-6), and primary focus (HR=1.87, P=0.0413) were independent prognostic indicators for OS. The Clark level II and Breslow value showed significance in the univariate Cox analysis but lost in the multivariate Cox analysis. No remarkable gender difference was observed (**Supplementary Table 2**). The results of **Figures 9A–D** showed the Schoenfeld tests value (Global Schoenfeld test = 0.8366, Age, p = 0.8829; Stage2, p = 0.3545; Primary, p = 0.9737; Risk score, p = 0.4448), indicating that each variable met the requirements for proportional hazards test (PH) (PH>0.05). Four significant prognostic variables identified in the Cox regression model were introduced to construct the nomogram model. As shown in **Figure 9E**, each factor was given a score on the axis, the points of all variables were joined together and the outcome was depended on the position on the survival axis based on the total score. Calibration curves confirmed the degree of precision of the nomogram, and the OS predicted by the nomogram was in accordance with 5-year OS and 10-year OS (**Figure 9F**). The AUC values under the ROC curve were 0.752 and 0.845, respectively, in predicting the 5-year and 10-year OS for melanoma patients (**Figure 9G**). Survival analysis showed a significant difference in term of OS between the two groups (p< 0.0001) (**Figure 9H**).

Interference of TBC1D7 Expression Inhibits Melanoma Cell Proliferation, Migration, and Invasion

In order to further investigate the function role of TBC proteins in melanoma, TBC1D7, one of TBC proteins was chosen for subsequent functional validation. As shown in **Figure 10A**,

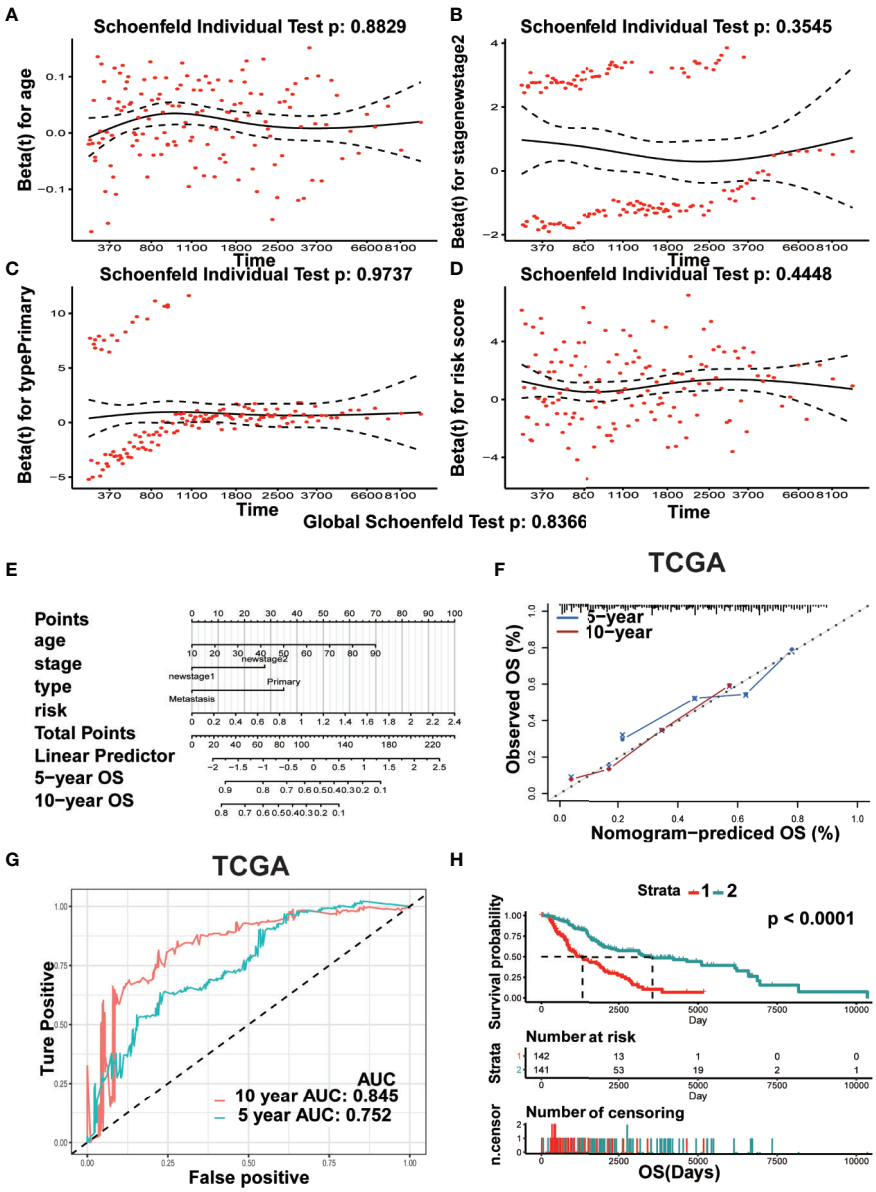

FIGURE 9 | Prognostic nomogram model was constructed for predicting OS. **(A–D)** The plots of Schoenfeld residual were showed for age **(A)** stage II **(B)** Primary **(C)** risk **(D)** in the prognostic nomogram. **(E)** The prognostic nomogram for melanoma patients was established dependent on four crucial factors. **(F)** The calibration curve of OS predicted by nomogram. The predicted possibility of OS is responded to x-axis and the observed OS is responded to the y-axis. **(G)** The curve of ROC based on the prognostic nomogram at 5-year and 10-year OS. **(H)** Comparison of OS between two groups (Strata 1 vs Strata 2).

TBC1D7 mRNA expression in both melanoma cell lines A375 and Sk-Mel-28 were successfully interfered with siRNA which was confirmed by RT-PCR, and two sequences of them were selected to explore the effect of TBC1D7 on melanoma cells. TBC1D7 deficiency induced by siRNA suppressed the proliferation of melanoma cells A375 and Sk-Mel-28 obviously (**Figure 10B**). To further determine whether TBC1D7 could inhibit the metastasis of melanoma, Boyden chambers were used to assess melanoma cell migration and invasion. The results showed that depletion of TBC1D7 in both melanoma cell lines A375 and Sk-Mel-28 impeded the ability of migration (**Figure 10C**). Similarly, suppression of TBC1D7 with siRNA also inhibited the invasion of melanoma cells remarkably (**Figure 10D**). Collectively, these results suggested that TBC1D7 inhibits the migration and invasion ability of melanoma cells.

DISCUSSION

Melanoma is a highly mutated and metastatic cancer originated from the malignant transformation of melanocytes. Men are at a 40% increased risk in their lifetime to be diagnosed with melanoma (21).

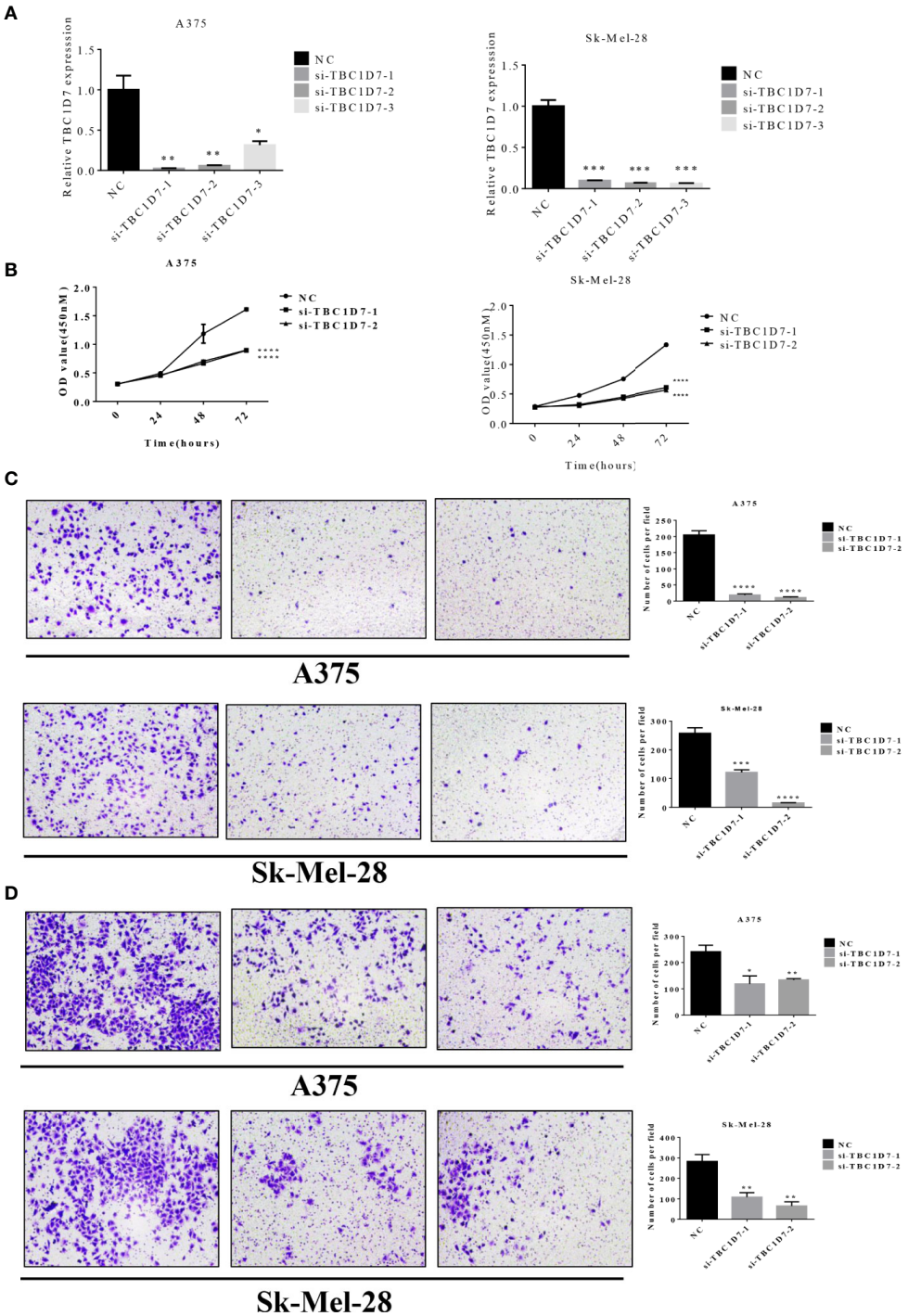

FIGURE 10 | Interference of TBC1D7 expression inhibits melanoma cell migration and invasion. **(A)** The relative mRNA levels of TBC1D7 at 36 h after transfection with si-TBC1D7-1, si-TBC1D7-2, si-TBC1D7-3 and NC as control in melanoma cells A375 and Sk-Mel-28 were measured by RT-PCR. GAPDH was used as a control. *p <, **p < 0.01, ***p < 0.001. **(B)** Melanoma cells A375 and Sk-Mel-28 interfered with si-TBC1D7, 2.0 x 103 cells planted into 96-well cultured for 24, 48, 72 h, CCK-8 kits were used to detect the proliferation at OD450nM following the manufacturer's instruction. Each group have 5 replicates(n=5) with 3 independent experiments. ****p < 0.0001. **(C)** A number of 1 x 10^4 cells were seeded into the upper chambers with 550ul medium containing 30% FBS put into the lower chambers. Chambers after cultured for 24 h were fixed with 4% paraformaldehyde, stained with crystal violet and imaged by microscope. Representative images of migration of A375 and Sk-Mel-28, the numbers of magration cells per field were calculated, and the results are presented as the mean ± SD (n = 3). ***p < 0.001, ****p < 0.0001. **(D)** 5 x 10^4 cells were seeded in the chambers embed with matrigel cultured for 30 h and performed as material and methods. Representative images of invasion of A375 and Sk-Mel-28, the numbers of invasion cells per field were also calculated. *p < 0.05, **p < 0.01.

As the incidence of melanoma progressively increasing, illuminating the complicated pathogenesis and risk factors are crucial. TBC family members are classical GAPs negatively regulating the hydrolysis of GTP, the latter is engaged in the cycles of RABs (22). TBCs are involved in the pathogenesis of various diseases such as dermatitis, obesity, bacterial infection and tumorigenesis (8). Some TBCs may act as oncogenes that affect disease survival and metastasis. For example, TBC1D3 is observed to be overexpressed in breast cancer by promoting oxidized low-density lipoprotein receptor 1 expression required for cell migration involving in TNFα/NF-κB signaling (23). Daigo Y et al. discovered the activation of TBC1D7 in lung cancer and suppression of TBC1D7 inhibited the growth of lung cancer cells (12). However, few studies have focused on functions of TBC family members in melanoma.

In this study, we conducted a comprehensive analysis of the characteristics of 33 *TBC* genes in melanoma. We firstly analyzed the relationship between mRNA expression of *TBC* genes and clinical features such as age, gender, tumor type and stage in melanoma. We observed a strong correlation between mRNA expressions of some of TBC genes such as *TBC1D10C, TBC1D4, TBC1D23* and clinical-pathological features (**Figure 2**). Seven prognosis associated TBCs genes including *TBC1D13*, *TBC1D16*, *TBC1D7*, *TBC1D10C*, *TBC1D19*, *TBC1D8B*, and *TBC1D15* were identified in melanoma. Few studies have focused on the roles of these *TBC* genes in melanoma. TBC1D13 is a specific GAP of RAB35 that plays a crucial effect on the trafficking of GLUT4 in adipocytes (24). Interestingly, the role of TBC1D13 in melanoma remains unknown. Evidence has shown that TBC1D16 is a driver of melanoma (13). Hypomethylation of TBC1D16 leads to the activation of TBC1D16 transcription in melanoma, and the short isoform of TBC1D16 (TBC1D16-47KDa) promotes melanoma growth and metastasis through interacting with RAB5C and regulating EGFR signaling (25). Knockdown of TBC1D7 resulted in the activation of mTORC1 signaling, and enhanced cell growth (26). Interests in TBC1D10C are mainly focused on immune response (27, 28). Two pieces of literature reported TBC1D19, one showed that TBC1D19 acted upon cell polarity and decreased TBC1D19 expression contributed to the disruption of odontoblast polarity and apoptosis (29). Interference of TBC1D8B increased basal autophagy and exocytosis through inhibiting the expression of RAB11 which plays a crucial role in the pathogenesis of nephrotic syndrome (30). TBC1D15 controlled glucose uptake through RAB7 in late endosomal pathway impacting GLUT4 translocation (31). Bibliography retrieval on above genes showed that the function of these *TBC* genes is unclear, the role of these TBCs in the melanoma is largely unknown. Somatic alteration analysis showed genomic alterations in both the high- and low-risk groups, and the mutant frequency of *TBC1D8* is the highest among the seven TBC genes (**Figure 4**). Hemizygous missense mutations in *TBC1D8B* have also been reported in families with nephrotic syndrome (30). However, little is known about the functional significance of genomic alteration of these TBCs.

We used LASSO Cox regression analysis to calculate the risk score according to the seven most meaningful TBC genes in this study. We observed a higher risk score related to clinical-pathological characteristics of melanoma such as Breslow value (>3), Clark level IV, V, vital status (dead), tumor status (with tumor), tumor type (metastasis). In addition, a higher risk score was also associated with shorter OS and DSS (**Figure 5**). Consensus clustering analysis grouped the patients into two clusters, the principal component analysis further demonstrated differential expression of the TBC genes between the two clusters. Cluser1 showed shorter OS and DSS (**Figure 6**). The potential function of TBC genes in melanoma may include vesicular transport such as protein export, amino acid transport, and protein transmembrane import (**Figure 7**). Take TBC1D15 as an example, Ishihara N et al. reported that Fis1 acts as a mitochondrial recruitment factor for TBC1D15 which is engaged in the regulation of mitochondrial morphology (32). Senga T et al. discovered that knockdown of TBC1D15 resulted in the activation of RhoA and membrane blebbing, which was blocked by inhibiting RhoA signaling (33). TBC1D15 acts as a GAP of Rab7 in regulation of the lysosomal morphology (34). Aberrant intracellular transport is involved in type 2 diabetes, immune deficiencies and cancer (35),. Besides, correlation analysis indicated a positive correlation with signal molecule synthesis, apoptosis and cell cycle arrest (36, 37). TBC/RABGAPs regulate the malignant behavior involved in the regulation of RABs. Nearly a half of RABs have been identified as substrates for TBC/RABGAP family members. Results of correlation analysis for the seven prognostic associated TBCs and RABs in our study indicated that the same TBC gene might be regulated by various RABs, and the same RAB gene might be regulated by different TBCs. TBC1D8B is observed to regulate autophagy and exocytosis interacting with RAB11 (30). As could be seen from **Figure 7**, TBC1D8B might be regulated by RAB18, RAB12, RAB14, RAB33B, RAB2A, RAB8B, RAB10, RAB22A, RAB17 except for RAB11A. Meanwhile, RAB18 might be regulated by TBC1D8B, TBC1D15, TBC1D19, which gave us hints that the complex mechanism of TBCs regulated by RABs. We also investigated the correlation of the seven prognostic-associated TBCs between MMP-related genes (MMP2, MMP9, MMP7, MMP14, BSG, EGFR, MMP1, MMP3) and EMT-associated genes (TWIST1, VIM, CDH2, ACTA2, ZEB1), which also indicated a central role of TBCs in melanoma. As reported in the literature, TBC1D16 as a driver of melanoma is a Rab4A GAP that is engaged in the trafficking of transferrin receptor and EGFR (38). TBC1D8B can interact with RAB11B that is involved in vesicular recycling (30, 39).

Immune microenvironment is also key important for tumors (40–42). Melanoma patients are supposed to develop immune responses against specific tumor antigens (43). Therefore, We also investigate the role of immune cells in melanoma, and correlation analysis of the seven prognostic-associated TBC genes with immune cells showed that differential variations of the seven genes regarding immune cells, especially for TBC1D10C (**Figure 8**). As reported, TBC1D10C is identified to be related with immune response in head and neck squamous cell carcinoma (27), and artificial neural networks analysis also confirmed the involvement of TBC1D10C in immune response through TCGA (28),

suggesting the possible mechanisms of these TBCs in regulation of the immune microenvironment.

We also constructed a prognostic nomogram for predicting OS of melanoma and found the independent prognostic indicators such as age, risk score based on the expression levels of the seven TBC genes, stage 2 and primary focus (**Figure 9**). What's more, TBC1D7, one of the seven TBC proteins was chosen for further experimental validation, TBC1D7 is the third subunit of TSC1/TSC2 associated with autophagy (26). It has been reported that TBC1D7 is related with various diseases such as intellectual disability, megalencephaly (44), diabetes (45) and tumor (12). Highly expression of TBC1D7 was related with poor outcome in non-small cell lung cancer (NSCLC), and suppression of TBC1D7 inhibits the growth of lung cancer cells, which might be a promising target in cancer therapy (12). By using mass spectrometry-based quantitative proteomic method, a recent study by Qi et al. observed that TBC1D7 is a potential driver for melanoma cell invasion by transwell assay, and higher TBC1D7 expression is associated with poor outcome as analyzed by the TCGA and GEO (GSE65904) data (46). In our study, we also observed that interference of TBC1D7 expression inhibited the proliferation, migration and invasion of melanoma cells A375 and Sk-Mel-28 *in vitro* (**Figure 10**), suggesting the potential role of TBC1D7 in melanoma. Different from the study by Qi et al., we investigated the association of mRNA expression of TBCs and the clinical traits in melanoma, and we observed that in spite of TBC1D7, six other prognostic-associated TBC genes TBC1D13, TBC1D16, TBC1D7, TBC1D8B, TBC1D15, TBC1D19, and TBC1D10C were also identified by LASSO Cox regression analysis In addition, mutations profile of these genes was also analyzed. A risk score model, cluster model and prognostic nomogram model which were well established to predict the OS. What's more, the pathway analysis and correlation analysis of the seven prognostic-associated TBC genes with RAB proteins, invasion-associated genes (i.e *BSG*, *EGFR* and *MMP*) and EMT-associated genes (i.e *TWIST1*, *VIM*, *CDH2*, *ACTA2*, and *ZEB1*) were also explored. Immune microenvironment is another key factor promoting the malignant phenotype of melanoma, and we also conducted an analysis to understand the relationship between the seven prognostic-associated TBC genes and immune cells hoping for finding clues under the view of immune microenvironment for melanoma. However, more experiments needed to be performed to investigate the detailed mechanism of TBC1D7 in melanoma cells, and the biological function of the seven prognostic-associated TBCs in melanoma is still largely unknown, further study should be clarified the effect of TBCs on melanoma.

CONCLUSION

This study identified seven prognostic-associated TBCs based on comprehensive bioinformatics analysis of TBCs expression profiles and clinical features. The prognostic model of the seven prognostic-associated TBCs showed a good performance in the prediction of survival. Correlation between the prognostic-associated TBCs and RAB family members, invasion-related genes and immune cells are also observed. The nomogram integrating the seven prognostic-associated TBCs and clinical features could be more accurate in predicting the survival of melanoma patients. What's more, Interference of TBC1D7 was confirmed to inhibit the migration and invasion in melanoma cells *in vitro*, indicating the potential therapeutic role of TBC proteins in melanoma.

DATA AVAILABILITY STATEMENT

The original contributions presented in the study are included in the article/**Supplementary Material**. Further inquiries can be directed to the corresponding authors.

AUTHOR CONTRIBUTIONS

XC, X-PC, and CP conceived and designed the idea for the manuscript and financial support. LT was responsible for writing this paper. S-SZ, ZZ, and HL contributed the collection and interpretation of data. QC provided analysis tools and analyzed the data. All authors contributed to the article and approved the submitted version.

FUNDING

This work was supported by the Major Projects of International Cooperation and Exchanges NSFC (grant number 81620108024) and the National Natural Science Foundation (grant number 81572679, 81430075, 81673518), National Science and Technology Major Project (grant number 2013zx09509107), and the Independent Exploration and Innovation Project of Central South University in China (grant number 2019zzts344).

ACKNOWLEDGMENTS

The authors would like to thank TCGA and GEO projects for data sharing.

SUPPLEMENTARY MATERIAL

The Supplementary Material for this article can be found online at: https://www.frontiersin.org/articles/10.3389/fonc.2020.579625/full#supplementary-material

SUPPLEMENTARY FIGURE 1 | Relationship between TBCs mRNA expression with clinical features in melanoma. The heat maps based on clustering analysis according to the subgroups exhibited the differential expression patterns of TBCs (Tumor status: tumor-free vs with-tumor, Metastasis type: RCS vs RLN vs DM and Age: young vs old). *p < 0.05, **p < 0.01, ***p < 0.001, **** < 0.0001.

SUPPLEMENTARY FIGURE 2 | The differential expression of the seven prognostic-associated TBC genes. The differential expression of the seven

prognostic-associated TBC genes between normal tissues and tumor tissues in the TCGA dataset. ***p <0.001, NS. p > 0.05.

SUPPLEMENTARY FIGURE 3 | Protein expression of TBCs detecting by immunohistochemical assay based on online websites. Immunohistochemical staining showed the images of the protein expression of TBC1D10C **(A)**, TBC1D19 **(B)**, TBC1D16 **(C)**, and TBC1D13 **(D)** in normal skin tissues and melanoma tissues from the Human Protein Atlas website (www.proteinatlas.org).

SUPPLEMENTARY FIGURE 4 | Survival analyses based on risk score and clusters. **(A)** Kaplan ± Meier survival analyses demonstrated the differences in OS, PFI and DSS based on risk scores (High vs Low) in primary tissues from TCGA. **(B)** Kaplan ± Meier survival analyses demonstrated the differences in DMS and DSS based on risk scores (High vs Low) in tumor tissues from the GEO dataset (65904). **(C)** Kaplan ± Meier survival analyses demonstrated the differences in PFI based on clusters (cluster 1 vs cluster 2) in tumor tissues. **(D)** Kaplan ± Meier survival analyses demonstrated the differences in PFI based on clusters (cluster 1 vs cluster 2) in metastasis tissues. **(E)** Kaplan ± Meier survival analyses demonstrated the differences in OS, PFI and DSS based on clusters (cluster 1 vs cluster 2) in primary tissues.

SUPPLEMENTARY FIGURE 5 | GO and KEGG analysis. **(A, B)** Correlation analysis between the seven prognostic TBCs and the top 10 significant pathways from GO and KEGG analysis.

REFERENCES

1. Houghton AN, Polsky D. Focus on melanoma. *Cancer Cell* (2002) 2(4):275–8.
2. Schadendorf D, van Akkooi ACJ, Berking C, Griewank KG, Gutzmer R, Hauschild A, et al. Melanoma. *Lancet* (2018) 392(10151):971–84.
3. Liu-Smith F, Farhat AM, Arce A, Ziogas A, Taylor T, Wang Z, et al. Sex differences in the association of cutaneous melanoma incidence rates and geographic ultraviolet light exposure. *J Am Acad Dermatol* (2017) 76(3):499–505.e3.
4. Carr S, Smith C, Wernberg J. Epidemiology and Risk Factors of Melanoma. *Surg Clinics North Am* (2020) 100(1):1–12.
5. Tracey EH, Vij A. Updates in Melanoma. *Dermatol Clin* (2019) 37(1):73–82.
6. Mishra H, Mishra PK, Ekielski A, Jaggi M, Iqbal Z, Talegaonkar S. Melanoma treatment: from conventional to nanotechnology. *J Cancer Res Clin Oncol* (2018) 144(12):2283–302.
7. Wei Z, Zhang M, Li C, Huang W, Fan Y, Guo J, et al. Specific TBC Domain-Containing Proteins Control the ER-Golgi-Plasma Membrane Trafficking of GPCRs. *Cell Rep* (2019) 28(2):554–66.e4.
8. Frasa MA, Koessmeier KT, Ahmadian MR, Braga VM. Illuminating the functional and structural repertoire of human TBC/RABGAPs. *Nat Rev Mol Cell Biol* (2012) 13(2):67–73.
9. Chen S, Wasserman DH, MacKintosh C, Sakamoto K. Mice with AS160/TBC1D4-Thr649Ala knockin mutation are glucose intolerant with reduced insulin sensitivity and altered GLUT4 trafficking. *Cell Metab* (2011) 13(1):68–79.
10. Kane S, Sano H, Liu SC, Asara JM, Lane WS, Garner CC, et al. A method to identify serine kinase substrates. Akt phosphorylates a novel adipocyte protein with a Rab GTPase-activating protein (GAP) domain. *J Biol Chem* (2002) 277 (25):22115–8.
11. Pei L, Peng Y, Yang Y, Ling XB, Van Eyndhoven WG, Nguyen KC, et al. PRC17, a novel oncogene encoding a Rab GTPase-activating protein, is amplified in prostate cancer. *Cancer Res* (2002) 62(19):5420–4.
12. Sato N, Koinuma J, Ito T, Tsuchiya E, Kondo S, Nakamura Y, et al. Activation of an oncogenic TBC1D7 (TBC1 domain family, member 7) protein in pulmonary carcinogenesis. *Genes Chromosomes Cancer* (2010) 49(4):353–67.
13. Akavia UD, Litvin O, Kim J, Sanchez-Garcia F, Kotliar D, Causton HC, et al. An integrated approach to uncover drivers of cancer. *Cell* (2010) 143(6):1005–17.
14. Goeman JJ. L1 penalized estimation in the Cox proportional hazards model. *Biom J Biom Z* (2010) 52(1):70–84.
15. Mermel CH, Schumacher SE, Hill B, Meyerson ML, Beroukhim R, Getz G. GISTIC2.0 facilitates sensitive and confident localization of the targets of focal somatic copy-number alteration in human cancers. *Genome Biol* (2011) 12(4):R41.
16. Wilkerson MD, Hayes DN. ConsensusClusterPlus: a class discovery tool with confidence assessments and item tracking. *Bioinf (Oxford Engl)* (2010) 26 (12):1572–3.
17. Datta S, Datta S. Comparisons and validation of statistical clustering techniques for microarray gene expression data. *Bioinf (Oxford Engl)* (2003) 19(4):459–66.
18. Hanzelmann S, Castelo R, Guinney J. GSVA: gene set variation analysis for microarray and RNA-seq data. *BMC Bioinf* (2013) 14:7.
19. Liberzon A, Birger C, Thorvaldsdottir H, Ghandi M, Mesirov JP, Tamayo P. The Molecular Signatures Database (MSigDB) hallmark gene set collection. *Cell Syst* (2015) 1(6):417–25.
20. Nunez E, Steyerberg EW, Nunez J. [Regression modeling strategies]. *Rev Espanola Cardiol* (2011) 64(6):501–7.
21. Prado G, Svoboda RM, Rigel DS. What's New in Melanoma. *Dermatol Clin* (2019) 37(2):159–68.
22. Gabernet-Castello C, O'Reilly AJ, Dacks JB, Field MC. Evolution of Tre-2/Bub2/Cdc16 (TBC) Rab GTPase-activating proteins. *Mol Biol Cell* (2013) 24 (10):1574–83.
23. Wang B, Zhao H, Zhao L, Zhang Y, Wan Q, Shen Y, et al. Up-regulation of OLR1 expression by TBC1D3 through activation of TNFalpha/NF-kappaB pathway promotes the migration of human breast cancer cells. *Cancer Lett* (2017) 408:60–70.
24. Davey JR, Humphrey SJ, Junutula JR, Mishra AK, Lambright DG, James DE, et al. TBC1D13 is a RAB35 specific GAP that plays an important role in GLUT4 trafficking in adipocytes. *Traffic (Copenhagen Denmark)* (2012) 13 (10):1429–41.
25. Vizoso M, Ferreira HJ, Lopez-Serra P, Carmona FJ, Martinez-Cardus A, Girotti MR, et al. Epigenetic activation of a cryptic TBC1D16 transcript enhances melanoma progression by targeting EGFR. *Nat Med* (2015) 21 (7):741–50.
26. Dibble CC, Elis W, Menon S, Qin W, Klekota J, Asara JM, et al. TBC1D7 is a third subunit of the TSC1-TSC2 complex upstream of mTORC1. *Mol Cell* (2012) 47(4):535–46.
27. Song Y, Pan Y, Liu J. The relevance between the immune response-related gene module and clinical traits in head and neck squamous cell carcinoma. *Cancer Manage Res* (2019) 11:7455–72.
28. Choy CT, Wong CH, Chan SL. Embedding of Genes Using Cancer Gene Expression Data: Biological Relevance and Potential Application on Biomarker Discovery. *Front Genet* (2018) 9:682.
29. Choi SJ, Song IS, Feng JQ, Gao T, Haruyama N, Gautam P, et al. Mutant DLX 3 disrupts odontoblast polarization and dentin formation. *Dev Biol* (2010) 344 (2):682–92.
30. Kampf LL, Schneider R, Gerstner L, Thunauer R, Chen M, Helmstadter M, et al. TBC1D8B Mutations Implicate RAB11-Dependent Vesicular Trafficking in the Pathogenesis of Nephrotic Syndrome. *J Am Soc Nephrol* (2019) 30: (12):2338–53.
31. Wu J, Cheng D, Liu L, Lv Z, Liu K. TBC1D15 affects glucose uptake by regulating GLUT4 translocation. *Gene* (2019) 683:210–5.
32. Onoue K, Jofuku A, Ban-Ishihara R, Ishihara T, Maeda M, Koshiba T, et al. Fis1 acts as a mitochondrial recruitment factor for TBC1D15 that is involved in regulation of mitochondrial morphology. *J Cell Sci* (2013) 126(Pt 1):176–85.
33. Takahara Y, Maeda M, Hasegawa H, Ito S, Hyodo T, Asano E, et al. Silencing of TBC1D15 promotes RhoA activation and membrane blebbing. *Mol Cell Biochem* (2014) 389(1-2):9–16.
34. Peralta ER, Martin BC, Edinger AL. Differential effects of TBC1D15 and mammalian Vps39 on Rab7 activation state, lysosomal morphology, and growth factor dependence. *J Biol Chem* (2010) 285(22):16814–21.
35. Yang Z, Shen H, He W, Ouyang L, Guo Y, Qian F, et al. Expression of TBC1D16 Is Associated with Favorable Prognosis of Epithelial Ovarian Cancer. *Tohoku J Exp Med* (2018) 245(3):141–8.
36. Haley R, Wang Y, Zhou Z. The small GTPase RAB-35 defines a third pathway that is required for the recognition and degradation of apoptotic cells. *PLoS Genet* (2018) 14(8):e1007558.

37. Li W, Zou W, Zhao D, Yan J, Zhu Z, Lu J, et al. C. elegans Rab GTPase activating protein TBC-2 promotes cell corpse degradation by regulating the small GTPase RAB-5. *Dev (Cambridge Engl)* (2009) 136(14):2445–55.
38. Vizoso M, Esteller M. Targeting melanoma: unusual epigenetics reveals the dynamic rewiring of metastatic cells. *Epigenomics* (2015) 7(7):1079–81.
39. Dorval G, Kuzmuk V, Gribouval O, Welsh GI, Bierzynska A, Schmitt A, et al. TBC1D8B Loss-of-Function Mutations Lead to X-Linked Nephrotic Syndrome via Defective Trafficking Pathways. *Am J Hum Genet* (2019) 104 (2):348–55.
40. Chen J, Chen Z. The effect of immune microenvironment on the progression and prognosis of colorectal cancer. *Med Oncol (Northwood Lond Engl)* (2014) 31(8):82.
41. Li DY, Tang YP, Zhao LY, Geng CY, Tang JT. Antitumor effect and immune response induced by local hyperthermia in B16 murine melanoma: Effect of thermal dose. *Oncol Lett* (2012) 4(4):711–8.
42. Yang MQ, Du Q, Varley PR, Goswami J, Liang Z, Wang R, et al. Interferon regulatory factor 1 priming of tumour-derived exosomes enhances the antitumour immune response. *Br J Cancer* (2018) 118(1):62–71.
43. Ouyang Z, Wu H, Li L, Luo Y, Li X, Huang G. Regulatory T cells in the immunotherapy of melanoma. *Tumour Biol J Int Soc Oncodev Biol Med* (2016) 37(1):77–85.
44. Gai Z, Chu W, Deng W, Li W, Li H, He A, et al. Structure of the TBC1D7-TSC1 complex reveals that TBC1D7 stabilizes dimerization of the TSC1 C-terminal coiled coil region. *J Mol Cell Biol* (2016) 8(5):411–25.
45. Ren S, Huang Z, Jiang Y, Wang T. dTBC1D7 regulates systemic growth independently of TSC through insulin signaling. *J Cell Biol* (2018) 217(2):517–26.
46. Qi TF, Guo L, Huang M, Li L, Miao W, Wang Y. Discovery of TBC1D7 as a Potential Driver for Melanoma Cell Invasion. *Proteomics* (2020) 20(14): e1900347.

Conflict of Interest: The authors declare that the research was conducted in the absence of any commercial or financial relationships that could be construed as a potential conflict of interest.

frontiers in Oncology

REVIEW
published: 04 February 2021
doi: 10.3389/fonc.2020.626129

Decoding Melanoma Development and Progression: Identification of Therapeutic Vulnerabilities

Kevinn Eddy[1,2], *Raj Shah*[2,3] *and Suzie Chen*[1,2,4,5]*

[1] Graduate Program in Cellular and Molecular Pharmacology, School of Graduate Studies, Rutgers University, Piscataway, NJ, United States, [2] Susan Lehman Cullman Laboratory for Cancer Research, Rutgers University, Piscataway, NJ, United States, [3] Joint Graduate Program in Toxicology, Rutgers University, Piscataway, NJ, United States, [4] Rutgers Cancer Institute of New Jersey, New Brunswick, NJ, United States, [5] Environmental & Occupational Health Sciences Institute, Rutgers University, Piscataway, NJ, United States

Melanoma, a cancer of the skin, arises from transformed melanocytes. Melanoma has the highest mutational burden of any cancer partially attributed to UV induced DNA damage. Localized melanoma is "curable" by surgical resection and is followed by radiation therapy to eliminate any remaining cancer cells. Targeted therapies against components of the MAPK signaling cascade and immunotherapies which block immune checkpoints have shown remarkable clinical responses, however with the onset of resistance in most patients, and, disease relapse, these patients eventually become refractory to treatments. Although great advances have been made in our understanding of the metastatic process in cancers including melanoma, therapy failure suggests that much remains to be learned and understood about the multi-step process of tumor metastasis. In this review we provide an overview of melanocytic transformation into malignant melanoma and key molecular events that occur during this evolution. A better understanding of the complex processes entailing cancer cell dissemination will improve the mechanistic driven design of therapies that target specific steps involved in cancer metastasis to improve clinical response rates and overall survival in all cancer patients.

Keywords: melanoma, melanoma progression, metastasis, signaling pathways, melanoma therapies

OPEN ACCESS

Edited by:
Vladimir Spiegelman, Penn State Milton S. Hershey Medical Center, United States

Reviewed by:
Pamela Bond Cassidy, Oregon Health and Science University, United States
John August D'Orazio, University of Kentucky, United States

***Correspondence:**
Suzie Chen
suziec@pharmacy.rutgers.edu

Specialty section:
This article was submitted to Skin Cancer, a section of the journal Frontiers in Oncology

Received: *04 November 2020*
Accepted: *21 December 2020*
Published: *04 February 2021*

Citation:
Eddy K, Shah R and Chen S (2021) Decoding Melanoma Development and Progression: Identification of Therapeutic Vulnerabilities. Front. Oncol. 10:626129. doi: 10.3389/fonc.2020.626129

INTRODUCTION TO MELANOMA

In the United States, cancer is the second leading cause of death and is expected to surpass heart disease in a few years (1). Skin cancer is by far the most common of all cancers, with an increasing frequency in the past three decades that includes basal cell carcinoma (BCC), squamous cell carcinoma (SCC), and melanoma. Although melanoma accounts for merely 1% of all skin cancers, it is responsible for the majority of skin cancer related fatalities. Melanoma is the most aggressive and dangerous forms of skin cancer that develops from the transformed pigment forming cells of the skin, melanocytes (2). Diagnosing melanoma in its early stages, *in situ*, is crucial for the prognosis and survival of this deadly disease as the 5-year survival rate for primary melanoma is 99% and for metastatic melanoma is only 27% (1). Global incidence rates for melanoma have steadily increased over the years; in the United States approximately 100,000 new cases of invasive melanoma will be

diagnosed in 2021 and about 7,000 of those melanoma patients will die from this disease (1, 3). There are various risk factors associated with melanoma: a family history of skin cancer, being a male, fair skin, number of moles, age, and UV exposure (1, 3–9). The most common inherited genetic defects associated with a predisposition to developing melanoma are the cell cycle regulating genes: *CDKN2A*, *CDK4*, a gene responsible for skin pigmentation: *MC1R*, and the genetic disorder xeroderma pigmentosum (XP) that disrupts the proper repair of UV induced DNA damage thereby leading to a higher mutation rate (10–17).

A dermatologist usually diagnoses melanoma on a patient using the ABCDEF criteria with the help of a dermascope, a tool that removes skin surface reflections to accurately distinguish between a benign or malignant lesion (18–20). The ABCDEF criteria are: Asymmetry, Border irregularity, Color variegation, Diameter >6 mm, Evolution of a nevi and Funny looking, where a malignant nevi does not conform to the common profiles of nevi found on a patient (18). Once diagnosed, the melanoma is staged using a set of principles developed by the American Joint Committee on Cancer (AJCC) to guide patient treatment and prognosis (21). Melanoma patients can be classified into five distinct stages, 0, I, II, III, and IV, as the stage increases the prognosis is worse (21). Stage 0 is defined as melanoma *in situ* while stage IV melanoma is known as metastatic melanoma. Metastatic melanoma is defined by the dissemination of primary melanoma cells to distant organs including but not limited to the lymph nodes, lungs, liver, brain, and bone (21, 22). AJCC criteria uses different permutations of the TNM system, to categorize melanoma from early stage to late stage melanoma (21). The TNM system is defined as: Tumor thickness with or without ulceration, Nodal involvement, and Metastasis (21). Great advances have been made in the understanding of melanoma pathogenesis that have resulted in improved disease treatment outcomes including targeted therapies: BRAF and MEK inhibitors and immunotherapies: monoclonal antibodies that target CTLA-4, PD-1 and PD-L1, however not all patients respond, and resistance eventually develops to these agents. This underscores the importance of dissecting the molecular pathways mediating metastasis, the processes of transitioning of an immobile melanoma cell into a motile cell that can successfully colonize distant organs. A better understanding of these pathways will help in the identification of biological markers (biomarkers) for better diagnosis and provide rational therapeutic strategies to predict favorable treatment responses.

TUMOR INTRINSIC AND EXTRINSIC FUNCTIONS NECESSARY FOR SUCCESSFUL TUMOR CELL DISSEMINATION

Stepwise Molecular Evolution for the Transition of Primary Melanoma to Metastatic Melanoma

Melanoma has the highest mutational burden of any cancer as a result of UV induced DNA damage and/or DNA replication errors (8, 23). All these mutations contribute to various aspects of melanocytic neoplasia; however, certain mutations are considered driver mutations as they are likely to initiate melanocytic transformation, the early steps of tumor formation, progression, and dissemination. Vogelstein et al., and Shain et al., have elegantly described the genetic evolution transpiring during the transformation of a melanocytic lesion into malignant melanoma (**Figure 1**) (6, 24, 25). First a normal melanocyte acquires an initiating driver mutation that leads to melanocyte hyperplasia and nevi development (6, 25–28). These

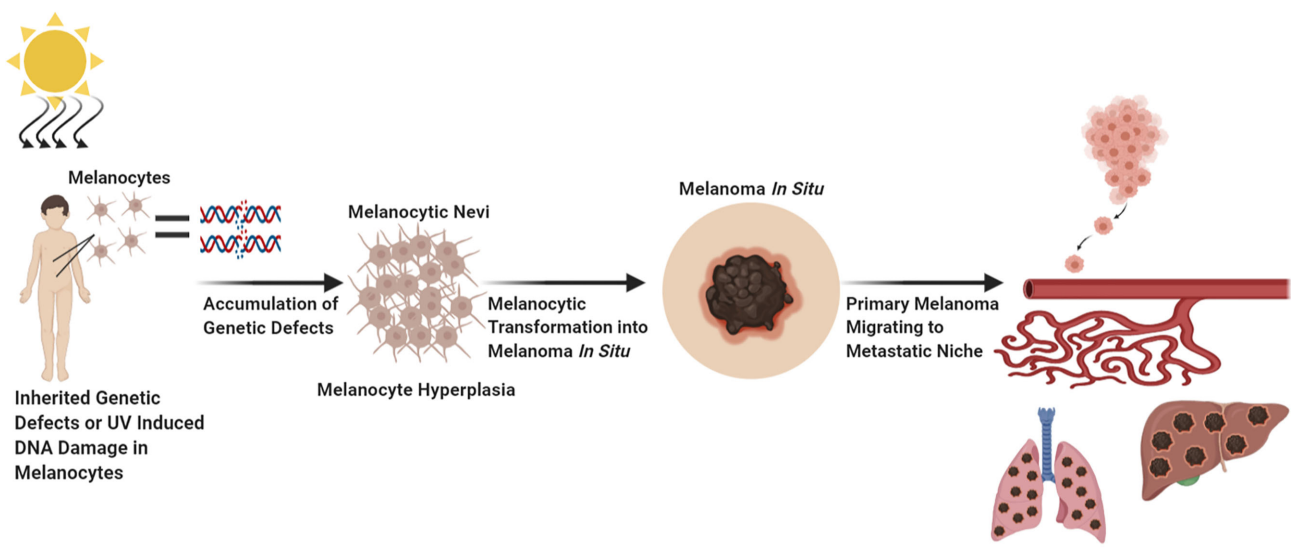

FIGURE 1 | Factors Which Contribute to Melanocytic Transformation. Created with BioRender.com.

steps are known as the breakthrough phase, with a low mutational burden, and copy number alterations (24, 25). Common mutations found in melanocyte nevi are *BRAF* mutations (26–28). Mutations in *BRAF* and *NRAS* are frequently mutually exclusive, with *NRAS* mutations sometimes found in nevi, especially congenital nevi (29, 30). The next step known as the expansion phase where some of the melanocytic nevi progress into intermediate lesions and overtime develop into melanoma *in situ*, that is accompanied with the acquisition of the *TERT* promoter mutations, and a high mutational burden (6, 24, 25, 31). The *TERT* gene encodes for telomerase reverse transcriptase, the catalytic component of telomerase, an enzyme required for the maintenance of telomeres (31). Aberrant expression of telomerase allows melanoma cells to become replicative immortal (31). After the accumulation of various mutations such as: *CDKN2A*, *TP53*, *PTEN*, and genes encoding SWI/SWF chromatin remodeling complex subunits, primary melanoma enters the invasive phase and becomes malignant melanoma (6, 24, 25). This phase is characterized by a high tumor mutational burden and increased copy number alterations (6, 25). To note, only 20–40% of melanomas arise from nevi and the rest are *de novo*, however *de novo* melanomas may arise from clinically undetectable precursor lesions, and these lesions may follow similar trajectory as detectable lesions (**Figure 1**) (6, 25, 32, 33).

In addition to the genetic defects associated with metastatic melanoma development there are several dysregulated key signaling pathways that occur during melanoma progression such as the WNT, MAPK, and PI3K/AKT pathways (22, 34, 35). These pathways are involved in melanoma cell proliferation, growth, survival, evading cell death, and acquiring metastatic properties (34, 35). The MAPK and PI3K/AKT pathways can cooperate with each other in the transduction of survival signals (36). The WNT signaling cascade plays a fundamental role in embryogenesis (37). The involvement of such a central pathway, the WNT pathway, in melanoma cell dissemination suggests that the reactivation of elements associated with embryogenesis is crucial in elucidating cancer cell metastases (37, 38). Embryogenesis requires a single cell to proliferate and differentiate into various cell types and acquire migratory/invasive properties required for body patterning that parallels carcinogenesis (37, 38). Signal transduction of the WNT, MAPK, and PI3K/AKT pathways in melanoma cells promotes altered expression of cell adhesion molecules and peptidases allowing for the remodeling of the extracellular matrix (ECM) to facilitate in cancer cell migration (34, 39–42). During melanoma progression, elevated matrix metallopeptidase (MMP) expression and function have been detected (34, 43, 44). MMP facilitates the degradation of the ECM that supports melanoma growth during early stages and eventual migration to distant organs (34, 43, 44). Increased MMP avidity in the tumor microenvironment is contributed by both tumor production of MMP as well as tumor induced fibroblast production of MMPs (39–47). Loss of the ECM enables melanoma cells to become anchorage independent and anoikis resistance that support melanoma dissemination through the circulatory system. In addition to MMP cleaving connections between melanoma cells and ECM, the loss of adhesion molecules such as integrins and cadherins also contribute to the motility of melanoma cells from the primary site (22, 34, 48–51). Cell adhesion molecules are required for cell attachment to the basement membrane and cell-cell interactions allowing for the proper development of tissues and organs. Under normal physiology, cell adhesion molecules, integrins and E-cadherins are involved in the attachment of melanocytes to the basement membrane and mediating the interactions between keratinocytes and melanocytes (52, 53). During melanoma progression, E-cadherins are progressively reduced to allow for the dissociation between melanocytes and keratinocytes followed by concomitant upregulation of N-cadherins to support melanoma cell survival, and migration through tissues, a process regulated by the PI3K/AKT pathway (54–56). In addition to modulations in the expression of cadherins during metastasis, integrins can be modulated to support motility and migration into hospitable metastatic niches by modifying basement membrane interactions, supporting angiogenesis formation and expression of MMPs (34, 51, 57–59). There are specific micro RNAs (miRNA), metastamiRs, that were shown to potentiate cancer cell metastasis by regulating critical steps associated with epithelial and mesenchymal transition (EMT), angiogenesis, colonization, adhesion, migration, and invasion (60). Melanoma cell interactions with neighboring cells are essential for their survival, proliferation, and dissemination, in line with this we will discuss the importance of immune evasion in melanoma metastasis.

Interactions Between the Host Immune System and Melanoma Cells to Support Melanoma Cell Growth and Dissemination

Our immune system is essential for defending us from foreign pathogens that invade our body. Cancer is a distorted version of our normal self, and under this guise it can evade immune destruction through the process of immune editing (61, 62). It takes many years through the process of immune editing for a clinically detectable melanoma (or other cancers) to emerge (61, 62). Immune editing is composed of three phases: elimination, equilibrium, and escape phases (61, 62). Immunogenic melanoma clones during the elimination phase are detected by antigen presenting cells, phagocytosed and cross-presented to melanoma specific cytotoxic T-cells for activation to induce an anti-tumor responses against melanoma associated antigens (61). This process inherently allows for the selection of low immunogenic melanoma cell clones to survive and evade host immune detection while highly immunogenic cell clones are eliminated, a process termed as the equilibrium phase (61). Immune resistant melanoma cell clones that have survived are able to proliferate and migrate to distant organs without immune detection, a term coined as the escape phase (61). The process of immune editing is supported by the notion that the first site of melanoma metastasis is detected in the lymph nodes, an organ composed of many cytotoxic immune cells (**Figure 2**) (22). If the immune system is not suppressed, then these melanoma cells would not be able to survive and thrive at this site (**Figure 2**). The

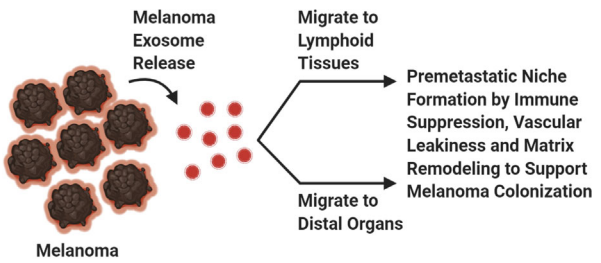

FIGURE 2 | Exosomes. Melanoma exosomes create a pre-metastatic niche at distal sites to support melanoma cell dissemination. Created with BioRender.com.

migration of low immunogenic primary melanoma cells into lymph nodes may not be attributed solely to the passive migration of these cells from the primary niche to the metastatic niche, but rather a preferential migration to the lymph nodes to improve tumor fitness and colonization abilities (63–65). The migration of melanoma cells from the skin to the lymph nodes is attributed to their ability to secrete soluble factors, in addition to the presence of small vesicles, exosomes, which contain cargo that promote the lymphatic system to expand its vasculature (65) (**Figure 2**). Furthermore, lymphatic endothelial cells secrete cytokines and chemokines that support the movement of tumor cells to the lymph nodes (65). All these factors are key contributors to the successful colonization of melanoma cells to the lymphatic tissues (65). One of the rate limiting steps in the establishment of distant metastasis is oxidative stress (65). To overcome this barrier, primary melanoma cells preferentially migrate to the lymph nodes where they are educated to become resistant to oxidative stress (65). This adaptation allows these tumor cells to successfully seed and colonize distant organs compared to circulating melanoma cells (64, 65). Next, we will discuss the critical players in tumor metastasis including genetic mutations, signaling pathways, tumor microenvironment and the involvement of small vesicles, exosomes (**Figure 2**).

Experimental Models to Study Melanoma Metastasis

Experimental models that recapitulate the onset and progression of human disorders is essential in biomedical research to bridge the gap between basic science and the treatment of diseases. There are very few animal models for tumor metastasis, with the B16 mouse melanoma cell line being a very popular one. The B16 parental cell line was derived from a C57BL/6 mouse which spontaneously developed lesions and were subsequently adapted to grow in cultured conditions (66). There are several subclones of B16 cells with differing metastatic capabilities (66, 67). These subclones were derived by subcutaneously injecting B16 cells into syngeneic C57BL/6 mice (spontaneous metastasis), or by intravenous injection of these cells into circulation (experimental metastasis) (66). Our spontaneous melanoma-prone mouse model is driven by the ectopic expression of a normal neuronal receptor, Metabotropic Glutamate Receptor 1 (protein: mGluR1; gene: *GRM1*) in melanocytes which is a useful model to study spontaneous metastasis in a biologically and physiologically relevant manner (68–72). We demonstrated this melanoma-prone mouse model has several advantages: it develops spontaneous metastatic melanoma with 100% penetrance, the progression of the disease mimics human melanoma progression and metastatic dissemination with melanomas being detectable first in the lymph nodes and at later stages in the lung, brain, and other sites (68–72). In some cases, the melanotic tumors can undergo phenotypic changes into amelanotic metastatic tumors similar to human melanomas (72). Recently, Kos and co-workers used fluorescence imaging to trace melanoma cell dissemination in an intact *in vivo* setting using crosses of our mice, this new strain will be a useful tool to study spontaneous metastasis (73). The study of spontaneous metastasis is hindered since the required interval for spontaneous metastasis to occur *in vivo* takes much longer than the commonly used intravenous inoculation of tumor cells, in addition animal wellness rules in almost all institutions, frequently discourages the practice to keeping tumor-bearing mice for a long period of time.

MECHANISMS AND ROUTES FOR MELANOMA METASTASIS

EMT-to-MET Transition

There are numerous steps required for melanoma cells, as well as other cancer cells, to successfully spread to distant organs. Melanoma cells must first dissociate from the primary tumor and undergo Epithelial Mesenchymal Transition (EMT), a process by which epithelial cells undergo morphological and phenotypic changes that allow them to become more migratory and invasive through tissues and enter circulation. Tsuji and colleagues have proposed that tumor cells that have not undergone EMT, termed non -EMT tumor cells are attached to EMT tumor cells and "come along for the ride" to distal organs (**Figure 3**) (74). Bockhorn and colleagues suggested the notions of passive and active intravasations (75). In passive intravasation tumor cells are passively shed during tumor progression as a result of a highly stressful environment (**Figure 3**) (75). Active intravasation is when cancer cells are actively undergoing molecular alterations to a metastatic phenotype and follow a chemokine gradient to arrive at the site of metastasis (**Figure 3**) (75). We propose that both passive and active intravasations occur as tumor progresses, since the surrounding extracellular matrix (ECM) is degraded and enables both EMT and non-EMT tumor cells to intravasate into circulation (**Figure 3**) (74, 75). In this scenario, EMT cells are actively intravasating into circulation and non-EMT cells are the passengers as in passive intravasation (**Figure 3**) (74, 75). Once in circulation, these traveling melanoma cells will migrate to their preferential metastatic organs mediated by chemotaxis of specific chemokine ligand-receptor interactions or by passive migration (22, 74, 75). In circulation, melanoma cells can transdifferentiate into endothelial cells where they remain dormant at the intravascular niche near the metastatic

site (**Figure 3**) (73). Quiescent in-transit melanoma cells are resistant to therapies, suggesting that these melanoma cells may have transdifferentiated into endothelial-like cells and contribute to melanoma relapse in patients who have previously responded to therapy (73). Interestingly, it was shown that highly metastatic melanoma cells can form their own vascular tubes to improve blood flow to the tumor site and promote cancer cell dissemination, a phenomenon known as vascular mimicry (76, 77). It has been proposed that these transdifferentiated quiescent melanoma cells may undergo an endothelial to mesenchymal transition (EndMT) to extravasate into the metastatic niche (73). Therefore, it is possible that there are at least two distinct mechanisms for circulating melanoma cells to successfully establish at the secondary site depending on if they are active or dormant cancer cells: 1) the canonical extravasation or 2) the proposed transition of a quiescent-like endothelial melanoma cell to convert into a mesenchymal phenotype in order to successfully extravasate into the metastatic niche (**Figure 3**) (73, 78). If the environment of the metastatic niche is favorable, melanoma cells can successfully colonize there and become clinical detectable tumors. Alternate mechanisms of tumor cell dissemination have been proposed. One of these mechanisms is that melanoma metastasis occurs in parallel with the primary tumor rather in a stepwise manner, a distinct idea from EMT (6). This concept is based on the observation that in some melanoma patients with localized melanomas who have had their sentinel lymph nodes removed but did not show improvement in their survival suggests that the tumor cells may already have migrated to distal organs (6, 63, 79, 80). Furthermore, patients who have localized melanomas or no metastasis at all have shown the presence of circulating melanoma cells (6, 81). Another intriguing proposal is that benign melanocyte nevi can migrate to distal sites and acquire oncogenic mutations enabling

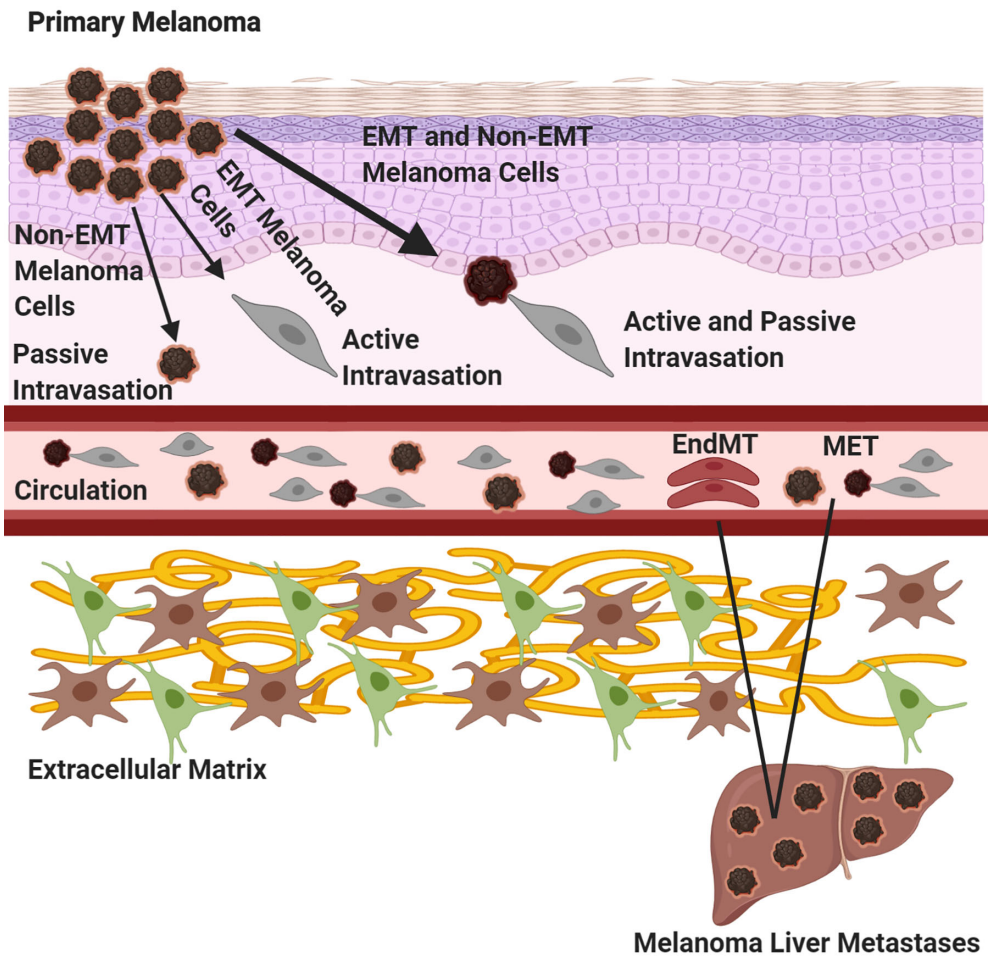

FIGURE 3 | Melanoma Metastasis. Three routes of primary melanoma dissemination are outlined. A primary melanoma can undergo 1) passive shedding of tumor cells, non-EMT (epithelial to mesenchymal transition) followed by passive intravasation, 2) tumor cells can undergo EMT and active intravasation or 3) melanoma cells can undergo EMT and bring along non-EMT tumor cells, where the EMT cells are actively intravasating while the non-EMT cell are undergoing passive intravasation. Once in circulation, tumor cells will migrate to site of metastasis. If the tumor cells are active, they will undergo the canonical extravasation by mesenchymal to epithelial transition (MET). If the tumor cells are dormant, they will transdifferentiate into endothelial cells at the intravascular niche, undergo endothelial to mesenchymal transition (EndMT) and extravasate into the niche. Created with BioRender.com.

their transformation into melanoma cells at the metastatic site, a process known as benign metastasis (6, 82–84). Benign metastasis may explain how 4% of melanoma patients develop "metastasized" melanomas despite the absence of detectable primary tumors (6). These findings further complicate our understanding of melanoma metastasis; however, it is possible that in some cases both stepwise and parallel melanoma dissemination occur simultaneously.

Angiogenesis

Angiogenesis is a biological process that marks a critical stage in tumor progression where the cells transition from an avascular to a vascular phase, serving as a turning point in melanoma tumor growth and metastasis (**Figure 4**). Melanoma cells serve as the source of several classical angiogenic growth factors including but not limited to vascular endothelial growth factor (VEGF), also known as the vascular permeability factor (VPF), fibroblast growth factor (FGF), interleukin-8 (IL-8), and placental growth factor (PlGF), all potent contributors of angiogenesis (**Figure 4**) (85). VEGF is often considered to be one of the most important mediators of angiogenesis and was shown to have elevated expression in all known solid tumors including malignant melanoma (86). Melanoma cells produce and secrete VEGF into the extracellular matrix (87). Expression of a specific VEGF isoform in an otherwise non-tumorigenic, non-VEGF expressing melanoma cell line results in an aggressive tumor with a highly extensive supporting vasculature, suggesting its undisputed role in promoting angiogenesis (88). Upregulation of IL-8 and VEGF have also been postulated to contribute to the development of resistance to chemotherapeutic agents in melanoma (89). VEGF mediates its effects by interacting with and stimulating its high-affinity transmembrane family of tyrosine kinase receptors, VEGF receptors (VEGFRs). At the molecular level, interactions between VEGF and VEGFR-mediated signal transduction, promote reprogramming of specific gene expression in endothelial cells, including upregulated expression of several proteins encompassing the procoagulant tissue factor, proteins associated with the fibrinolytic pathway, MMPs and a number of anti-apoptotic factors (90, 91). The consequences of this altered gene expression includes stimulation in endothelial cell proliferation and migration, lumen formation, increased vessel dilation and permeability thereby enabling constant supply of both oxygen and nutrients to support the growing tumor (92). Inhibition of angiogenesis through targeting of various driver genes, predominantly VEGF, has been touted as a novel alternative or supplement to conventional cancer therapy (93–95). Since anti-angiogenic agents were shown to effectively slow the growth and metastasis of human melanoma, it is not surprising that the efficacy of these agents in augmenting the benefits of other promising therapies is being tested in clinical trials (87, 96). Unfortunately, anti-angiogenic monotherapies in melanoma did not show remarkable clinical responses and it has been suggested that vascular mimicry plays an important role in improving blood supply to the tumor to support its growth and dissemination (97, 98). It is possible that delivering therapeutics that block angiogenesis or vascular mimicry to early-stage melanoma patients, may impede metastasis in two ways: 1) block nutrient and oxygen flow to the primary tumor and 2) hamper primary tumor cells' dissemination by inhibiting entry into circulation.

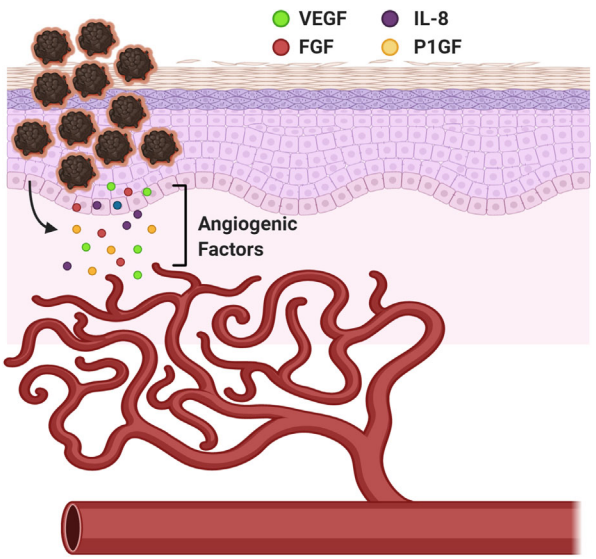

FIGURE 4 | Angiogenesis in Melanoma. A mechanism to provide nourishment to the growing tumor cells and establish routes to distant metastatic sites. Vascular Endothelial Growth Factor (VEGF), Fibroblast Growth Factor (FGF), Interleukin-8 (IL-8), and Placental Growth Factor (PlGF). Created with BioRender.com.

Exosomes

All cell types release exosomes but cancer cells release higher amounts of exosomes compared to their normal counterparts (2). Cancer exosomes play important roles in creating a favorable environment for cancer cells to thrive in; which can be attributed to the suppression of an anti-tumor immune response and establishment of a pre-metastatic niche (**Figure 2**) (2). Accumulating evidence suggests that the horizontal transfer of tumor exosomal cargo, composed of nucleic acid, lipids, and proteins, into recipient cells within lymphoid tissue promotes immune suppression resulting in defective antigen presentation, reduced antigen specific anti-tumor immune response and upregulation of immunosuppressive cytokines that support melanoma metastasis to the lymph nodes and beyond (**Figure 2**) (99–105). These unique features plus PD-L1 expression on the exosome surface, contribute to defective immune effector cell function at both local and systemic levels (106–108). In addition to their roles in modulating the immune system, other functions have been attributed to exosomal cargo including enhanced vascular leakiness, fibronectin deposition, and delivery of soluble factors that are involved in ECM remodeling to support formation of a metastatic niche for tumor cells, including melanomas (**Figure 2**) (2, 104, 109–112). Exosomes support the "seed and soil" hypothesis of cancer cell dissemination (111–113). Melanoma exosomes located at the most common sites of metastasis, lymph nodes, liver, and lungs, create a "fertile soil" for melanoma cells to

"seed" upon arrival then proliferate and manifest into a malignant tumor (111–113). In our mGluR1 driven melanoma model, we have demonstrated that mGluR1$^+$ melanoma exosomes when taken up by mGluR1$^-$ recipient cells promote these cells to become more migratory, invasive and develop an anchorage-independent growth phenotype compared to mGluR1$^-$ melanoma exosomes (114). Taken together, it is clear that every step of tumor dissemination is critical for its successful colonization to distant sites. Better understanding of these necessary molecular and theoretical steps will provide rational therapeutic designs to improve the efficacy of treatments as well as reduce disease relapse.

BIOMARKERS IN MALIGNANT MELANOMA

Melanoma biomarkers can be divided into different categories based on their level of expression compared to normal tissues as well as their ability to serve as prognostic or predictive markers (115). These markers can be further classified into two groups (serum-specific and tissue-specific) depending on their dominant location of expression. Due to the complexity and heterogeneity of melanoma tumors, immunohistochemical staining for tissue-specific melanocytic markers is often used to diagnose melanoma. Microphthalmia-associated transcription factor (MITF), a predominant tissue-specific marker, plays a critical role in lineage commitment of melanocytes and melanoma (116). Normal melanocyte differentiation and proliferation are under the regulation of MITF. MITF expression is also essential for melanoma cell proliferation and survival (117). With integrative genomic analysis, it was found to be amplified in ~16% of melanomas. *BRAF*^{V600E} mutation together with ectopic expression of MITF has been shown to transform primary melanocytes into malignant melanoma (118). In addition, MITF also stimulates the cell cycle regulator, *INK4A*, for efficient melanocyte differentiation (119). Several studies have investigated the potential of MITF in specificity and sensitivity in distinguishing melanoma from other cancers, however, the discovery of the presence of MITF in other non-melanocytic cell types in the tumor microenvironment has complicated this notion (120–122). Similar concerns pertaining to other tissue-specific biomarkers including tyrosinase, MMPs, cyclooxegenase-2 (COX-2), chondroitin sulfate proteoglycan 4 (CSPG4), and human melanoma black-45 (HMB-45) among others also have been reported (123). A lack of "tumor-specific" non-invasive and affordable tools including specific antibodies have greatly hampered the use of biomarkers in diagnosis, prognosis, and prediction of treatment outcomes. It is critical to improve biomarker discoveries and detection tools. Promising candidates are "OMICS" studies that include a variety of cancer and normal tissue specimens along with machine learning approaches may have the potential to promote such findings.

Regarding serum-specific biomarkers, lactate dehydrogenase (LDH) is one of the best prognostic factors in metastatic melanoma (124). Cancer cells including melanoma employ a different metabolic strategy than normal cells to satisfy their energy requirements and sustain cellular proliferation. Under aerobic conditions, normal cells acquire their energy primarily from the conversion of glucose to pyruvate by a process known as glycolysis that occurs in the cytosol. Pyruvate then enters the tricarboxylic acid (TCA) cycle where it converts into carbon dioxide in the mitochondria *via* oxygen-consuming cellular respiration (125, 126). However, under hypoxic conditions such as in most tumors, where oxygen is not readily available, cells prefer to rely more on anaerobic glycolysis that converts glucose into lactate instead of pyruvate. Elevated levels of LDH, an enzyme that catalyzes the conversion of pyruvate to lactate, in systemic circulation was shown to predict survival in patients with metastatic melanoma (127). The increase in serum LDH is associated with poor survival, one of the consequences of melanoma cells outgrowing and surpassing the blood supply (124). Similar to tissue-specific biomarkers, differential sensitivity and specificity are also reported in serum-specific markers including but not limited to LDH, S100 and melanoma-inhibitory activity (MIA) (128). The importance of cancer exosomes in mediating tumor progression has led many investigators to evaluate its diagnostic and prognostic value as a biomarker (2). Cancer exosomes that carry specific molecules such as, PD-L1, CD63, Caveloin-1, MIA, S100B, Glypican-1, and non-coding RNA to name a few, were shown to stratify patients participating in various clinical trials into responders versus non-responders, healthy controls and disease-free patients *versus* cancer patients, and/or cancer patients with differing survival outcomes (104, 107, 129–133). Taken together, the challenges that confront the identification of a reliable melanoma biomarker emphasizes the need to investigate and validate emerging biomarker candidates in the clinic to realize their diagnostic, prognostic, and predictive values.

The identification of a reliable predictive clinical biomarker is crucial for precision medicine. Predictive biomarkers are biological molecules detected in most patients and are frequently correlated with treatment responses (134). Personalized/precision medicine is the future for human disease treatments, and it is essential to identify clinically relevant biomarkers that can be easily applied in the clinic. Most pre-clinical cancer studies only assess for the efficacy of drug(s) in tumor progression, but it is crucial to also identify predictive biomarkers for treatment responses. Identification of these biomarkers will provide clinicians with the opportunity to make suitable and rational decisions in therapeutic options.

MELANOMA TREATMENTS

Chemotherapies and Targeted Therapies

For patients diagnosed with primary melanoma, surgical removal of the tumor(s) provides the best chance of definitive cure. Late-stage melanoma is difficult to treat due to metastasis, refractile to most treatment modalities and a high genomic variability of a heterogeneous melanocytic tumor (135). The understanding of how various genetic mutations are associated with the onset and progression of melanoma allows for innovation and subsequent implementation of novel therapeutic strategies targeting specific oncogenes. Within the last decade, much progress has been made

in the treatment of metastatic melanoma. Earlier studies showed that treatment with Sorafenib (BAY 43-9006), a general multi-kinase inhibitor resulted in inhibition of melanoma cell proliferation *in vitro* and *in vivo* (136). However, in the Phase 2 randomized Sorafenib clinical trial little or no anti-tumor activity was detected in advanced melanoma patients, therefore, the trial was discontinued (137). A highly selective small molecule inhibitor, Vemurafenib/Zelboraf (PLX4720/PLX4032), against cells that harbor the most common mutation in melanoma, mutated $BRAF^{V600E}$, was initially reported to have therapeutic effects in patients with advanced melanoma but its effectiveness was marred by patient relapse within 8–12 months (138–141). The treatment responses were short-lived due to the reactivation of the MAPK pathway and/or other mutations (36, 142–144). Combining BRAF inhibitors with other small molecule inhibitors that target other components of the MAPK pathway such as MEK and ERK appear to be an improvement over single-agent therapy but also has increased toxicities (36, 145, 146). It is noteworthy that until recently, it had not been possible to develop an inhibitor towards RAS (147). Christensen et al., reported a $KRAS^{G12C}$ inhibitor that demonstrated pronounced tumor regression in multiple *KRAS*-mutant tumor models (148). *KRAS* mutations are rare in melanoma, where it accounts for about 1.7% and is almost exclusively in codon G12 however it is not known if the recently developed $KRAS^{G12C}$ inhibitor will have any effects in *KRAS* mutated melanomas, furthermore, possible efficacies of the mutated KRAS inhibitor toward *NRAS* mutated melanomas was not tested (149). Despite the nominal successes described above for some patients they only represent a minority of all patients.

Immunotherapies

Melanoma is one of the most immunogenic types of cancers, hence making it a strong candidate for immune checkpoint blockade (ICB) therapy (150). This therapy utilizes a patient's own immune system to attack cancer cells with a robust anti-tumor response, long-term immunity, and durable survival. The concept of immunotherapy has been around for approximately 130 years with the early usage of Coley's toxin, then almost a century later, the uses of interferon (IFN), high dose interleukin-2 (IL-2) and the cancer vaccine, Bacillus-Calmette-Guerin (BCG) have been described for the treatment of melanoma (151–153). These early immunotherapies were non-specific, however within the past decade the utilization of targeted immunotherapies have risen with monoclonal antibodies that block immune checkpoint molecules, such as cytotoxic T-lymphocyte associated protein–4 (CTLA-4), programmed cell death protein-1 (PD-1), and programmed death ligand-1 (PD-L1), adoptive T-cell therapies and oncolytic viruses (151, 153–155). These new targeted immunotherapies have shown remarkable anti-tumor immune responses with improved survival; however, they only benefit a subset of patients.

During infection, immune activity is heightened in order to properly identify and eliminate the source of infection. To reduce the likelihood of the development of autoimmunity the body uses immune checkpoints such as CTLA-4, PD-1, and PD-L1 to rein in the overactive immune response (156–161). Cancer cells utilize these immune checkpoints to induce local and systemic immune suppression. Since cancer is a chronic disease, T-cells within the lymph nodes are continuously exposed to cancer antigens resulting in the upregulation of CTLA-4 on their cell surface and inhibition of proper T-cell activation, disrupting anti-tumor cytotoxic T-cell functions that results in T-cell anergy (162–164). The PD-1/PD-L1 axis functions within the tumor microenvironment, the PD-1 receptors are expressed on the surface of T-cells and tumor cells express its ligand, PD-L1 (152). The PD-1/PD-L1 axis inhibits cytotoxic T-cell response against tumor cells (152). Interestingly, it was shown that this axis contributes to T-cell anergy within tumor draining lymph nodes and that PD-1/PD-L1 interactions within tumor draining lymph nodes can be used as a prognostic marker to determine melanoma treatment outcomes (165). Monoclonal antibodies were developed to block these immune checkpoint interactions. Ipilimumab blocking CTLA-4, and Pembrolizumab/Nivolumab blocking PD-1. The FDA has approved these antibodies for patients with unresectable or metastatic melanoma and these agents were shown to have strong durable responses with improved survival in a subset of patients (151, 152, 166–169). Stage III melanoma patients who have had their melanomas resected can undergo different regimens based on their *BRAF* genotype (170). Patients who harbor mutated *BRAF* are given adjuvant anti-PD-1 therapy in combination with BRAF and MEK inhibitors, while patients with wild-type *BRAF* are given anti-PD-1, as opposed to anti-CTLA-4 due to toxicity (170). The anti-PD-L1 antibody, Atezolizumab has been approved for unresectable or metastatic melanoma patients with the *BRAF V600* mutation in combination with BRAF and MEK inhibitors, Vemurafenib and Cobimetinib (153). It is not surprising that various combinatorial studies utilizing various permutations of drugs to combine with anti-PD-1/anti-PD-L1 may improve patients' responsiveness to immune checkpoint blockade therapy have been one of the most sought-after clinical trials in human cancers including melanoma (169).

DISCUSSION AND FUTURE PERSPECTIVES

A better understanding of the metastatic processes that govern migration of primary melanoma to distant metastatic niches such as lymph nodes, liver, lung, and brain can aid in the clinical development of novel anti-cancer treatments in the future. Several therapies that target driver pathways of melanoma metastasis have been developed: BRAF and MEK inhibitors, anti-angiogenic therapies and immunotherapies that rejuvenate the immune system to detect and eliminate cancer cells. These therapies have remarkable efficacy in the outcomes of treating malignant melanoma in the past decade, however only a small subset of patients respond. This implies that our understanding of melanoma progression is incomplete. To improve our understanding of the signaling cascades involve in melanoma progression (or other cancers) we suggest conducting a large-scale unbiased biomarker serum profiling screen of healthy donors, disease free patients and melanoma patients at different

melanoma stages. Biomarkers are molecules that are linked to disease pathogenesis and identification of biomarkers will reveal biological pathway(s) involved in melanoma progression. Identification of upregulated or downregulated serum markers such as nucleic acids, proteins, exosomes, lipids, and circulating tumor cells may unravel novel or key metastatic pathways that can be further dissected, and therapies developed against them. This proposed concept mirrors forward genetics, we know the external phenotype is melanoma, therefore doing a high throughput unbiased screen for serum biomarkers will reveal expression changes of biomarkers between healthy controls, disease-free patients, and melanoma patients, which will provide insights into key driver pathways regulating metastasis. Using this approach will be the nucleation point to further dissect these pathways and develop a more robust anti-metastatic drug with better responses than current therapies. Furthermore, the identification of a reliable melanoma biomarker that can accurately predict disease treatment outcome in patients and correctly identify patients who will benefit from therapy is still underway. Since melanoma is a molecularly complex and heterogeneous disease with intra- and inter-tumoral variabilities, evaluating multiple biomarkers simultaneously may improve the accuracy and precision of predictive markers than each individual marker.

AUTHOR CONTRIBUTIONS

Conceptualization, KE, RS, and SC. Writing—Original Draft Preparation, KE and RS. Writing—Review and Editing, KE, RS, and SC. Supervision, SC. Funding Acquisition, KE, RS, and SC. All authors contributed to the article and approved the submitted version.

FUNDING

This work was funded by New Jersey Commission on Cancer Research (NJCCR) Pre-Doctoral Fellowship (DCHS19PPC027) to KE, National Cancer Institute Small Business Innovation Research (NCI SBIR) (R44CA156781-04) to SC, Veterans Administration Research Merit Award (101BX003742) to SC. SC and RS are grateful for the support of the NIEHS T32 training grant in Environmental Toxicology (ES007148). The authors also declare that this study received funding from the Bristol-Myers Squibb Graduate Research Fellowship, for RS. The funder was not involved in the study design, collection, analysis, interpretation of data, the writing of this article or the decision to submit it for publication.

REFERENCES

1. Siegel RL, Miller KD, Fuchs HE, Jemal A. Cancer statistics, 2021. *CA Cancer J Clin* (2021) 70(1):7–33. doi: 10.3322/caac.21654
2. Isola AL, Eddy K, Chen S. Biology, Therapy and Implications of Tumor Exosomes in the Progression of Melanoma. *Cancers (Basel)* (2016) 8 (12):110. doi: 10.3390/cancers8120110
3. Matthews NH, Li WQ, Qureshi AA, Weinstock MA, Cho E. "Epidemiology of Melanoma". In: WH Ward and JM Farma, editors. *Cutaneous Melanoma: Etiology and Therapy*. Brisbane (AU: Codon Publications (2017). The Authors.
4. White LP. Studies on Melanoma. *N Engl J Med* (1959) 260(16):789–97. doi: 10.1056/nejm195904162601601
5. Scoggins CR, Ross MI, Reintgen DS, Noyes RD, Goydos JS, Beitsch PD, et al. Gender-related differences in outcome for melanoma patients. *Ann Surg* (2006) 243(5):693–8; discussion 8-700. doi: 10.1097/01.sla.0000216771.81362.6b
6. Shain AH, Bastian BC. From melanocytes to melanomas. *Nat Rev Cancer* (2016) 16(6):345–58. doi: 10.1038/nrc.2016.37
7. Holly EA, Kelly JW, Shpall SN, Chiu S-H. Number of melanocytic nevi as a major risk factor for malignant melanoma. *J Am Acad Dermatol* (1987) 17 (3):459–68. doi: 10.1016/S0190-9622(87)70230-8
8. Alexandrov LB, Nik-Zainal S, Wedge DC, Aparicio SA, Behjati S, Biankin AV, et al. Signatures of mutational processes in human cancer. *Nature* (2013) 500(7463):415–21. doi: 10.1038/nature12477
9. Ford D, Bliss JM, Swerdlow AJ, Armstrong BK, Franceschi S, Green A, et al. Risk of cutaneous melanoma associated with a family history of the disease. The International Melanoma Analysis Group (IMAGE). *Int J Cancer* (1995) 62(4):377–81. doi: 10.1002/ijc.2910620403
10. Soufir N, Avril M-F, Chompret A, Demenais F, Bombled J, Spatz A, et al. Prevalence of p16 and CDK4 Germline Mutations in 48 Melanoma-Prone Families in France. *Hum Mol Genet* (1998) 7(2):209–16. doi: 10.1093/hmg/7.2.209
11. Puntervoll HE, Yang XR, Vetti HH, Bachmann IM, Avril MF, Benfodda M, et al. Melanoma prone families with CDK4 germline mutation: phenotypic profile and associations with MC1R variants. *J Med Genet* (2013) 50(4):264–70. doi: 10.1136/jmedgenet-2012-101455
12. Hussussian CJ, Struewing JP, Goldstein AM, Higgins PA, Ally DS, Sheahan MD, et al. Germline p16 mutations in familial melanoma. *Nat Genet* (1994) 8(1):15–21. doi: 10.1038/ng0994-15
13. Zuo L, Weger J, Yang Q, Goldstein AM, Tucker MA, Walker GJ, et al. Germline mutations in the p16INK4a binding domain of CDK4 in familial melanoma. *Nat Genet* (1996) 12(1):97–9. doi: 10.1038/ng0196-97
14. Kamb A, Shattuck-Eidens D, Eeles R, Liu Q, Gruis NA, Ding W, et al. Analysis of the p16 gene (CDKN2) as a candidate for the chromosome 9p melanoma susceptibility locus. *Nat Genet* (1994) 8(1):22–6. doi: 10.1038/ng0994-22
15. Molven A, Grimstvedt MB, Steine SJ, Harland M, Avril M-F, Hayward NK, et al. A large Norwegian family with inherited malignant melanoma, multiple atypical nevi, and CDK4 mutation. *Genes Chromosomes Cancer* (2005) 44(1):10–8. doi: 10.1002/gcc.20202
16. Tagliabue E, Gandini S, Bellocco R, Maisonneuve P, Newton-Bishop J, Polsky D, et al. MC1R variants as melanoma risk factors independent of at-risk phenotypic characteristics: a pooled analysis from the M-SKIP project. *Cancer Manag Res* (2018) 10:1143–54. doi: 10.2147/cmar.S155283
17. Black JO. Xeroderma Pigmentosum. *Head Neck Pathol* (2016) 10(2):139–44. doi: 10.1007/s12105-016-0707-8
18. Daniel Jensen J, Elewski BE. The ABCDEF Rule: Combining the "ABCDE Rule" and the "Ugly Duckling Sign" in an Effort to Improve Patient Self-Screening Examinations. *J Clin Aesthet Dermatol* (2015) 8(2):15.
19. Holmes GA, Vassantachart JM, Limone BA, Zumwalt M, Hirokane J, Jacob SE. Using Dermoscopy to Identify Melanoma and Improve Diagnostic Discrimination. *Fed Pract* (2018) 35(Suppl 4):S39–45.
20. Sonthalia S, Kaliyadan F. *Dermoscopy Overview and Extradiagnostic Applications*. *StatPearls*. Treasure Island (FL: StatPearls Publishing Copyright © 2020, StatPearls Publishing LLC (2020).
21. Gershenwald JE, Scolyer RA, Hess KR, Sondak VK, Long GV, Ross MI, et al. Melanoma staging: Evidence-based changes in the American Joint Committee on Cancer eighth edition cancer staging manual. *CA Cancer J Clin* (2017) 67(6):472–92. doi: 10.3322/caac.21409
22. Damsky WE, Rosenbaum LE, Bosenberg M. Decoding melanoma metastasis. *Cancers (Basel)* (2010) 3(1):126–63. doi: 10.3390/cancers 3010126
23. Lawrence MS, Stojanov P, Polak P, Kryukov GV, Cibulskis K, Sivachenko A, et al. Mutational heterogeneity in cancer and the search for new cancer-associated genes. *Nature* (2013) 499(7457):214–8. doi: 10.1038/nature12213
24. Vogelstein B, Kinzler KW. The Path to Cancer –Three Strikes and You're Out. *N Engl J Med* (2015) 373(20):1895–8. doi: 10.1056/NEJMp1508811

25. Shain AH, Yeh I, Kovalyshyn I, Sriharan A, Talevich E, Gagnon A, et al. The Genetic Evolution of Melanoma from Precursor Lesions. *N Engl J Med* (2015) 373(20):1926–36. doi: 10.1056/NEJMoa1502583
26. Sensi M, Nicolini G, Petti C, Bersani I, Lozupone F, Molla A, et al. Mutually exclusive NRASQ61R and BRAFV600E mutations at the single-cell level in the same human melanoma. *Oncogene* (2006) 25(24):3357–64. doi: 10.1038/sj.onc.1209379
27. Poynter JN, Elder JT, Fullen DR, Nair RP, Soengas MS, Johnson TM, et al. BRAF and NRAS mutations in melanoma and melanocytic nevi. *Melanoma Res* (2006) 16(4):267–73. doi: 10.1097/01.cmr.0000222600.73179.f3
28. Pollock PM, Harper UL, Hansen KS, Yudt LM, Stark M, Robbins CM, et al. High frequency of BRAF mutations in nevi. *Nat Genet* (2003) 33(1):19–20. doi: 10.1038/ng1054
29. Bauer J, Curtin JA, Pinkel D, Bastian BC. Congenital melanocytic nevi frequently harbor NRAS mutations but no BRAF mutations. *J Invest Dermatol* (2007) 127(1):179–82. doi: 10.1038/sj.jid.5700490
30. Martins da Silva V, Martinez-Barrios E, Tell-Martí G, Dabad M, Carrera C, Aguilera P, et al. Genetic Abnormalities in Large to Giant Congenital Nevi: Beyond NRAS Mutations. *J Invest Dermatol* (2019) 139(4):900–8. doi: 10.1016/j.jid.2018.07.045
31. Chiba K, Lorbeer FK, Shain AH, McSwiggen DT, Schruf E, Oh A, et al. Mutations in the promoter of the telomerase gene TERT contribute to tumorigenesis by a two-step mechanism. *Science* (2017) 357(6358):1416–20. doi: 10.1126/science.aao0535
32. Shitara D, Nascimento MM, Puig S, Yamada S, Enokihara MM, Michalany N, et al. Nevus-associated melanomas: clinicopathologic features. *Am J Clin Pathol* (2014) 142(4):485–91. doi: 10.1309/ajcp4l5cjgktjvdd
33. Elder DE, Bastian BC, Cree IA, Massi D, Scolyer RA. The 2018 World Health Organization Classification of Cutaneous, Mucosal, and Uveal Melanoma: Detailed Analysis of 9 Distinct Subtypes Defined by Their Evolutionary Pathway. *Arch Pathol Lab Med* (2020) 144(4):500–22. doi: 10.5858/arpa.2019-0561-RA
34. Monteiro AC, Toricelli M, Jasiulionis MG. "Signaling Pathways Altered During the Metastatic Progression of Melanoma. (April 1st 2015". In: . *Melanoma - Current Clinical Management and Future Therapeutics [Internet]* (2015). Available at: https://www.intechopen.com/books/melanoma-current-clinical-management-and-future-therapeutics/signaling-pathways-altered-during-the-metastatic-progression-of-melanoma.
35. Lopez-Bergami P, Fitchman B, Ronai Z. Understanding signaling cascades in melanoma. *Photochem Photobiol* (2008) 84(2):289–306. doi: 10.1111/j.1751-1097.2007.00254.x
36. McCubrey JA, Steelman LS, Chappell WH, Abrams SL, Franklin RA, Montalto G, et al. Ras/Raf/MEK/ERK and PI3K/PTEN/Akt/mTOR cascade inhibitors: how mutations can result in therapy resistance and how to overcome resistance. *Oncotarget* (2012) 3(10):1068–111. doi: 10.18632/oncotarget.659
37. Shah K, Patel S, Mirza S, Rawal RM. Unravelling the link between embryogenesis and cancer metastasis. *Gene* (2018) 642:447–52. doi: 10.1016/j.gene.2017.11.056
38. Manzo G. Similarities Between Embryo Development and Cancer Process Suggest New Strategies for Research and Therapy of Tumors: A New Point of View. *Front Cell Dev Biol* (2019) 7:20. doi: 10.3389/fcell.2019.00020
39. Huntington JT, Shields JM, Der CJ, Wyatt CA, Benbow U, Slingluff CLJr., et al. Overexpression of collagenase 1 (MMP-1) is mediated by the ERK pathway in invasive melanoma cells: role of BRAF mutation and fibroblast growth factor signaling. *J Biol Chem* (2004) 279(32):33168–76. doi: 10.1074/jbc.M405102200
40. Lee KR, Lee JS, Kim YR, Song IG, Hong EK. Polysaccharide from Inonotus obliquus inhibits migration and invasion in B16-F10 cells by suppressing MMP-2 and MMP-9 via downregulation of NF-κB signaling pathway. *Oncol Rep* (2014) 31(5):2447–53. doi: 10.3892/or.2014.3103
41. Yao X, Jiang W, Yu D, Yan Z. Luteolin inhibits proliferation and induces apoptosis of human melanoma cells in vivo and in vitro by suppressing MMP-2 and MMP-9 through the PI3K/AKT pathway. *Food Funct* (2019) 10(2):703–12. doi: 10.1039/c8fo02013b
42. Hess AR, Seftor EA, Seftor RE, Hendrix MJ. Phosphoinositide 3-kinase regulates membrane Type 1-matrix metalloproteinase (MMP) and MMP-2 activity during melanoma cell vasculogenic mimicry. *Cancer Res* (2003) 63(16):4757–62.
43. Hofmann UB, Westphal JR, Waas ET, Zendman AJ, Cornelissen IM, Ruiter DJ, et al. Matrix metalloproteinases in human melanoma cell lines and xenografts: increased expression of activated matrix metalloproteinase-2 (MMP-2) correlates with melanoma progression. *Br J Cancer* (1999) 81(5):774–82. doi: 10.1038/sj.bjc.6690763
44. Hofmann UB, Westphal JR, Zendman AJ, Becker JC, Ruiter DJ, van Muijen GN. Expression and activation of matrix metalloproteinase-2 (MMP-2) and its co-localization with membrane-type 1 matrix metalloproteinase (MT1-MMP) correlate with melanoma progression. *J Pathol* (2000) 191(3):245–56. doi: 10.1002/1096-9896(2000)9999:9999<::Aid-path632>3.0.Co;2-
45. Löffek S, Zigrino P, Angel P, Anwald B, Krieg T, Mauch C. High invasive melanoma cells induce matrix metalloproteinase-1 synthesis in fibroblasts by interleukin-1alpha and basic fibroblast growth factor-mediated mechanisms. *J Invest Dermatol* (2005) 124(3):638–43. doi: 10.1111/j.0022-202X.2005.23629.x
46. Ntayi C, Hornebeck W, Bernard P. Influence of cultured dermal fibroblasts on human melanoma cell proliferation, matrix metalloproteinase-2 (MMP-2) expression and invasion in vitro. *Arch Dermatol Res* (2003) 295(6):236–41. doi: 10.1007/s00403-003-0429-0
47. Moore-Smith LD, Isayeva T, Lee JH, Frost A, Ponnazhagan S. Silencing of TGF-β1 in tumor cells impacts MMP-9 in tumor microenvironment. *Sci Rep* (2017) 7(1):8678. doi: 10.1038/s41598-017-09062-y
48. Paluncic J, Kovacevic Z, Jansson PJ, Kalinowski D, Merlot AM, Huang ML, et al. Roads to melanoma: Key pathways and emerging players in melanoma progression and oncogenic signaling. *Biochim Biophys Acta* (2016) 1863(4):770–84. doi: 10.1016/j.bbamcr.2016.01.025
49. Tucci MG, Lucarini G, Brancorsini D, Zizzi A, Pugnaloni A, Giacchetti A, et al. Involvement of E-cadherin, beta-catenin, Cdc42 and CXCR4 in the progression and prognosis of cutaneous melanoma. *Br J Dermatol* (2007) 157(6):1212–6. doi: 10.1111/j.1365-2133.2007.08246.x
50. Hsu MY, Wheelock MJ, Johnson KR, Herlyn M. Shifts in cadherin profiles between human normal melanocytes and melanomas. *J Invest Dermatol Symp Proc* (1996) 1(2):188–94.
51. Seftor RE, Seftor EA, Hendrix MJ. Molecular role(s) for integrins in human melanoma invasion. *Cancer Metastasis Rev* (1999) 18(3):359–75. doi: 10.1023/a:1006317125454
52. Kim JE, Finlay GJ, Baguley BC. The role of the hippo pathway in melanocytes and melanoma. *Front Oncol* (2013) 3:123. doi: 10.3389/fonc.2013.00123
53. Tang A, Eller MS, Hara M, Yaar M, Hirohashi S, Gilchrest BA. E-cadherin is the major mediator of human melanocyte adhesion to keratinocytes in vitro. *J Cell Sci* (1994) 107(Pt 4):983–92.
54. McGary EC, Lev DC, Bar-Eli M. Cellular adhesion pathways and metastatic potential of human melanoma. *Cancer Biol Ther* (2002) 1(5):459–65. doi: 10.4161/cbt.1.5.158
55. Lade-Keller J, Riber-Hansen R, Guldberg P, Schmidt H, Hamilton-Dutoit SJ. Steiniche T. E- to N-cadherin switch in melanoma is associated with decreased expression of phosphatase and tensin homolog and cancer progression. *Br J Dermatol* (2013) 169(3):618–28. doi: 10.1111/bjd.12426
56. Hao L, Ha JR, Kuzel P, Garcia E, Persad S. Cadherin switch from E- to N-cadherin in melanoma progression is regulated by the PI3K/PTEN pathway through Twist and Snail. *Br J Dermatol* (2012) 166(6):1184–97. doi: 10.1111/j.1365-2133.2012.10824.x
57. Kumar CC, Malkowski M, Yin Z, Tanghetti E, Yaremko B, Nechuta T, et al. Inhibition of angiogenesis and tumor growth by SCH221153, a dual alpha(v) beta3 and alpha(v)beta5 integrin receptor antagonist. *Cancer Res* (2001) 61(5):2232–8.
58. Jiao Y, Feng X, Zhan Y, Wang R, Zheng S, Liu W, et al. Matrix metalloproteinase-2 promotes αvβ3 integrin-mediated adhesion and migration of human melanoma cells by cleaving fibronectin. *PLoS One* (2012) 7(7):e41591. doi: 10.1371/journal.pone.0041591
59. Das A, Monteiro M, Barai A, Kumar S, Sen S. MMP proteolytic activity regulates cancer invasiveness by modulating integrins. *Sci Rep* (2017) 7(1):14219. doi: 10.1038/s41598-017-14340-w
60. Hurst DR, Edmonds MD, Welch DR. Metastamir: the field of metastasis-regulatory microRNA is spreading. *Cancer Res* (2009) 69(19):7495–8. doi: 10.1158/0008-5472.Can-09-2111

61. Tucci M, Passarelli A, Mannavola F, Felici C, Stucci LS, Cives M, et al. Immune System Evasion as Hallmark of Melanoma Progression: The Role of Dendritic Cells. *Front Oncol* (2019) 9:1148. doi: 10.3389/fonc.2019.01148
62. Escors D. Tumour immunogenicity, antigen presentation and immunological barriers in cancer immunotherapy. *New J Sci* (2014) 2014. doi: 10.1155/2014/734515
63. Brown M, Assen FP, Leithner A, Abe J, Schachner H, Asfour G, et al. Lymph node blood vessels provide exit routes for metastatic tumor cell dissemination in mice. *Science* (2018) 359(6382):1408–11. doi: 10.1126/science.aal3662
64. Ubellacker JM, Tasdogan A, Ramesh V, Shen B, Mitchell EC, Martin-Sandoval MS, et al. Lymph protects metastasizing melanoma cells from ferroptosis. *Nature* (2020) 585(7823):113–8. doi: 10.1038/s41586-020-2623-z
65. Lund AW, Soengas MS. Lymph: (Fe)rrying Melanoma to Safety. *Cancer Cell* (2020) 38(4):446–8. doi: 10.1016/j.ccell.2020.08.011
66. Poste G, Doll J, Brown AE, Tzeng J, Zeidman I. Comparison of the metastatic properties of B16 melanoma clones isolated from cultured cell lines, subcutaneous tumors, and individual lung metastases. *Cancer Res* (1982) 42(7):2770–8.
67. Stackpole CW. Generation of phenotypic diversity in the B16 mouse melanoma relative to spontaneous metastasis. *Cancer Res* (1983) 43 (7):3057–65.
68. Pollock PM, Cohen-Solal K, Sood R, Namkoong J, Martino JJ, Koganti A, et al. Melanoma mouse model implicates metabotropic glutamate signaling in melanocytic neoplasia. *Nat Genet* (2003) 34(1):108–12. doi: 10.1038/ng1148
69. Chen S, Zhu H, Wetzel WJ, Philbert MA. Spontaneous melanocytosis in transgenic mice. *J Invest Dermatol* (1996) 106(5):1145–51. doi: 10.1111/1523-1747.ep12340194
70. Zhu H, Reuhl K, Zhang X, Botha R, Ryan K, Wei J, et al. Development of heritable melanoma in transgenic mice. *J Invest Dermatol* (1998) 110 (3):247–52. doi: 10.1046/j.1523-1747.1998.00133.x
71. Shin SS, Namkoong J, Wall BA, Gleason R, Lee HJ, Chen S. Oncogenic activities of metabotropic glutamate receptor 1 (Grm1) in melanocyte transformation. *Pigment Cell Melanoma Res* (2008) 21(3):368–78. doi: 10.1111/j.1755-148X.2008.00452.x
72. Schiffner S, Chen S, Becker JC, Bosserhoff AK. Highly pigmented Tg(Grm1) mouse melanoma develops non-pigmented melanoma cells in distant metastases. *Exp Dermatol* (2012) 21(10):786–8. doi: 10.1111/j.1600-0625.2012.01560.x
73. Li X, Karras P, Torres R, Rambow F, van den Oord J, Marine JC, et al. Disseminated Melanoma Cells Transdifferentiate into Endothelial Cells in Intravascular Niches at Metastatic Sites. *Cell Rep* (2020) 31(11):107765. doi: 10.1016/j.celrep.2020.107765
74. Tsuji T, Ibaragi S, Hu GF. Epithelial-mesenchymal transition and cell cooperativity in metastasis. *Cancer Res* (2009) 69(18):7135–9. doi: 10.1158/0008-5472.Can-09-1618
75. Bockhorn M, Jain RK, Munn LL. Active versus passive mechanisms in metastasis: do cancer cells crawl into vessels, or are they pushed? *Lancet Oncol* (2007) 8(5):444–8. doi: 10.1016/s1470-2045(07)70140-7
76. Maniotis AJ, Folberg R, Hess A, Seftor EA, Gardner LM, Pe'er J, et al. Vascular channel formation by human melanoma cells in vivo and in vitro: vasculogenic mimicry. *Am J Pathol* (1999) 155(3):739–52. doi: 10.1016/s0002-9440(10)65173-5
77. Folberg R, Hendrix MJ, Maniotis AJ. Vasculogenic mimicry and tumor angiogenesis. *Am J Pathol* (2000) 156(2):361–81. doi: 10.1016/s0002-9440(10)64739-6
78. Yao D, Dai C, Peng S. Mechanism of the mesenchymal-epithelial transition and its relationship with metastatic tumor formation. *Mol Cancer Res* (2011) 9(12):1608–20. doi: 10.1158/1541-7786.Mcr-10-0568
79. Balch CM, Soong SJ, Bartolucci AA, Urist MM, Karakousis CP, Smith TJ, et al. Efficacy of an elective regional lymph node dissection of 1 to 4 mm thick melanomas for patients 60 years of age and younger. *Ann Surg* (1996) 224(3):255–63; discussion 63-6. doi: 10.1097/00000658-199609000-00002
80. Morton DL, Thompson JF, Cochran AJ, Mozzillo N, Nieweg OE, Roses DF, et al. Final trial report of sentinel-node biopsy versus nodal observation in melanoma. *N Engl J Med* (2014) 370(7):599–609. doi: 10.1056/NEJMoa1310460
81. Reid AL, Millward M, Pearce R, Lee M, Frank MH, Ireland A, et al. Markers of circulating tumour cells in the peripheral blood of patients with melanoma correlate with disease recurrence and progression. *Br J Dermatol* (2013) 168(1):85–92. doi: 10.1111/bjd.12057
82. Carson KF, Wen DR, Li PX, Lana AM, Bailly C, Morton DL, et al. Nodal nevi and cutaneous melanomas. *Am J Surg Pathol* (1996) 20(7):834–40. doi: 10.1097/00000478-199607000-00006
83. Bautista NC, Cohen S, Anders KH. Benign melanocytic nevus cells in axillary lymph nodes. A prospective incidence and immunohistochemical study with literature review. *Am J Clin Pathol* (1994) 102(1):102–8. doi: 10.1093/ajcp/102.1.102
84. Holt JB, Sangueza OP, Levine EA, Shen P, Bergman S, Geisinger KR, et al. Nodal melanocytic nevi in sentinel lymph nodes. Correlation with melanoma-associated cutaneous nevi. *Am J Clin Pathol* (2004) 121(1):58–63. doi: 10.1309/y5qa-d623-mya2-1puy
85. Wanebo HJ, Argiris A, Bergsland E, Agarwala S, Rugo H. Targeting growth factors and angiogenesis; using small molecules in malignancy. *Cancer Metastasis Rev* (2006) 25(2):279–92. doi: 10.1007/s10555-006-8508-2
86. Dvorak HF. Vascular permeability factor/vascular endothelial growth factor: a critical cytokine in tumor angiogenesis and a potential target for diagnosis and therapy. *J Clin Oncol* (2002) 20(21):4368–80. doi: 10.1200/jco.2002.10.088
87. Rofstad EK, Halsør EF. Vascular endothelial growth factor, interleukin 8, platelet-derived endothelial cell growth factor, and basic fibroblast growth factor promote angiogenesis and metastasis in human melanoma xenografts. *Cancer Res* (2000) 60(17):4932–8.
88. Yu JL, Rak JW, Klement G, Kerbel RS. Vascular endothelial growth factor isoform expression as a determinant of blood vessel patterning in human melanoma xenografts. *Cancer Res* (2002) 62(6):1838–46.
89. Huang S, Mills L, Mian B, Tellez C, McCarty M, Yang XD, et al. Fully humanized neutralizing antibodies to interleukin-8 (ABX-IL8) inhibit angiogenesis, tumor growth, and metastasis of human melanoma. *Am J Pathol* (2002) 161(1):125–34. doi: 10.1016/s0002-9440(10)64164-8
90. Brown LF, Detmar M, Claffey K, Nagy JA, Feng D, Dvorak AM, et al. Vascular permeability factor/vascular endothelial growth factor: a multifunctional angiogenic cytokine. *Exs* (1997) 79:233–69. doi: 10.1007/978-3-0348-9006-9_10
91. Ferrara N. Molecular and biological properties of vascular endothelial growth factor. *J Mol Med (Berl)* (1999) 77(7):527–43. doi: 10.1007/s001099900019
92. Bates DO, Hillman NJ, Williams B, Neal CR, Pocock TM. Regulation of microvascular permeability by vascular endothelial growth factors. *J Anat* (2002) 200(6):581–97. doi: 10.1046/j.1469-7580.2002.00066.x
93. Kerbel RS. Inhibition of tumor angiogenesis as a strategy to circumvent acquired resistance to anti-cancer therapeutic agents. *BioEssays News Rev Mol Cell Dev Biol* (1991) 13(1):31–6. doi: 10.1002/bies.950130106
94. Folkman J. Angiogenesis and angiogenesis inhibition: an overview. *Exs* (1997) 79:1–8. doi: 10.1007/978-3-0348-9006-9_1
95. Robert EG, Hunt JD. Lipid messengers as targets for antiangiogenic therapy. *Curr Pharm Des* (2001) 7(16):1615–26. doi: 10.2174/1381612013397203
96. Oku T, Tjuvajev JG, Miyagawa T, Sasajima T, Joshi A, Joshi R, et al. Tumor growth modulation by sense and antisense vascular endothelial growth factor gene expression: effects on angiogenesis, vascular permeability, blood volume, blood flow, fluorodeoxyglucose uptake, and proliferation of human melanoma intracerebral xenografts. *Cancer Res* (1998) 58(18):4185–92.
97. Fathi Maroufi N, Taefehshokr S, Rashidi MR, Taefehshokr N, Khoshakhlagh M, Isazadeh A, et al. Vascular mimicry: changing the therapeutic paradigms in cancer. *Mol Biol Rep* (2020) 47(6):4749–65. doi: 10.1007/s11033-020-05515-2
98. Felcht M, Thomas M. Angiogenesis in malignant melanoma. *J Der Deutschen Dermatol Gesellschaft J German Soc Dermatol JDDG* (2015) 13 (2):125–36. doi: 10.1111/ddg.12580
99. Hood JL, San RS, Wickline SA. Exosomes released by melanoma cells prepare sentinel lymph nodes for tumor metastasis. *Cancer Res* (2011) 71 (11):3792–801. doi: 10.1158/0008-5472.Can-10-4455
100. Hu L, Wickline SA, Hood JL. Magnetic resonance imaging of melanoma exosomes in lymph nodes. *Magn Reson Med* (2015) 74(1):266–71. doi: 10.1002/mrm.25376
101. Düchler M, Czernek L, Peczek L, Cypryk W, Sztiller-Sikorska M, Czyz M. Melanoma-Derived Extracellular Vesicles Bear the Potential for the

Induction of Antigen-Specific Tolerance. *Cells* (2019) 8(7):665. doi: 10.3390/cells8070665
102. Gerloff D, Lützkendorf J, Moritz RKC, Wersig T, Mäder K, Müller LP, et al. Melanoma-Derived Exosomal miR-125b-5p Educates Tumor Associated Macrophages (TAMs) by Targeting Lysosomal Acid Lipase A (LIPA). *Cancers (Basel)* (2020) 12(2):464. doi: 10.3390/cancers12020464
103. Xiang X, Poliakov A, Liu C, Liu Y, Deng ZB, Wang J, et al. Induction of myeloid-derived suppressor cells by tumor exosomes. *Int J Cancer* (2009) 124(11):2621–33. doi: 10.1002/ijc.24249
104. Peinado H, Alečković M, Lavotshkin S, Matei I, Costa-Silva B, Moreno-Bueno G, et al. Melanoma exosomes educate bone marrow progenitor cells toward a pro-metastatic phenotype through MET. *Nat Med* (2012) 18 (6):883–91. doi: 10.1038/nm.2753
105. Chow A, Zhou W, Liu L, Fong MY, Champer J, Van Haute D, et al. Macrophage immunomodulation by breast cancer-derived exosomes requires Toll-like receptor 2-mediated activation of NF-κB. *Sci Rep* (2014) 4:5750. doi: 10.1038/srep05750
106. Sharma P, Diergaarde B, Ferrone S, Kirkwood JM, Whiteside TL. Melanoma cell-derived exosomes in plasma of melanoma patients suppress functions of immune effector cells. *Sci Rep* (2020) 10(1):92. doi: 10.1038/s41598-019-56542-4
107. Chen G, Huang AC, Zhang W, Zhang G, Wu M, Xu W, et al. Exosomal PD-L1 contributes to immunosuppression and is associated with anti-PD-1 response. *Nature* (2018) 560(7718):382–6. doi: 10.1038/s41586-018-0392-8
108. Poggio M, Hu T, Pai CC, Chu B, Belair CD, Chang A, et al. Suppression of Exosomal PD-L1 Induces Systemic Anti-tumor Immunity and Memory. *Cell* (2019) 177(2):414–27.e13. doi: 10.1016/j.cell.2019.02.016
109. Erler JT, Bennewith KL, Cox TR, Lang G, Bird D, Koong A, et al. Hypoxia-induced lysyl oxidase is a critical mediator of bone marrow cell recruitment to form the premetastatic niche. *Cancer Cell* (2009) 15(1):35–44. doi: 10.1016/j.ccr.2008.11.012
110. Costa-Silva B, Aiello NM, Ocean AJ, Singh S, Zhang H, Thakur BK, et al. Pancreatic cancer exosomes initiate pre-metastatic niche formation in the liver. *Nat Cell Biol* (2015) 17(6):816–26. doi: 10.1038/ncb3169
111. Morishita M, Takahashi Y, Nishikawa M, Sano K, Kato K, Yamashita T, et al. Quantitative analysis of tissue distribution of the B16BL6-derived exosomes using a streptavidin-lactadherin fusion protein and iodine-125-labeled biotin derivative after intravenous injection in mice. *J Pharm Sci* (2015) 104(2):705–13. doi: 10.1002/jps.24251
112. Takahashi Y, Nishikawa M, Shinotsuka H, Matsui Y, Ohara S, Imai T, et al. Visualization and in vivo tracking of the exosomes of murine melanoma B16-BL6 cells in mice after intravenous injection. *J Biotechnol* (2013) 165 (2):77–84. doi: 10.1016/j.jbiotec.2013.03.013
113. Paget S. The distribution of secondary growths in cancer of the breast. 1889. *Cancer Metastasis Rev* (1989) 8(2):98–101.
114. Isola AL, Eddy K, Zembrzuski K, Goydos JS, Chen S. Exosomes released by metabotropic glutamate receptor 1 (GRM1) expressing melanoma cells increase cell migration and invasiveness. *Oncotarget* (2017) 9(1):1187–99. doi: 10.18632/oncotarget.23455
115. Vereecken P, Cornelis F, Van Baren N, Vandersleyen V, Baurain JF. A synopsis of serum biomarkers in cutaneous melanoma patients. *Dermatol Res Pract* (2012) 2012:260643. doi: 10.1155/2012/260643
116. Tachibana M, Takeda K, Nobukuni Y, Urabe K, Long JE, Meyers KA, et al. Ectopic expression of MITF, a gene for Waardenburg syndrome type 2, converts fibroblasts to cells with melanocyte characteristics. *Nat Genet* (1996) 14(1):50–4. doi: 10.1038/ng0996-50
117. Levy C, Khaled M, Fisher DE. MITF: master regulator of melanocyte development and melanoma oncogene. *Trends Mol Med* (2006) 12(9):406–14. doi: 10.1016/j.molmed.2006.07.008
118. Garraway LA, Widlund HR, Rubin MA, Getz G, Berger AJ, Ramaswamy S, et al. Integrative genomic analyses identify MITF as a lineage survival oncogene amplified in malignant melanoma. *Nature* (2005a) 436 (7047):117–22. doi: 10.1038/nature03664
119. Loercher AE, Tank EMH, Delston RB, Harbour JW. MITF links differentiation with cell cycle arrest in melanocytes by transcriptional activation of INK4A. *J Cell Biol* (2005) 168(1):35–40. doi: 10.1083/jcb.200410115
120. Dorvault CC, Weilbaecher KN, Yee H, Fisher DE, Chiriboga LA, Xu Y, et al. Microphthalmia transcription factor: a sensitive and specific marker for malignant melanoma in cytologic specimens. *Cancer* (2001) 93(5):337–43. doi: 10.1002/cncr.9049
121. King R, Weilbaecher KN, McGill G, Cooley E, Mihm M, Fisher DE. Microphthalmia transcription factor. A sensitive and specific melanocyte marker for MelanomaDiagnosis. *Am J Pathol* (1999) 155(3):731–8. doi: 10.1016/s0002-9440(10)65172-3
122. Miettinen M, Fernandez M, Franssila K, Gatalica Z, Lasota J, Sarlomo-Rikala M. Microphthalmia transcription factor in the immunohistochemical diagnosis of metastatic melanoma: comparison with four other melanoma markers. *Am J Surg Pathol* (2001) 25(2):205–11. doi: 10.1097/00000478-200102000-00008
123. Weinstein D, Leininger J, Hamby C, Safai B. Diagnostic and prognostic biomarkers in melanoma. *J Clin Aesthetic Dermatol* (2014) 7(6):13–24.
124. Balch CM, Buzaid AC, Soong SJ, Atkins MB, Cascinelli N, Coit DG, et al. Final version of the American Joint Committee on Cancer staging system for cutaneous melanoma. *J Clin Oncol* (2001) 19(16):3635–48. doi: 10.1200/JCO.2001.19.16.3635
125. Vander Heiden MG, Cantley LC, Thompson CB. Understanding the Warburg Effect: The Metabolic Requirements of Cell Proliferation. *Science (New York NY)* (2009) 324(5930):1029–33. doi: 10.1126/science.1160809
126. Lunt SY, Heiden MGV. Aerobic Glycolysis: Meeting the Metabolic Requirements of Cell Proliferation. *Annu Rev Cell Dev Biol* (2011) 27 (1):441–64. doi: 10.1146/annurev-cellbio-092910-154237
127. Gray MR, SMd C, Zhang X, Zhang H, FF S, WEC III, et al. Metastatic Melanoma: Lactate Dehydrogenase Levels and CT Imaging Findings of Tumor Devascularization Allow Accurate Prediction of Survival in Patients Treated with Bevacizumab. *Radiology* (2014) 270(2):425–34. doi: 10.1148/radiol.13130776
128. Uslu U, Schliep S, Schliep K, Erdmann M, Koch HU, Parsch H, et al. Comparison of the Serum Tumor Markers S100 and Melanoma-inhibitory Activity (MIA) in the Monitoring of Patients with Metastatic Melanoma Receiving Vaccination Immunotherapy with Dendritic Cells. *Anticancer Res* (2017) 37(9):5033–7. doi: 10.21873/anticanres.11918
129. Logozzi M, De Milito A, Lugini L, Borghi M, Calabrò L, Spada M, et al. High levels of exosomes expressing CD63 and caveolin-1 in plasma of melanoma patients. *PLoS One* (2009) 4(4):e5219. doi: 10.1371/journal.pone.0005219
130. Alegre E, Zubiri L, Perez-Gracia JL, González-Cao M, Soria L, Martín-Algarra S, et al. Circulating melanoma exosomes as diagnostic and prognosis biomarkers. *Clin Chim Acta* (2016) 454:28–32. doi: 10.1016/j.cca.2015.12.031
131. Melo SA, Sugimoto H, O'Connell JT, Kato N, Villanueva A, Vidal A, et al. Cancer exosomes perform cell-independent microRNA biogenesis and promote tumorigenesis. *Cancer Cell* (2014) 26(5):707–21. doi: 10.1016/j.ccell.2014.09.005
132. Melo SA, Luecke LB, Kahlert C, Fernandez AF, Gammon ST, Kaye J, et al. Glypican-1 identifies cancer exosomes and detects early pancreatic cancer. *Nature* (2015) 523(7559):177–82. doi: 10.1038/nature14581
133. Zebrowska A, Widlak P, Whiteside T, Pietrowska M. Signaling of Tumor-Derived sEV Impacts Melanoma Progression. *Int J Mol Sci* (2020) 21 (14):5066. doi: 10.3390/ijms21145066
134. Group F-NBW. *Understanding Prognostic versus Predictive Biomarkers*. F Adminstration, editor. Silver Spring (MD): National Institutes of Health (2016).
135. Sabel MS, Liu Y, Lubman DM. Proteomics in Melanoma Biomarker Discovery: Great Potential, Many Obstacles. *Int J Proteomics* (2011) 2011:181890. doi: 10.1155/2011/181890
136. Karasarides M, Chiloeches A, Hayward R, Niculescu-Duvaz D, Scanlon I, Friedlos F, et al. B-RAF is a therapeutic target in melanoma. *Oncogene* (2004) 23(37):6292–8. doi: 10.1038/sj.onc.1207785
137. Eisen T, Ahmad T, Flaherty KT, Gore M, Kaye S, Marais R, et al. Sorafenib in advanced melanoma: a Phase II randomised discontinuation trial analysis. *Br J Cancer* (2006) 95(5):581–6. doi: 10.1038/sj.bjc.6603291
138. Bucheit AD, Davies MA. Emerging insights into resistance to BRAF inhibitors in melanoma. *Biochem Pharmacol* (2014) 87:381–9. doi: 10.1016/j.bcp.2013.11.013
139. Johnson DB, Sosman JA. Therapeutic Advances and Treatment Options in Metastatic Melanoma. *JAMA Oncol* (2015) 1(3):380–6. doi: 10.1001/jamaoncol.2015.0565. doi: 2276102 [pii].
140. Bollag G, Hirth P, Tsai J, Zhang J, Ibrahim PN, Cho H, et al. Clinical efficacy of a RAF inhibitor needs broad target blockade in BRAF-mutant melanoma. *Nature* (2010) 467(7315):596–9. doi: 10.1038/nature09454

141. Flaherty KT, Puzanov I, Kim KB, Ribas A, McArthur GA, Sosman JA, et al. Inhibition of mutated, activated BRAF in metastatic melanoma. *N Engl J Med* (2010) 363(9):809–19. doi: 10.1056/NEJMoa1002011
142. Teh JL, Chen S. Glutamatergic signaling in cellular transformation. *Pigment Cell Melanoma Res* (2012) 25(3):331–42. doi: 10.1111/j.1755-148X.2012.00983.x
143. Siegel RL, Miller KD, Jemal A. Cancer statistics, 2016. *CA: A Cancer J Clin* (2016) 66(1):7–30. doi: 10.3322/caac.21332
144. Chapman PB, Hauschild A, Robert C, Haanen JB, Ascierto P, Larkin J, et al. Improved survival with vemurafenib in melanoma with BRAF V600E mutation. *N Engl J Med* (2011) 364(26):2507–16. doi: 10.1056/NEJMoa1103782
145. Beloueche-Babari M, Jamin Y, Arunan V, Walker-Samuel S, Revill M, Smith PD, et al. Acute tumour response to the MEK1/2 inhibitor selumetinib (AZD6244, ARRY-142886) evaluated by non-invasive diffusion-weighted MRI. *Br J Cancer* (2013) 109(6):1562–9. doi: 10.1038/bjc.2013.456
146. Hatzivassiliou G, Song K, Yen I, Brandhuber BJ, Anderson DJ, Alvarado R, et al. RAF inhibitors prime wild-type RAF to activate the MAPK pathway and enhance growth. *Nature* (7287) 2010) 464:431–5. doi: 10.1038/nature08833. doi: nature08833 [pii].
147. Baines AT, Xu D, Der CJ. Inhibition of Ras for cancer treatment: the search continues. *Future Med Chem* (2011) 3(14):1787–808. doi: 10.4155/fmc.11.121
148. Christensen JG, Hallin J, Engstrom LD, Hargis L, Calinisan A, Aranda R, et al. The KRASG12C Inhibitor, MRTX849, Provides Insight Toward Therapeutic Susceptibility of KRAS Mutant Cancers in Mouse Models and Patients. *Cancer Discov* (2019) 10(1):CD–19-1167. doi: 10.1158/2159-8290.Cd-19-1167
149. Milagre C, Dhomen N, Geyer FC, Hayward R, Lambros M, Reis-Filho JS, et al. A mouse model of melanoma driven by oncogenic KRAS. *Cancer Res* (2010) 70(13):5549–57. doi: 10.1158/0008-5472.Can-09-4254
150. Haanen JBAG. Immunotherapy of melanoma. *EJC Suppl* (2013) 11(2):97–105. doi: 10.1016/j.ejcsup.2013.07.013
151. Green J, Ariyan C. Update on immunotherapy in melanoma. *Surg Oncol Clin N Am* (2015) 24(2):337–46. doi: 10.1016/j.soc.2014.12.010
152. Ribas A, Wolchok JD. Cancer immunotherapy using checkpoint blockade. *Science* (2018) 359(6382):1350–5. doi: 10.1126/science.aar4060
153. Eddy K, Chen S. Overcoming Immune Evasion in Melanoma. *Int J Mol Sci* (2020) 21(23):8984. doi: 10.3390/ijms21238984
154. Bommareddy PK, Shettigar M, Kaufman HL. Integrating oncolytic viruses in combination cancer immunotherapy. *Nat Rev Immunol* (2018) 18(8):498–513. doi: 10.1038/s41577-018-0014-6
155. Waldman AD, Fritz JM, Lenardo MJ. A guide to cancer immunotherapy: from T cell basic science to clinical practice. *Nat Rev Immunol* (2020) 20:1–18. doi: 10.1038/s41577-020-0306-5
156. Nishimura H, Okazaki T, Tanaka Y, Nakatani K, Hara M, Matsumori A, et al. Autoimmune dilated cardiomyopathy in PD-1 receptor-deficient mice. *Science* (2001) 291(5502):319–22. doi: 10.1126/science.291.5502.319
157. Nishimura H, Nose M, Hiai H, Minato N, Honjo T. Development of lupus-like autoimmune diseases by disruption of the PD-1 gene encoding an ITIM motif-carrying immunoreceptor. *Immunity* (1999) 11(2):141–51. doi: 10.1016/s1074-7613(00)80089-8
158. Klocke K, Sakaguchi S, Holmdahl R, Wing K. Induction of autoimmune disease by deletion of CTLA-4 in mice in adulthood. *Proc Natl Acad Sci U S A* (2016) 113(17):E2383–92. doi: 10.1073/pnas.1603892113
159. Waterhouse P, Penninger JM, Timms E, Wakeham A, Shahinian A, Lee KP, et al. Lymphoproliferative disorders with early lethality in mice deficient in Ctla-4. *Science* (1995) 270(5238):985–8. doi: 10.1126/science.270.5238.985
160. Tivol EA, Borriello F, Schweitzer AN, Lynch WP, Bluestone JA, Sharpe AH. Loss of CTLA-4 leads to massive lymphoproliferation and fatal multiorgan tissue destruction, revealing a critical negative regulatory role of CTLA-4. *Immunity* (1995) 3(5):541–7. doi: 10.1016/1074-7613(95)90125-6
161. Latchman YE, Liang SC, Wu Y, Chernova T, Sobel RA, Klemm M, et al. PD-L1-deficient mice show that PD-L1 on T cells, antigen-presenting cells, and host tissues negatively regulates T cells. *Proc Natl Acad Sci U S A* (2004) 101(29):10691–6. doi: 10.1073/pnas.0307252101
162. Ribas A, Shin DS, Zaretsky J, Frederiksen J, Cornish A, Avramis E, et al. PD-1 blockade expands intratumoral T memory cells. *Cancer Immunol Res* (2016) 4(3):194–203. doi: 10.1158/2326-6066.CIR-15-0210
163. Guntermann C, Alexander DR. CTLA-4 suppresses proximal TCR signaling in resting human CD4(+) T cells by inhibiting ZAP-70 Tyr(319) phosphorylation: a potential role for tyrosine phosphatases. *J Immunol* (2002) 168(9):4420–9. doi: 10.4049/jimmunol.168.9.4420
164. Chambers CA, Kuhns MS, Egen JG, Allison JP. CTLA-4-mediated inhibition in regulation of T cell responses: mechanisms and manipulation in tumor immunotherapy. *Annu Rev Immunol* (2001) 19:565–94. doi: 10.1146/annurev.immunol.19.1.565
165. Dammeijer F, van Gulijk M, Mulder EE, Lukkes M, Klaase L, van den Bosch T, et al. The PD-1/PD-L1-Checkpoint Restrains T cell Immunity in Tumor-Draining Lymph Nodes. *Cancer Cell* (2020) 38(35):685–700. doi: 10.1016/j.ccell.2020.09.001
166. Hodi FS, O'Day SJ, McDermott DF, Weber RW, Sosman JA, Haanen JB, et al. Improved survival with ipilimumab in patients with metastatic melanoma. *N Engl J Med* (2010) 363(8):711–23. doi: 10.1056/NEJMoa1003466. doi: NEJMoa1003466 [pii].
167. Eroglu Z, Kim DW, Wang X, Camacho LH, Chmielowski B, Seja E, et al. Long term survival with cytotoxic T lymphocyte-associated antigen 4 blockade using tremelimumab. *Eur J Cancer* (2015) 51(17):2689–97. doi: 10.1016/j.ejca.2015.08.012
168. Schadendorf D, Hodi FS, Robert C, Weber JS, Margolin K, Hamid O, et al. Pooled Analysis of Long-Term Survival Data From Phase II and Phase III Trials of Ipilimumab in Unresectable or Metastatic Melanoma. *J Clin Oncol* (2015) 33(17):1889–94. doi: 10.1200/jco.2014.56.2736
169. Carretero-González A, Lora D, Ghanem I, Zugazagoitia J, Castellano D, Sepúlveda JM, et al. Analysis of response rate with ANTI PD1/PD-L1 monoclonal antibodies in advanced solid tumors: a meta-analysis of randomized clinical trials. *Oncotarget* (2018) 9(9):8706–15. doi: 10.18632/oncotarget.24283
170. Kudchadkar RR, Michielin O, van Akkooi ACJ. Practice-Changing Developments in Stage III Melanoma: Surgery, Adjuvant Targeted Therapy, and Immunotherapy. *Am Soc Clin Oncol Educ Book Am Soc Clin Oncol Annu Meet* (2018) 38:759–62. doi: 10.1200/edbk_200241

Conflict of Interest: The authors declare that the research was conducted in the absence of any commercial or financial relationships that could be construed as a potential conflict of interest.

frontiers in Oncology

REVIEW
published: 08 February 2021
doi: 10.3389/fonc.2020.628367

The Paradoxical Behavior of microRNA-211 in Melanomas and Other Human Cancers

Animesh Ray[1,2], *Haritha Kunhiraman*[3] *and Ranjan J. Perera*[3,4]*

[1] Riggs School of Applied Life Sciences, Keck Graduate Institute, Claremont, CA, United States, [2] Division of Biology and Biological Engineering, California Institute of Technology, Pasadena, CA, United States, [3] Cancer & Blood Disorder Institute, Johns Hopkins All Children's Hospital, South, St. Petersburg, FL, United States, [4] Department of Oncology, Sidney Kimmel Comprehensive Cancer Center, School of Medicine, Johns Hopkins University, Baltimore, MD, United States

Cancer initiation, progression, and metastasis leverage many regulatory agents, such as signaling molecules, transcription factors, and regulatory RNA molecules. Among these, regulatory non-coding RNAs have emerged as molecules that control multiple cancer types and their pathologic properties. The human microRNA-211 (MIR211) is one such molecule, which affects several cancer types, including melanoma, glioblastoma, lung adenocarcinomas, breast, ovarian, prostate, and colorectal carcinoma. Previous studies suggested that in certain tumors MIR211 acts as a tumor suppressor while in others it behaves as an oncogenic regulator. Here we summarize the known molecular genetic mechanisms that regulate *MIR211* gene expression and molecular pathways that are in turn controlled by MIR211 itself. We discuss how cellular and epigenetic contexts modulate the biological effects of MIR211, which exhibit pleiotropic effects. For example, up-regulation of *MIR211* expression down-regulates Warburg effect in melanoma tumor cells associated with an inhibition of the growth of human melanoma cells *in vitro*, and yet these conditions robustly increase tumor growth in xenografted mice. Signaling through the DUSP6-ERK5 pathway is modulated by MIR211 in $BRAF^{V600E}$ driven melanoma tumors, and this function is involved in the resistance of tumor cells to the BRAF inhibitor, Vemurafenib. We discuss several alternate but testable models, involving stochastic cell-to-cell expression heterogeneity due to multiple equilibria involving feedback circuits, intracellular communication, and genetic variation at miRNA target sties, to reconcile the paradoxical effects of MIR211 on tumorigenesis. Understanding the precise role of this miRNA is crucial to understanding the genetic basis of melanoma as well as the other cancer types where this regulatory molecule has important influences. We hope this review will inspire novel directions in this field.

Keywords: microRNA-211, melanoma, tumor-promoter, tumor suppresser, epigenetics, miRNA, bistability, MIR211

OPEN ACCESS

Edited by:
Vladimir Spiegelman, Penn State Milton S. Hershey Medical Center, United States

Reviewed by:
Consuelo Amantini, University of Camerino, Italy
Gerolama Condorelli, University of Naples Federico II, Italy

***Correspondence:**
Ranjan J. Perera
jperera2@jh.edu

Specialty section:
This article was submitted to Skin Cancer, a section of the journal Frontiers in Oncology

Received: *11 November 2020*
Accepted: *21 December 2020*
Published: *08 February 2021*

Citation:
Ray A, Kunhiraman H and Perera RJ (2021) The Paradoxical Behavior of microRNA-211 in Melanomas and Other Human Cancers. Front. Oncol. 10:628367. doi: 10.3389/fonc.2020.628367

INTRODUCTION

MicroRNAs[1] (miRNAs) are highly conserved small non-coding RNA molecules of approximately 22 nucleotides that control gene expression either by direct translational inhibition of protein synthesis or by affecting the degradation of the target mRNA (2). miRNA biogenesis occurs through biochemical pathways that are well conserved among metazoans (3), which is described briefly below [miRNA biogenesis has been reviewed recently (4)]. In animals, miRNA transcription begins by the binding of RNA polymerase II enzyme (Pol II) to transcriptional regulatory regions. The primary pol II transcript (Pri-miRNA) molecules, which are precursors of the mature miRNAs, often contain multiple and complex intramolecularly bases-paired looped structures and are subsequently processed by the nuclear enzyme Drosha to produce the intermediate precursor molecules termed Pre-miRNA. Pre-miRNA molecules generally possess a single hairpin loop. Pre-miRNAs are then exported to the cytoplasm by Exportin-5 (Ex-5) and are further processed to generate a mature miRNA duplex without a hairpin by the Dicer enzyme. Mature miRNA molecules, which can be either the 5′ (miRNA-5p) or the 3' (miRNA-3p) component of the Pre-miRNA double-stranded stems of the hairpin, are loaded into the multi-protein RNA-induced silencing complex (RISC) to generate single-stranded guide miRNAs. Such guide miRNA molecules preloaded into the RISC complex interact with various target mRNAs by complementary base pairing over short regions of perfect or near-perfect sequence complementarity, most frequently at the 3'untranslated regions (3'UTR) of the target mRNAs (4). In animals, long 3'UTRs of target mRNAs are often recognized by multiple miRNAs (5, 6). Most such mRNAs with long 3'UTR are known to be involved in cellular fate-determination and developmental processes (4, 7), whereas target genes with relatively short 3'UTR regions generally encode proteins that participate in fundamental cellular biochemistry and stress response (7, 8). For example, genes encoding ribosomal RNAs and proteins have shorter 3'UTR sequences; therefore, these RNA molecules present less complex regulatory potential through the binding of a small number of different miRNAs than do genes encoding longer 3'UTRs, which are generally associated with mRNA of regulatory proteins. Less frequently, biologically important miRNA binding sites are also located in 5'UTR regions, coding regions and promoter regions of coding genes (9, 10). This dichotomy in 3'UTR or 5'UTR lengths have dynamical consequences: genes encoding proteins that participate in fundamental biochemistry/metabolism of the cells ("housekeeping" genes) are regulated quantitatively, as a rheostat does, through a graded response to regulation by miRNAs (11). By contrast, genes encoding regulatory proteins such as transcription factors, each exhibiting multiple miRNA targets, are regulated through complex analog-logical circuits that often result in a switch-like behavior in their expression levels. To understand the biological effects of a miRNA, therefore, it is important to understand how the expression of the miRNA is regulated as well as how that specific miRNA molecule regulates other genes. We illustrate some of these complexities with MIR211, which is one of the major regulators in human cancer, specifically in human melanomas (12–17). Specifically, this molecule can act both as a tumor suppressor and an oncogene based on the cellular context and thus demonstrates a paradoxical behavior in melanoma and other cancers.

[1]We use the convention for human miRNAs as proposed in (1), where a human miRNA is MIRNA followed by a number, and its corresponding gene is italicized.

DIRECT TRANSCRIPTIONAL REGULATION OF *MIR211* EXPRESSION

MIR211 gene is located on chromosome 15q13.3, encoded within the sixth intron of the *Transient Receptor Potential cation channel subfamily M member1* gene (*TRPM1*, Melastatin). The primary human melanocytes exhibit a high expression level of MIR211 (12). Normal human organs such as the eye (18) and the heart (19) also exhibit high expression levels of the primary *TRPM1* transcript. As expected, the levels of *TRPM1* and *MIR211* expression are positively correlated (20).

MIR211 has now been recognized as an important player in the molecular pathogenesis of skin cancers. The Melanocyte Inducing Transcription Factor (MITF) regulates *MIR211*'s host gene *TRPM1* by serving as its primary transcriptional regulator. MITF is one of the critical regulators of melanocyte differentiation and melanoma formation (12, 21, 22). A positive correlation of gene expression levels between *MIR211* and other MITF target genes such as *TYRP1, TYR, MLANA, CDK2*, and *SILV* has also been reported, further supporting the role of MITF in regulating *MIR211* expression (12, 23), and allowing the inclusion of *MIR211* into the gene ontology (24) cluster of "melanosome pigment granule related genes" (FDR corrected $P = 4.36 \times 10^{-8}$). An *MITF-MIR211-BRN2* regulatory feedback loop has been demonstrated (**Figure 1**), and this regulatory mechanism may be important for cell state specification in both melanoblasts and melanoma cells (25–28). BRN2 (Brain-Specific Homeobox/POU Domain Protein class 3 transcription Factor 2 or POU3F2), a transcription factor, is associated with aggressive melanoma development, and MIR211 is a strong suppressor of *BRN2* mediated invasiveness (25). In this feedback model BRN2 is a direct target of MIR211: predictably, BRN2 expression shows an inverse correlation with *MITF* expression. On the other hand, BRN2 has been shown to be a repressor of *MITF* transcription (29). This is predicted to induce bistable states in different subpopulations of cells (21): one in which *MIR211* expression and in the other BRN2 expression would dominate, thus producing different cellular behaviors due to mutually exclusive expression of these two genes in the two subpopulations (see later for a significance of this feedback loop).

The transcription regulatory gene *Recombination signal Binding Protein for immunoglobulin kappa J region* (*RBPJ*), one of the primary downstream molecular effectors of Notch signaling, shares a similar gene expression profile with that of MITF, suggesting a conserved biological function (30). Indeed, the expression levels of *RBPJ* and *MITF* exhibit a positive

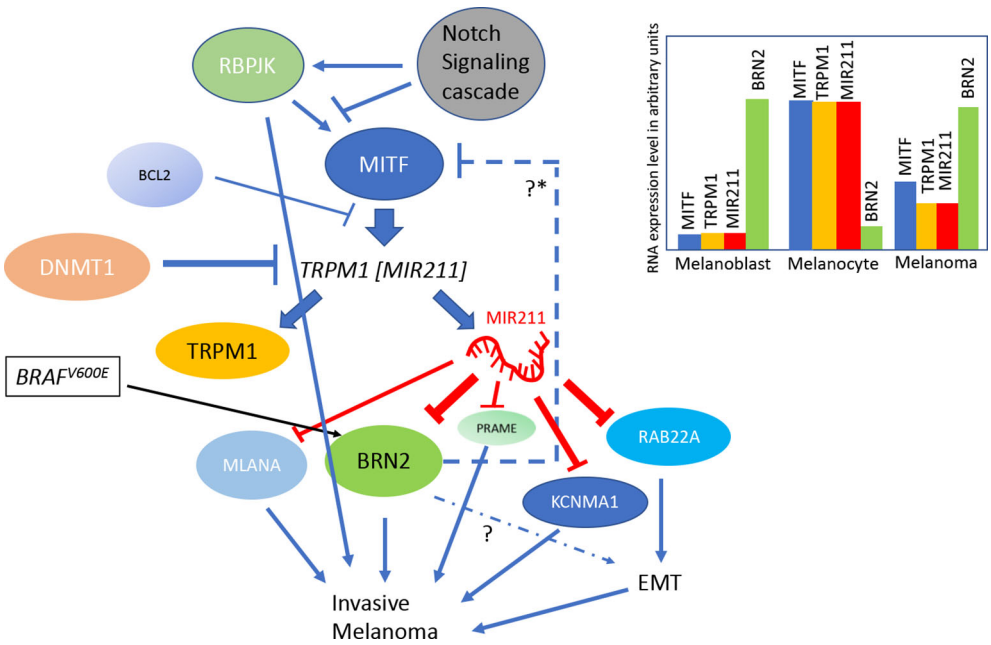

FIGURE 1 | A model summarizing the regulation of MIR211 gene expression: *MIR211* gene is nested within the *TRMP1* transcript. *TRPM1* transcription is promoted by the transcription factor MITF, and the latter's transcription is in turn regulated by the Notch signaling pathway *via* the expression of RBPJK. The DNA methyl transferase DNMT1 regulates the epigenetic state of *TRPM1* gene *via* promoter methylation. MIR211 negatively regulates various genes, including MLANA, PRAME, RABB22A, KCNMA1, and BRN2. Simultaneously *BRN2* gene product induces *MIR211*expression through an unknown mechanism. Apart from that, *MIR211* expression also negatively regulated by pro-apoptotic protein BCL2 through MITF inhibition. The BRAFV600E mutation, a frequent driver mutation for melanoma, activates BRN2, which is negatively regulated by MIR211. EMT is Epithelial Mesenchymal Transition. The inset is a color-coded summary of salient mRNA expression patterns in different cell types related to melanoma formation (blue, MITF; orange, TRPM1; red, MIR211; green, BRN2). The Y-axis is an arbitrary scale of gene expression levels, used as a schematic representation of the salient points on how *MIR211* expression varies in various cell types. See text for evidence regarding these circuits and the gene expression levels from the following sources (12, 14, 25–33). *Proposed negative regulation.

correlation (R=0.47, $P<10^{-10}$) in the Genotype-Tissue Expression (GTEx) datasets for healthy skin (both sun-exposed and unexposed), but this correlation is absent in melanoma cells (34). Furthermore, *RBPJ* occupies and regulates the *TRPM1* promoter in a *MITF* dependent manner and thereby increases the expression of *MIR211* (30, 31). Bcl-2, a pro-apoptotic protein, regulates the expression of *MIR211* by modulating *MITF* expression in melanoma cell lines, in addition to the reciprocal regulation of *BCL2* by MITF (32). **Figure 1** summarizes these pathways of regulation of *MIR211* gene.

THE EPIGENETIC REGULATION OF *MIR211*

Transcriptional silencing associated with methylation of CpG islands is an important correlate that is thought to be responsible for the regulation of tumor suppressor genes (35–37). DNA methyltransferase 1 (DNMT1) mediated methylation of *TRPM1/MIR211* promoter reduces *MIR211* expression levels in melanoma cells (26). Decreased MIR211 levels were correlated with increased cell proliferation and Epithelial to Mesenchymal Transition (EMT, a morphogenetic state transition that is important for the development of numerous cancer types) of melanoma cells (26). The 3'UTR of the oncogenic *Ras-related protein Rab-22A* (*RAB22A*) gene's mRNA was found to be a direct target MIR211 (33) suggesting that the suppressive effects of MIR211 on oncogenic properties might be at least partially through the inhibition of RAB22A expression. Similarly, epigenetic silencing of *TRPM1/MIR211* gene by EZH2-induced (Enhancer Of Zeste Homolog 2 protein) histone H3K27 trimethylation and DNMT1 mediated promoter methylation were associated with cell proliferation, increased AKT/β-catenin signaling, and the induction of EMT, whereas restoration of *MIR211* expression reduced cell proliferation, inhibited AKT/β-catenin signaling and reversed EMT in glioblastoma multiformi (38). Thus, the EZH2/DNMT1/MIR211/RAB22A axis might provide novel insights into the molecular pathogenesis of both melanoma and glioblastoma, particularly on the EMT processes in these two different cancers. In a separate study, Li N *et al.* reported that the silencing of *MIR211* expression by methylation is associated with reduced cisplatin sensitivity in melanoma (39). This observation, however, may be interpreted as an indirect consequence of reduced EMT in MIR211 deficient cells, because increased EMT increases the resistance of cells to cisplatin (40).

TUMOR SUPPRESSOR EFFECTS OF *MIR211*

As expected of a regulatory molecule with a potential tumor-suppressor activity, MIR211 was first identified as one of the most differentially under-expressed miRNA molecules in non-pigmented human melanoma cell lines and in a majority of clinical melanoma tissue samples relative to those expressed in normal melanocytes or in matched normal patient tissues, respectively (12, 14). Conversely, when MIR211 levels were increased artificially in melanoma cells, a significant inhibition of growth and *in vitro* invasive properties were observed, which could again be reversed by inhibiting MIR211 by an antagomir (12–14), fulfilling the criteria for a tumor-suppressor molecule. Consistently, several MIR211 targets genes, all of which were previously known to be oncogenic, were identified, including the *calcium-activated potassium channel subunit a-1* (*KCNMA1*) (12), *Insulin-like Growth Factor 2 Receptor* (*IGF2R*) (14), *TGF-beta Receptor 2* (*TGFBR2*) (41), *Insulin Growth Factor Binding Protein 5* (*IGFBP5*) (42, 43), *POU domain-containing transcription factor BRN2* (25), and *Nuclear Factor of Activated T-cells 5* (*NFAT5*) (14). These evidences together are consistent with the proposal that MIR211 exerts its tumor suppressor properties by means of direct negative regulation of potentially oncogenic mRNAs (44). This proposal is also consistent with the tumor suppressor role of *MITF* as a directly activating transcription factor of *MIR211* gene (12). Subsequently, a series of additional evidences solidified the proposal of miR-211 action as akin to a tumor suppressor for melanomas (13) as well as several other cancer types, including epithelial ovarian cancer (45), ovarian carcinoma (46), breast cancer (47), hepatocellular carcinoma (48), renal cancer (49), and thyroid tumors (50), among others (see **Table 1** for a more complete list).

ONCOGENIC EFFECTS OF *MIR211*

Paradoxically, when *MIR211* expression was artificially induced in human melanoma cell lines, where its expression is generally reduced relative to those in melanocytes, which were xenografted into immunodeficient mice they resulted into aggressive tumor growth (68). Interestingly, this surprising observation is consistent with similar oncogenic effects associated with *MIR211* expression in a number of other cancer types,

TABLE 1 | Summary of MIR211 target genes and their roles in various cancer types.

	TUMOR/CANCER TYPE	TARGET GENES	ASSOCIATED DYSREGULATED MECHANISMS	REFERENCES
1	MELANOMA	*BRN2 (POU3F2)*	INVASION	(14, 25, 26, 32, 51–53)
		PDK4	CELL GROWTH	
		TGFBR2	INVASION	
		NFAT5	INVASION	
		RAB22A	EMT	
		IL6	INVASION	
		IGF2R	CELL GROWTH	
		BCL2	APOPTOSIS	
		EDEM	PIGMENTATION	
		IGFBP5		
		AP1S2		
		SOX11		
		SERINC3		
2	MALIGANANT MELANOMA	*PRAME*		(54)
3	MULTIPLE MYELOMA	*CHOP*	APOPTOSIS	(55)
4	THYROID CANCER	*SOX11*	APOPTOSIS	(50)
5	EPITHELIAL OVARIAN CANCER	*CYCLIN D1CDK1*	CELL CYCLE, APOPTOSIS	(45)
7	CERVICAL CANCER	*MUC4*	INVASION & EMT	(16, 56, 57)
		SPARC	EMT	
		ZEB1	PROLIFERATION AND METASTSIS	
10	GASTRIC CANCER	*MMP-9*	EMT	(58, 59)
		SOX4	CANCER METASTASIS	
12	BLADDER CANCER	*SNAI1*	CANCER METASTASIS	(60)
13	OVARIAN CANCER	*PHF-19*	PROLIFERATION, MIGRATION AND APOPTOSIS	(46)
15	GLIOBLASTIOMA	*MCM3AP-AS1*	ANGIOGENESIS	(61)
		KLF5	ANGIOGENESIS	
17	HEPATOCELLULAR CARCINOMA	*SATB2*	PROLIFERATION AND INVSION	(48, 62)
		SPARC		
19	BREAST CANCER	*CDC25B*	PROLIFERATION, MIGRATION AND INVASION	(63)
		CCNB1		
		FOXM1		
22	COLORECTAL CANCER	*CDH5*	PROLIFERATION AND MIGRATION	(64)
23	ORAL SQUAMOUS CANCER	*BIN1*	PROLIFERATION, MIGRATION AND INVASION	(65)
24	NON SMALL CELL LUNG CANCER	*SRC1N1*	INVASION	(66)
25	HEAD AND NECK SQUAMOUS CELL CARCINOMA	*TGFβRII*	METASTASIS	(67)

including oral carcinoma (65, 69), head and neck carcinoma (67), Burkitt lymphoma (70), breast cancer cell lines (71), and non-small-cell lung cancer (66).

There is no *a priori* reason why a regulatory molecule cannot be a tumor suppressor in one cancer type but oncogenic in another because the identity of differentially regulated downstream target genes in different cancer types might be the obvious mechanism. Indeed, separate sets of target genes of MIR211 have been shown to be responsible for its tumor-enhancing role (66, 69, 71). However, such an explanation does not easily explain how a regulatory molecule can be both a tumor suppressor and an oncogene in the same cancer type, such as seen with *MIR211* in melanoma. We propose below several mechanisms that should help resolve this important paradox.

CELLULAR AND/OR GENETIC CONTEXTS DETERMINE THE EFFECTS OF MIR211 EXPRESSION

We and others have reported that *MIR211* expression is reduced in amelanotic melanoma cell lines (12) and in clinical melanoma samples (44, 72), driving efforts to use *MIR211* as a clinical diagnostic test to discriminate melanomas from benign nevi (52). We also reported that the artificial over-expression of *MIR211* in amelanotic melanoma cells (A375) increases mitochondrial respiration by inhibiting *Pyruvate Dehydrogenase Kinase 4* (*PDK4*) mRNA levels, which was associated with reduced cell survival and lessened invasive properties under cell culture conditions (13). Consistently, miRNA profiling studies revealed that *MIR211* expression is down-regulated not only in melanoma (12, 54), but also in other cancers such as glioma (73) and glioblastoma (38), prostate cancer (74), hepatocellular carcinoma (48), epithelial ovarian cancer (45), cervical cancer (16, 56), and breast cancer (75). These foregoing results together point towards a general tumor-suppressor role of *MIR211*. By contrast, *MIR211* is also known exhibit high expression levels in certain melanoma subtypes and in other cancers: *MIR211* expression is high in a majority (6/8) of melanoma lines in the NCI-60 cancer cell panel (76), and in 9/29 clinical melanoma samples (12), suggesting that either MIR211 level by itself is irrelevant to the tumor-like status or malignancy or that in certain cancer cells MIR211 levels might have tumor-promoting activity.

The dual role of *MIRNA211* described above may hinge on the cellular context, similar to context-dependent regulation that was previously reported for other miRNA genes, in particular with *MIR7* (77, 78), *MIR125B* (79) and *MIR155* (80). This fascinating paradox—whether and how a particular miRNA could either inhibit or augment cancer growth and development depending on the particular cellular context—raises several questions concerning the importance of *MIR211* in melanocyte dedifferentiation (43), melanoma genesis (25), aging and senescence (81), and cardiac development (19).

On the basis of the observations that MIR211 over-expression in the amelanotic melanoma cell line A375 decreased Warburg effect and simultaneously decreased cell proliferation and invasiveness (13), it was anticipated that these cells when transplanted as murine xenografts would also reduce tumor size relative to those by the control (normal MIR211 levels) A375 cells. Paradoxically, exactly the opposite results were observed (68), in which extraordinarily aggressive tumors were formed by the xenografted cells over-expressing MIR211. The *PDK4* gene, the target gene of MIR211 which was previously thought to be an effector of the metabolic switch controlled by MIR211, was indeed downregulated in these xenografts, and therefore the response of this target gene was unable to explain the paradoxical behavior of MIR211 on tumorigenesis. Deletion of *MIR211* gene in these xenografted cells produced much reduced tumors, supporting the conclusion that this MIR211 was directly responsible for the hypertrophic tumor phenotype. RNAseq analysis of mRNA molecules co-immunoprecipitated with the Argonaut-2 protein suggested that these mRNA molecules are associated with the RISC complex in cells with or without MIR211 (68). These studies further revealed several additional target mRNAs, including DUSP6 and BIRC2, which were then confirmed to be causally related to tumor hypertrophy *via* a modulation of the ERK5/MEK kinase signaling pathway (68) (**Figure 2**). These cells simultaneously became more resistant to the BRAF inhibitor vemurafenib and the MEK inhibitor cobimetinib, suggesting that the modulation of the DUSP6/ERK5 signaling pathway by MIR211 is related to the development of BRAF/MEK inhibitor resistant melanoma (68).

BROADLY PLEIOTROPIC TUMOR SUPPRESSOR AND ONCOGENIC BEHAVIOR OF MIR211 CAN BE EXPLAINED BY THE DIVERSITY OF ITS TARGET MRNAS

As described above, MIR211 acts as a tumor suppressor in a variety of cancer types, it can also act as an oncogenic regulator in others. Therefore an understanding of the paradoxical behavior of MIR211 is of paramount importance for understanding cancer biology.

Though the functional role of MIR211 has not been studied extensively in primary human melanocytes, its tumor suppressor role in pigmented melanoma has reported widely and suggested to be due to a multitude of target genes [see citations above, and also (44, 83)]. Endoplasmic reticulum stress initiates the activation of three important signaling molecules like Ire-1α/β, ATF 6, and PERK, whose function is to enable adaptation to the ER stress. PERK (Eukaryotic translation initiation factor 2-alpha kinase 3, also known as protein kinase R (PKR)-like endoplasmic reticulum kinase), is an enzyme that in humans is encoded by the EIF2AK3 gene. PERK has been reported to induce the expression of MIR211, which in turn reduces the stress-dependent expression of GAD153/CHOP, a pro-apoptotic transcription factor at early stages of ER stress (84). If the ER stress is sustained, *MIR211* expression is turned off and increases the expression of CHOP and thereby apoptosis (84). A reduction in

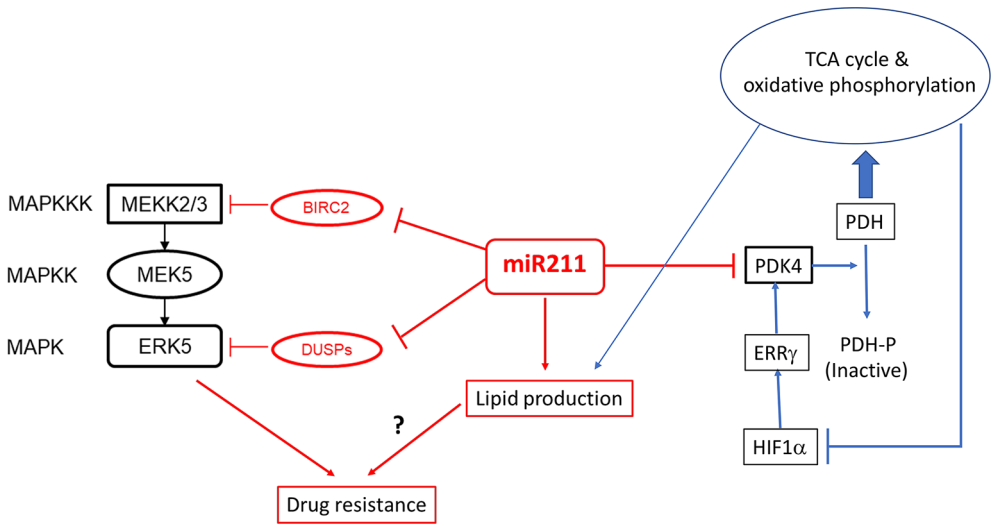

FIGURE 2 | The regulatory cascade of MIR211 involving the BRAF/ERK5/DUSP and PDK4. MIR211 is a negative regulator of at least two negative regulators (BIRC2, DUSP6 and possibly other DUSP mRNAs) of the ERK5/MEK signaling pathway. The latter is involved in resistance of melanoma to vemurafenib and cobimetinib. PDK4 is a pyruvate dehydrogenase kinase, which inactivates pyruvate dehydrogenase (PDH) by phosphorylation, which therefore cannot catalyze the entry of pyruvate to tricarboxylic acid (TCA) cycle. Metabolites of the TCA cycle induces lipid biosynthesis and inhibits hypoxia inducing factor HIF1α, which is a transcriptional activator of ERRβ, which in turn is a transcriptional activator of *PDK4* gene. Evidence for these pathways are obtained from Lee *et al.* (2016 and 2020) (68, 82).

the expression of MIR211 in multiple myeloma is associated with increased expression of pro-apoptotic factor CHOP which in turn triggers ER stress mediated apoptosis (55). In epithelial ovarian cancer (EOC) cells, *MIR211* expression was down-regulated and increased the expression of cyclin D1 and CDK1 and thereby apoptosis (45). Levy et al. reported that MIR211 can directly inhibit the *TGFBR2* and *NFAT5* and can indirectly inhibit *IGF2R*, which leads to the reduced invasive potential of malignant melanomas (14).

EMT is a highly dynamic process that can convert nonmotile epithelial cells to motile mesenchymal cells (85), which involves molecular reprogramming and phenotypic changes that lead to tumor metastasis. EMT in cancer is associated with a decrease in the expression of epithelial cell markers such as γ-catenin and E cadherin, and with an increase in the expression of mesenchymal markers such as vimentin and N-cadherin (86). Mucin 4 (MUC4) is a glycoprotein that covers the epithelial cells and belongs to a large MUCIN family of glycoproteins. Mucin could be used as a lineage marker in benign cervical tissue, whose expression might be higher in cervical cancer (87). MIR211 could directly target MUC4 mRNA and thereby can inhibit the invasion and EMT in cervical cancer cells (57). In melanoma cells, MIR211 can modulate EMT by targeting RAB22A, a member of the RAB family of small GTPase, which regulates tumor invasion and metastasis in various cancer types (32).

Secreted protein acidic and rich in cysteine (SPARC) is a matricellular family of proteins, which modulates cell-matrix interactions and tissue remodeling and, thereby, EMT. In cervical cancer, MIR211 directly targets SPARC and thus acts as a tumor suppressor gene (16). MIR211 regulates Matrix metalloproteinase-9 (MMP-9) and thereby reduces EMT in gastric cancer (58). Sex-determining region Y-related high-mobility group box 4 (SOX4) is another crucial transcription factor that contributes to tumor cell survival, metastasis, and possibly to the maintenance of cancer stem cell properties. In gastric cancer cells, overexpression of MIR211 directly inhibits SOX4 expression and thereby down regulates tumor metastasis (88), suggesting the involvement of cancer stem cells. The Snail family transcriptional repressor 1 (SNAI1) has a significant role in regulating genes required for cell-cell interaction and EMT. By targeting SNAI1 mRNA, MIR211 directly regulates the metastatic behavior of tumor cells in renal cancer cells (49). PHF19 is a member of polycomb repressive complex 2 Complex, which mediates transcriptional repression of developmental regulatory genes and modulates embryonic stem cell differentiation. A recent report suggests that MIR211 can target PHF19 and thereby inhibit cell proliferation, migration and apoptosis in ovarian cancer (89). At the same time, MALAT1, a long non-coding RNA antagonizes the effect of MIR211 in ovarian cancer cells (46). The Secreted protein acidic and rich in cysteine (SPARC) is an oncogene, which is highly expressed in various tumors such as glioma, melanoma, prostate, and gastric carcinoma. SPARC belongs to the matricellular family and has a significant role in tissue repair and remodeling (90). MIR211 is a direct regulator of SPARC expression, and thereby down-regulates other metastasis-associated genes (62). ZEB1, a member of the zinc finger family protein, is reported to be upregulated in ovarian, breast, prostate, and endometrial cancer (91–94). MIR211 directly targets ZEB1 mRNA and reduces the proliferation and metastasis of cervical cancer cells (56).

Apart from regulating the apoptosis, Endoplasmic reticulum stress and EMT, MIR211 also regulates various other processes important for cancer, including angiogenesis, through influencing multiple signaling pathways. In hepatocellular carcinoma MIR211 down-regulates SATB2 (Human special AT-rich sequence-binding protein-2) and reduces its invasion and proliferation (48). Another important study demonstrated that in tongue squamous cell carcinoma the long non-coding RNA KCNQ1OT1 sponges MIR211 and thereby activates Ezrin/Fak/Src signaling pathways (95). Mazar *et al.* reported that MIR211 directly targets pyruvate dehydrogenase kinase 4 (*PDK4*) mRNA, and the ectopic expression of *MIR211* reduced hypoxia-inducible factor 1α (HIF-1α) protein levels and decreased cell growth during hypoxia (13). Ribonucleotide reductase M2 (RRM2) is associated with tumor progression and metastasis; and in colorectal cancer k–ras mutation reduces the expression of MIR211 which thereby enhances the expression of RRM2 (96). In melanotic melanoma cells, MIR211 is induced by BRAFi/MEKi and favors their pro-pigmentation activity by targeting EDEM1, hence promoting TYR expression and melanin accumulation (53). In another interesting study with breast cancer cells it was suggested that MIR211 targeted CDC25B, CCNB1, and FOXM1 and thereby inhibited cell cycle and reduced genomic stability, proliferation, migration, and invasion in triple-negative breast cancer cells (63). It was recently shown that adipocytes secret IL6, which leads to downregulation of MIR211 in melanoma which further promotes melanoma invasion (51).

In contrast to the tumor suppressor activities of MIR211 mentioned above, increased expression of MIR211 is reportedly oncogenic [see above, and (67, 97)]. Some of its oncogenic properties can also be traced to its target genes. For example, MIR211 appears to up-regulate cell cycle progression by targeting the tumor suppressor gene *CHD5* (64), thus modulating the p53 pathway, and *via* several protein kinases (98). MIR211 acts as an oncogene in Acute Myeloid Leukemia (97) by down-regulating the expression of *BIN1* and by activating the EGFR/MAPK pathway. Increased expression of MIR211 in head and neck squamous cell carcinoma (HNSCC) inhibited TGFβRII and thus decreased the SMAD3 phosphorylation and increased c-myc expression (67). MIR211 contributes to melanoma progression not only by targeting genes of melanoma cells but also by modulating the tumor niche in melanoma microenvironment *via* communication through melanosomes (15, 51). Melanosomal-MIR211 released from melanoma cells are transferred into the surrounding primary skin fibroblasts and which then induce their reprogramming into cancer-associated fibroblasts (CAFs) by targeting the IGF2R mRNA and through regulating MAPK signaling (15). The target genes of MIR211 which are considered to be important in various cancer types are summarized in **Table 1**.

PARALOGS OF THE MIR211 FAMILY

A second *miRNA* gene that belongs to the same family as *MIR211* is *MIR204*, which is located within the *TRPM3* gene at 9q21.12, and is believed to be a paralog of *MIR211* (71). Both of these two mature MIRNAs share a similar seed sequence, but they differ in two nucleotides within their 3' regions; these two MIRNAs share multiple common mRNA targets (99). Among these shared targets are the mRNAs of the following tumor-suppressing genes: *XIAP Associated Factor 1* (*XAF I*) (71, 100, 101), whose loss of function mutation causes gastric carcinoma, *HRAS-Like-Suppressor4* (or *HRASLS4*) (71, 101, 102), also associated with mutations in gastric cancer, *Homeodomain Interacting Protein Kinase 2* (*HIPK2*) (71, 103), mutations in which gene are associated with keratocanthoma (a rare skin cancer), breast cancer, and *Thioredoxin Interacting Protein* (*TXNIP*) (71, 104), associated with exocervical carcinoma. In the opposite direction, TargetScan (www.targetscan.org) analysis of MIR211-5p and MIR204-5p also yields the following common oncogene or oncogene-like genes as high-confidence targets: *Ras-Related Protein Rab-22A* (*RAB22A*), *Paired Like Homeobox 2B* (*PHOX2B*) whose high expression is associated with neuroblastoma (105), and *Adaptor Related Protein Complex 1 Subunit Sigma 2* (*AP1S2*) whose mRNA expression is enhanced in melanoma and is associated with significantly poorer survival of melanoma patients (although confers a better survival probability to ovarian and breast cancer patients). In summary, MIR211 and its paralog MIR204 together regulate a number of genes whose expression are related to both tumor suppressor and oncogenic activities in a number of different cancer types including melanoma. As a result, the complexity of phenotypes associated with *MIR211* could also be due to the combined as well as single negative effects on a number of different oncogenic and tumor suppressor mRNA levels, which at least in theory may produce rather complex net dynamics depending on the expression signatures of a large number of genes and the relative levels of the two microRNAs.

MODELS EXPLAINING THE PARADOXICAL EFFECTS OF MIR211

The paradoxical behavior of MIR211 brings to mind the early controversy of p53, acting, as initially proposed, to promote tumor growth (106) but later understood to be a tumor suppressor (107). While as yet there is no direct relationship between p53 and MIR211, by reminding ourselves of the importance of paradoxes in science (108), especially concerning the p53 controversy, we suggest that MIR211 biology is important for understanding cancer biology.

There might be at least three different mechanisms that can explain the paradoxical behavior of a miRNA on a biological process: (a) differences in the allelic variants at miRNA targets; (b) differences in the cellular micro-environment, (c) stochastic fluctuations in the expression levels of the miRNA which set into motion different trajectories of regulatory influences in different cells. **Figure 3** summarizes the three models. It is unclear at this time which of these models is true of *MIR211*. These models are offered as the rationale to guide future experiments. The models are general, in the sense that these could formally apply to all

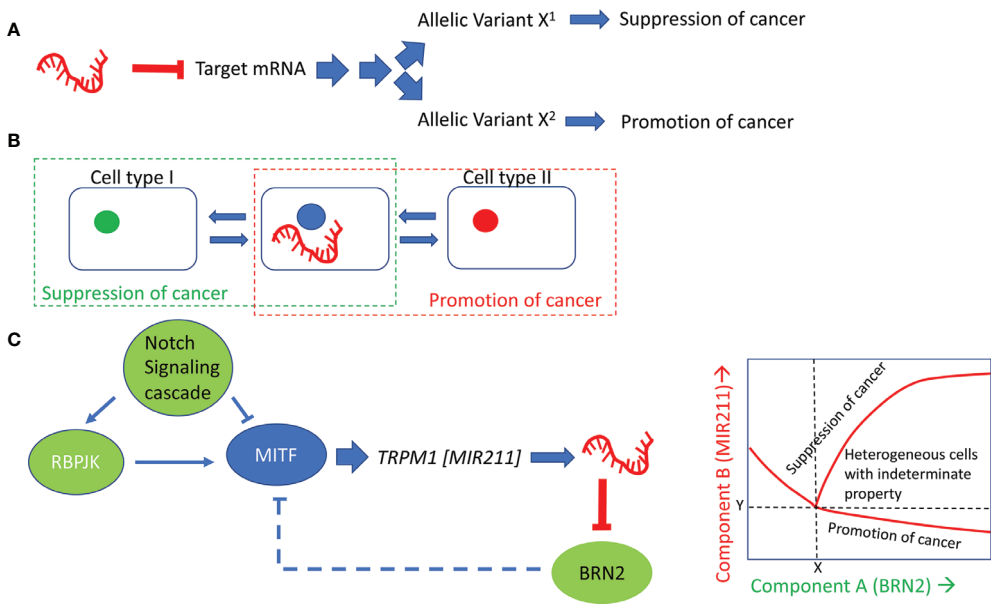

FIGURE 3 | Models that explain the paradoxical effects of MIR211 on cancer development. **(A)** posits that allelic variants in MIR211 target genes explain the behavior of cells with respect to tumorigenesis. **(B)** assumes that the cellular type and the microenvironment, including cell-cell communication, determines the context for whether MIR211 will be tumorigenic or tumor suppressive. MIR211 secreted within exosomes, and/or signaling molecules or metabolites secreted by cells with high or low expression of MIR211 may influence adjacent tumor cells in concentration dependent manner, thus helping to establish distinct morphogenetic fields within the tumors and contribute to tumor heterogeneity. **(C)** explains the mutually opposite effects of MIR211 on the basis of cell to cell heterogeneity and dynamics of gene expression related to MIR211. In this last model, feed-forward and negative feedback with time delays set up opportunities for complex dynamical patterns of expression involving the two genes, *MIR211* and *BRN2*. The inset shows a schematic of such a dynamical pattern, in which stochastic fluctuation in the initial levels of MIR211 or BRN2 could lead to the transition at the parameter values (X,Y) of a cell to a tumor progression (high BRN2/low MIR211) or to a tumor suppressive (high BRN2/high MIR211) state and thus lock in the characteristic state. Intermediate states (high BRN2/intermediate MIR211) could represent cells that could be driven to either direction through other (environmental) factors, which has been shown to occur with melanoma cells with respect to their vemurafenib resistance phenotype (109).

cases where the same miRNA has multiple, mutually opposite, biological effects depending on the cellular contexts.

The allelic variant model (**Figure 3A**) proposes that nucleotide differences at the target site, especially within the seed sequences of the miRNA, are responsible for the cell-line to cell-line variability of its biological effects. Such variability might be inherited in the germline, or maybe due to somatic mutations. This model is consistent with several previous observations on miRNA target site sequence variations (110–112).

The micro-environment influence model (**Figure 3B**) posits that the expression of MIR211 triggers cell-nonautonomous events. Some cells in the tumor micro-environment sense the downstream effectors of MIR211, through either direct exosomal contribution of MIR211 to the neighboring cells or indirectly *via* cell-to-cell signaling and/or metabolites secreted by the primary cells. This proposal assumes the presence of morphogenetically heterogeneous cells within the tumor micro-environment, which takes into account the following previous observations: (i) Melanocytes are derived from non-pigmented melanocyte precursor stem cells, and non-pigmented melanomas are thought to be mainly derived from these stem cells through oncogenic transformation (113); (ii) pigmented melanoma cells are derived from dedifferentiation and transformation of melanocytes); (iii) *MIR211* expression is low in undifferentiated precursor cells, is high in melanocytes, low in non-pigmented melanoma, but high in pigmented melanoma cells (12); (iv) MIR211 targets PDK4, which causes high $NADP^+$/NADPH ratio (13); (v) High $NADP^+$/NADPH ratio causes high ROS levels (114). Diffusion of these molecules is in principle sufficient to set up distinct morphogenetic fields within the tumors (115).

The stochastic single-cell expression model (**Figure 3C**) posits that *MIR211* expression fluctuates stochastically from cell to cell (116), which leads to cell-to-cell fluctuations in the relative levels of *MITF* (component X) and *BRN2* (component Y). A well-known consequence of such fluctuations of two regulatory components in a mutually negative feedback regulatory loop is the establishment of multiple distinct equilibrium regions of expression levels of the two components in which they are both low, both high or one high/one low. Tumor gene expression systems have been shown to operate under such multiple equilibria, producing heterogenous cell populations within the tumors, leading to vastly different biological consequences (117). Importantly, the three models proposed here are not mutually exclusive; elements of each can coexist with those of the other two in defining the full range of biological complexity associated with this regulatory molecule.

SUMMARY AND RECOMMENDATIONS

MIR211 shows both tumor suppressive and oncogenic activities in the same or different cancer types. Since MIR211 has also been shown to be associated with various human diseases apart from cancers, it is regarded as one of the most promising miRNA molecules for therapeutic applications. To our knowledge no clinical trial is currently on-going with this miRNA. Although numerous studies have illuminated the molecular mechanisms associated with the tumor-suppressive and oncogenic characteristics of MIR211, there are many important questions that need to be answered in the future, and we have provided three different frameworks for approaching these mechanisms. We suggest that further work on this interesting regulatory molecule should focus on (a) deciphering the source of mutually opposite behavior of MIR211 in cancer, (b) understanding the mechanisms of cell-to-cell expression variances of *MIR211*, and (c) how such variations could be utilized for diagnostic, prognostic or therapeutic applications.

AUTHOR CONTRIBUTIONS

AR and RP incepted the idea on the paradoxical behavior of the MIR-211 in melanoma and other cancers. All authors (AR, RP, and HK) contributed to the writing. All authors contributed to the article and approved the submitted version.

FUNDING

This study was supported by P30 CA006973 (JHU SKCCC) and Florida Department of Health, Bankhead-Coley Cancer Research Program (5BC08) to RP, and CDMRP/DTRA grant W81XWH-16-1-0170 to AR.

ACKNOWLEDGMENTS

We would like to thank Drs. Carmit Levy and Tamar Golan for their initial suggestion and comments on this manuscript.

REFERENCES

1. Desvignes T, Batzel P, Berezikov E, Eilbeck K, Eppig JT, McAndrews MS, et al. microRNA nomenclature: A view incorporating genetic origins, biosynthetic pathways, and sequence variants. *Trends Genet* (2015) 31:613–26. doi: 10.1016/j.tig.2015.09.002
2. Dexheimer PJ, Cochella L. MicroRNAs: From Mechanism to Organism. *Front Cell Dev Biol* (2020) 8:1–18. doi: 10.3389/fcell.2020.00409
3. Meunier J, Lemoine F, Soumillon M, Liechti A, Weier M, Guschanski K, et al. Birth and expression evolution of mammalian microRNA genes. *Genome Res* (2013) 23:34–45. doi: 10.1101/gr.140269.112
4. Bartel DP. Metazoan MicroRNAs. *Cell* (2018) 173:20–51. doi: 10.1016/j.cell.2018.03.006
5. Grimson A, Farh KK-H, Johnston WK, Garrett-Engele P, Lim LP, Bartel DP. MicroRNA targeting specificity in mammals: determinants beyond seed pairing. *Mol Cell* (2007) 27:91–105. doi: 10.1016/j.molcel.2007.06.017
6. Sætrom P, Heale BSE, Snøve O, Aagaard L, Alluin J, Rossi JJ. Distance constraints between microRNA target sites dictate efficacy and cooperativity. *Nucleic Acids Res* (2007) 35:2333–42. doi: 10.1093/nar/gkm133
7. Zhang Y, Tang C, Yu T, Zhang R, Zheng H, Yan W. MicroRNAs control mRNA fate by compartmentalization based on 3′ UTR length in male germ cells. *Genome Biology* (2017) 18:105. doi: 10.1186/s13059-017-1243-x
8. Zheng D, Wang R, Ding Q, Wang T, Xie B, Wei L, et al. Cellular stress alters 3′UTR landscape through alternative polyadenylation and isoform-specific degradation. *Nature Communication* (2018) 9:2268. doi: 10.1038/s41467-018-04730-7
9. Gu W, Xu Y, Xie X, Wang T, Ko J-H, Zhou T. The role of RNA structure at 5′ untranslated region in microRNA-mediated gene regulation. *RNA* (2014) 20:1369–75. doi: 10.1261/rna.044792.114
10. Lee I, Ajay SS, Yook JI, Kim HS, Hong SH, Kim NH, et al. New class of microRNA targets containing simultaneous 5′-UTR and 3′-UTR interaction sites. *Genome Res* (2009) 19:1175–83. doi: 10.1101/gr.089367.108
11. Siciliano V, Garzilli I, Fracassi C, Criscuolo S, Ventre S, di Bernardo D. miRNAs confer phenotypic robustness to gene networks by suppressing biological noise. *Nat Commun* (2013) 4:2364. doi: 10.1038/ncomms3364
12. Mazar J, DeYoung K, Khaitan D, Meister E, Almodovar A, Goydos J, et al. The regulation of miRNA-211 expression and its role in melanoma cell invasiveness. *PloS One* (2010) 5:e13779. doi: 10.1371/journal.pone.0013779
13. Mazar J, Qi F, Lee B, Marchica J, Govindarajan S, Shelley J, et al. MicroRNA 211 Functions as a Metabolic Switch in Human Melanoma Cells. *Mol Cell Biol* (2016) 36:1090–108. doi: 10.1128/MCB.00762-15
14. Levy C, Khaled M, Iliopoulos D, Janas MM, Schubert S, Pinner S, et al. Intronic miR-211 assumes the tumor suppressive function of its host gene in melanoma. *Mol Cell* (2010) 40:841–9. doi: 10.1016/j.molcel.2010.11.020
15. Dror S, Sander L, Schwartz H, Sheinboim D, Barzilai A, Dishon Y, et al. Melanoma miRNA trafficking controls tumour primary niche formation. *Nat Cell Biol* (2016) 18:1006–17. doi: 10.1038/ncb3399
16. Qu X, Gao D, Ren Q, Jiang X, Bai J, Sheng L. miR-211 inhibits proliferation, invasion and migration of cervical cancer via targeting SPARC. *Oncol Lett* (2018) 16:853–60. doi: 10.3892/ol.2018.8735
17. Pei Y, Yao Q, Li Y, Zhang X, Xie B. microRNA-211 regulates cell proliferation, apoptosis and migration/invasion in human osteosarcoma via targeting EZRIN. *Cellular & Molecular Biological Letter* (2019) 24:48. doi: 10.1186/s11658-019-0173-x
18. Gagliano C, Russo A, Ragusa M, Caltabiano R, Puzzo L, Avitabile T, et al. MicroRNAs in vitreous humor from patients with ocular disease: preliminary results. *Invest Ophthalmol Vis Sci* (2013) 54:6365–5.
19. Thomas T, Galuppo P, Wolf C, Fiedler J, Kneitz S, van Laake LW, et al. MicroRNAs in the Human Heart. *Circulation* (2007) 116:258–67. doi: 10.1161/CIRCULATIONAHA.107.687947
20. Lonsdale J, Thomas J, Salvatore M, Phillips R, Lo E, Shad S, et al. The Genotype-Tissue Expression (GTEx) project. *Nature Genetics* (2013) 45:580–5. doi: 10.1038/ng.2653
21. Goding CR, Arnheiter H. MITF—the first 25 years. *Genes Dev* (2019) 33:1–25. doi: 10.1101/gad.324657.119
22. Levy C, Khaled M, Fisher DE. MITF: master regulator of melanocyte development and melanoma oncogene. *Trends Mol Med* (2006) 12:406–14. doi: 10.1016/j.molmed.2006.07.008
23. Wu G, Feng X, Stein L. A human functional protein interaction network and its application to cancer data analysis. *Genome Biology* (2010) 11:R53. doi: 10.1186/gb-2010-11-5-r53
24. The Gene Ontology Consortium. Gene Ontology Consortium: going forward. *Nucleic Acids Res* (2015) 43:D1049–56. doi: 10.1093/nar/gku1179
25. Boyle GM, Woods SL, Bonazzi VF, Stark MS, Hacker E, Aoude LG, et al. Melanoma cell invasiveness is regulated by miR-211 suppression of the BRN2 transcription factor. *Pigment Cell Melanoma Research* (2011) 24:525–37. doi: 10.1111/j.1755-148X.2011.00849.x
26. Yu H, Yang W. MiR-211 is epigenetically regulated by DNMT1 mediated methylation and inhibits EMT of melanoma cells by targeting RAB22A. *Biochem Biophys Res Commun* (2016) 476:400–5. doi: 10.1016/j.bbrc.2016.05.133
27. De Luca T, Pelosi A, Trisciuoglio D, D'Aguanno S, Desideri M, Farini V, et al. miR-211 and MITF modulation by Bcl-2 protein in melanoma cells. *Mol Carcinog* (2016) 55:2304–12. doi: 10.1002/mc.22437

28. Miller AJ, Du J, Rowan S, Hershey CL, Widlund HR, Fisher DE. Transcriptional Regulation of the Melanoma Prognostic Marker Melastatin (TRPM1) by MITF in Melanocytes and Melanoma. *Cancer Res* (2004) 64:509–16. doi: 10.1158/0008-5472.CAN-03-2440
29. Goodall J, Carreira S, Denat L, Kobi D, Davidson I, Nuciforo P, et al. Brn-2 represses microphthalmia-associated transcription factor expression and marks a distinct subpopulation of microphthalmia-associated transcription factor-negative melanoma cells. *Cancer Res* (2008) 68:7788–94. doi: 10.1158/0008-5472.CAN-08-1053
30. Tabach Y, Golan T, Hernández-Hernández A, Messer AR, Fukuda T, Kouznetsova A, et al. Human disease locus discovery and mapping to molecular pathways through phylogenetic profiling. *Mol Syst Biol* (2013) 9:692. doi: 10.1038/msb.2013.50
31. Golan T, Levy C. Negative Regulatory Loop between Microphthalmia-Associated Transcription Factor (MITF) and Notch Signaling. *Int J Mol Sci* (2019) 20. doi: 10.3390/ijms20030576
32. McGill GG, Horstmann M, Widlund HR, Du J, Motyckova G, Nishimura EK, et al. Bcl2 regulation by the melanocyte master regulator Mitf modulates lineage survival and melanoma cell viability. *Cell* (2002) 109:707–18. doi: 10.1016/s0092-8674<(>02<)>00762-6
33. Su F, Chen Y, Zhu S, Li F, Zhao S, Wu L, et al. RAB22A overexpression promotes the tumor growth of melanoma. *Oncotarget* (2016) 7:71744–53. doi: 10.18632/oncotarget.12329
34. Tang Z, Li C, Kang B, Gao G, Li C, Zhang Z. GEPIA: a web server for cancer and normal gene expression profiling and interactive analyses. *Nucleic Acids Res* (2017) 45:W98–W102. doi: 10.1093/nar/gkx247
35. Jones PA, Laird PW. Cancer epigenetics comes of age. *Nat Genet* (1999) 21:163–7. doi: 10.1038/5947
36. Baylin SB, Esteller M, Rountree MR, Bachman KE, Schuebel K, Herman JG. Aberrant patterns of DNA methylation, chromatin formation and gene expression in cancer. *Hum Mol Genet* (2001) 10:687–92. doi: 10.1093/hmg/10.7.687
37. Esteller M. CpG island hypermethylation and tumor suppressor genes: a booming present, a brighter future. *Oncogene* (2002) 21:5427–40. doi: 10.1038/sj.onc.1205600
38. Li W, Miao X, Liu L, Zhang Y, Jin X, Luo X, et al. Methylation-mediated silencing of microRNA-211 promotes cell growth and epithelial to mesenchymal transition through activation of the AKT/β-catenin pathway in GBM. *Oncotarget* (2017) 8:25167–76. doi: 10.18632/oncotarget.15531
39. Li N, Liu Y, Pang H, Lee D, Zhou Y, Xiao Z. Methylation-Mediated Silencing of MicroRNA-211 Decreases the Sensitivity of Melanoma Cells to Cisplatin. *Med Sci Monit* (2019) 25:1590–9. doi: 10.12659/MSM.911862
40. Ashrafizadeh M, Zarrabi A, Hushmandi K, Kalantari M, Mohammadinejad R, Javaheri T, et al. Association of the Epithelial-Mesenchymal Transition (EMT) with Cisplatin Resistance. *Int J Mol Sci* (2020) 21:4002–48. doi: 10.3390/ijms21114002
41. Dai X, Rao C, Li H, Chen Y, Fan L, Geng H, et al. Regulation of pigmentation by microRNAs: MITF-dependent microRNA-211 targets TGF-β receptor 2. *Pigment Cell Melanoma Res* (2015) 28:217–22. doi: 10.1111/pcmr.12334
42. Díaz-Martínez M, Benito-Jardón L, Alonso L, Koetz-Ploch L, Hernando E, Teixidó J. miR-204-5p and miR-211-5p Contribute to BRAF Inhibitor Resistance in Melanoma. *Cancer Res* (2018) 78:1017–30. doi: 10.1158/0008-5472.CAN-17-1318
43. Margue C, Philippidou D, Reinsbach SE, Schmitt M, Behrmann I, Kreis S. New target genes of MITF-induced microRNA-211 contribute to melanoma cell invasion. *PloS One* (2013) 8:e73473. doi: 10.1371/journal.pone.0073473
44. Xu Y, Brenn T, Brown ERS, Doherty V, Melton DW. Differential expression of microRNAs during melanoma progression: miR-200c, miR-205 and miR-211 are downregulated in melanoma and act as tumour suppressors. *Br J Cancer* (2012) 106:553–61. doi: 10.1038/bjc.2011.568
45. Xia B, Yang S, Liu T, Lou G. miR-211 suppresses epithelial ovarian cancer proliferation and cell-cycle progression by targeting Cyclin D1 and CDK6. *Mol Cancer* (2015) 14:57–70. doi: 10.1186/s12943-015-0322-4
46. Tao F, Tian X, Ruan S, Shen M, Zhang Z. miR-211 sponges lncRNA MALAT1 to suppress tumor growth and progression through inhibiting PHF19 in ovarian carcinoma. *FASEB J* (2018) 32:6330–43. doi: 10.1096/fj.201800495RR
47. Li X, Wang S, Li Z, Long X, Guo Z, Zhang G, et al. The lncRNA NEAT1 facilitates cell growth and invasion via the miR-211/HMGA2 axis in breast cancer. *International Journal of Biological Macromolecules* (2017) 105:346–53. doi: 10.1016/j.ijbiomac.2017.07.053
48. Jiang G, Cui Y, Yu X, Wu Z, Ding G, Cao L. miR-211 suppresses hepatocellular carcinoma by downregulating SATB2. *Oncotarget* (2015) 6:9457–66. doi: 10.18632/oncotarget.3265
49. Wang K, Jin W, Jin P, Fei X, Wang X, Chen X. miR-211-5p Suppresses Metastatic Behavior by Targeting SNAI1 in Renal Cancer. *Mol Cancer Res* (2017) 15:448–56. doi: 10.1158/1541-7786.MCR-16-0288
50. Wang L, Shen Y, Shi Z, Shang X, Jin D, Xi F. Overexpression miR-211-5p hinders the proliferation, migration, and invasion of thyroid tumor cells by downregulating SOX11. *J Clin Lab Anal* (2018) 32:e22293. doi: 10.1002/jcla.22293
51. Golan T, Parikh R, Jacob E, Vaknine H, Zemser-Werner V, Hershkovitz D, et al. Adipocytes sensitize melanoma cells to environmental TGF-β cues by repressing the expression of miR-211. *Sci Signal* (2019) 12:1–15. doi: 10.1126/scisignal.aav6847
52. Babapoor S, Horwich M, Wu R, Levinson S, Gandhi M, Makkar H, et al. microRNA in situ hybridization for miR-211 detection as an ancillary test in melanoma diagnosis. *Modern Pathol* (2016) 29:461–75. doi: 10.1038/modpathol.2016.44
53. Vitiello M, Tuccoli A, D'Aurizio R, Sarti S, Giannecchini L, Lubrano S, et al. Context-dependent miR-204 and miR-211 affect the biological properties of amelanotic and melanotic melanoma cells. *Oncotarget* (2017) 8:25395–417. doi: 10.18632/oncotarget.15915
54. Sakurai E, Maesawa C, Shibazaki M, Yasuhira S, Oikawa H, Sato M, et al. Downregulation of microRNA-211 is involved in expression of preferentially expressed antigen of melanoma in melanoma cells. *Int J Oncol* (2011) 39:665–72. doi: 10.3892/ijo.2011.1084
55. Cha JA, Song H-S, Kang B, Park MN, Park KS, Kim S-H, et al. miR-211 Plays a Critical Role in Cnidium officinale Makino Extract-Induced, ROS/ER Stress-Mediated Apoptosis in U937 and U266 Cells. *Int J Mol Sci* (2018) 19:865. doi: 10.3390/ijms19030865
56. Chen G, Huang P, Xie J, Li R. microRNA−211 suppresses the growth and metastasis of cervical cancer by directly targeting ZEB1. *Mol Med Rep* (2018) 17:1275–82. doi: 10.3892/mmr.2017.8006
57. Xu D, Liu S, Zhang L, Song L. MiR-211 inhibits invasion and epithelial-to-mesenchymal transition (EMT) of cervical cancer cells via targeting MUC4. *Biochem Biophys Res Commun* (2017) 485:556–62. doi: 10.1016/j.bbrc.2016.12.020
58. Wang X-D, Wen F-X, Liu B-C, Song Y. MiR-211 inhibits cell epithelial-mesenchymal transition by targeting MMP9 in gastric cancer. *Int J Clin Exp Pathol* (2017) 10:7551–8.
59. Geethadevi. An interplay between MicroRNA and SOX4 in the regulation of epithelial–mesenchymal transition and cancer progression. Available at: https://www.cancertm.com/article.asp?issn=2395-3977;year=2018;volume=4;issue=1;spage=17;epage=27;aulast=Geethadevi (Accessed December 15, 2020).
60. Liu D, Li Y, Luo G, Xiao X, Tao D, Wu X, et al. LncRNA SPRY4-IT1 sponges miR-101-3p to promote proliferation and metastasis of bladder cancer cells through up-regulating EZH2. *Cancer Lett* (2017) 388:281–91. doi: 10.1016/j.canlet.2016.12.005
61. Yang C, Zheng J, Xue Y, Yu H, Liu X, Ma J, et al. The Effect of MCM3AP-AS1/miR-211/KLF5/AGGF1 Axis Regulating Glioblastoma Angiogenesis. *Front Mol Neurosci* (2018) 10:1–14. doi: 10.3389/fnmol.2017.00437
62. Deng B, Qu L, Li J, Fang J, Yang S, Cao Z, et al. MiRNA-211 suppresses cell proliferation, migration and invasion by targeting SPARC in human hepatocellular carcinoma. *Sci Rep* (2016) 6:26679. doi: 10.1038/srep26679
63. Song G, Zhao Y. MicroRNA-211, a direct negative regulator of CDC25B expression, inhibits triple-negative breast cancer cells' growth and migration. *Tumour Biol* (2015) 36:5001–9. doi: 10.1007/s13277-015-3151-6
64. Cai C, Ashktorab H, Pang X, Zhao Y, Sha W, Liu Y, et al. MicroRNA-211 Expression Promotes Colorectal Cancer Cell Growth In Vitro and In Vivo by Targeting Tumor Suppressor CHD5. *PloS One* (2012) 7:e29750. doi: 10.1371/journal.pone.0029750
65. Chang K-W, Liu C-J, Chu T-H, Cheng H-W, Hung P-S, Hu W-Y, et al. Association between High miR-211 microRNA Expression and the Poor

Prognosis of Oral Carcinoma. *J Dent Res* (2008) 87:1063–8. doi: 10.1177/154405910808701116
66. Hong W, Yu S, Zhuang Y, Zhang Q, Wang J, Gao X. SRCIN1 Regulated by circCCDC66/miR-211 Is Upregulated and Promotes Cell Proliferation in Non-Small-Cell Lung Cancer. *BioMed Res Int* (2020) 2020:e5307641. doi: 10.1155/2020/5307641
67. Chu T-H, Yang C-C, Liu C-J, Lui M-T, Lin S-C, Chang K-W. miR-211 promotes the progression of head and neck carcinomas by targeting TGFβRII. *Cancer Lett* (2013) 337:115–24. doi: 10.1016/j.canlet.2013.05.032
68. Lee B, Sahoo A, Sawada J, Marchica J, Sahoo S, Layng FIAL, et al. MicroRNA-211 Modulates the DUSP6-ERK5 Signaling Axis to Promote BRAFV600E-Driven Melanoma Growth In Vivo and BRAF/MEK Inhibitor Resistance. *J Invest Dermatol* (2021) 141:385–94. doi: 10.1016/j.jid.2020.06.038
69. Chen Y-F, Yang C-C, Kao S-Y, Liu C-J, Lin S-C, Chang K-W. MicroRNA-211 Enhances the Oncogenicity of Carcinogen-Induced Oral Carcinoma by Repressing TCF12 and Increasing Antioxidant Activity. *Cancer Res* (2016) 76:4872–86. doi: 10.1158/0008-5472.CAN-15-1664
70. Bu Y, Yoshida A, Chitnis N, Altman BJ, Tameire F, Oran A, et al. A PERK–miR-211 axis suppresses circadian regulators and protein synthesis to promote cancer cell survival. *Nat Cell Biol* (2018) 20:104–15. doi: 10.1038/s41556-017-0006-y
71. Lee H, Lee S, Bae H, Kang H-S, Kim SJ. Genome-wide identification of target genes for miR-204 and miR-211 identifies their proliferation stimulatory role in breast cancer cells. *Sci Rep* (2016) 6:25287. doi: 10.1038/srep25287
72. Kozubek J, Ma Z, Fleming E, Duggan T, Wu R, Shin D-G, et al. In-depth characterization of microRNA transcriptome in melanoma. *PloS One* (2013) 8:e72699. doi: 10.1371/journal.pone.0072699
73. Zhang J, Lv J, Zhang F, Che H, Liao Q, Huang W, et al. MicroRNA-211 expression is down-regulated and associated with poor prognosis in human glioma. *J Neurooncol* (2017) 133:553–9. doi: 10.1007/s11060-017-2464-2
74. Hao P, Kang B, Yao G, Hao W, Ma F. MicroRNA-211 suppresses prostate cancer proliferation by targeting SPARC. *Oncol Lett* (2018) 15:4323–9. doi: 10.3892/ol.2018.7877
75. Guda MR, Asuthkar S, Labak CM, Tsung AJ, Alexandrov I, Mackenzie MJ, et al. Targeting PDK4 inhibits breast cancer metabolism. *Am J Cancer Res* (2018) 8:1725–38.
76. Gaur A, Jewell DA, Liang Y, Ridzon D, Moore JH, Chen C, et al. Characterization of microRNA expression levels and their biological correlates in human cancer cell lines. *Cancer Res* (2007) 67:2456–68. doi: 10.1158/0008-5472.CAN-06-2698
77. Chou Y-T, Lin H-H, Lien Y-C, Wang Y-H, Hong C-F, Kao Y-R, et al. EGFR promotes lung tumorigenesis by activating miR-7 through a Ras/ERK/Myc pathway that targets the Ets2 transcriptional repressor ERF. *Cancer Res* (2010) 70:8822–31. doi: 10.1158/0008-5472.CAN-10-0638
78. Kalinowski FC, Brown RAM, Ganda C, Giles KM, Epis MR, Horsham J, et al. microRNA-7: a tumor suppressor miRNA with therapeutic potential. *Int J Biochem Cell Biol* (2014) 54:312–7. doi: 10.1016/j.biocel.2014.05.040
79. Banzhaf-Strathmann J, Edbauer D. Good guy or bad guy: the opposing roles of microRNA 125b in cancer. *Cell Commun Signal* (2014) 12:30. doi: 10.1186/1478-811X-12-30
80. Svoronos AA, Engelman DM, Slack FJ. OncomiR or Tumor Suppressor? The Duplicity of MicroRNAs in Cancer. *Cancer Res* (2016) 76:3666–70. doi: 10.1158/0008-5472.CAN-16-0359
81. Bu H, Wedel S, Cavinato M, Jansen-Dürr P. MicroRNA Regulation of Oxidative Stress-Induced Cellular Senescence. *Oxid Med Cell Longevity* (2017) 2017:e2398696. doi: 10.1155/2017/2398696
82. Lee B, Sahoo A, Marchica J, Holzhauser E, Chen X, Li J-L, et al. The long noncoding RNA *SPRIGHTLY* acts as an intranuclear organizing hub for pre-mRNA molecules. *Sci Adv* (2017) 3:e1602505. doi: 10.1126/sciadv.1602505
83. Bell RE, Khaled M, Netanely D, Schubert S, Golan T, Buxbaum A, et al. Transcription factor/microRNA axis blocks melanoma invasion program by miR-211 targeting NUAK1. *J Invest Dermatol* (2014) 134:441–51. doi: 10.1038/jid.2013.340
84. Chitnis NS, Pytel D, Bobrovnikova-Marjon E, Pant D, Zheng H, Maas NL, et al. miR-211 is a prosurvival microRNA that regulates chop expression in a PERK-dependent manner. *Mol Cell* (2012) 48:353–64. doi: 10.1016/j.molcel.2012.08.025
85. Nisticò P, Bissell MJ, Radisky DC. Epithelial-Mesenchymal Transition: General Principles and Pathological Relevance with Special Emphasis on the Role of Matrix Metalloproteinases. *Cold Spring Harb Perspect Biol* (2012) 4(2):a011908. doi: 10.1101/cshperspect.a011908
86. Micalizzi DS, Farabaugh SM, Ford HL. Epithelial-mesenchymal transition in cancer: parallels between normal development and tumor progression. *J Mammary Gland Biol Neoplasia* (2010) 15:117–34. doi: 10.1007/s10911-010-9178-9
87. Munro EG, Jain M, Oliva E, Kamal N, Lele SM, Lynch MP, et al. Upregulation of MUC4 in cervical squamous cell carcinoma: pathologic significance. *Int J Gynecol Pathol* (2009) 28:127–33. doi: 10.1097/PGP.0b013e318184f3e0
88. Wang C-Y, Hua L, Sun J, Yao K-H, Chen J-T, Zhang J-J, et al. MiR-211 inhibits cell proliferation and invasion of gastric cancer by down-regulating SOX4. *Int J Clin Exp Pathol* (2015) 8:14013–20.
89. Ruan S, Zhang H, Tian X, Zhang Z, Huang H, Shi C, et al. PHD Finger Protein 19 Enhances the Resistance of Ovarian Cancer Cells to Compound Fuling Granule by Protecting Cell Growth, Invasion, Migration, and Stemness. *Front Pharmacol* (2020) 11:150. doi: 10.3389/fphar.2020.00150
90. Jayakumar AR, Apeksha A, Norenberg MD. Role of Matricellular Proteins in Disorders of the Central Nervous System. *Neurochem Res* (2017) 42:858–75. doi: 10.1007/s11064-016-2088-5
91. Hurt EM, Saykally JN, Anose BM, Kalli KR, Sanders MM. Expression of the ZEB1 (δEF1) transcription factor in human: additional insights. *Mol Cell Biochem* (2008) 318:89–99. doi: 10.1007/s11010-008-9860-z
92. Singh M, Spoelstra NS, Jean A, Howe E, Torkko KC, Clark HR, et al. ZEB1 expression in type I vs type II endometrial cancers: a marker of aggressive disease. *Mod Pathol* (2008) 21:912–23. doi: 10.1038/modpathol.2008.82
93. Graham TR, Zhau HE, Odero-Marah VA, Osunkoya AO, Kimbro KS, Tighiouart M, et al. Insulin-like growth factor-I-dependent up-regulation of ZEB1 drives epithelial-to-mesenchymal transition in human prostate cancer cells. *Cancer Res* (2008) 68:2479–88. doi: 10.1158/0008-5472.CAN-07-2559
94. Drake JM, Strohbehn G, Bair TB, Moreland JG, Henry MD. ZEB1 enhances transendothelial migration and represses the epithelial phenotype of prostate cancer cells. *Mol Biol Cell* (2009) 20:2207–17. doi: 10.1091/mbc.e08-10-1076
95. Zhang S, Ma H, Zhang D, Xie S, Wang W, Li Q, et al. LncRNA KCNQ1OT1 regulates proliferation and cisplatin resistance in tongue cancer via miR-211-5p mediated Ezrin/Fak/Src signaling. *Cell Death Dis* (2018) 9:1–16. doi: 10.1038/s41419-018-0793-5
96. Chang C-C, Lin C-C, Wang C-H, Huang C-C, Ke T-W, Wei P-L, et al. miR-211 regulates the expression of RRM2 in tumoral metastasis and recurrence in colorectal cancer patients with a k-ras gene mutation. *Oncol Lett* (2018) 15:8107–17. doi: 10.3892/ol.2018.8295
97. Narayan N, Morenos L, Yuen HLA, Chen M, Fornerod M, Zwaan CM, et al. Microrna-211 - a Novel Oncogene in Acute Myeloid Leukemia. *Blood* (2017) 130:2507–7. doi: 10.1182/blood.V130.Suppl_1.2507.2507
98. Zheng J, Wang J, Jia Y, Liu T, Duan Y, Liang X, et al. microRNA-211 promotes proliferation, migration, and invasion ability of oral squamous cell carcinoma cells via targeting the bridging integrator 1 protein. *J Cell Biochem* (2019) 120:4644–53. doi: 10.1002/jcb.27753
99. Griffiths-Jones S. The microRNA Registry. *Nucleic Acids Res* (2004) 32:D109–11. doi: 10.1093/nar/gkh023
100. Liston P, Fong WG, Kelly NL, Toji S, Miyazaki T, Conte D, et al. Identification of XAF1 as an antagonist of XIAP anti-Caspase activity. *Nat Cell Biol* (2001) 3:128–33. doi: 10.1038/35055027
101. DiSepio D, Ghosn C, Eckert RL, Deucher A, Robinson N, Duvic M, et al. Identification and characterization of a retinoid-induced class II tumor suppressor/growth regulatory gene. *Proc Natl Acad Sci USA* (1998) 95:14811–5. doi: 10.1073/pnas.95.25.14811
102. Higuchi E, Chandraratna RAS, Hong WK, Lotan R. Induction of TIG3, a putative class II tumor suppressor gene, by retinoic acid in head and neck and lung carcinoma cells and its association with suppression of the transformed phenotype. *Oncogene* (2003) 22:4627–35. doi: 10.1038/sj.onc.1206235
103. Hofmann TG, Glas C, Bitomsky N. HIPK2: A tumour suppressor that controls DNA damage-induced cell fate and cytokinesis. *Bioessays* (2013) 35:55–64. doi: 10.1002/bies.201200060

104. Jiao D, Huan Y, Zheng J, Wei M, Zheng G, Han D, et al. UHRF1 promotes renal cell carcinoma progression through epigenetic regulation of TXNIP. *Oncogene* (2019) 38:5686–99. doi: 10.1038/s41388-019-0822-6
105. Thwin KKM, Ishida T, Uemura S, Yamamoto N, Lin KS, Tamura A, et al. Level of Seven Neuroblastoma-Associated mRNAs Detected by Droplet Digital PCR Is Associated with Tumor Relapse/Regrowth of High-Risk Neuroblastoma Patients. *J Mol Diagn* (2020) 22:236–46. doi: 10.1016/j.jmoldx.2019.10.012
106. Reich NC, Levine AJ. Growth regulation of a cellular tumour antigen, p53, in nontransformed cells. *Nature* (1984) 308:199–201. doi: 10.1038/308199a0
107. Finlay CA, Hinds PW, Levine AJ. The p53 proto-oncogene can act as a suppressor of transformation. *Cell* (1989) 57:1083–93. doi: 10.1016/0092-8674<(>89<)>90045-7
108. Popper K. *The Logic of Scientific Discovery*. London: Routledge (2005). doi: 10.4324/9780203994627
109. Shaffer SM, Dunagin MC, Torborg SR, Torre EA, Emert B, Krepler C, et al. Rare cell variability and drug-induced reprogramming as a mode of cancer drug resistance. *Nature* (2017) 546:431–5. doi: 10.1038/nature22794
110. Saunders MA, Liang H, Li W-H. Human polymorphism at microRNAs and microRNA target sites. *Proc Natl Acad Sci USA* (2007) 104:3300–5. doi: 10.1073/pnas.0611347104
111. Ryan BM, Robles AI, Harris CC. Genetic variation in microRNA networks: the implications for cancer research. *Nat Rev Cancer* (2010) 10:389–402. doi: 10.1038/nrc2867
112. Piletic K, Kunej T. MicroRNA-Target Interactions Reloaded: Identification of Potentially Functional Sequence Variants Within Validated MicroRNA-Target Interactions. *OMICS* (2018) 22:700–8. doi: 10.1089/omi.2018.0159
113. Becker JC, zur Hausen A. Cells of Origin in Skin Cancer. *J Invest Dermatol* (2014) 134:2491–3. doi: 10.1038/jid.2014.233
114. Murphy MP. How mitochondria produce reactive oxygen species. *Biochem J* (2009) 417:1–13. doi: 10.1042/BJ20081386
115. Levin M. Morphogenetic fields in embryogenesis, regeneration, and cancer: non-local control of complex patterning. *Biosystems* (2012) 109:243–61. doi: 10.1016/j.biosystems.2012.04.005
116. Sherman MS, Lorenz K, Lanier MH, Cohen BA. Cell-to-cell variability in the propensity to transcribe explains correlated fluctuations in gene expression. *Cell Syst* (2015) 1:315–25. doi: 10.1016/j.cels.2015.10.011
117. Hausser J, Alon U. Tumour heterogeneity and the evolutionary trade-offs of cancer. *Nat Rev Cancer* (2020) 20:247–57. doi: 10.1038/s41568-020-0241-6

Conflict of Interest: The authors declare that the research was conducted in the absence of any commercial or financial relationships that could be construed as a potential conflict of interest.

frontiers in Oncology

ORIGINAL RESEARCH
published: 17 March 2021
doi: 10.3389/fonc.2021.643613

LncRNA POU3F3 Contributes to Dacarbazine Resistance of Human Melanoma Through the MiR-650/MGMT Axis

*Kai Wu[1], Qiang Wang[2,3], Yu-Lin Liu[3], Zhuo Xiang[4], Qing-Qing Wang[2], Li Yin[2] and Shun-Li Liu[1]**

[1] Department of Burns and Plastic Surgery, People's Liberation Army (PLA) 960 Hospital, Jinan, China, [2] Oncology Department, Shandong Second Provincial General Hospital, Jinan, China, [3] Clinical Laboratory, Navy 971 Hospital of PLA, Qingdao, China, [4] Pharmacy Department, Navy 971 Hospital of PLA, Qingdao, China

OPEN ACCESS

Edited by:
Vladimir Spiegelman, Penn State Milton S. Hershey Medical Center, United States

Reviewed by:
Akinori Kawakami, Massachusetts General Hospital and Harvard Medical School, United States
Chandra K. Singh, University of Wisconsin-Madison, United States

***Correspondence:**
Shun-Li Liu
liushunli5678@163.com

Specialty section:
This article was submitted to Skin Cancer, a section of the journal Frontiers in Oncology

Received: 18 December 2020
Accepted: 08 February 2021
Published: 17 March 2021

Citation:
Wu K, Wang Q, Liu Y-L, Xiang Z, Wang Q-Q, Yin L and Liu S-L (2021) LncRNA POU3F3 Contributes to Dacarbazine Resistance of Human Melanoma Through the MiR-650/MGMT Axis. Front. Oncol. 11:643613. doi: 10.3389/fonc.2021.643613

Background: Alkylating agents are critical therapeutic options for melanoma, while dacarbazine (DTIC)-based chemotherapy showed poor sensitivity in clinical trials. Long non-coding RNAs (lncRNAs) were highlighted in the progression of malignant tumors in recent years, whereas little was known about their involvement in melanoma.

Methods: The functional role and molecular mechanism of lncRNA POU3F3 were evaluated on DTIC-resistant melanoma cells. Further studies analyzed its clinical role in the disease progression of melanoma.

Results: We observed elevated the expression of lncRNA POU3F3 in the DTIC-resistant melanoma cells. Gain-of-function assays showed that the overexpression of lncRNA POU3F3 maintained cell survival with DTIC treatment, while the knockdown of lncRNA POU3F3 restored cell sensitivity to DTIC. A positive correlation of the expression O6-methylguanine-DNA-methyltransferase (MGMT) was observed with lncRNA POU3F3 *in vitro* and *in vivo*. Bioinformatic analyses predicted that miR-650 was involved in the lncRNA POU3F3-regulated MGMT expression. Molecular analysis indicated that lncRNA POU3F3 worked as a competitive endogenous RNA to regulate the levels of miR-650, and the lncRNA POU3F3/miR-650 axis determined the transcription of MGMT in melanoma cells to a greater extent. Further clinical studies supported that lncRNA POU3F3 was a risk factor for the disease progression of melanoma.

Conclusion: LncRNA POU3F3 upregulated the expression of MGMT by sponging miR-650, which is a crucial way for DTIC resistance in melanoma. Our results indicated that lncRNA POU3F3 was a valuable biomarker for the disease progression of melanoma.

Keywords: lncRNA POU3F3, melanoma, chemo-resistance, dacarbazine, MGMT

INTRODUCTION

Wide multidisciplinary approaches, along with the immune checkpoint inhibitors and targeted therapies have substantially improved the survival of patients with melanoma (1). Combined treatment with alkylating agents and targeted therapies is a recommended option for metastatic melanoma, whereas the treatment with alkylating agents, such as dacarbazine (DTIC), showed a complete response rate of < 5% (2, 3). Nevertheless, it was calculated that the increasing incidence of malignant melanoma and low survival rate occurred in the late-stage patients (4). It was critical to assess the mechanism of therapeutic resistance to improve the available therapies (5, 6).

Extensive studies indicate various strategies for DTIC-resistant melanoma cells (7). Among them, O^6-methylguanine-DNA-methyltransferase (MGMT), a damage-reversal suicide enzyme, plays an important role in the chemotherapy resistance related to alkylating agents (8). The MGMT transfers an alkyl group from the O^6-guanine of DNA to protect the cells against the DTIC-induced DNA damage. Clinical trials identified elevated MGMT expression in melanoma metastases as an indicator for DTIC-based therapy resistance (9). Therefore, further research for MGMT regulation is valuable to explore a novel strategy for reversing the chemotherapy resistance.

Recent studies on long non-coding RNAs (lncRNAs) indicated that lncRNAs played crucial roles in chromosome modification, gene transcription, and intranuclear translocation (10). However, rear studies explore the significance of lncRNA in malignant melanoma. Earlier, we screened out increased levels of lncRNA POU3F3 (also LINC01158) in DTIC-resistant melanoma cells, indicating a promising role of lncRNA POU3F3 in the acquired DTIC resistance. LncRNA POU3F3 is a 747 bp transcript located in Chr2q12.1, which shows absolute conservation among different orthologous species (11). Moreover, the elevated lncRNA POU3F3 expression was also reported in glioma (12), esophageal cancer (13), and cervical cancer (14), which was correlated with cell proliferation, migration, and invasion. Extensive research on the molecular mechanisms, including the crosstalk with miRNA, was needed for the lncRNA POU3F3-participated DTIC-resistance.

Thus, we explored the biological role of lncRNA POU3F3 in regulating DTIC-resistant melanoma cells, as well as their clinical significance in patients with malignant melanoma.

MATERIALS AND METHODS

Cell Culture

Human melanoma cell lines, namely A375 and MV3, were obtained from the American Type Culture Collection (ATCC) (Manassas, USA). The cells were cultured in an RPMI-1640 medium with 10% fetal bovine serum (FBS). The DTIC (Sigma-Aldrich, St. Louis, USA) was dissolved in 1 M hydrochloric acid and diluted to various concentrations in a culture medium. Gradient concentration of DTIC was added in the medium for 6 months to generate the DTIC-resistant cells (A375/DTIC and MV3/DTIC).

Cell Transfection

The pIRSE2-lncRNA POU3F3, full-length MGMT, MGMT-3′-untranslated regions (3′-UTRs), and small interfering RNAs (siRNAs) for MGMT as well as the mutant ones were synthesized in Sangon Biotech (Shanghai, China). The siMGMT were designed as reported by Veil et al. (15). The miRNA-650 mimic and the inhibitor were prepared in GenePharma (Shanghai, China). Cell transfection was performed with Lipofectamine 2000 (Invitrogen, Carlsbad, CA) and verified by quantitative real-time-PCR (qRT-PCR) assays.

Quantitative Real-Time PCR (qRT-PCR)

Total RNA of cultured cells was prepared with the TRIzol reagent (Invitrogen, CA, USA). The AMV Reverse tTanscriptase XL (Takara Bio, Otsu, Japan) and RevertAid^{TM} H Minus First Strand cDNA Synthesis Kit (Takara) were used for reverse transcription. The expression levels of lncRNA and micRNA were measured with the One Step SYBR Prime Script RT-PCR Kit (Takara Bio, CA, USA). The GAPDH and U6 were used as their endogenous controls. All experiments were independently repeated at least three times. The sequences of the primers are listed in the **Supplementary Table 1**.

MTT Assay

Transfected cells were seeded into 96-well plates and treated with the DTIC of indicated concentration for 48 h. Cell viability was analyzed with the MTT Cell Proliferation and Cytotoxicity Assay Kit (C0009, Beyotime, Shanghai, China), which was performed according to the instructions of the manufacturer. Cell viability was measured at OD450 nm with a microplate reader.

Colony Formation Assay

In total, 1,000 transfected cells were cultured with 12-well plates for 14 days. Giemsa-stained cell colonies were counted and photographed. All experiments were independently repeated at least three times.

Cell Apoptosis Assay

We collected all the attached and floating cells after the indicated treatment and resuspended them in an HEPES buffer. Cell apoptosis was determined with the Annexin V-FITC/PI kit (Beyotime, Shanghai, China) as the instructions of the manufacturer, which was measured with the BD FACSAria II flow cytometer (BD Biosciences, CA, USA).

Western Blot

A radioimmunoprecipitation assay buffer (Cell-Signaling Tech., MA, USA) was used for total protein extraction. Primary antibodies against MGMT (ab108630) and GAPDH (ab181602) were obtained from Abcam (Cambridge, USA). Western blot assays were performed as previously reported (16). The GAPDH was used as a loading control.

Xenograft Model

In total, 12 BALB/c-nude mice were provided by the Shanghai Laboratory Animal Resource Center (Shanghai, China). The infected A375 cells (5×10^6) were subcutaneously planted (six mice in each group) and grew until 100 mm^3. The DTIC was

dissolved into 0.9% NaCl solution and intraperitoneally (IP) administered (5 mg/kg weight, every 2 days) as reported by Tsubaki et al. (17). The xenograft volume was measured every 3 days with the following formula:

$$Volume = (length \times width^2)/2.$$

The mice were anesthetized and sacrificed after 15 days of DTIC treatment. The tumor tissue from each mouse was excised and photographed.

Immunohistochemical Staining

Paraffin-embedded xenograft sections were prepared. Primary antibodies for MGMT and Bcl-2 (ab32124) were obtained for Abcam. The immunohistochemical (IHC) staining was performed with DAKO REAL EnVision K5007 (Glostrup, Denmark) according to the instructions of the manufacturer.

Luciferase Reporter Assay

Dual-luciferase pmirGLO-lncPOU3F3-wt and mutant reporter vectors were designed as present in the schematic diagram. HEK-293 cells were co-transfected with reporters and with miR-NC or miR-650. The luciferase activity was measured with the Dual-Luciferase Reporter Assay System (Promega, Madison, WI) after 48 h.

RNA Immunoprecipitation

The RNA immunoprecipitation of A375/DTIC cells was performed with the Imprint RNA Immunoprecipitation Kit (Sigma Aldrich, MO, USA). The immunoprecipitates were collected with anti-argonaute 2 (Ago2) or anti-IgG antibody, which were conjugated with magnetic beads. Then, qRT-PCR assays were performed for the abundance of lncRNA and miRNA in the purified RNA.

RNA Pull-Down Assay

The miR-650-wt or miR-650-mut was transfected into A375 cells. Streptavidin-coated magnetic beads (Life Technologies, Carlsbad, USA) were used to collect the biotin-coupled RNA complex. Then, a qRT-PCR assay was performed to measure the levels of lncRNA.

Statistical Analysis

The statistical data were presented as mean ± SD from at least three independent experiments. The comparison between two or more groups was performed with the paired Student's *t*-test

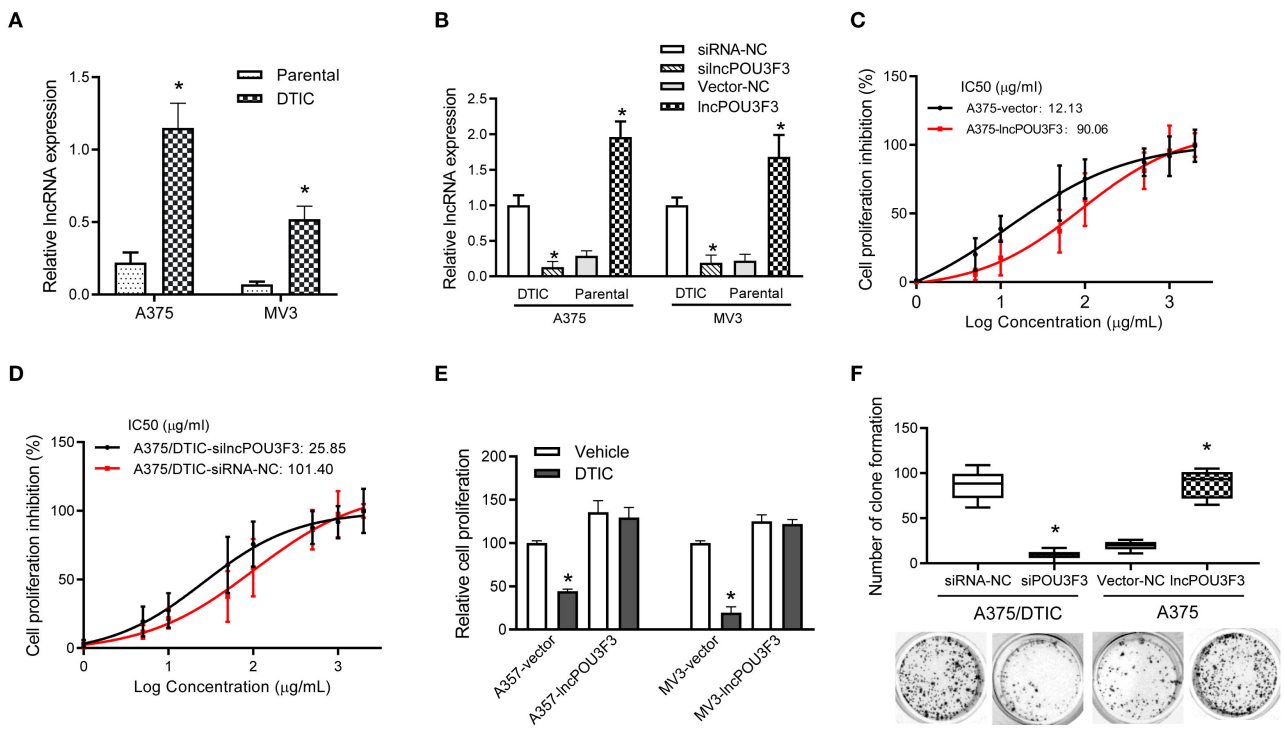

FIGURE 1 | LncRNA POU3F3 maintains melanoma cell survival with DTIC treatment. **(A)** The lncRNA POU3F3 expression level was measured in DTIC-resistant melanoma cells and parental A375 and MV3 melanoma cells. GAPDH was used as the control. **(B)** The DTIC-resistant or parental A375 and MV3 cells were transfected with siRNA-NC/siRNA-lncRNA POU3F3 or Vector-NC/lncRNA POU3F3. The lncRNA POU3F3 expression levels were measured with qRT-PCR assays. **(C,D)** The transfected parental and DTIC-resistant A375 cells were treated with a series dose of DTIC (1–2,000 μg/ml) for 48 h, and cell viability was determined by MTT assays. IC50 was analyzed with the percentage of cell viability inhibition. **(E)** LncRNA POU3F3 overexpressing cells and control cells were treated with DTIC (25 μg/ml) for 3 days. The cell proliferation was detected with MTT assays. **(F)** In total, 1,000 transfected DTIC-resistant and parental A375 cells were cultured with DTIC (25 μg/ml) for 10 days. Cell colony number was compared among the groups. The data are presented as mean ± SD of three independent experiments, where $^*p < 0.01$. LncRNA, long non-coding RNAs; DTIC, dacarbazine; siRNA, small interfering RNAs; qRT-PCR, quantitative real-time PCR.

or the one-way ANOVA test. Correlation between the clinical variables was analyzed with the Chi-square test. The Kaplan–Meier analysis with the log-rank test and Cox proportional hazard methods were used for the survival estimation. The value of $p < 0.05$ was considered as a significant difference.

RESULTS

LncRNA POU3F3 Maintains Melanoma Cell Survival With DTIC Treatment

First, the expression levels of lncRNA POU3F3 were monitored in the DTIC-resistant cells and parental cells, which showed an increased expression of lncRNA POU3F3 in the DTIC-resistant cells than in the parental ones (**Figure 1A**). Then, we assessed the functional role of lncRNA POU3F3 in melanoma cells. The knockdown of lncRNA POU3F3 was verified after si-lncPOU3F3 transfection in the DTIC-resistant cells (**Figure 1B**). Exogenous expression of lncRNA POU3F3 was performed with parental melanoma cells, in which an empty vector was used as a control (**Figure 1B**). The MTT assays were performed for the cell viability of the transfected cells with gradient concentrations of DTIC for 48 h. Then, we analyzed the IC50 for each cell group. An increased IC50 value was observed in lncRNA POU3F3 overexpressing cells (**Figure 1C** and **Supplementary Figure 1A**), while the knockdown of lncRNA POU3F3 induced a decrease of IC50 in the DTIC-resistant cells (**Figure 1D**). The transfected cells were cultured with 25 μg/ml DTIC for 3 days. The cell viability analysis indicated that the expression of lncRNA POU3F3 maintained the survival of melanoma cells with DTIC treatment (**Figure 1E**). Moreover, the colony formation assay showed increased cell colonies in lncRNA

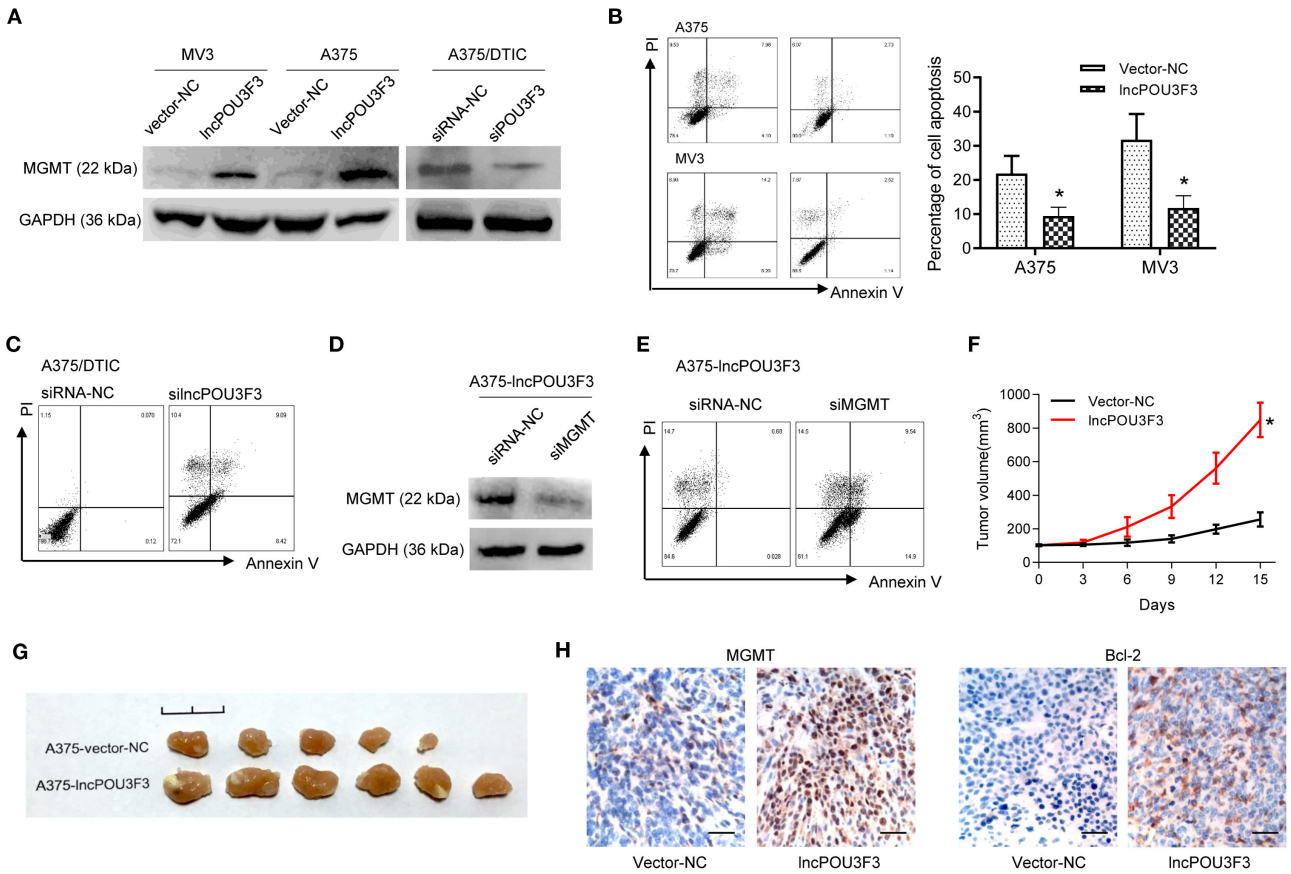

FIGURE 2 | LncRNA POU3F3 contributes to MGMT-induced DTIC resistance. **(A)** Western blot assay for the MGMT expression was performed with lncRNA POU3F3 overexpressing cells, knockdown cells, and control cells. GAPDH was used as the loading control. **(B)** The transfected cells were pretreated with DTIC (A375 cells: 25 μg/ml; MV3: 10 μg/ml) for 48 h. Cell apoptosis was detected with the flow cytometry analysis. **(C)** A375/DTIC-silncPOU3F3 cells and control cells were treated with 25 μg/ml DTIC for 48 h and cell apoptosis was analyzed with a flow cytometer. **(D)** Western blot assay for the MGMT expression was performed with shMGMT transfected A375-lncPOU3F3 cells. **(E)** The transfected cells were treated with 25 μg/ml DTIC for 48 h and cell apoptosis was analyzed with a flow cytometer. The cell apoptosis data are presented as mean ± SD of at least three independent experiments. **(F)** The lncRNA POU3F3 overexpressing and controlled A375 cells were subcutaneously implanted for xenografts. DTIC (5 mg/kg) was IP administered every 2 days after the average volume of xenografts was 100 mm^3. The volume of the xenografts was recorded every 3 days. **(G)** The volume of A375-lncPOU3F3 xenografts was compared between A375-vector and A375-lncPOU3F3 ones. **(H)** The expression levels of MGMT and Bcl-2 were determined by IHC staining with the xenografts as indicated in **(G)**, where $^*p < 0.01$. LncRNA, long non-coding RNAs; DTIC, dacarbazine; MGMT, O6-methylguanine-DNA-methyltransferase; IP, intraperitoneally; IHC, immunohistochemical.

POU3F3 overexpressing cells with DTIC treatment, whereas the knockdown of lncRNA POU3F3 decreased the ability of cell colonies compared to the corresponding control group (**Figure 1F**). Similar results were also observed in the transfected MV3 cells (**Supplementary Figure 1B**). The results supported that lncRNA POU3F3 participated in the DTIC resistance of melanoma cells.

lncRNA POU3F3 Contributes to MGMT-Induced DTIC Resistance

We further accessed the correlation of lncRNA POU3F3 and MGMT in the DTIC resistance of melanoma cells. We examined the protein levels of MGMT in transfected cells. Western blot assays showed an increased MGMT protein level in lncRNA POU3F3 overexpressing cells, whereas the knockdown of lncRNA POU3F3 reduced the MGMT levels (**Figure 2A**). A cell apoptosis analysis was performed with the transfected melanoma cells. The results showed that the overexpression of lncRNA POU3F3 induced a low percentage of cell apoptosis than the corresponding control cells (**Figure 2B**), whereas a higher percentage of cell apoptosis in the knockdown of lncRNA POU3F3 A375/DTIC cells than control cells (**Figure 2C**). The knockdown of MGMT was performed with lncRNA POU3F3 overexpressing cells and verified with the Western blot assay (**Figure 2D**). Increased cell apoptosis was observed in the MGMT knockdown cells, compared with the control group (**Figure 2E**).

In vivo assays were performed with lncRNA POU3F3 overexpressing A375 cells and empty control cells. The DTIC was administrated when the xenograft volumes were around 100 mm^3. Increased tumor growth was observed in the

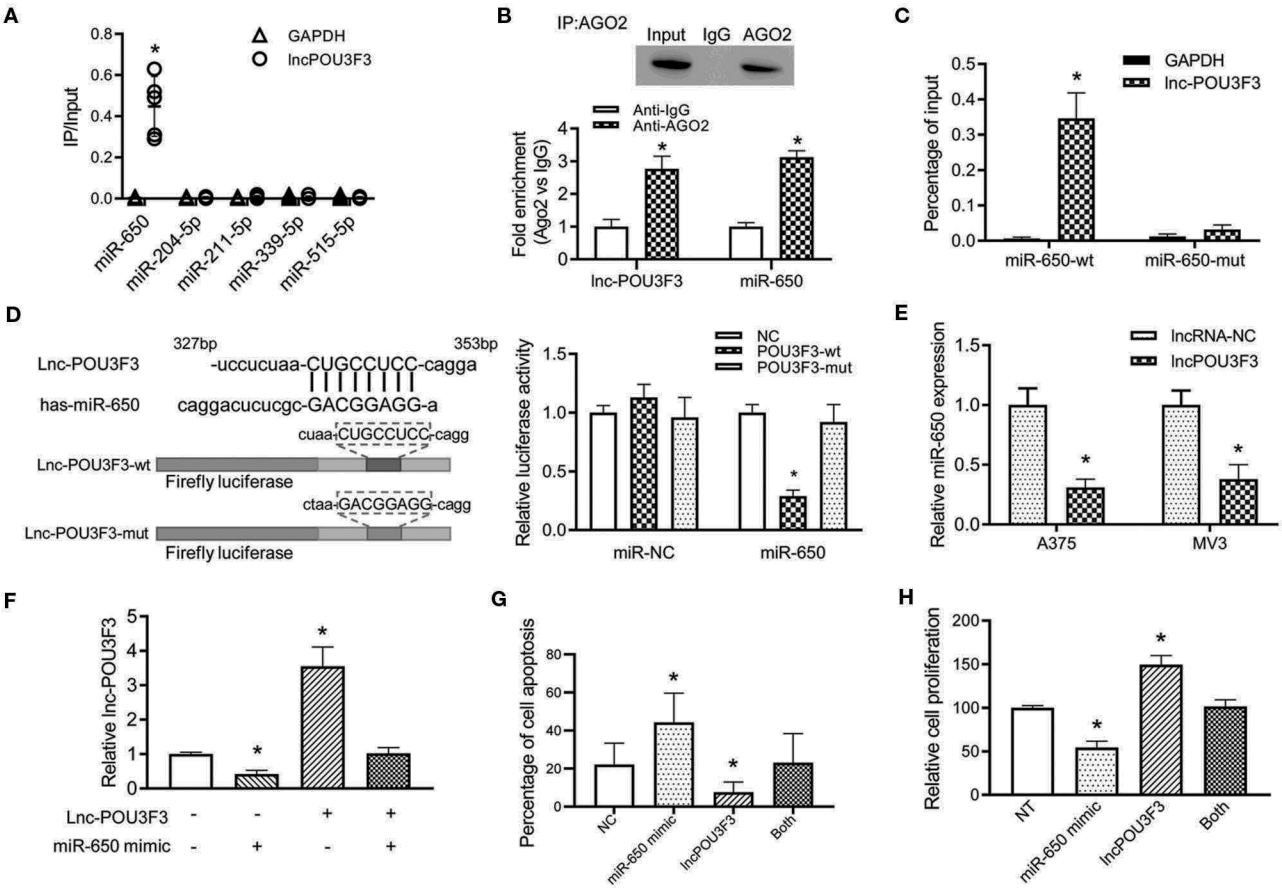

FIGURE 3 | LncRNA POU3F3 regulates miR-650 as a competing endogenous RNA. **(A)** A375 cells were transfected with biotinylated miRNAs. The RNA levels of lncRNA POU3F3 and GAPDH were analyzed for the relative ratio of IP input with qRT-qPCR. **(B)** The lncRNA POU3F3 and miR-650 levels were measured in anti-AGO2 immunoprecipitates, which were analyzed with anti-Ago2 RIP assays. **(C)** The content of lncRNA POU3F3 was compared between miR-650-wt and miR-650-mut transfected A375 cells. **(D)** The predicted binding site of lncRNA POU3F3 and miR-650 was shown in the schematic diagram. Wild type and mutant lncRNA POU3F3 firefly luciferase reporters were prepared as shown in the sequence. The luciferase activity of different transfected cells was compared using a histogram. **(E)** The miR-650 expression level was analyzed in lncRNA POU3F3 overexpressing cells and vector control cells, which was measured by the qRT-PCR assay. **(F)** Relative expression levels of lncRNA POU3F3 were analyzed in the A375 cells co-infected with or without miR-650 using qRT-PCR assays. **(G)** The cell apoptosis percentage of the transfected cells **(F)** was analyzed with a flow cytometer after DTIC treatment for 48 h. **(H)** The transfected cells were treated with DTIC (25 μg/ml) for 3 days. Cell viability was detected with MTT assays. The data are presented as mean ± SD of at least three independent experiments, where $^*p < 0.01$. LncRNA, long non-coding RNAs; DTIC, dacarbazine; IP, intrapotential; miRNAs, micro RNAs; qRT-PCR, quantitative real-time-PCR.

tumors of lncRNA POU3F3 overexpressing cells (**Figure 2F**), and the xenografts showed a larger volume than the control group (**Figure 2G**). Moreover, the IHC staining showed an increased positive expression of MGMT and of bcl-2 in the xenografts of A375-lncRNA POU3F3 cells than in the control group (**Figure 2H**). These data suggested that lncRNA POU3F3 inhibited DTIC-induced melanoma cell apoptosis, which was correlated with an expression of increased MGMT.

lncRNA POU3F3 Regulates miR-650 as a Competing Endogenous RNA

Previous studies indicated that a variety of lncRNAs absorbed miRNAs to regulate the transcription of the targeted mRNA (10). Then, we analyzed the reverse complementary recognition sequence of lncRNA POU3F3 to predict the target miRNAs, which was analyzed with LncBase v.2 (http://carolina.imis.athena-innovation.gr/diana_tools/web/index.php?r=lncbasev2/index). Moreover, candidate miRNAs, to regulate the MGMT expression, were also analyzed with Targetscan 7.2 (http://www.targetscan.org/vert_72/). An overlap analysis found five candidate miRNAs for further verification. An RNA pull-down analysis indicated the most relevant target miRNA of lncRNA POU3F3, which was more abundant in miR-650 than others (**Figure 3A**). Further analysis was performed for the interaction between lncRNA POU3F3 and miR650. RIP assays were performed with precipitated Ago2 protein. Our results showed that lncRNA POU3F3 and miR-650 were associated with the Ago2 in A375 cells (**Figure 3B**). Moreover, the miR-650 and lncRNA POU3F3 levels showed over 2-fold increase than the IgG control (**Figure 3B**). The RNA pull-down assays also indicated higher levels of lncRNA POU3F3 in miR-650-wt than in the mutant ones (**Figure 3C**). Further, luciferase reporter assays were conducted with the lncRNA POU3F3-wt reporter or mutant

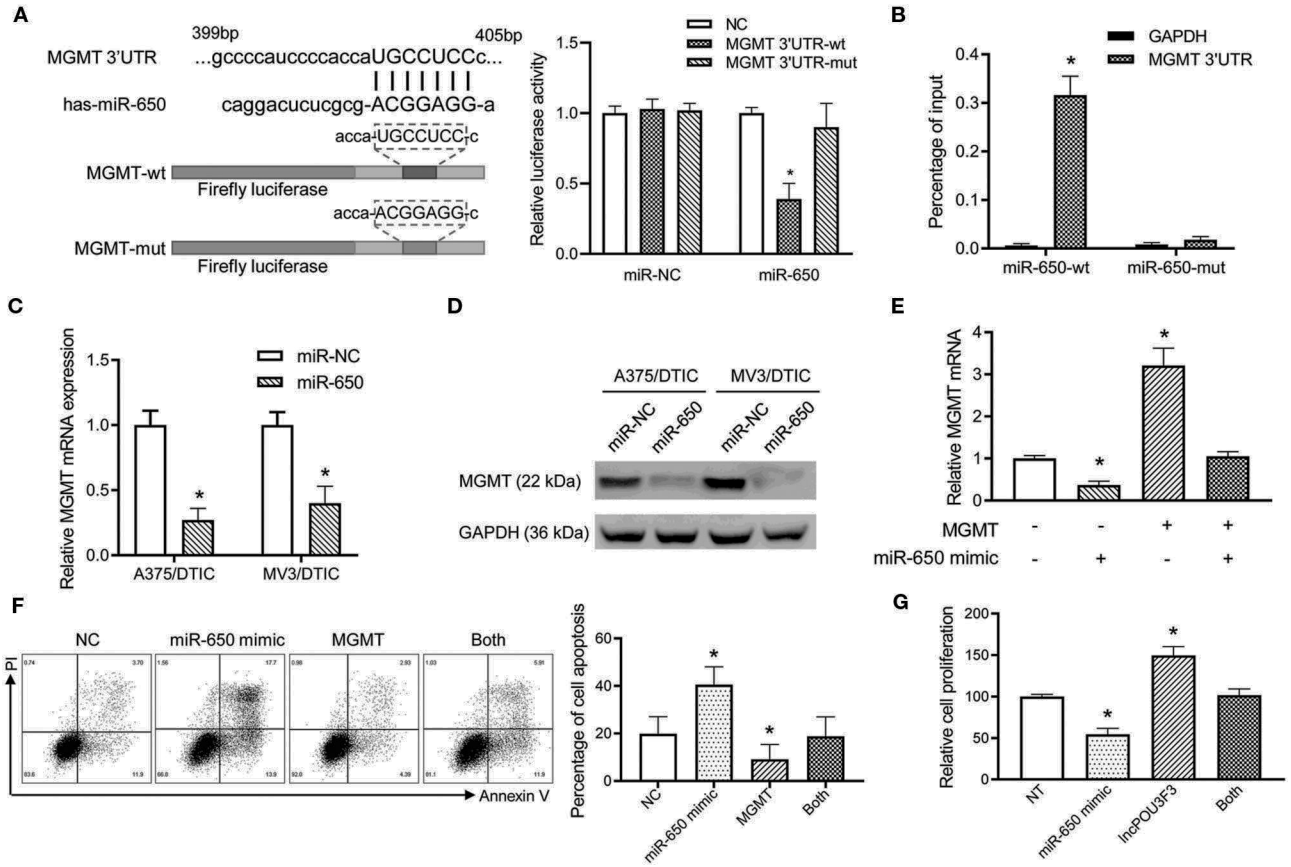

FIGURE 4 | The miR-650 regulates the expression of MGMT in the melanoma cells. **(A)** The schematic diagram showed the predicted binding site of MGMT-3′UTR and miR-650. A luciferase reporter gene assay was performed for the luciferase activity in A375 cells with wild-type and mutant MGMT-3′UTR. **(B)** The MGMT-3′UTR and GAPDH RNA levels were measured with a qRT-PCR assay after the transfection of biotinylated miR-650-wt or mutant in A375/DTIC cells. The histogram showed the relative ratio to the intraperitoneal input. **(C)** The expression of MGMT mRNAs was measured with the qRT-PCR assay in miR-650 transfected melanoma cells. **(D)** The protein levels of MGMT were analyzed in miR-650 transfected cells with the Western bolt assay. **(E)** Relative MGMT mRNA expression levels were compared with the A375 cells which were transfected with the miR-650 mimic or MGMT. **(F)** The percentage of cell apoptosis of the transfected cells indicated in **(E)** was analyzed with a flow cytometer after DTIC treatment for 48 h. **(G)** The transfected cells were treated with DTIC (25 μg/ml) for 3 days. Cell viability was detected with MTT assays. The data are presented as mean ± SD of at least three independent experiments, where $*p < 0.01$. DTIC, dacarbazine; miRNAs, micro RNAs; qRT-PCR, quantitative real-time PCR; MGMT, O6-methylguanine-DNA-methyltransferase.

vector transfection. Our results showed lower luciferase activity in the cells transfected with the wild-type reporter and miR-650 than those transfected with miR-NC. However, cells transfected with the lncRNA POU3F3-mut reporter showed comparable luciferase activity in the cells co-transfected with miR-650 and miR-NC (**Figure 3D**). In addition, a decreased miR-650 level was observed in lncRNA POU3F3 overexpressed melanoma cells in the qRT-PCR assay (**Figure 3E**). A rescue experiment was performed with co-infection of miR-650 and lncRNA POU3F3. The qRT-PCR assay indicated that the lncRNA POU3F3 level was downregulated to a greater extent with the transfection with the miR-650 mimic (**Figure 3F**). Moreover, the flow cytometry analysis indicated that the miR-650 mimic transfection increased cell apoptosis with DTIC treatment, which reversed the overexpression of lncRNA POU3F3 induced the DTIC resistance in melanoma cells (**Figure 3G** and **Supplementary Figure 1C**). Moreover, the transfection of miR-650 mimic could also attenuate the cell proliferation ability in melanoma cells with DTIC treatment (**Figure 3H**).

The miR-650 Regulates MGMT Expression in the Melanoma Cells

Further analysis was performed for the MGMT transcription regulation by miR-650. Luciferase reporters were prepared with a wild type or mutant MGMT 3′-UTR. The luciferase activity

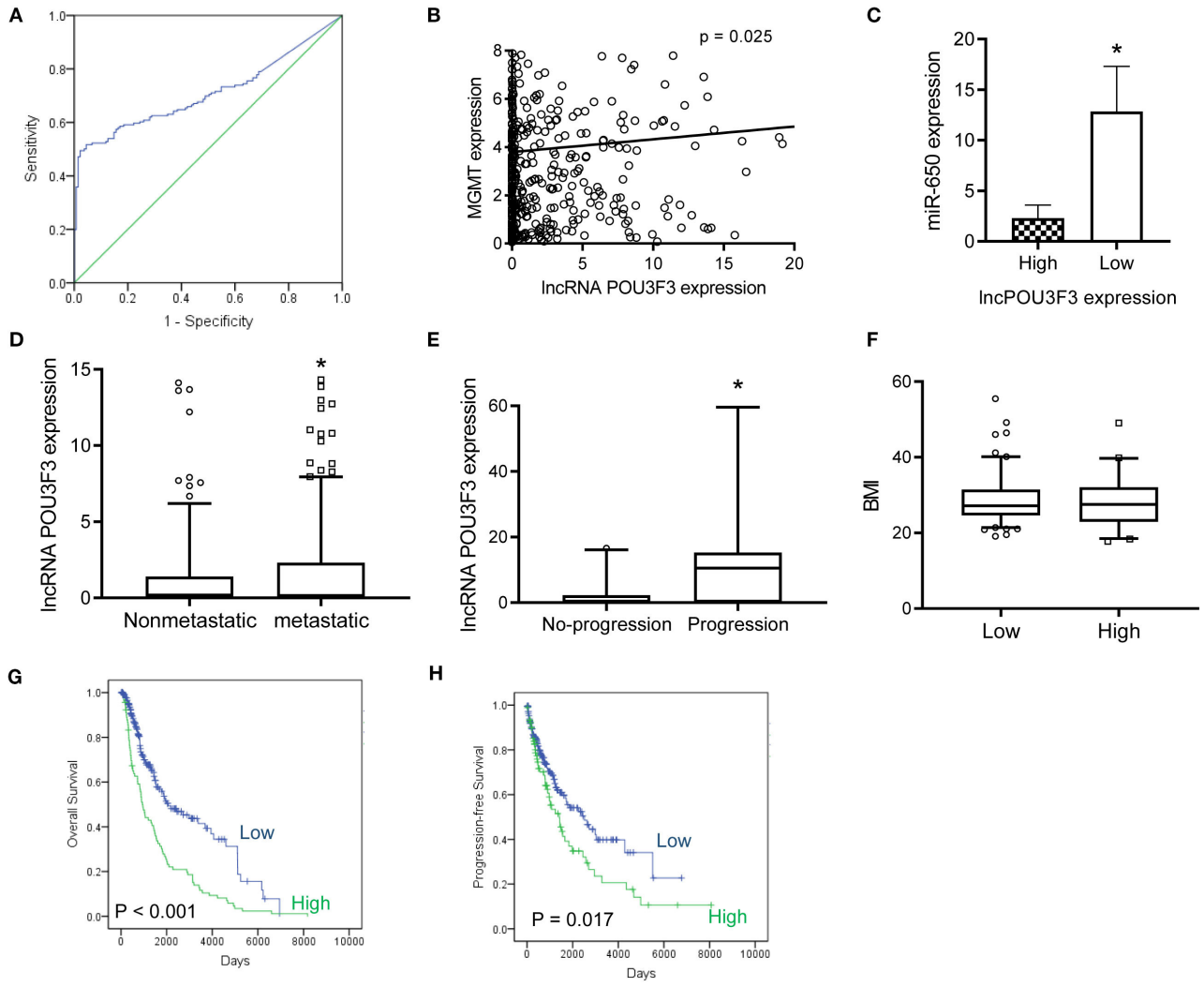

FIGURE 5 | The lncRNA POU3F3 contributes to the disease progression of melanoma. **(A)** From the TCGA database, an ROC curve analysis was performed for the cut-off value of lncRNA POU3F3 in patients with melanoma ($p < 0.01$). **(B,C)** The correlation was analyzed between the expression levels of lncRNA POU3F3, MGMT, and miR-650. **(D)** The expression levels of the lncRNA POU3F3 were compared between patients with metastasis and patients without metastasis. **(E)** The lncRNA POU3F3 expression comparison was performed among 33 patients either with disease progression or without the disease progression. All patients received DTIC treatment. **(F)** The BMI was compared between the patients with high or low lncRNA POU3F3 expression, where $^*p < 0.01$. **(G,H)** Kaplan–Meier analysis was performed for the overall survival **(G)** and progression-free survival **(H)** according to the lncRNA POU3F3 expression status. LncRNA, long non-coding RNAs; ROC, receiver operating characteristics; DTIC, dacarbazine; IP, intrapotential; MGMT, O6-methylguanine-DNA-methyltransferase.

TABLE 1 | Clinical characteristics of the 309 patients with melanoma.

Characteristic	All	Low lncRNA POU3F3	High lncRNA POU3F3	*p*-value
Total	309	218	91	
Age				
<60	155	101	54	0.037
≥60	154	117	37	
Gender				
Female	111	78	33	0.936
Male	198	140	58	
TNM stage				
I–II	176	126	50	0.644
III–IV	133	92	41	

TNM, tumor, node, metastasis.

TABLE 2 | Univariate and multivariate analyses of patients with the disease progression of melanoma.

Variable	Univariate analysis	*p*-value	Multivariate analysis	*p*-value
Age (≥60 vs. <60)	1.432 (0.995–2.061)	0.053		
Gender (Male vs. Female)	0.981 (0.679–1.419)	0.981		
BMI (≥24 vs. <24)	0.637 (0.371–1.096)	0.103		
TNM stage (III–IV vs. I–II)	2.699 (1.887–3.860)	<0.001	2.357 (1.429–3.890)	0.001
lncPOU3F3 (High vs. Low)	1.541 (1.079–2.202)	0.017	1.591 (0.955–2.649)	0.074

BMI, Body mass index.

analysis indicated that the wild-type MGMT luciferase activity was inhibited by miR-650, while there was no significant impact by miR-NC (**Figure 4A**). Moreover, the mutant-type MGMT-3′UTR showed no significant change in the luciferase activity with miR-650 or miR-NC (**Figure 4A**). The RNA pull-down assay also indicated higher levels of MGMT 3′-UTR in wild-type miR-650 transfected with A357/DTIC cells than in the mutant-type ones (**Figure 4B**). Furthermore, a decreased MGMT expression was observed with the miR-650 mimic transfection in DTIC-resistant melanoma cells, which was examined with qRT-PCR assays and Western blot assays (**Figures 4C,D**). Moreover, MGMT plasmid and miR-650 mimics were co-transfected into A375 cells. We found that the exogenous expression of full-length MGMT was partially attenuated by the ectopic miR-650 expression (**Figure 4E**). The transfected cells were treated with DTIC for 48 h to analyze cell apoptosis. The results showed that the ectopic miR-650 expression increased cell apoptosis, which also attenuated the MGMT-induced DTIC resistance in melanoma cells (**Figure 4F**). Moreover, the infection of miR-650 mimics in melanoma cells also inhibited the cell viability of melanoma cells with DTIC treatment, which was also observed in the MGMT expressing cells (**Figure 4G**).

lncRNA POU3F3 Contributes to Disease Progression in Melanoma

After obtaining complete clinical information from the TCGA database, we assessed the clinical significance of the lncRNA POU3F3 expression in 309 patients with cutaneous melanoma. The ROC analysis indicated the cut-off value of lncRNA POU3F3 as 1.384 (**Figure 5A**). A significant positive correlation was observed in the expression of lncRNA POU3F3 and MGMT (**Figure 5B**). A reverse correlation was observed between lncRNA POU3F3 and miR-650 (**Figure 5C**). Further analysis showed an increased lncRNA POU3F3 expression in the metastatic tumors than in the localized ones ($p = 0.01$, **Figure 5D**). In addition, a total of 33 patients received DTIC-based chemotherapy. We found higher lncRNA POU3F3 levels in patients with disease progression than others ($p < 0.001$, **Figure 5E**). Further correlation analysis indicated a significant correlation between the expression of lncRNA POU3F3 and age ($p = 0.037$), whereas there was no significant correlation between gender, TNM stage, and BMI (**Table 1** and **Figure 5F**). A univariate Cox regression analysis indicated that the TNM stage and the expression of lncRNA POU3F3 were correlated with the disease progression of melanoma (**Table 2**), while a multivariate analysis showed that only the TNM stage was statistically significant in the disease progression of melanoma (**Table 2**). The Kaplan–Meier analysis indicated a worse overall survival and progression-free survival estimation for positive patients with lncRNA POU3F3 than the others (**Figures 5G,H**). Our results supported that lncRNA POU3F3 was a detrimental factor for the disease progression of melanoma.

DISCUSSION

LncRNA POU3F3 is located in the bidirectional promoter of POU3F3 at Chr2q12.1. The oncogenic role of lncRNA POU3F3 was verified in glioma and triple-negative breast cancer (12, 18). Recent studies identified that lncRNA POU3F3 promoted cell proliferation, invasion, and G1 cell cycle arrest *in vitro*, as well as arteriole formation *in vivo* (18–20). Our study identified an increased lncRNA POU3F3 level in DTIC-resistant melanoma cells. The gain of function assays indicated that the knockdown of lncRNA POU3F3 reversed the DTIC-resistance of melanoma cell lines, as well as decreased the ability of cell growth. The exogenous expression of lncRNA POU3F3 decreased cell sensitivity to DTIC *in vitro* and *in vivo*. Studies suggested that lncRNA POU3F3 conferred the DTIC-resistant ability of melanoma cells, which shed light to improve the therapeutic efficiency of DTIC-based chemotherapy (21).

The crosstalk between lncRNAs and miRNAs was discovered to promote malignant disease progression in various aspects of tumors, such as LINC00673/miR-150-5p in NSCLC (22). Previous studies discovered that lncRNA POU3F3 promoted the methylation of the POU3F3 gene for transcriptional repression in glioma and esophageal squamous cell carcinoma (11, 12).

However, rear studies were performed for the mechanism of DTIC-related chemotherapy resistance (23, 24). In this study, a positive correlation was observed between lncRNA POU3F3 and the MGMT expression in DTIC-resistant melanoma cells *in vivo* and *in vitro*. As a dominant molecular, MGMT transports cytotoxic adducts from O^6-guanine of DNA to avoid genomic mutation. Excessive MGMT levels induce therapeutic resistance to the treatment based on alkylating agents (25). Further studies supported that MGMT was also a predictor for clinical response to the DTIC-based therapy in patients with metastatic melanoma (26). Our study explored the mechanism of lncRNA POU3F3-induced DTIC resistance in melanoma. MiR-650 was identified and validated to mediate the transcriptional regulation of MGMT, in which the lncRNA POU3F3 sponged miR650 in DTIC-resistant cells. Endogenous competition between lncRNA POU3F3 and miR-650 regulates the expression levels of MGMT, which determines the tolerance of melanoma cells to DTIC treatment to some extent.

MicroRNAs participate in the regulation of the cellular process as post-transcriptional regulators, which directly targeted the 3′-UTRs of mRNA to repress a broad spectrum of gene expression (27). It was a ubiquitous regulation of the feedback loop between miRNAs and target genes. Various functional roles of miR-650 are regarded in different tumors, which are dependent on the target genes in a particular histological type (28). An elevated miR-650 expression is observed in hepatocellular cancer, lung adenocarcinoma, and prostate cancer, which correlates with tumor metastasis and poor prognosis (29–32). Nevertheless, the overexpression of miR-650 also indicates favorable survival estimation in chronic lymphocytic leukemia and colorectal cancer (33, 34). In this study, the tumor suppressor role of miR-650 was identified in DTIC-resistant melanoma cells. Downregulation of miR-650 by lncRNA POU3F3 facilitates the expression of MGMT in the development of DTIC resistance. MGMT is identified as a detrimental factor in alkylating agent-based chemotherapy. Further rescue experiments supported the tumor suppressor role of miR-650 in the chemotherapy for melanoma. However, there were also some limitations in the investigation mechanism. Other pathways to mediate the crosstalk between the expression of lncRNA and MGMT, including canonical signaling pathways regulation, still deserve further research.

Accumulated studies indicate that lncRNAs potentially contribute to the development of various malignant tumors (10, 22). The tumor promoting effects of lncRNA POU3F3 were reported in esophageal squamous cell carcinoma and cervical cancer (13, 14). LncRNA POU3F3 is a candidate biomarker for diagnosis and prognosis (13). We evaluated the expression status of lncRNA POU3F3/miR-650/MGMT in melanoma tissues. Our results showed an increased MGMT expression in those with high lncRNA POU3F3 levels. A negative correlation between miR-650 and MGMT was also observed in melanoma tissues. Further studies also supported high lncRNA POU3F3 levels in the disease progression of patients with melanoma who received the DTIC-based chemotherapy. Cox-regression and survival analysis indicated that the expression of lncRNA POU3F3 was a detrimental factor for the progression of melanoma. The patients with lncRNA POU3F3-positive melanoma showed a shorter survival time than other patients. Our results supported a promising survival estimation value of lncRNA POU3F3 in patients with melanoma.

Our study suggested that the lncRNA POU3F3/miR-650/MGMT pathway is a novel target for improving the therapeutic efficiency of alkylating agents-based chemotherapy for melanoma. Given that the limited survival time was calculated for patients in the late stage of melanoma and the increasing trends of the incidence, further clinical trials for an lncRNA POU3F3-targeted therapy is considered as a promising strategy for melanoma treatment.

DATA AVAILABILITY STATEMENT

The original contributions presented in the study are included in the article/**Supplementary Material**, further inquiries can be directed to the corresponding author/s.

ETHICS STATEMENT

The animal study was reviewed and approved by the Animal Care and Use Committees of PLA 960th Hospital.

AUTHOR CONTRIBUTIONS

KW, QW, and S-LL were involved in the concept and design of the study. KW, QW, Y-LL, ZX, and Q-QW contributed to acquiring the data. KW, QW, LY, and S-LL contributed to the analysis and interpretation of the data. KW and S-LL drafted the manuscript. All authors revised the manuscript and approved the final version.

FUNDING

This research was supported by grants from the National Natural Science Foundation of China (81972793, 81803400, and 81502283), the Presidential Foundation of the PLA960 Hospital (2014MSO4), the Qingdao Science and Technology Program for Benefiting People Special Project 2019 (19-6-1-25-nsh), and the Qingdao Outstanding Health Professional Development Fund.

SUPPLEMENTARY MATERIAL

The Supplementary Material for this article can be found online at: https://www.frontiersin.org/articles/10.3389/fonc.2021.643613/full#supplementary-material

REFERENCES

1. Ugurel S, Rohmel J, Ascierto PA, Flaherty KT, Grob JJ, Hauschild A, et al. Survival of patients with advanced metastatic melanoma: the impact of novel therapies-update 2017. *Eur J Cancer.* (2017) 83:247–57. doi: 10.1016/j.ejca.2017.06.028
2. Weide B, Eigentler T, Catania C, Ascierto PA, Cascinu S, Becker JC, et al. A phase II study of the L19IL2 immunocytokine in combination with dacarbazine in advanced metastatic melanoma patients. *Cancer Immunol Immunother.* (2019) 68:1547–59. doi: 10.1007/s00262-019-02383-z
3. Tang J, Zhou H, Hou X, Wang L, Li Y, Pang Y, et al. Enhanced anti-tumor efficacy of temozolomide-loaded carboxylated poly(amido-amine) combined with photothermal/photodynamic therapy for melanoma treatment. *Cancer Lett.* (2018) 423:16–26. doi: 10.1016/j.canlet.2018.03.002
4. Gershenwald JE, Guy GP Jr. Stemming the rising incidence of melanoma: calling prevention to action. *J Natl Cancer Inst.* (2016) 108:djv381. doi: 10.1093/jnci/djv381
5. Tentori L, Lacal PM, Graziani G. Challenging resistance mechanisms to therapies for metastatic melanoma. *Trends Pharmacol Sci.* (2013) 34:656–66. doi: 10.1016/j.tips.2013.10.003
6. Davey RJ, van der Westhuizen A, Bowden NA. Metastatic melanoma treatment: combining old and new therapies. *Crit Rev Oncol Hematol.* (2016) 98:242–53. doi: 10.1016/j.critrevonc.2015.11.011
7. Arozarena I, Wellbrock C. Phenotype plasticity as enabler of melanoma progression and therapy resistance. *Nat Rev Cancer.* (2019) 19:377–91. doi: 10.1038/s41568-019-0154-4
8. Tawbi HA, Villaruz L, Tarhini A, Moschos S, Sulecki M, Viverette F, et al. Inhibition of DNA repair with MGMT pseudosubstrates: phase I study of lomeguatrib in combination with dacarbazine in patients with advanced melanoma and other solid tumours. *Br J Cancer.* (2011) 105:773–7. doi: 10.1038/bjc.2011.285
9. Naumann SC, Roos WP, Jost E, Belohlavek C, Lennerz V, Schmidt CW, et al. Temozolomide- and fotemustine-induced apoptosis in human malignant melanoma cells: response related to MGMT, MMR, DSBs, and p53. *Br J Cancer.* (2009) 100:322–33. doi: 10.1038/sj.bjc.6604856
10. Kopp F, Mendell JT. Functional classification and experimental dissection of long noncoding RNAs. *Cell.* (2018) 172:393–407. doi: 10.1016/j.cell.2018.01.011
11. Li W, Zheng J, Deng J, You Y, Wu H, Li N, et al. Increased levels of the long intergenic non-protein coding RNA POU3F3 promote DNA methylation in esophageal squamous cell carcinoma cells. *Gastroenterology.* (2014) 146:1714–26.e15. doi: 10.1053/j.gastro.2014.03.002
12. Guo H, Wu L, Yang Q, Ye M, Zhu X. Functional linc-POU3F3 is overexpressed and contributes to tumorigenesis in glioma. *Gene.* (2015) 554:114–9. doi: 10.1016/j.gene.2014.10.038
13. Tong YS, Wang XW, Zhou XL, Liu ZH, Yang TX, Shi WH, et al. Identification of the long non-coding RNA POU3F3 in plasma as a novel biomarker for diagnosis of esophageal squamous cell carcinoma. *Mol Cancer.* (2015) 14:3. doi: 10.1186/1476-4598-14-3
14. Chang S, Sun L, Feng G. SP1-mediated long noncoding RNA POU3F3 accelerates the cervical cancer through miR-127-5p/FOXD1. *Biomed Pharmacother.* (2019) 117:109133. doi: 10.1016/j.biopha.2019.109133
15. Viel T, Monfared P, Schelhaas S, Fricke IB, Kuhlmann MT, Fraefel C, et al. Optimizing glioblastoma temozolomide chemotherapy employing lentiviral-based anti-MGMT shRNA technology. *Mol Ther.* (2013) 21:570–9. doi: 10.1038/mt.2012.278
16. Wang Q, Jiang J, Ying G, Xie XQ, Zhang X, Xu W, et al. Tamoxifen enhances stemness and promotes metastasis of ERalpha36(+) breast cancer by upregulating ALDH1A1 in cancer cells. *Cell Res.* (2018) 28:336–58. doi: 10.1038/cr.2018.15
17. Tsubaki M, Takeda T, Obata N, Kawashima K, Tabata M, Imano M, et al. Combination therapy with dacarbazine and statins improved the survival rate in mice with metastatic melanoma. *J Cell Physiol.* (2019) 234:17975–89. doi: 10.1002/jcp.28430
18. Yang J, Meng X, Yu Y, Pan L, Zheng Q, Lin W. LncRNA POU3F3 promotes proliferation and inhibits apoptosis of cancer cells in triple-negative breast cancer by inactivating caspase 9. *Biosci Biotechnol Biochem.* (2019) 83:1117–23. doi: 10.1080/09168451.2019.1588097
19. Wan X, Xiang J, Zhang Q, Bian C. Long noncoding RNA POU3F3 promotes cancer cell proliferation in prostate carcinoma by upregulating rho-associated protein kinase 1. *J Cell Biochem.* (2018) 10:1002. doi: 10.1002/jcb.28101
20. Lang HL, Hu GW, Chen Y, Liu Y, Tu W, Lu YM, et al. Glioma cells promote angiogenesis through the release of exosomes containing long non-coding RNA POU3F3. *Eur Rev Med Pharmacol Sci.* (2017) 21:959–72. Available online at: https://www.europeanreview.org/article/12314
21. Erdmann S, Seidel D, Jahnke HG, Eichler M, Simon JC, Robitzki AA. Induced cross-resistance of BRAF(V600E) melanoma cells to standard chemotherapeutic dacarbazine after chronic PLX4032 treatment. *Sci Rep.* (2019) 9:30. doi: 10.1038/s41598-018-37188-0
22. Peng WX, Koirala P, Mo YY. LncRNA-mediated regulation of cell signaling in cancer. *Oncogene.* (2017) 36:5661–7. doi: 10.1038/onc.2017.184
23. Eich M, Roos WP, Nikolova T, Kaina B. Contribution of ATM and ATR to the resistance of glioblastoma and malignant melanoma cells to the methylating anticancer drug temozolomide. *Mol Cancer Ther.* (2013) 12:2529–40. doi: 10.1158/1535-7163.MCT-13-0136
24. Toricelli M, Melo FHM, Hunger A, Zanatta D, Strauss BE, Jasiulionis MG. Timp1 promotes cell survival by activating the PDK1 signaling pathway in melanoma. *Cancers.* (2017) 9:37. doi: 10.3390/cancers9040037
25. Yu W, Zhang L, Wei Q, Shao A. O(6)-Methylguanine-DNA methyltransferase (MGMT): challenges and new opportunities in glioma chemotherapy. *Front Oncol.* (2019) 9:1547. doi: 10.3389/fonc.2019.01547
26. Ma S, Egyhazi S, Ueno T, Lindholm C, Kreklau EL, Stierner U, et al. O6-methylguanine-DNA-methyltransferase expression and gene polymorphisms in relation to chemotherapeutic response in metastatic melanoma. *Br J Cancer.* (2003) 89:1517–23. doi: 10.1038/sj.bjc.6601270
27. Bhaskaran M, Mohan M. MicroRNAs: history, biogenesis, and their evolving role in animal development and disease. *Vet Pathol.* (2014) 51:759–74. doi: 10.1177/0300985813502820
28. Farooqi AA, Qureshi MZ, Coskunpinar E, Naqvi SK, Yaylim I, Ismail M. MiR-421, miR-155 and miR-650: emerging trends of regulation of cancer and apoptosis. *Asian Pac J Cancer Prev.* (2014) 15:1909–12. doi: 10.7314/APJCP.2014.15.5.1909
29. Han LL, Yin XR, Zhang SQ. miR-650 promotes the metastasis and epithelial-mesenchymal transition of hepatocellular carcinoma by directly inhibiting LATS2 expression. *Cell Physiol Biochem.* (2018) 51:1179–92. doi: 10.1159/000495495
30. Zhao Y, Zhu Z, Shi S, Wang J, Li N. Long non-coding RNA MEG3 regulates migration and invasion of lung cancer stem cells via miR-650/SLC34A2 axis. *Biomed Pharmacother.* (2019) 120:109457. doi: 10.1016/j.biopha.2019.109457
31. Zuo ZH, Yu YP, Ding Y, Liu S, Martin A, Tseng G, et al. Oncogenic activity of miR-650 in prostate cancer is mediated by suppression of CSR1 expression. *Am J Pathol.* (2015) 185:1991–9. doi: 10.1016/j.ajpath.2015.03.015
32. Orlandella FM, Mariniello RM, Iervolino PLC, Imperlini E, Mandola A, Verde A, et al. miR-650 promotes motility of anaplastic thyroid cancer cells by targeting PPP2CA. *Endocrine.* (2019) 65:582–94. doi: 10.1007/s12020-019-01910-3
33. Mraz M, Dolezalova D, Plevova K, Stano Kozubik K, Mayerova V, Cerna K, et al. MicroRNA-650 expression is influenced by immunoglobulin gene rearrangement and affects the biology of chronic lymphocytic leukemia. *Blood.* (2012) 119:2110–3. doi: 10.1182/blood-2011-11-394874
34. Feng L, Xie Y, Zhang H, Wu Y. Down-regulation of NDRG2 gene expression in human colorectal cancer involves promoter methylation and microRNA-650. *Biochem Biophys Res Commun.* (2011) 406:534–38. doi: 10.1016/j.bbrc.2011.02.081

Conflict of Interest: The authors declare that the research was conducted in the absence of any commercial or financial relationships that could be construed as a potential conflict of interest.

frontiers in Oncology

ORIGINAL RESEARCH
published: 31 March 2021
doi: 10.3389/fonc.2021.650165

Proteome Analysis of USP7 Substrates Revealed Its Role in Melanoma Through PI3K/Akt/FOXO and AMPK Pathways

Lanyang Gao[1,2†], Danli Zhu[1†], Qin Wang[1†], Zheng Bao[1], Shigang Yin[2,3], Huiyan Qiang[4], Heinrich Wieland[1], Jinyue Zhang[1], Alexander Teichmann[1] and Jing Jia[5,6*]*

[1] Sichuan Provincial Center for Gynaecology and Breast Disease, The Affiliated Hospital of Southwest Medical University, Luzhou, China, [2] Academician (Expert) Workstation of Sichuan Province, The Affiliated Hospital of Southwest Medical University, Luzhou, China, [3] Laboratory of Nervous System Disease and Brain Functions, The Affiliated Hospital of Southwest Medical University, Luzhou, China, [4] Department of Outpatient, The Affiliated Hospital of Southwest Medical University, Luzhou, China, [5] Department of Anesthesiology, The Affiliated Hospital of Southwest Medical University, Luzhou, China, [6] Laboratory of Anesthesiology, Southwest Medical University, Luzhou, China

OPEN ACCESS

Edited by:
Suzie Chen,
The State University of New Jersey, United States

Reviewed by:
Gagan Chhabra,
University of Wisconsin-Madison, United States
Changzhao Li,
Creighton University, United States

***Correspondence:**
Jing Jia
jiajing@swmu.edu.cn
Alexander Teichmann
teichmann2020@163.com

[†]These authors have contributed equally to this work

Specialty section:
This article was submitted to Skin Cancer, a section of the journal Frontiers in Oncology

Received: 07 January 2021
Accepted: 15 March 2021
Published: 31 March 2021

Citation:
Gao L, Zhu D, Wang Q, Bao Z, Yin S, Qiang H, Wieland H, Zhang J, Teichmann A and Jia J (2021) Proteome Analysis of USP7 Substrates Revealed Its Role in Melanoma Through PI3K/Akt/FOXO and AMPK Pathways. Front. Oncol. 11:650165. doi: 10.3389/fonc.2021.650165

The ubiquitin-specific protease 7 (USP7), as a deubiquitinating enzyme, plays an important role in tumor progression by various mechanisms and serves as a potential therapeutic target. However, the functional role of USP7 in melanoma remains elusive. Here, we found that USP7 is overexpressed in human melanoma by tissue microarray. We performed TMT-based quantitative proteomic analysis to evaluate the A375 human melanoma cells treated with siRNA of USP7. Our data revealed specific proteins as well as multiple pathways and processes that are impacted by USP7. We found that the phosphatidylinositol-3-kinases/Akt (PI3K-Akt), forkhead box O (FOXO), and AMP-activated protein kinase (AMPK) signaling pathways may be closely related to USP7 expression in melanoma. Moreover, knockdown of USP7 in A375 cells, particularly USP7 knockout using CRISPR-Cas9, verified that USP7 regulates cell proliferation *in vivo* and *in vitro*. The results showed that inhibition of USP7 increases expression of the AMPK beta (PRKAB1), caspase 7(CASP7), and protein phosphatase 2 subunit B R3 isoform (PPP2R3A), while attenuating expression of C subunit of vacuolar ATPase (ATP6V0C), and peroxisomal biogenesis factor 11 beta (PEX11B). In summary, these findings reveal an important role of USP7 in regulating melanoma progression *via* PI3K/Akt/FOXO and AMPK signaling pathways and implicate USP7 as an attractive anticancer target for melanoma.

Keywords: melanoma, USP7, deubiquitinating enzyme, quantitative proteomics, PI3K/Akt/FOXO pathways

INTRODUCTION

Malignant melanomas are an extremely aggressive skin cancer induced by ultraviolet (UV) radiation that arises from melanocytes (1). The global prevalence of melanomas has been growing at an alarming rate over the last several years (2). Until now, there has been no effective therapy for melanoma due to its metastatic potential. Therefore, it is crucial to explore the molecular mechanisms of melanoma progression.

USP7, as a deubiquitinating enzyme (DUB), participates in regulating many cellular process, including tumor progression (3, 4), immune dysfunction (5), DNA damage (6), and epigenetic regulation (7). Among these processes, the roles of USP7 in tumor progression have been extensively characterized as either p53-dependent or p53-independent. Under normal conditions, USP7 prefers to associate with murine double minute2 (MDM2), a E3 ubiquitin ligase targeting p53 for degradation by the proteasome, and stabilizes MDM2, resulting in p53 turnover (8, 9). However, upon cellular stress, USP7 switches from stabilizing MDM2 to p53 (8). Beyond the USP7-MDM2-p53 axis, USP7 also affects oncogenesis through other modulators, including regulation of oncoproteins (such as REST, TRRAP, and cMyc) (10, 11), PTEN (12), FOXO proteins (13), and the Rb protein (14). Therefore, in the past decades, researchers have explored its effects on tissues including the bladder (15), prostate (12), colon (16), lung (17), liver (18), ovary (19), brain (14), breast (20), and glioma (21). All these studies demonstrated that the role of USP7 is tumor suppressive or oncogenic, depending on the context of the cancers and its substrates. However, the expression and role of USP7 in melanoma remains to be elucidated.

We confirmed that USP7 was highly expressed in clinical melanoma tissues and its loss of function significantly inhibited proliferation of melanoma cells and promoted apoptosis. In this study, mass spectrometry-based deep proteomic analysis was carried out following USP7 knockdown to explore the mechanism of action of USP7 in regulating melanoma growth. Our results revealed that USP7 acts as an oncogene in melanoma through mediating PI3K/AKT/FOXO as well as AMPK signaling pathways, and through some new pathways, such as peroxisome and lysosome signaling pathways. Concomitantly, we found ATP6V0C and PEX11B may be new substrates of USP7, which requires further confirmation. In summary, these data suggest that USP7 is a tumor promoter and can serve as a therapeutic target for melanoma, potentially as a novel therapeutic strategy to respond to the resistance of advanced melanoma to chemotherapy.

MATERIALS AND METHODS

Tissue Microarray and TCGA Analysis

The tissue microarray (ME241b) was purchased from Alenabio (Xian, Shanxi, China). This microarray have total 21 tissue sample, including normal skin tissue, melanoma from skin, esophagus, parotid, anus and rectum. All experiments were performed following the protocols and ethical standards of this company. Anti-USP7 (Santa Cruz, 1:50) was used to immunolabel the paraffin-embedded sections. USP7 expression in tissues was evaluated. Kaplan–Meier survival analyses for The Cancer Genome Atlas (TCGA) dataset was conducted using the online database (www.oncolnc.org). P values were calculated with log-rank test. Patients were stratified into "low" and "high" expression based on autoselect best cutoff in the database.

Immunohistochemical Staining and Intensity Analysis

Immunohistochemistry was performed as previously described (22). The tissues sections were blocked by goat serum and incubated with primary antibody (1:50) and then incubated with biotinylated secondary antibody (1:100). Finally, the data were analyzed with ImageJ software.

Cell Lines and Cell Culture

A375 human melanoma cells, mouse B16 melanoma cells, and 293T cells were cultured in Dulbecco's modified Eagle's medium (HyClone) with high glucose (4.5 g/l) containing 100 IU/ml penicillin/streptomycin and 10% fetal bovine serum (Gibco). All of the cells were cultured at 37°C with 5% CO_2.

Transfection Assay

For siRNA transfection, siRNAs targeting USP7 and lipofectamine RNAiMax reagent (Invitrogen) were prepared according to the manufacturer's instructions. The siRNA sequences were as follows: si-NC (sense 5'-UUC UCC GAA CGU GUC ACG UTT-3; antisense 5'-ACG UGA CAC GUU CGG AGA ATT-3') and si-USP7 (sense 5'-GGA CUA UGA CGU GUC UCU UTT-3'; antisense 5'-AAG AGA CAC GUC AUA GUC CTT-3').

Stable A375 USP7-ShRNA Knockdown Establishment

Sequences of shRNAs are shown as following: ShRNA-NC: 5'-CCTAAGGTTAAGTCGCCCTCG-3'; ShRNA-USP7: 5'-CGTGGTGTCAAGGTGTACTAA-3'.

pCMV-dR8.2 dvpr, pLP/VSVG, and lentiviral DNA constructs (pLKO.1-TRC for USP7) were co-transfected into 293T cells using LipoFilter (HANBIO). Supernatant was collected after 24 h transfection then added to infect A375 cells, cells were selected with puromycin (1 ug/ml) over 7 days.

Stable B16 CAS9-USP7 Knockout Establishment

USP7 CRISPR/Cas9 plasmid was purchased from Santa Cruz and transfected into B16 cells. After 48 h transfection, B16 cells were cultured into 96-well plates at a concentration of 1 cell/well. Single colonies were detected by immunoblotting analysis. USP7 knockout B16 cells and control cells were defined as B16 USP7 KO and B16 WT, respectively.

Western Blot Analysis

Total cellular proteins were obtained and denatured, and the A375 nucleus and cytoplasm proteins were obtained by using the Nucleus and Cytoplasmic Protein Extraction Kit (Sangon Biotech), separated by sodium dodecylsulfate polyacrylamide gel electrophoresis (SDS–PAGE) and transferred to nitrocellulose filter membranes NC membranes. The antibodies used are shown in **Table 1**.

TABLE 1 | List of All Antibodies and Sources.

antibody	product code	company	host species	dilution
β-Actin	BS6007M	Bioworld	mouse	1:5000
Usp7	sc-377147	Santa Cruz	mouse	1:400
Casp7	A1524	Abclonal	rabbit	1:1000
ATP6V0C	A16350	Abclonal	rabbit	1:500
PRKAB1	A12491	Abclonal	rabbit	1:1000
PEX11B	A18321	Abclonal	rabbit	1:500
PARP1	A19596	Abclonal	rabbit	1:500
Phospho-FOXO4-S197	AP0177	Abclonal	rabbit	1:1000
FOXO4	A3307	Abclonal	rabbit	1:500
PPP2R3A	A17395	Abclonal	rabbit	1:500
AKT	#9272	Cell Signaling	rabbit	1:1000
P-Akt1(Ser473)	AF1546	Beyotime	rabbit	1:600
p-FOX01(Thr24)/Fox03a(Thr32)/Fox04(Thr28)	#2599	Cell Signaling	rabbit	1:1000
P-AMPKB1-S108	AP0597	Abclonal	rabbit	1:600
Ki-67	Sc-23900	Santa Cruz	mouse	1:200
P53	#2524	Cell Signaling	mouse	1.1000
MDM2	Sc-965	Santa Cruz	mouse	1:500
Rabbit IgG	AS014	Abclonal	—	1:20000
Mouse IgG	AS003	Abclonal	—	1:20000

Cell Clonogenic Assay

A clonogenic assay was performed as previously described (23). Wild-type cells and USP7 loss cells (A375 shRNA-USP7 and B16 WT/USP7-KO) were plated into six well plates in triplicate. Then wild-type cells were exposed to the USP7 inhibitor gen6776 (10 μm). The plates were washed with PBS and stained with crystal violet on the 14th day. The cells were observed and photographed.

Immunofluorescence

A375 cells were transfected with si-NC/USP7. After 24 h, cells were fixed with 4% paraformaldehyde and blocked with 0.2% Triton X-100 and 5% FBS in PBS. Samples were incubated with primary antibody FOXO4 (1:100, Abclonal) and Ki-67 (1:200, Santa Cruz) in PBS overnight at 4 °C. Samples were incubated with secondary FITC-labeled anti-rabbit and Cy3-labeled anti-mouse antibody (Beyotime) for 1 h at ambient temperature. Cells were visualized with an Olympus X71 fluorescence microscope.

Cell Cycle and Apoptosis Assay

For the cell cycle assay, 1 ml of 70% ethanol was added to cells and cells were resuspended overnight. Then the cells were incubated with 50 μg/ml of propidium iodide (PI), 0.2% of Triton-X-100, and 100 μg/ml of RNase complex for 30 min in the dark. For the cell apoptosis analysis, cells were resuspended for 30 min with a complex of 500 μl Annexin VFITC binding buffer, 5 μl PI, and 5 μl Annexin V-FITC. Finally, the two samples were assessed by flow cytometry.

Quantitative Reverse Transcription PCR (RT-qPCR) Analysis

Total RNA was extracted by TRIzol reagent (Invitrogen), and HiScript III RT SuperMix for RT-qPCR (Vazyme) was used for reverse transcription according to the manufacturer's instructions. The primers used for RT-qPCR are shown as follows: p27^{Kip1} (forward): 5'-GGCTAACTCTGAGGACACGCA-3'; p27^{Kip1} (reverse): 5'-TGGGGAACCGTCTGAAACAT-3'; GAPDH (forward): 5'-GGAGCGAGATCCCTCCAAAAT-3'; and GAPDH (reverse): 5'-GGCTGTTGTCATACTTCTCATGG-3'.

Proteomic Sample Preparation

The siRNA transfected A375 cell samples were disrupted in SDT (4% (w/v)) SDS, 100 mM Tris/HCl (pH7.6, 0.1M DTT) lysis buffer. The protein concentration was determined by BCA (bicinchoninic acid) assay.

Tandem mass tag (TMT) labeling and high pH reversed-phase peptide fractionation and LC-MS/MS analysis. Proteomic samples were analyzed by LC-MS/MS as described in **Supplement 1**.

Protein Identification and Quantitation

LC-MS/MS spectra were searched using the MASCOT engine (Matrix Science, London, UK; version 2.2) embedded into Proteome Discoverer 1.4 (Thermo Scientific). The protein ratios were calculated as the median of only unique peptides of the protein. All peptide ratios were normalized by the median protein ratio. The median protein ratio should be 1 after the normalization.

Animal Experiments

Nude female mice (Balb/c) and C57BL/6 female mice were purchased from the Chengdu Dossy Laboratory Animals Company. All of the animal procedures were approved by the Laboratory Animal Management Committee of the Affiliated Hospital of Southwest Medical University. The animals were treated as described in **Supplement 2**.

Statistical Analysis

The data shown in the figures are representative of three or more independent experiments and were analyzed by the one-way Student's *t*-test, and $P < 0.05$ was considered statistically significant. Where exact P-values are not shown, statistical significance is shown as $^*P < 0.05$, $^{**}P < 0.01$.

RESULTS

USP7 Is Overexpressed in Melanoma and Predicts Clinical Outcomes

Previous studies have demonstrated that USP7 plays a prominent role in tumor development and progression (12, 14, 18). We found that the expression of the USP7 protein was increased in melanoma tissues compared with normal tissue by immunohistochemistry (**Figures 1A, B**). Furthermore, we performed Kaplan–Meier analysis in melanoma patients of TCGA. The results showed that USP7 expression was negatively correlated with overall survival of melanoma patients in the TCGA dataset ($P < 0.05$, **Figure 1C**). Collectively, these results demonstrate that USP7 is overexpressed in human melanoma and predicts clinical outcomes.

USP7 Loss Suppresses Melanoma Growth

To explore USP7 expression levels relative to melanoma development and progression, we built USP7 knockdown A375 cells by shRNA or siRNA and USP7 KO B16 cells (**Figure 2A**). The cell colony formation assay results revealed that loss of USP7 function dramatically suppressed colony formation (**Figure 2B**). Furthermore, **Figures 2C–E** showed that poly ADP-ribose polymerase (PARP) cleavage and cellular apoptosis were induced by USP7 inhibition. Concomitantly, USP7 downregulation significantly arrested the cell cycle, increasing the proportion of A375 cells in the G1 phase and decreasing the proportion in the S phase (**Figures 2G, H**). Expression of the proliferation marker Ki67 was also reduced by USP7 downregulation (**Figure 2F**). These findings support a role for USP7 in promoting growth of melanoma cells.

Protein Identification and Bioinformatics Analysis

To clarify the mechanism of action of USP7 in melanoma, we compared whole-cell proteomes in WT and USP7 knockdown A375 cells using TMT quantitative proteomics technology. As a result, we identified a total of 5696 proteins with expression changes of 1.1 times or more and P values of < 0.05. In the si-USP7 vs si-NC group, we found 101 upregulated differentially expressed proteins (DEPs) and 71 downregulated DEPs

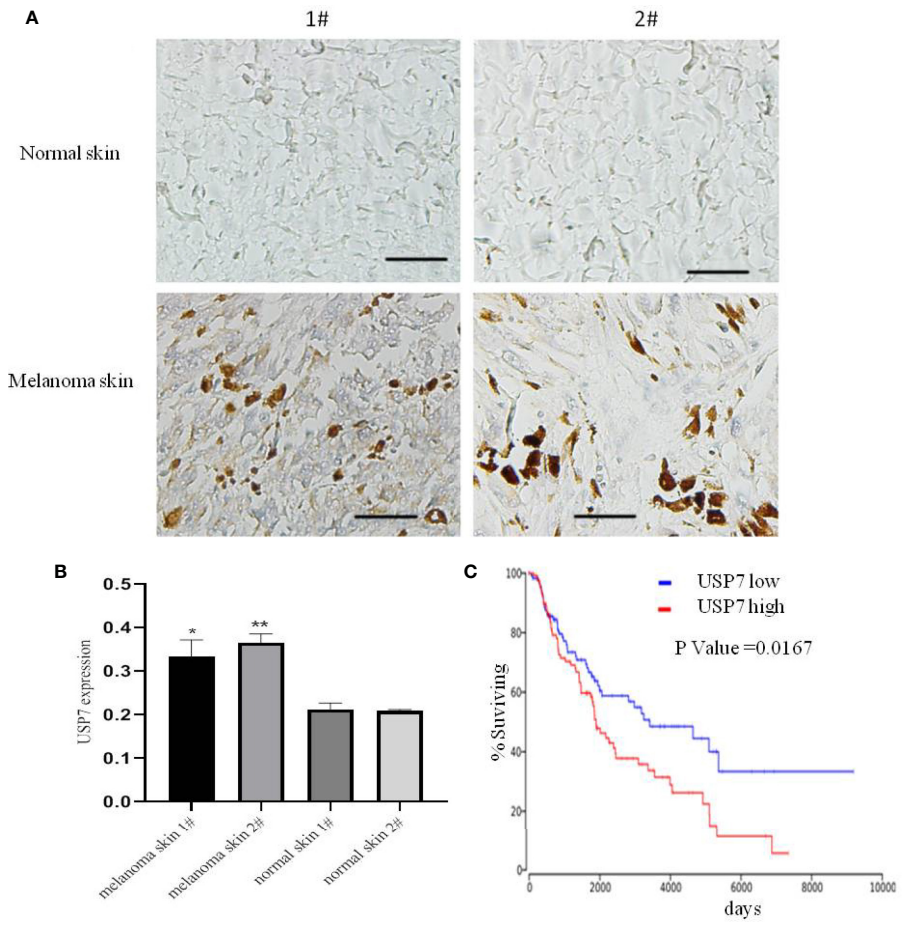

FIGURE 1 | USP7 is overexpressed in melanoma and predicts clinical outcome. **(A, B)** Immunohistochemical analysis of USP7 in human normal skin and melanoma tissue. The data were analyzed with ImageJ software. Scale bar, 50 μm. *p<0.05,**p<0.01. **(C)** Kaplan-Meier curves from patients with melanoma expressing low and high USP7 from the TCGA protein expression array data.

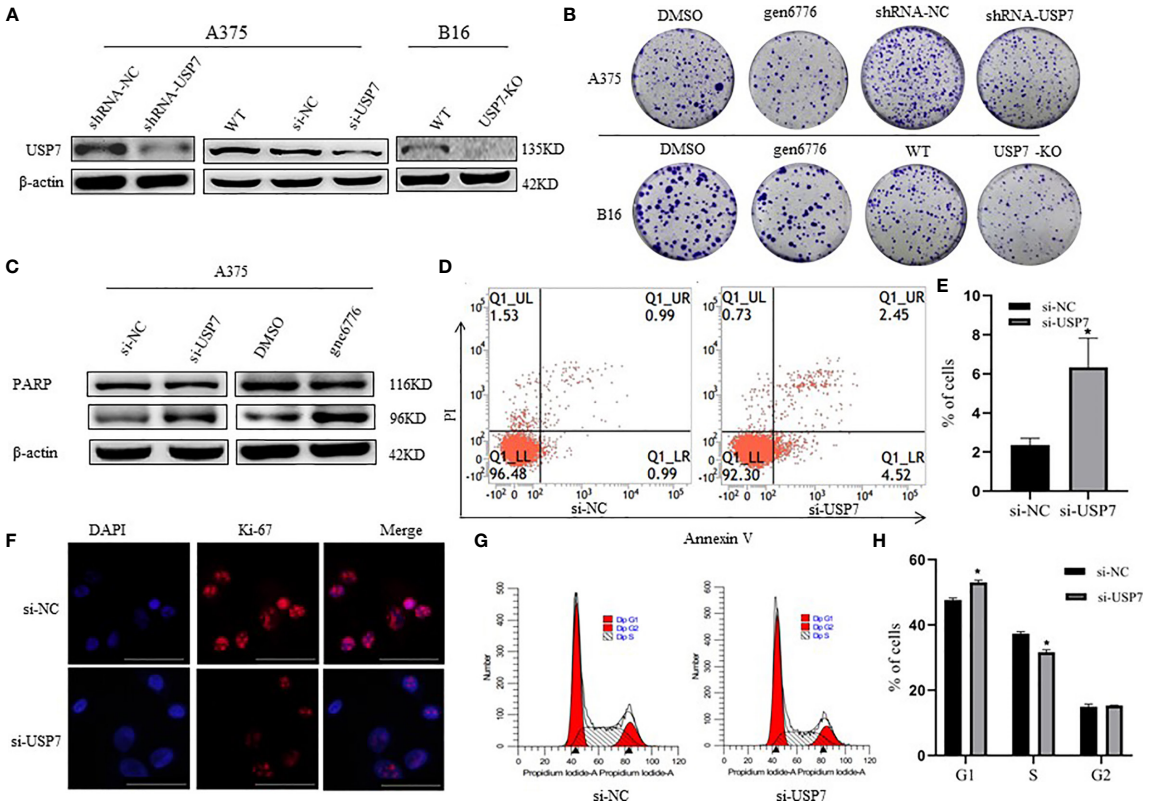

FIGURE 2 | Effects of USP7 on melanoma cell line growth. **(A, B)** Protein lysates were extracted from A375 cells transiently expressing USP7 siRNA and stable control shRNA or USP7 shRNA and B16 cells deleted the USP7 gene using the CRISPR/Cas9 editing system (USP7 KO). Western blotting analysis was performed to determine the expression of USP7. **(B)** Cells were collected from the indicated cells with gen6776 (USP7 inhibitor), USP7 shRNA or USP7 knockout treatment. Colony formation assay was performed and representative images are shown. **(C–E)** A375 cells were transfected with USP7 siRNAs for 48 h and detected with Annexin V-FITC/PI staining followed by flow cytometry analysis. Cell death populations are shown. Western blotting analysis was used for PARP expression. **(F–H)** A375 cells were treated as described in **(C–E)**. Immunofluorescence staining of Ki-67 of A375 cells was observed using fluorescence microscope. Red: Ki-67; blue: nucleus. Typical images are shown. Scale bars: 50 μm. Analysis of cell cycle by FCM is described in the *Materials and Methods*. Data are represented as the mean ± SEM of three independent experiments, each in triplicate; bars, SEM. *P ≤ 0.05 vs. control.

(**Supplement 4**). **Supplement 1B** shows a hierarchical clustering analysis of all 172 DEPs.

A total of 5696 proteins were annotated to molecular function, biological process, and cellular components by GO analysis. Then, the Fisher's exact test was used to analyze the GO function enrichment of the DEPs. The top 10 enriched GO terms within each major functional category are shown in **Figure 3A** and **Supplement 1C**. In the three categories, the most significant terms are all associated with microtubule-related functions (**Figure 3C**).

In the biological process and molecular function category, we noted that many terms are related to nucleoside-containing compound biosynthesis and metabolism (**Figure 3A**). We also identified significantly altered protein-protein interaction networks in the protein sets, as shown in **Figure 3B**. Among proteins involved in ion transport and binding (**Figure 3B**), ATP6V0C had the most decreased protein expression following USP7 knockdown, which was also confirmed by western blot (**Figure 4A**). Protein-protein interaction networks then revealed another four distinct clusters (**Figure 3B**), corresponding to proteins related to DNA repair, post-translational protein modification, microtubule motor activity, and ubiquitin-protein transferase activity.

To explore how USP7 plays roles in melanoma by these cellular processes, DEPs were then mapped to the reference pathway in the KEGG database. There were 172 DEPs that were mapped to 178 signaling pathways. Phosphatidylinositol 4,5-bisphosphate 3-kinase catalytic subunit beta isoform (PIK3CB) is the protein that most commonly participates in signaling pathways, followed by PRKAB1, CASP7, PPP2R3A, and ATP6V0C. We confirmed these proteins in both A375 and B16 cell lines (**Figure 4A**). Concomitantly, only the pathways with at least three or more DEPs are shown in **Figure 3C**. In this study, we mainly focused on the PI3K-Akt, FOXO, and AMPK signaling pathways to clarify the roles of USP7 in melanoma.

Validation of Proteomic Data

To validate our mass spectrometry results, we investigated the most striking DEPs including ATP6V0C and PEX11B, PRKAB1 (AMPK), CASP7, and PPP2R3A, which participate in many pathways (**Figure 4A**). Altogether, these proteins were confirmed in both melanoma cell lines after USP7 loss, which indicated that

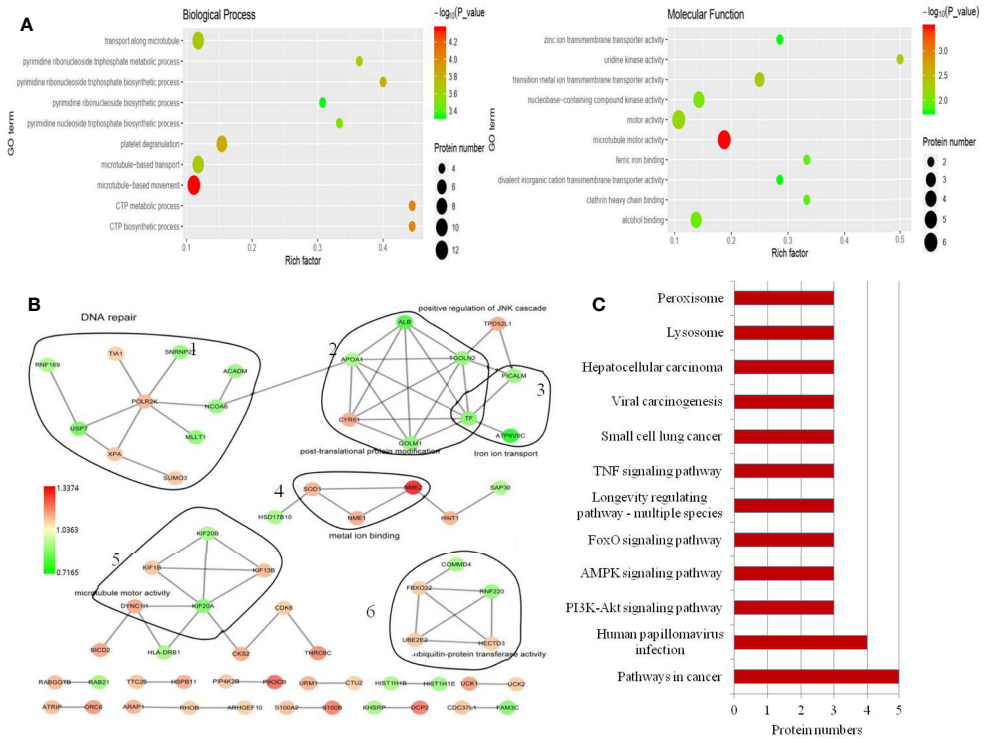

FIGURE 3 | GO annotation and KEGG pathway analysis of the DEPs. **(A)** Top 10 enriched GO terms under "biological process". Term01, microtubule-based movement; term02, CTP metabolic process; term03, CTP biosynthetic process; term04, platelet degranulation; term05, pyrimidine ribonucleoside triphosphate biosynthetic process; term06, microtubule-based transport; term07, transport along microtubule; term08, pyrimidine ribonucleoside triphosphate metabolic process; term09, pyrimidine nucleoside triphosphate biosynthetic process; term10, pyrimidine ribonucleoside biosynthetic process. Top 10 enriched GO terms under "molecular function". Term01, microtubule motor activity; term02, transition metal ion transmembrane transporter activity; term03, uridine kinase activity; term04, motor activity; term05, nucleobase-containing compound kinase activity; term06, alcohol binding; term07, clathrin heavy chain binding; term08, ferric iron binding; term09, zinc ion transmembrane transporter activity; term10, divalent inorganic cation transmembrane transporter activity. **(B)** Protein–protein interaction network generated with STRING and visualized with Cytoscape for DEPs. DEPs are represented as round nodes. The red node indicates upregulation and green node indicates downregulation of the DEPs. Corresponding to proteins related to DNA repair (1), post-translational protein modification and iron ion transport (2), microtubule motor activity (3), metal ion binding (4) and ubiquitin-protein transferase activity (5), ubiquitin-protein transferase activity (6). **(C)** Enriched KEGG pathways.

USP7 may control the signaling pathways involving in these proteins to promote melanoma development and progression. For example, Kaplan–Meier analysis of ATP6V0C and CASP7 in melanoma patients of TCGA showed that expression of the two proteins was negatively and positively correlated with overall survival of melanoma patients (**Supplement 5**), respectively.

Reduction of USP7 Mediates Signaling Pathways Associated With Cancer Activity

Immunoblotting results showed that phosphorylated AMPK was significantly increased following USP7 loss in both cell lines A375 and B16 (**Figure 4B**), which may be due to an increase in PRKAB1. Previous studies have proposed a tumor-suppressing function of activated AMPK (24, 25). Accordingly, USP7 loss inhibits melanoma growth by partially activating the AMPK signaling pathway.

Consistent with previous studies on USP7 (12, 13, 26), our results suggest that USP7 can activate the PI3K/Akt signaling pathway to promote cell survival by phosphorylating and inhibiting FOXO transcription factors, such as FOXO1, FOXO3a, and FOXO4. As shown in **Figures 4A** and **B**, phosphorylated Akt decreases due to the increase in PPP2R3A, which can dephosphorylate Akt. Further research has found that Akt phosphorylation reduction results in FOXO dephosphorylation at Akt-induced sites, including P-FOXO4(Thr28), P-FOXO3a(Thr32), and P-FOXO1(Thr24) (**Figure 4B**). Previous studies have indicated that a decrease in FOXO phosphorylation promotes their entry into the nucleus and ultimately increases transcriptional activity towards target genes, including the cell cycle arrest gene $p27^{kip1}$ (26). To further confirm this result in melanoma, FOXO4 was selected for detecting its intracellular localization by immunofluorescence and nuclear/cytosol protein fractionation assay and its target gene $p27^{kip1}$ expression levels. Our results showed that FOXO4 was mainly present in the nuclear compartment after USP7 downregulation (**Figures 4C, D**), which ultimately promoted $p27^{kip1}$ expression (**Figure 4E**).

Taken together, our results suggest that loss of USP7 function inhibits the melanoma cell cycle and promotes cell apoptosis by mediating AMPK and PI3K/Akt/FOXO signaling pathway activity. The results also demonstrated that USP7 can upregulate MDM2, and inhibit the expression of p53.

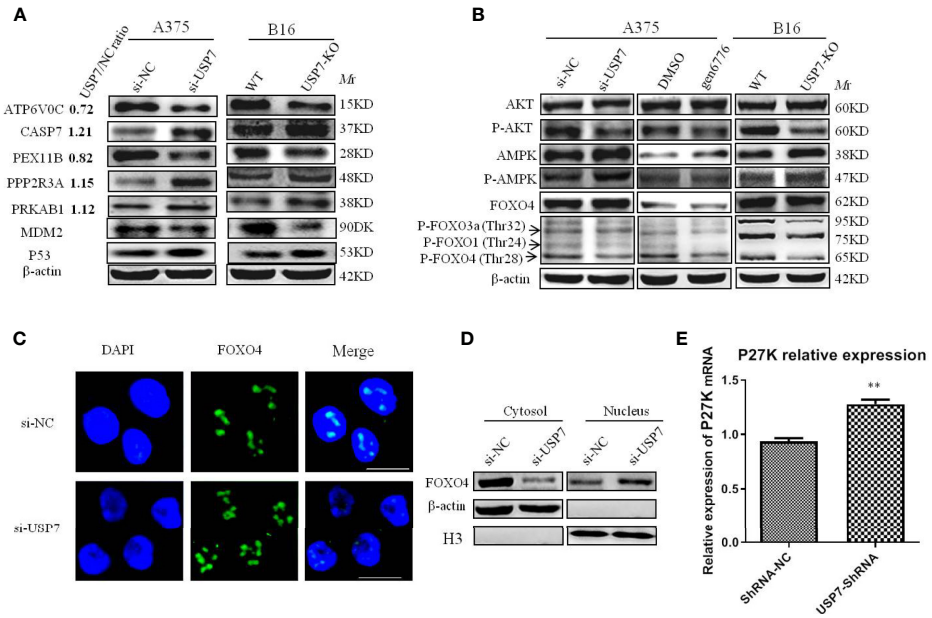

FIGURE 4 | Multiple proteins and PI3K/AKT/FOXO and AMPK signaling pathways are affected by removal of USP7. USP7 was inhibited by siRNA or inhibitor gen 6776 in A375 cells and was knocked out through CRISPR/Cas9 in B16 cells. **(A)** Proteins exhibiting significant changes between USP7 knockdown A375 cells and A375 cells and USP7-KO B16 cells. Protein names, USP7/NC ratio, and the expression of indicated proteins by western blotting are shown. **(B)** The key proteins levels of the PI3K/Akt/FOXO and AMPK signaling pathways were analyzed by western blotting after inactivation of USP7 in A375 cells and B16 cells. **(C, D)** The expression of FOXO4 in the nucleus and cytosol was detected by immunofluorescence and western blotting, respectively. Green, FOXO4; blue, nucleus. Scale bar 50 μm. **(E)** Representative levels of $P27^{kip1}$ by quantitative real-time PCR. Data are represented as the mean ± SEM of three independent experiments, each in triplicate; bars, SEM. **P ≤ 0.01 vs. control.

USP7 Loss Suppresses Melanoma Growth in A375 and B16 Xenografts

ShRNA-USP7 A375 cell and USP7-KO B16 cell xenograft models were established in Balb/c nude mice and C57BL/6 mice, respectively. As shown in **Figures 5A–C**, there was a significant reduction in tumor growth and tumor weight after USP7 loss, with tumor volumes inhibited by 64.7% for A375 and 46.4% for B16. No significant change was observed in the body weight between the control and USP7 loss groups.

To further validate the mechanism of action of USP7 as an oncogene in melanoma *in vivo*, the expression levels of the proteins indicated in **Figure 5** were analyzed by immunoblotting and immunohistochemistry. **Figures 5E** (The Western blot analysis of proteins in mice tumors were evaluated **Supplement 6**) and **5F** show that in line with the proteomic results, the indicated proteins have significant changes on levels in both A375 and B16 cells after USP7 loss.

DISCUSSION

We proved that USP7 levels are higher in melanoma than that of normal skin and are associated with poorer prognosis based on analysis from TCGA datasets. These findings implied that USP7 is implicated in melanoma development and progression. In this study, we demonstrated that loss of USP7 function inhibits cell growth by promoting cell cycle arrest and apoptosis in A375 and B16 cells. Furthermore, proteomic data analysis and western blot results showed the importance of the classical signaling pathways PI3K/Akt/FOXO and AMPK, and that new biological processes involve proteins such as ATP6V0C, CASP7, and PEX11B, which play crucial roles in USP7 mediating melanoma growth. USP7 knockdown decreases Akt phosphorylation and then causes FOXO phosphorylation reduction, which ultimately increases FOXO accumulation in the nucleus and promotes $P27^{kip1}$ gene expression that arrests the cell cycle (**Figure 4**).

In addition to our studies, several groups have shown that there are two factors of Akt phosphorylation reduction that must be addressed. The first involves PPP2R3A, a regulatory subunit of the protein phosphatase 2 (PP2A), which is significantly increased after USP7 downregulation. A previous study has shown that PP2A can directly dephosphorylate Akt, inhibiting PI3K/Akt signaling pathway activity (27). The second relates to the intracellular localization of PTEN, which antagonizes the PI3K-AKT pathway. Previous reports have demonstrated that USP7 induces PTEN deubiquitination, causing exclusion of PTEN from the nucleus and subsequently increasing in the PI3K/AKT signaling pathway (28). Therefore, USP7 downregulation accumulates monoubiquitinated PTEN in the nucleus, reducing Akt phosphorylation. Collectively, these two factors explain how USP7 plays a role in melanoma through the PI3K-AKT pathway.

Further research has shown that Akt phosphorylation reduction induces FOXO dephosphorylation at Akt-induced sites. It has been reported that phosphorylated FOXO induced by activated Akt stays

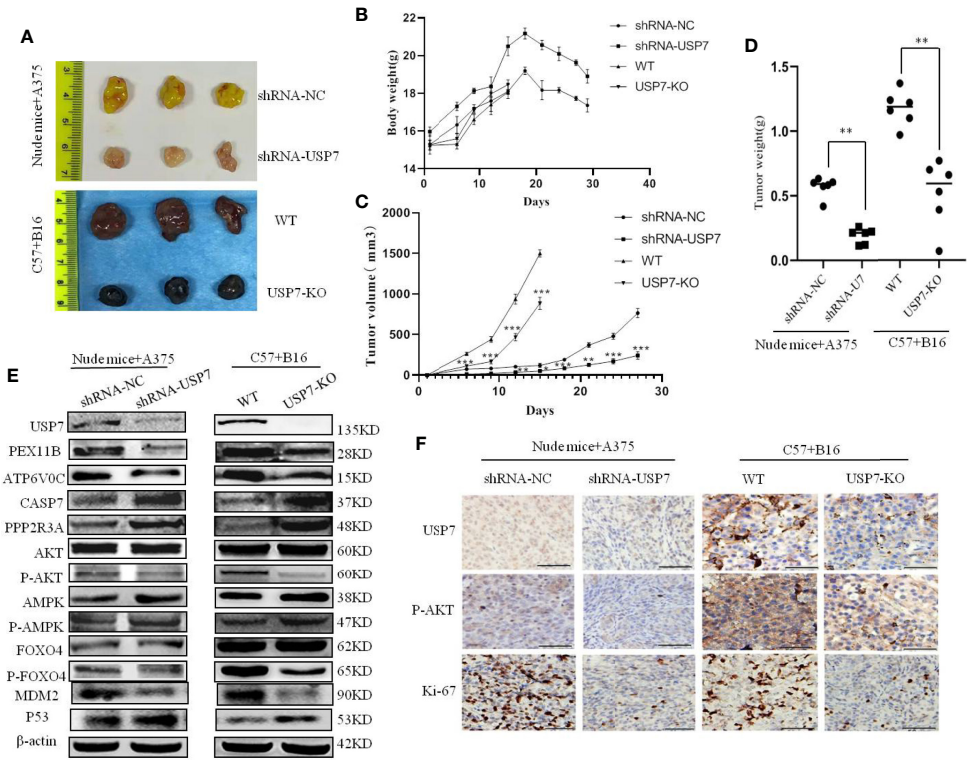

FIGURE 5 | Loss of USP7 function suppresses melanoma tumor growth *in vivo*. Balb/c nude mice and C57BL/6 mice were subcutaneously transplanted with A375 cells stably expressing USP7 shRNA and USP7-KO B16 cells, respectively, as indicated in the *Materials and Methods*. **(A)** Images of harvested mice and tumors after treatment from A375 shRNA-NC cells, A375 shRNA-USP7 cells, B16 WT melanoma cells, or B16 USP7-KO melanoma cells. **(B)** Mouse weight evolution during the experiment. The values are expressed as the mean. **(C)** Tumor size was determined by caliper measurement and the data was converted to tumor growth curves. **(D)** Tumor tissues were harvested and weighed at the end of study (**P < 0.01. Error bar = S.D.). **(E, F)** Expression of indicated proteins in tumor tissues was measured by western blotting and immunohistochemistry.

in the cytosol and is imported to the nucleus through dephosphorylation to induce the expression of a series of target proteins that regulate metabolism, the cell cycle, and apoptosis (29). Our results indicate that phosphorylation of FOXO4 (Thr28), FOXO3a (Thr32), and FOXO1 (Thr24) significantly decreases and FOXO4 substantially accumulates in the nucleus following USP7 knockdown. FOXO4 accumulation in the nucleus may be caused by weak deubiquitination of USP7 downregulation. Similar to PTEN, USP7-induced FOXO4 deubiquitination results in nuclear export and eliminates its transcriptional activity (13).

KEGG analysis of the proteomic data and western blot results reveal that the AMPK signaling pathway plays a role in USP7 mediating melanoma growth. PRKAB1, a regulatory subunit of AMPK, has a remarkable up-regulation following loss of USP7 function, which ultimately raises AMPK phosphorylation and activates AMPK signaling. It is well-documented that AMPK signaling has an anti-proliferative role. Dai et al. have reported that activated AMPK signaling inhibits survival and proliferation and activates apoptosis in colorectal cancer cells (30). Consequently, we conclude that USP7 plays a role in melanoma through AMPK signaling.

USP7 as a context-specific modulator mediates p53-dependent apoptosis *via* controlling MDM2 stability. Inhibition of USP7 also induces endoplasmic reticulum (ER) stress due to the accumulation of polyubiquitinated protein substrates in cancer cells, which leads to increased intracellular reactive oxygen species (ROS). Increased ROS can cause apoptosis in these cells. Our results indicated that USP7 knockdown also induces apoptosis (**Figure 2**). A lack of USP7-dependent deubiquitylation of MDM2 may lead, through enhanced breakdown of MDM2, to accumulation of p53 in melanoma. However, our data suggests additional involvement of USP7 in alternative apoptotic pathways, possibly *via* modification of a caspase7 dependent mechanism. In line with these observations, we found cleaved PARP1 levels increased upon USP7 removal. Similarly, in colon carcinoma cells, USP7 is involved in apoptotic pathways by modifying caspase3 levels (31). Therefore, we confirm that USP7 also as an oncogene inhibits p53-dependent apoptosis in melanoma, as in colon cancer.

ATP6V0C and PEX11B, proteins regulated by USP7, were confirmed in both melanoma cell lines by western blot. It has been reported that ATP6V0C is involved in the migration and invasion of prostate carcinoma cells (32). In addition, enriched KEGG pathways show that ATP6V0c and PEX11B are key protein of lysosome and peroxisome pathways, respectively. These findings provide a cue that USP7 plays roles in melanoma through these two pathways that have not been reported in other cancers.

Previous results have demonstrated that inhibition of USP7 induces genotoxic stress and DNA damage in chronic lymphocytic leukemia (CLL) cells (33). We also obtained similar results in melanoma cells following USP7 knockdown. GO analysis suggests that the DEPs RNF169, XPA, MLLT1, and NCOA6 participate in DNA repair (**Figure 3**). One of these, E3 ubiquitin ligase RNF169 is deubiquitylated and stabilized by USP7 in response to DNA double-strand breaks (34), and is significantly decreased in the USP7 knockdown, which suggests USP7 in melanoma also plays a role in DNA repair.

DATA AVAILABILITY STATEMENT

The authors acknowledge that the data presented in this study must be deposited and made publicly available in an acceptable repository, prior to publication. Frontiers cannot accept an article that does not adhere to our open data policies.

ETHICS STATEMENT

The animal study was reviewed and approved by the Laboratory Animal Management Committee of the Affiliated Hospital of Southwest Medical University.

AUTHOR CONTRIBUTIONS

JJ and AT designed the study. LG and JZ drafted the manuscript. DZ, JJ, and LG conducted experiments, and the other authors took part in literature collection and data analysis. All authors contributed to the article and approved the submitted version.

FUNDING

This work was supported by the Key Fund and the Youth Fund and the Transformation Project of Science and Technology Achievements of Southwest Medical University (2018-ZRQN-014), Scientific research project of the education department of Sichuan province (17ZA0436), Scientific Research Foundation for Doctors of the Affiliated Hospital of Southwest Medical University (to Lanyang Gao, Jing Jia and Shigang Yin), and Special project of talent introduction in Luzhou (0903-00040055).

SUPPLEMENTARY MATERIAL

The Supplementary Material for this article can be found online at: https://www.frontiersin.org/articles/10.3389/fonc.2021.650165/full#supplementary-material

REFERENCES

1. Menezes AC, Raposo S, Simões S, Ribeiro H, Oliveira H, Ascenso A. Prevention of Photocarcinogenesis by Agonists of 5-HT1A and Antagonists of 5-HT2A Receptors. *Mol Neurobiol* (2016) 53(2): 1145–64. doi: 10.1007/s12035-014-9068-z
2. Belanger F, Rajotte V, Drobetsky EA. A majority of human melanoma cell lines exhibits an S phase-specific defect in excision of UV-induced DNA photoproducts. *PloS One* (2014) 9:e85294. doi: 10.1371/journal.pone.0085294
3. Tavana O, Li D, Dai C, Lopez G, Banerjee D, Kon N, et al. HAUSP deubiquitinates and stabilizes N-Myc in neuroblastoma. *Nat Med* (2016) 22 (10):1180–6. doi: 10.1038/nm.4180
4. Hernandez-Perez S, Cabrera E, Salido E, Lim M, Reid L , Lakhani SR , et al. DUB3 and USP7 de-ubiquitinating enzymes control replication inhibitor Geminin: molecular characterization and associations with breast cancer. *Oncogene* (2017) 36(33):4817. doi: 10.1038/onc.2017.220
5. van Loosdregt J, Fleskens V, Fu J, Brenkman AB, Bekker CP, Pals CE, et al. Stabilization of the transcription factor Foxp3 by the deubiquitinase USP7 increases Treg-cell-suppressive capacity. *Immunity* (2013) 39:(2)259–71. doi: 10.1016/j.immuni.2013.05.018
6. Kim H, Lee JM, Lee G, Bhin J, Oh SK, Kim K, et al. DNA damage-induced RORalpha is crucial for p53 stabilization and increased apoptosis. *Mol Cell* (2011) 44(5):797–810. doi: 10.1016/j.molcel.2011.09.023
7. Chauhan D, Tian Z, Nicholson B, Kumar KG, Zhou B, Carrasco R, et al. A small molecule inhibitor of ubiquitin-specific protease-7 induces apoptosis in multiple myeloma cells and overcomes bortezomib resistance. *Cancer Cell* (2012) 22(3):345–58. doi: 10.1016/j.ccr.2012.08.007
8. Li M, Chen D, Shiloh A, Luo J, Nikolaev AY, Qin J, et al. Deubiquitination of p53 by HAUSP is an important pathway for p53 stabilization. *Nature* (2002) 416 (6881):648–53. doi: 10.1038/nature737
9. Cummins JM, Rago C, Kohli M, Kinzler KW, Lengauer C, Vogelstein B. Tumour suppression: disruption of HAUSP gene stabilizes p53. *Nature* (2004) 428(6982):1 p following 486. doi: 10.1038/nature02501
10. Huang Z, Wu Q, Guryanova OA, Cheng L, Shou W, Rich JN, et al. Deubiquitylase HAUSP stabilizes REST and promotes maintenance of neural progenitor cells. *Nat Cell Biol* (2011) 13(2):142–52. doi: 10.1038/ncb2153
11. Bhattacharya S, Ghosh MK. HAUSP regulates c-MYC expression via de-ubiquitination of TRRAP. *Cell Oncol (Dordr)* (2015) 38:265–77. doi: 10.1007/s13402-015-0228-6
12. Song MS, Salmena L, Carracedo A, Egia A, Lo-Coco F, Teruya-Feldstein J, et al. The deubiquitinylation and localization of PTEN are regulated by a HAUSP-PML network. *Nature* (2008) 455(7214):813–7. doi: 10.1038/nature07290
13. van der Horst A, de Vries-Smits AM, Brenkman AB, van Triest MH, van den Broek N, Colland F, et al. FOXO4 transcriptional activity is regulated by monoubiquitination and USP7/HAUSP. *Nat Cell Biol* (2006) 8(10):1064–73. doi: 10.1038/ncb1469
14. Bhattacharya S, Ghosh MK. HAUSP, a novel deubiquitinase for Rb - MDM2 the critical regulator. *FEBS J* (2014) 281:3061–78. doi: 10.1111/febs.12843
15. Varol N, Konac E, Bilen CY. Does Wnt/beta-catenin pathway contribute to the stability of DNMT1 expression in urological cancer cell lines? *Exp Biol Med (Maywood)* (2015) 240:624–30. doi: 10.1177/1535370214556951
16. Becker K, Marchenko ND, Palacios G, Moll UM. A role of HAUSP in tumor suppression in a human colon carcinoma xenograft model. *Cell Cycle* (2008) 7:1205–13. doi: 10.4161/cc.7.9.5756
17. Masuya D, Huang C, Liu D, Nakashima T, Yokomise H, Ueno M, et al. The HAUSP gene plays an important role in non-small cell lung carcinogenesis through p53-dependent pathways. *J Pathol* (2006) 208(5):724–32. doi: 10.1002/path.1931
18. Cai JB, Shi GM, Dong ZR, Ke AW, Ma HH, Gao Q, et al. Ubiquitin-specific protease 7 accelerates p14(ARF) degradation by deubiquitinating thyroid hormone receptor-interacting protein 12 and promotes hepatocellular carcinoma progression. *Hepatology* (2015) 61(5):1603–14. doi: 10.1002/hep.27682
19. Zhang L, Wang H, Tian L, Li H. Expression of USP7 and MARCH7 Is Correlated with Poor Prognosis in Epithelial Ovarian Cancer. *Tohoku J Exp Med* (2016) 239:165–75. doi: 10.1620/tjem.239.165
20. Epping MT, Meijer LA, Krijgsman O, Bos JL, Pandolfi PP, Bernards R. TSPYL5 suppresses p53 levels and function by physical interaction with USP7. *Nat Cell Biol* (2011) 13(1):102–8. doi: 10.1038/ncb2142

21. Cheng C, Niu C, Yang Y, Wang Y, Lu M. Expression of HAUSP in gliomas correlates with disease progression and survival of patients. *Oncol Rep* (2013) 29(5):1730–6. doi: 10.3892/or.2013.2342
22. Huang H, Guo M, Liu N, Zhao C, Chen H, Wang X, et al. Bilirubin neurotoxicity is associated with proteasome inhibition. *Cell Death Dis* (2017) 8(6):e2877. doi: 10.1038/cddis.2017.274
23. Xia X, Liao Y, Huang C, Liu Y, He J, Shao Z, et al. Deubiquitination and stabilization of estrogen receptor alpha by ubiquitin-specific protease 7 promotes breast tumorigenesis. *Cancer Lett* (2019) 465:118–28. doi: 10.1016/j.canlet.2019.09.003
24. Plews RL, Mohd Yusof A, Wang C, Saji M, Zhang X, Chen CS, et al. A novel dual AMPK activator/mTOR inhibitor inhibits thyroid cancer cell growth. *J Clin Endocrinol Metab* (2015) 100(100):E748–56. doi: 10.1210/jc.2014-1777
25. Pineda CT, Potts PR. Oncogenic MAGEA-TRIM28 ubiquitin ligase downregulates autophagy by ubiquitinating and degrading AMPK in cancer. *Autophagy* (2015) 11:844–6. doi: 10.1080/15548627.2015.1034420
26. Brunet A, Bonni A, Zigmond MJ, Lin MZ, Juo P, Hu LS, et al. Akt promotes cell survival by phosphorylating and inhibiting a Forkhead transcription factor. *Cell* (1999) 96(6):857–68. doi: 10.1016/S0092-8674(00)80595-4
27. Wandzioch E, Pusey M, Werda A, Bail S, Bhaskar A, Nestor M, et al. PME-1 modulates protein phosphatase 2A activity to promote the malignant phenotype of endometrial cancer cells. *Cancer Res* (2014) 74(16):4295–305. doi: 10.1158/0008-5472.CAN-13-3130
28. Barata JT. The impact of PTEN regulation by CK2 on PI3K-dependent signaling and leukemia cell survival. *Adv Enzyme Regul* (2011) 51:37–49. doi: 10.1016/j.advenzreg.2010.09.012
29. Matsuzaki H, Ichino A, Hayashi T, Yamamoto T, Kikkawa U, et al. Regulation of intracellular localization and transcriptional activity of FOXO4 by protein kinase B through phosphorylation at the motif sites conserved among the FOXO family. *J Biochem* (2005) 138(4):485–91. doi: 10.1093/jb/mvi146
30. Dai C, Zhang X, Xie D, Tang P, Li C, Zuo Y, et al. Targeting PP2A activates AMPK signaling to inhibit colorectal cancer cells. *Oncotarget* (2017) 8:95810–23. doi: 10.18632/oncotarget.21336
31. Kessler BM, Fortunati E, Melis M, et al. Proteome changes induced by knock-down of the deubiquitylating enzyme HAUSP/USP7. *J Proteome Res* (2007) 6:4163–72. doi: 10.1021/pr0702161
32. Zou P, Yang Y, Xu X, et al. Silencing of vacuolar ATPase c subunit ATP6V0C inhibits the invasion of prostate cancer cells through a LASS2/TMSG1-independent manner. *Oncol Rep* (2018) 39:298–306. doi: 10.3892/or.2017.6092
33. Agathanggelou A, Smith E, Davies NJ, et al. USP7 inhibition alters homologous recombination repair and targets CLL cells independently of ATM/p53 functional status. *Blood* (2017) 130:156–66. doi: 10.1182/blood-2016-12-758219
34. An L, Jiang Y, Ng HH, et al. Dual-utility NLS drives RNF169-dependent DNA damage responses. *Proc Natl Acad Sci USA* (2017) 114:E2872–E81. doi: 10.1073/pnas.1616602114

Conflict of Interest: The authors declare that the research was conducted in the absence of any commercial or financial relationships that could be construed as a potential conflict of interest.

frontiers in Oncology

CORRECTION
published: 23 July 2021
doi: 10.3389/fonc.2021.736438

Corrigendum: Proteome Analysis of USP7 Substrates Revealed Its Role in Melanoma Through PI3K/Akt/FOXO and AMPK Pathways

Lanyang Gao[1,2†], Danli Zhu[1†], Qin Wang[1†], Zheng Bao[1], Shigang Yin[2,3], Huiyan Qiang[4], Heinrich Wieland[1], Jinyue Zhang[1], Alexander Teichmann[1] and Jing Jia[5,6*]*

[1] Sichuan Provincial Center for Gynaecology and Breast Disease, The Affiliated Hospital of Southwest Medical University, Luzhou, China, [2] Academician (Expert) Workstation of Sichuan Province, The Affiliated Hospital of Southwest Medical University, Luzhou, China, [3] Laboratory of Nervous System Disease and Brain Functions, The Affiliated Hospital of Southwest Medical University, Luzhou, China, [4] Department of Outpatient, The Affiliated Hospital of Southwest Medical University, Luzhou, China, [5] Department of Anesthesiology, The Affiliated Hospital of Southwest Medical University, Luzhou, China, [6] Laboratory of Anesthesiology, Southwest Medical University, Luzhou, China

OPEN ACCESS

Edited and reviewed by:
Suzie Chen,
Rutgers, The State University of New Jersey, United States

***Correspondence:**
Jing Jia
jiajing@swmu.edu.cn
Alexander Teichmann
teichmann2020@163.com

[†]These authors have contributed equally to this work

Specialty section:
This article was submitted to Skin Cancer, a section of the journal Frontiers in Oncology

Received: 05 July 2021
Accepted: 08 July 2021
Published: 23 July 2021

Citation:
Gao L, Zhu D, Wang Q, Bao Z, Yin S, Qiang H, Wieland H, Zhang J, Teichmann A and Jia J (2021) Corrigendum: Proteome Analysis of USP7 Substrates Revealed Its Role in Melanoma Through PI3K/Akt/FOXO and AMPK Pathways. Front. Oncol. 11:736438. doi: 10.3389/fonc.2021.736438

Keywords: melanoma, USP7, deubiquitinating enzyme, quantitative proteomics, PI3K/Akt/FOXO pathways

A Corrigendum on

Proteome Analysis of USP7 Substrates Revealed Its Role in Melanoma Through PI3K/Akt/FOXO and AMPK Pathways

By Gao L, Zhu D, Wang Q, Bao Z, Yin S, Qiang H, Wieland H, Zhang J, Teichmann A and Jia J (2021) Front. Oncol. 11:650165. doi: 10.3389/fonc.2021.650165

In the original article, there was a mistake in ***Figure 2C*** as published. In fact, we initially left a gap between 116kD and 96kD WB bands in the manuscript (***Figure 2C***), which might not be clear enough, eventually leading to a misunderstanding of the bands. Actually, the PARP antibody (Abclonal, A19596) we used in this study could detect the full length PARP (116kDa), as well as the cleaved PARP (96 kDa). The short time exposure showed an increased but fuzzy band of the cleaved PARP. As the PARP cleavage serves as a better indicator of apoptosis triggering, that we examine the cleaved PARP (96 kDa) with a long time exposure. The corrected ***Figure 2C*** appears below.

The authors apologize for this error and state that this does not change the scientific conclusions of the article in any way. The original article has been updated.

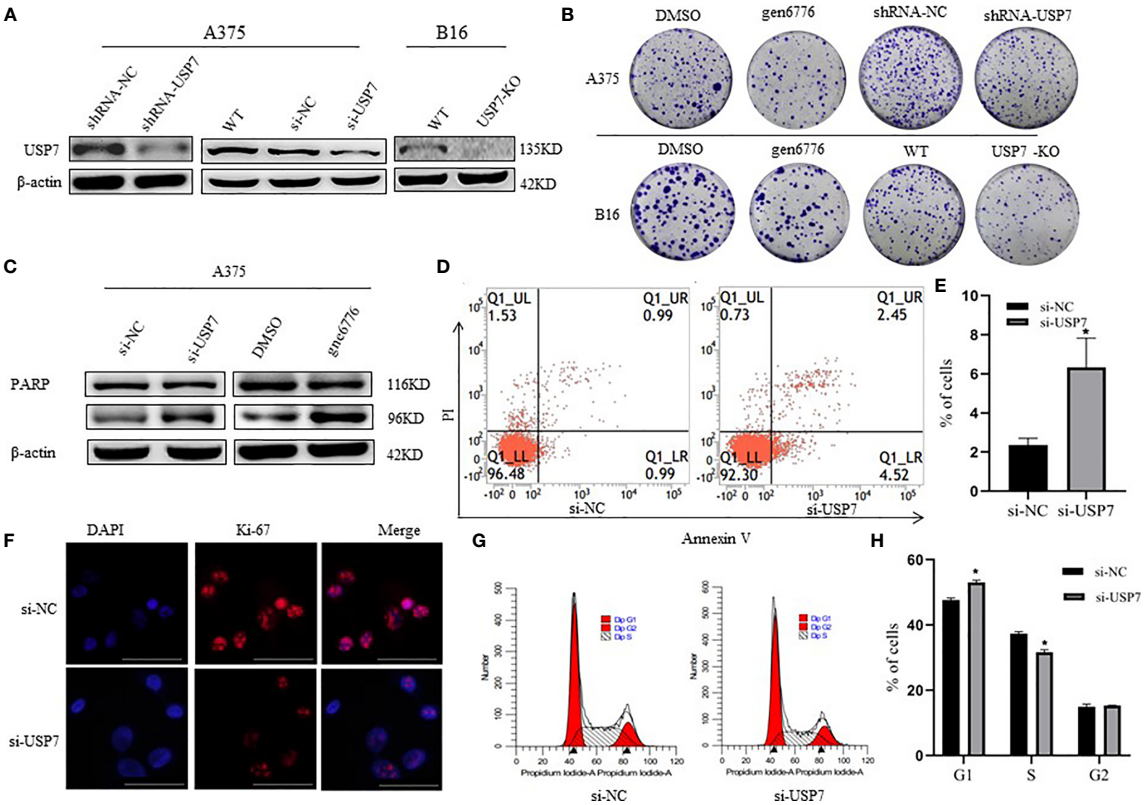

FIGURE 2 | Effects of USP7 on melanoma cell line growth. **(A, B)** Protein lysates were extracted from A375 cells transiently expressing USP7 siRNA and stable control shRNA or USP7 shRNA and B16 cells deleted the USP7 gene using the CRISPR/Cas9 editing system (USP7 KO). Western blotting analysis was performed to determine the expression of USP7. **(B)** Cells were collected from the indicated cells with gen6776 (USP7 inhibitor), USP7 shRNA or USP7 knockout treatment. Colony formation assay was performed and representative images are shown. **(C–E)** A375 cells were transfected with USP7 siRNAs for 48 h and detected with Annexin V-FITC/PI staining followed by flow cytometry analysis. Cell death populations are shown. Western blotting analysis was used for PARP expression. **(F–H)** A375 cells were treated as described in **(C–E)**. Immunofluorescence staining of Ki-67 of A375 cells was observed using fluorescence microscope. Red: Ki-67; blue: nucleus. Typical images are shown. Scale bars: 50 μm. Analysis of cell cycle by FCM is described in the Materials and Methods. Data are represented as the mean ± SEM of three independent experiments, each in triplicate; bars, SEM. *P ≤ 0.05 vs. control.

frontiers in Oncology

ORIGINAL RESEARCH
published: 16 April 2021
doi: 10.3389/fonc.2021.676077

Genetic Manipulation of Sirtuin 3 Causes Alterations of Key Metabolic Regulators in Melanoma

Chandra K. Singh[1], *Jasmine George*[1†], *Gagan Chhabra*[1], *Minakshi Nihal*[1], *Hao Chang*[1] *and Nihal Ahmad*[1,2*]

[1] Department of Dermatology, University of Wisconsin, Madison, WI, United States, [2] William S. Middleton VA Medical Center, Madison, WI, United States

OPEN ACCESS

Edited by:
Vladimir Spiegelman, Penn State Milton S. Hershey Medical Center, United States

Reviewed by:
Shiyong Wu, Ohio University, United States
Yu-Ying He, University of Chicago, United States

***Correspondence:**
Nihal Ahmad
nahmad@dermatology.wisc.edu

†Present address:
Jasmine George, Department of Obstetrics and Gynecology, Medical College of Wisconsin, Milwaukee, WI, United States

Specialty section:
This article was submitted to Skin Cancer, a section of the journal Frontiers in Oncology

Received: *04 March 2021*
Accepted: *29 March 2021*
Published: *16 April 2021*

Citation:
Singh CK, George J, Chhabra G, Nihal M, Chang H and Ahmad N (2021) Genetic Manipulation of Sirtuin 3 Causes Alterations of Key Metabolic Regulators in Melanoma. Front. Oncol. 11:676077. doi: 10.3389/fonc.2021.676077

The mitochondrial sirtuin SIRT3 plays key roles in cellular metabolism and energy production, which makes it an obvious target for the management of cancer, including melanoma. Previously, we have demonstrated that SIRT3 was constitutively upregulated in human melanoma and its inhibition resulted in anti-proliferative effects *in vitro* in human melanoma cells and *in vivo* in human melanoma xenografts. In this study, we expanded our data employing knockdown and overexpression strategies in cell culture and mouse xenografts to further validate and establish the pro-proliferative function of SIRT3 in melanocytic cells, and its associated potential mechanisms, especially focusing on the metabolic regulation. We found that short-hairpin RNA (shRNA) mediated SIRT3 knockdown in G361 melanoma cells showed diminished tumorigenesis in immunodeficient Nu/Nu mice. Conversely, SIRT3 overexpressing Hs294T melanoma cells showed increased tumor growth. These effects were consistent with changes in markers of proliferation (PCNA), survival (Survivin) and angiogenesis (VEGF) in xenografted tissues. Further, in *in vitro* culture system, we determined the effect of SIRT3 knockdown on glucose metabolism in SK-MEL-2 cells, using a PCR array. SIRT3 knockdown caused alterations in a total of 37 genes involved in the regulation and enzymatic pathways of glucose (32 genes) and glycogen (5 genes) metabolism. Functions annotation of these identified genes, using the ingenuity pathway analysis (IPA), predicted cumulative actions of decreased cell viability/proliferation, tumor growth and reactive oxygen species (ROS), and increased apoptosis in response to SIRT3 knockdown. Further, IPA gene network analysis of SIRT3 modulated genes revealed the interactions among these genes in addition to several melanoma-associated genes. Sirtuin pathway was identified as one of the top canonical pathways showing the interaction of SIRT3 with metabolic regulatory genes along with other sirtuins. IPA analysis also predicted the inhibition of HIF1α, PKM, KDM8, PPARGC1A, mTOR, and activation of P53 and CLPP; the genes involved in major cancer/melanoma-associated signaling events. Collectively, these results suggest that SIRT3 inhibition affects cellular metabolism, to impart an anti-proliferative response against melanoma.

Keywords: melanoma, sirtuins, SIRT3, shRNA, cellular metabolism

INTRODUCTION

Melanoma is the deadliest cancer of the skin, which arises from melanocytic cells that are derived from the neural crest and are primarily responsible for melanin production. Melanoma, if not treated early, possesses metastatic potential; and its incidence has been increasing over 30 years (1). Therefore, there is a critical need to develop novel mechanism-based strategies for an effective management of this neoplasm. Sirtuin-3 (SIRT3) is an important mitochondrial NAD^+-dependent deacetylase that is known to target mitochondrial proteins for deacetylation and regulates a variety of cellular functions. Although SIRT3 is a mitochondrial protein, it is reported to move from mitochondria to nucleus under cellular stress (2). SIRT3 plays key roles in mitochondrial dynamics, metabolism and energy regulation, and therefore their possible roles in the progression of cancer are being intensively investigated (3). Studies have suggested that SIRT3 coordinates global shifts in mitochondrial activity by deacetylating proteins involved in diverse mitochondrial functions including energy metabolism and mitochondrial biogenesis (4, 5). It also plays important roles in the regulation of a variety of cellular processes, including transcription, insulin secretion, apoptosis and redox signaling (6). SIRT3 has also been implicated in multiple cutaneous functions including skin renewal, and response to environmental stressors (7, 8).

Based on a number of studies, SIRT3 has been shown to act either as a tumor suppressor or promoter depending on the cell milieus (9). For example, SIRT3 has been shown to be downregulated in gastric cancer (10), hepatocellular carcinoma (11), and pancreatic cancer (12). Conversely, higher expression of SIRT3 has been reported in cancers of esophagus (13), breast (14) and colon (15). The higher expression of SIRT3 has also been connected to therapy resistance (16) and poor prognosis (17), and its inhibition has been shown to enhance radiotherapeutic and chemotherapeutic drug cytotoxicity (18). We have recently demonstrated that SIRT3 was overexpressed in human melanoma, and its small hairpin RNA (shRNA) mediated knockdown provoked the senescence and growth inhibition in melanoma cells, *in vitro* and *in vivo* (19). In addition, forced overexpression of SIRT3 resulted in enhanced proliferation of melanocytic cells (19).

Cancer cells are known to be metabolically more active and consume high cellular fuel than normal cells (20). Thus, understanding the regulatory mechanisms associated with cellular energy metabolism at the gene level may be of fundamental importance that could be potentially explored for cancer treatment. Increasing evidence show that SIRT3 is required for the maintenance of cellular and mitochondria homeostasis through regulating mitochondrial metabolism and cellular redox balance system (6, 21, 22). In this study, we expanded our findings in additional experiments, employing knockdown and overexpression strategies in human melanoma cells and mouse xenografts to further validate the pro-proliferative function of SIRT3 in melanoma, and establish its associated potential mechanisms, especially focusing on metabolic regulation.

MATERIALS AND METHODS

Cell Lines and Cell Culture

Human melanoma cell lines (SK-MEL-2, G361, and Hs294T), and human embryonic kidney cell line HEK293T were purchased from ATCC. SK-MEL-2 cells were maintained in Eagle's minimal essential medium (supplemented with 1 mM sodium pyruvate and non-essential amino acids), G361 in McCoy's 5a medium, and Hs294T and HEK293T cells in Dulbecco's modified eagle's medium with 10% fetal bovine serum at standard cell culture conditions (37°C, 5% CO_2).

Lentiviral SIRT3 Knockdown

SIRT3 knockdown was done in SK-MEL-2 and G361 cells and stable cell lines were established under puromycin selection, as described earlier (19). Briefly, for viral creation, HEK293T cells were transfected using calcium phosphate transfection method with empty vector pLKO.1 (SHC001V) and four different SIRT3 targeting short hairpin RNA (shRNA) procured from Sigma-Aldrich. Competent lentiviruses were harvested 48 h after transfection. The quality of lentivirus stock was assessed with Lenti-X GoStix (Clontech Laboratories). For transduction, viral media were added to SK-MEL-2 and G361 cells (at ~40% confluency) with 8 μg/ml of polybrene, 4-times over 2 days. On 3rd day, cells were collected and SIRT3 shRNA constructs were checked for SIRT3 knockdown. The most efficient SIRT3 shRNA construct (TRCN0000038889) was used for generating SIRT3 knockdown stable cell lines by selection with puromycin (SK-MEL-2, 1.5 μg/ml for 4 weeks; and G361, 2.0 μg/ml for 6 weeks), and maintained in their respective media with 1 μg/mL puromycin.

Forced Overexpression of SIRT3

For SIRT3 forced overexpression, as described earlier (19), bacterial glycerol stab with SIRT3-Flag plasmid (Addgene) was streaked onto agar plates containing ampicillin and incubated overnight at 37°C. Next day, four single colonies were picked and inoculated in LB medium. For SIRT3 overexpression, Hs294T cells were stably transfected with four isolated plasmid DNA of SIRT3-Flag and empty vector pcDNA 3.1(+) using Lipofectamine-2000 as per manufacturer's instructions (Invitrogen). After 48 h, geneticin (2 mg/ml G-418; Gibco BRL) was added in the medium until antibiotic-resistant colonies developed. Individual colonies were isolated and propagated, and SIRT3-Flag-tagged protein was detected by immunoblot analysis. The colonies expressing the highest levels of SIRT3-Flag were selected for further analysis.

Xenograft Studies

The xenograft experiments were performed under a protocol approved by the University of Wisconsin Animal Care and Use Committee. Female nude mice (Crl : NU-Foxn1nu) aged 6 weeks were procured from Charles River Laboratories. We conducted two sets of the experiment using twelve mice per experimental group. For SIRT3 knockdown, 2 x 10^6 cells (shNS-G361 and shSIRT3-G361) and for SIRT3 overexpression, 1 x 10^6 cells (Hs294T-pcDNA3.1 and Hs294T-SIRT3-Flag) mixed with

Matrigel (BD Biosciences) at the ratio of 1:1 were injected subcutaneously on the right flank of each mouse. Once tumors were palpable, they were measured twice per week (Hs294T-xenografts) or weekly (G361-xenografts) using digital calipers and tumor volumes were calculated according to the formula: 0.52 (height x length x width). Hs294T-xenografted mice were sacrificed when tumors reached 20 mm in any one dimension, in any group. However, a 10 mm cut-off point was selected for G361-xenografted mice due to slow-growing tumors in these mice.

RNA Isolation, Quantitative Real-Time PCR (RT-qPCR) and Glucose Metabolism PCR Array Analyses

RNA from cell lines and tissue samples were isolated using an RNeasy plus mini kit (Qiagen) as per the manufacture's protocol. Corresponding cDNAs were synthesized using Oligo DT primers, dNTPs and M-MLV reverse transcriptase (Promega). RT-qPCR analyses were performed as described earlier using SYBR Premix Ex Taq II (TaKaRa) and QuantStudio 3 (ThermoFisher Scientific) (23). The primers for SIRT3, PCNA, Survivin, VEGF and ACTB were selected from the PrimerBank database (24). Relative transcript of each gene of interest was calculated using the $\Delta\Delta C_T$ method and ACTB as an endogenous control.

The human glucose metabolism PCR array (Qiagen #PAHS-006Z) was run using cDNA isolated from shNS SK-MEL-2 and shSIRT3 SK-MEL-2 cells, and analyzed as described earlier (23). Briefly, the resulting cycle threshold (CT) values were uploaded onto GeneGlobe Data Analysis Center (Qiagen) (http://www.qiagen.com/us/shop/genes-and-pathways/data-analysis-center-overview-page/) to analyze fold change in transcripts in response to SIRT3 knockdown. Three housekeeping genes, *ACTB, HPRT1* and *RPLP0*, were used to normalize the data. Genes from the PCR array showing ≥1.96-fold change with statistical significance were selected for further analysis. Three biological replicates were used to assess the levels of the 84 metabolism-related genes.

Ingenuity Pathway Analysis (IPA)

To understand the pathways modulated in response to SIRT3 knockdown, differentially expressed genes from PCR array were uploaded on the IPA web portal (Qiagen; www.ingenuity.com). The data were analyzed to predict gene interaction network, cumulative functions, canonical pathways and upstream regulators for SIRT3-modulated genes.

Quantitative Immunodetection Analysis Using ProteinSimple

Protein from tumor tissues was isolated in 1X RIPA lysis buffer (Millipore), and quantified using Pierce BCA Protein assay kit (Thermo Scientific) as described earlier (25). Wes ProteinSimple, a capillary-based immunodetection system was used for protein analysis. Briefly, as per the manufacturer's protocol, Dithiothreitol, fluorescent 5× master mix, biotinylated ladder and luminol-peroxide solution were prepared. One part 5× fluorescent master mix was combined with 4 parts of protein lysate (0.5 µg/ul) in a microcentrifuge tube, and heated at 95°C for 5 min to denature the protein. These prepared proteins were loaded on 12–230 kDa Wes Separation Module (ProteinSimple), along with biotinylated ladder, antibody diluent (blocking reagent), primary antibodies, horseradish peroxidase (HRP)-conjugated secondary antibodies, streptavidin-HRP, luminol peroxide solution, and wash buffer, into the designated compartments. The primary antibodies were optimized and used at 1:50 dilution for VEGF (Proteintech #19003-1-AP), SIRT3, PCNA and Survivin (Cell Signaling #2627, 2586 and 2808, respectively). The produced chemiluminescence was detected at multiple exposure times and automatically quantified by the Compass for Simple Western software. The electropherograms showing automatically detected peak area for PCNA, Survivin or, VEGF were quantified and normalized to the total capillary area of the Total Protein Assay of the same sample.

Statistical Analysis

Statistical analyses were performed using GraphPad Prism 5 software. The statistical test applied for each data is indicated in their respective figure legends. Data are expressed as mean ± SEM of three replicates, and statistical significance is denoted as *p<0.05, **p<0.01, ***p<0.001, ****p<0.0001.

RESULTS

Tumorigenic Behavior of Genetically Manipulated Melanoma Cells for SIRT3 in Nu/Nu Mice Was Consistent With the Pro-Proliferative Role of SIRT3 in Melanoma

We have previously demonstrated that SIRT3 knockdown in NRAS-mutant SK-MEL-2 human melanoma cells inhibited tumor growth in a subcutaneous implanted Nu/Nu nude mouse model (19). Here, we expanded our work to confirm our previous results of SIRT3 knockdown in BRAF-mutant human melanoma cell line G361. For this purpose, Nu/Nu nude mice were subcutaneously implanted with shNS-G361 (control) and shSIRT3-G361 (SIRT3 knockdown) melanoma cells followed by assessing tumor development and progression (**Figure 1A**). Every mouse that received shNS-G361 developed a tumor approaching ~1000 mm^3 in volume by 56 days (**Figure 1B**). However, only 2 mice out of 12 implanted with shSIRT3-G361 cells developed extremely small size tumors measuring 150 mm^3 and 40 mm^3 respectively. At the termination of the study, we weighed wet tumors and found significant inhibition in tumor weight, as well. These results suggest that SIRT3 knockdown resulted in a significant effect in tumorigenicity of G361 cells, with almost complete inhibition of tumor growth in mice xenografts (**Figures 1B, C**).

The pro-proliferative role of SIRT3 was also shown in the xenograft experiment with SIRT3 overexpressing melanoma cells in Nu/Nu nude mice. We have earlier demonstrated that SIRT3 overexpression promotes the proliferative potential of Hs294T melanoma cells, *in vitro* (19). In this study, we determined the tumorigenic potential of SIRT3 overexpressing Hs294T cells in Nu/Nu mice. The mice were subcutaneously implanted with Hs294T-empty vector pcDNA 3.1(+) (control) and

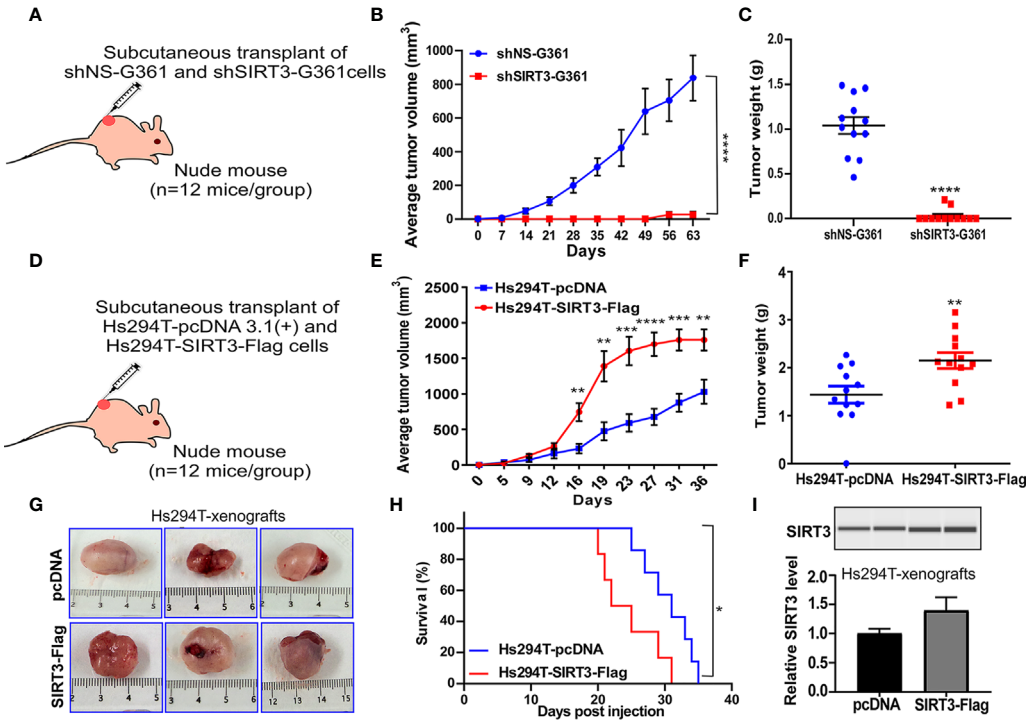

FIGURE 1 | Effect of SIRT3-knockdown (shSIRT3-G361) and overexpressing (Hs294T-SIRT3-Flag) melanoma cells in Nu/Nu mouse xenografts. SIRT3-knockdown and overexpressing melanoma cells were xenografted in Nu/Nu mice and followed for tumorigenesis. **(A)** SIRT3-knockdown study design, **(B)** Average tumor volume, and **(C)** Tumor weight for shNS-G361 and shSIRT3-G361 melanoma cells xenografted tumors (at the termination of the experiment). **(D)** SIRT3-overexpression study design, **(E)** Average tumor volume, **(F)** Tumor weight (at the termination of the experiment), **(G)** Representative images of tumors with scale bars, and **(H)** Survival probability analysis for Hs294T-empty vector pcDNA 3.1(+) (control) and Hs294T-SIRT3-Flag (SIRT3-overexpressing) melanoma cells xenografted tumors. **(I)** Wes ProteinSimple analysis confirming SIRT3 higher expression in the derived tumor tissues. The SIRT3 quantitative data was normalized using Total Protein Assay of the same sample. N=12 mice/experimental group. Statistical significance are indicated as *p < 0.05, **p < 0.01, ***p < 0.001, ****p < 0.0001. shNS, nonspecific shRNA; shSIRT3, SIRT3-knockdown; pcDNA (empty vector); SIRT3-Flag (SIRT3-overexpression).

Hs294T-SIRT3-Flag (SIRT3 overexpressing) melanoma cells and tumorigenicity of the cells was followed (**Figure 1D**). We found that SIRT3 overexpressing melanoma cells demonstrated significant increase in tumorigenicity, measured by both tumor volume and weight (**Figures 1E, F**). Representative images of resected tumors are shown in **Figure 1G**. Further, the Kaplan-Meier analysis showed that SIRT3 overexpression resulted in a significant survival detriment, in terms of reaching the tumor cutoff size 20 mm in one dimension (**Figure 1H**). SIRT3 expression was assessed in isolated tumor tissues and found a marked increase in SIRT3-Flag xenografts (**Figure 1I**). Though exogenous forced overexpression of SIRT3 may not represent physiologic phenomena as it generates supraphysiological SIRT3 levels, our results support the pro-proliferative function of SIRT3 in melanoma, further validating our earlier study (19).

Genetic Manipulation of SIRT3 Caused Modulations in Markers of Proliferation, Survival and Angiogenesis in Melanoma Xenografts

Due to an almost complete inhibition of tumor growth in shSIRT3-G361 implanted tumor group, we did not have sufficient tumor tissues from this group for further analyses. Therefore, we used archival tumor samples from our previous study, which utilized SIRT3 knockdown in SK-MEL-2 melanoma cells xenografted in Nu/Nu mice (19). We evaluated the effects of SIRT3 manipulation on markers of cell proliferation (PCNA), survival (Survivin) and angiogenesis (VEGF) using RT-qPCR and Wes ProteinSimple analyses. As shown in **Figure 2A**, significant decreases in PCNA, Survivin and VEGF transcripts were observed in SIRT3 knockdown tumor tissues. Similar results were noticed at the protein level for PCNA, Survivin and VEGF in SIRT3 knockdown tumor tissues (**Figures 2B, C**). We also analyzed the levels of PCNA, Survivin and VEGF transcripts and protein in SIRT3 overexpressing (Hs294T-SIRT3-Flag) tumor tissues. Our analysis found marked increase in PCNA, Survivin and VEGF transcripts in SIRT3 overexpressing tumor tissues (**Figure 2D**). However, at the protein level, a marked increase in VEGF and a marginal increase in Survivin were observed (**Figures 2E, F**). No change in PCNA was found probably due to the high background because of the higher number of PCNA positive proliferating cells in tumors. Overall, these data are consistent with the pro-proliferative role of SIRT3 in melanoma.

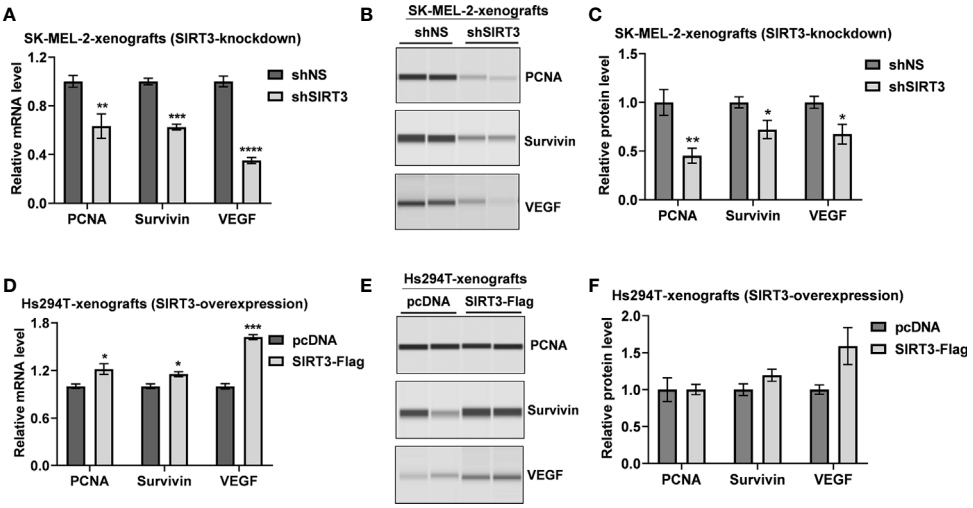

FIGURE 2 | Effect of SIRT3-knockdown and overexpression on the key tumor markers related to cell proliferation, survival and angiogenesis. Utilizing tumor tissues from SIRT3-knockdown (shSIRT3- SK-MEL-2) melanoma cell xenografts, **(A)** RT-qPCR and **(B)** Wes ProteinSimple analyses were performed for PCNA, Survivin and VEGF mRNA and protein levels. Next, utilizing tumor tissues from SIRT3-overexpressing (Hs294T-SIRT3-Flag) melanoma cell xenografts, **(C)** RT-qPCR and **(D)** Wes ProteinSimple analyses were performed for PCNA, Survivin and VEGF mRNA and protein levels. ACTB was used as an endogenous control for transcripts analysis. The protein quantitative data were normalized to the total capillary area of the Total Protein Assay of the same sample. Data are presented as the mean ± SEM of three biological pools (n = 6) with statistical significance (multiple t-test, *p < 0.05, **p < 0.01, ***p < 0.001, ****p < 0.0001). shNS, nonspecific shRNA; shSIRT3, SIRT3-knockdown; pcDNA (empty vector); SIRT3-Flag (SIRT3-overexpression).

SIRT3 Knockdown Altered the Expression of Key Metabolic Genes in Human Melanoma Cells *In Vitro*

Given the fact that SIRT3 plays important role in cellular metabolism (4, 5), and has been identified as a key player in promoting cancer metabolism and tumor growth (26), we investigated the effect of SIRT3 knockdown on genes involved in energy uptake metabolism in melanoma, employing a glucose metabolism PCR array containing 84 metabolism-related gene primers. shRNA-mediated knockdown of SIRT3 in SK-MEL-2 melanoma cells (**Figure 3A**) resulted in alteration in a number of metabolism-related genes (**Figure 3B**). For the analysis, we considered genes that were differentially expressed at least 1.96-fold when compared with the control cells (shNS-SK-MEL-2) and with P <0.05. We set the cut-off as 1.96 instead of 2 to include 3 more genes that were critical for the analysis. The next lowest cut-off point was 1.64-fold, which was not considered for analysis. The identified genes are depicted on metabolic pathways (**Figure 3C**). SIRT3 silencing significantly modulated genes related to glycolysis (ALDOC, ENO1, ENO2, ENO3, HK2, PFKL, PGAM2), gluconeogenesis (G6PC3, PCK2), Krebs cycle (ACLY, ACO2, CS, DLAT, FH, IDH2, IDH3A, MDH1, MDH2, OGDH, PCK2, PDHA1, SDHA, SDHB, SUCLG1, SUCLG2), and Pentose phosphate pathway (G6PD, H6PD, PRPS2, TALDO1) (**Figures 3B, C**). We also found SIRT3 knockdown-mediated alterations in the genes involved in the regulation of glucose metabolism (PDK2, PDK3, PDP2, and PDPR). Further, we observed significant changes in the genes involved in glycogen metabolism pathway (glycogen synthesis (UGP2), glycogen degradation (PYGL), and regulation of glycogen metabolism (GSK3A, PHKB, PHKG1) upon SIRT3 knockdown (**Figures 3B, C**). Collectively, these results suggest that inhibition of SIRT3 modulates cellular metabolism that may ultimately lead to an anti-proliferative response in melanoma cells.

Functions Annotation of Glucose Metabolism Genes Identified in Response to SIRT3 Knockdown Predicted Cumulative Action Against Melanoma Cell Survival

Next, to understand the effects of SIRT3-modulated metabolic genes, significantly altered genes were analyzed with IPA to predict their cumulative actions. Our analysis predicted the inhibition of cell viability, cell proliferation, tumor growth, and increased apoptosis (**Figures 4A–D**) in response to SIRT3 knockdown, which is in agreement with our *in vivo* findings. Though there are certain genes whose fold regulation with downstream effects are not consistent (yellow dotted lines) or predicted (gray dotted line), the cumulative effect remains the same. IPA also predicted a decrease in the generation of reactive oxygen species (ROS) in response to SIRT3 knockdown (**Figure 4E**). It is important to mention here that melanoma cells generate high ROS as a consequence of distorted melanosome structure (27), and thus, predicted inhibition of ROS supports the antitumor effect in response to SIRT3 inhibition in melanoma. The interaction of SIRT3 with hypoxia-inducible factor 1-alpha (HIF1α) has been shown to affect ROS homeostasis and glycolysis (28). Interestingly, the

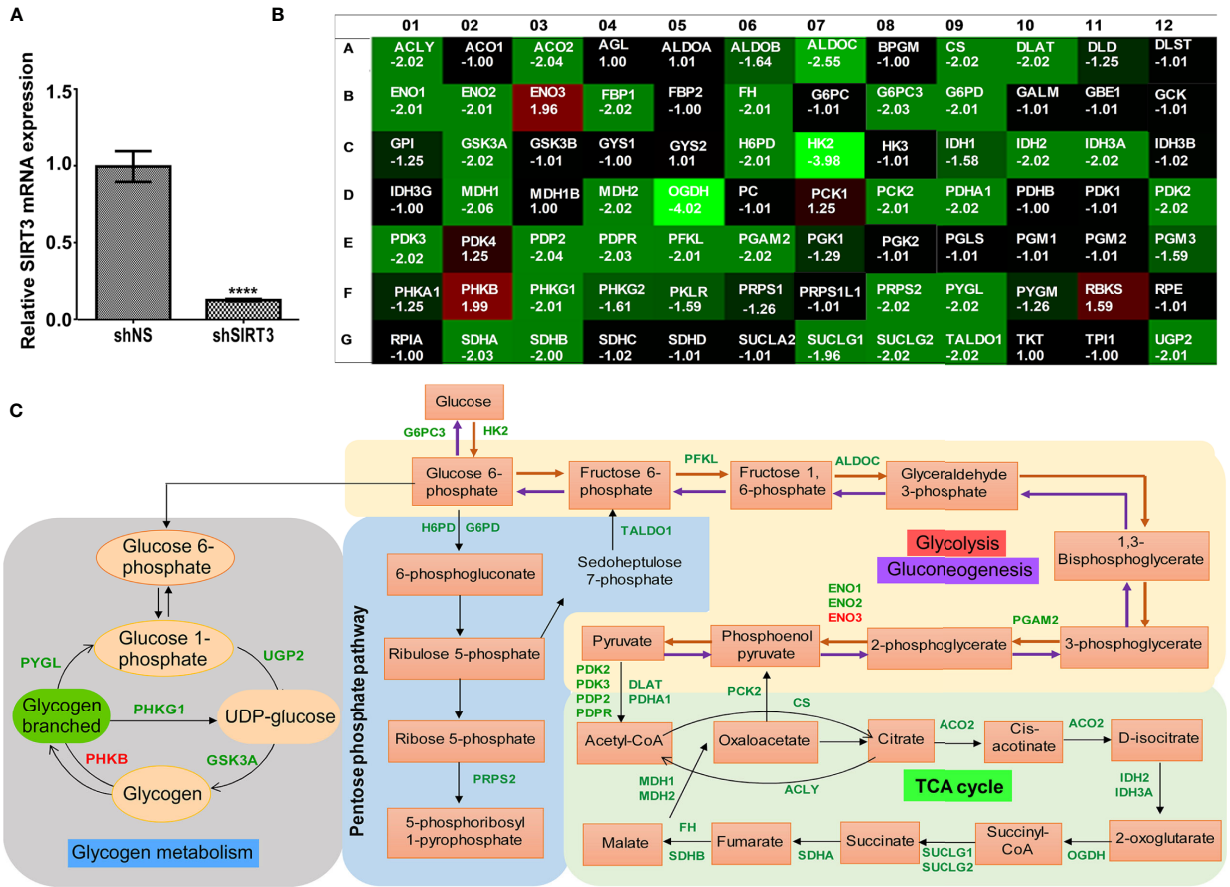

FIGURE 3 | Effect of SIRT3-knockdown on metabolism-related gene expression in SK-MEL-2 human melanoma cells. **(A)** RT-qPCR analysis confirming SIRT3 knockdown in SK-MEL-2 cells. ACTB was used as an endogenous control. Data is presented as mean ± SEM (t-test, ****$p < 0.0001$). **(B)** Utilizing cDNA from SIRT3-knockdown (shSIRT3- SK-MEL-2) melanoma cell, Glucose metabolism PCR array was run and analyzed to assess the expression levels of 84 metabolism-related genes. Heat map of average gene expression in shSIRT3 SK-MEL-2 cells compared to shNS- SK-MEL-2 (control) is presented as fold change regulation. An increase in gene expression is depicted in red, whereas a decrease in gene expression is represented by green color. No differences in expression are depicted in black. **(C)** Significantly modulated genes showing ≥1.96-fold regulation were distributed accordingly to their contribution in different metabolic pathways. Fold changes were calculated using the ΔΔCt method. The values represent the average fold change of three independent experiments.

upstream analysis of SIRT3-modulated genes identified in our PCR array predicted the inhibition of HIF1α (**Figure 4F**), further supporting the involvement of SIRT3-HIF1α-ROS connection in cancer metabolism.

Gene Network and canonical Pathway Analyses Showed Complex Interactions Among SIRT3 Modulated Genes and With Several Melanoma-Associated Genes

We employed IPA to explore the gene network and canonical pathway associated with SIRT3-modulated genes. Our analysis identified a gene network with 29 focus molecules (out of 37) indicating that these genes in the network were systematically associated (**Figure 5A**). The network pathway analysis of interacting genes predicted links to various other important genes (denoted with uncolored nodes). IPA exploration of the gene network indicated the connection of SIRT3 modulated genes along with several melanoma-associated genes (MYC, PI3K, AKT, CD3, ERK, and AMPK). Moreover, oncogenic MYC appeared as a central molecule interacting with most of the SIRT3-modulated genes and the molecules that appeared during network generation.

Further, IPA predicted five canonical pathways suggesting that these signaling pathways were constitutively affected in response to SIRT3 knockdown. These included Krebs cycle, glycolysis, gluconeogenesis, and pentose phosphate pathway. Interestingly, sirtuin signaling pathway appeared too as a canonical pathway (**Figure 5B**). SIRT3 was found to have interactions with several mitochondrial signaling molecules along with PDHA1, IDH2 and SDHA, identified in PCR array. SIRT3 also showed interaction with other mitochondrial sirtuins viz. SIRT4 and SIRT5. Interestingly, SIRT2, a cytoplasmic sirtuin was predicted to directly interact with ACLY, PCK2, PGAM2 and G6PD, which were also identified in PCR array, suggesting SIRT2/SIRT3 connection with cellular metabolism. Intriguingly, SIRT2 is also known to contribute in melanoma progression (29).

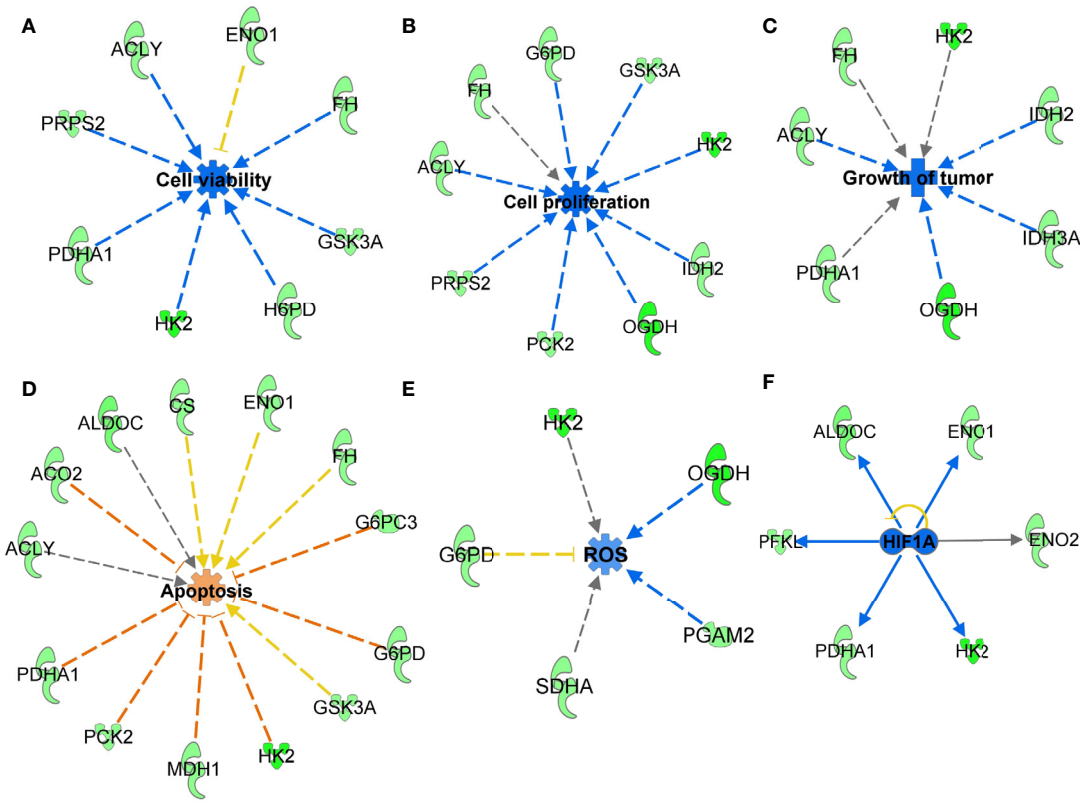

FIGURE 4 | Functions annotation of glucose metabolism genes identified in response to SIRT3 knockdown (shSIRT3- SK-MEL-2). The cumulative effect of SIRT3 modulated genes were analyzed using IPA and effects were predicted for **(A)** cell viability, **(B)** cell proliferation, **(C)** tumor growth, **(D)** apoptosis and **(E)** ROS. Genes from the array are in green (downregulated), while predicted functions and interaction lines are in blue (inhibition) or orange (activation). Yellow lines indicate inconsistent findings, and gray dotted lines show unpredicted effects. **(F)** Using IPA, upstream regulator analysis predicted inhibition of HIF1α. Though other upstream regulators are presented in Figure 6, HIF1α inhibition is presented here to discuss SIRT3-HIF1α-ROS connections in cancer metabolism.

Upstream Analysis of SIRT3-Modulated Genes Predicted Alteration in Major Cancer/Melanoma-Associated Signaling Events

Next, we performed the upstream analysis of SIRT3-modulated genes and identified alteration in several crucial upstream regulators that are known to affect cancer/melanoma development and progression. Specifically, our analysis predicted inhibition in pyruvate kinase muscle (PKM) isozyme, lysine demethylase 8 (KDM8), peroxisome proliferator-activated receptor gamma-coactivator 1 alpha (PPARGC1A) and mammalian target of rapamycin (mTOR) signaling (**Figures 6A–D**). Our analysis further predicted the activation of tumor suppressor P53 and mitochondrial caseinolytic protease P (CLPP) signaling (**Figure 6E, F**). Inhibition in HIF1α was also predicted (which has been discussed earlier in **Figure 4F**). Our data shows that most of the SIRT3 modulated genes were consistent with the state of upstream prediction. Those with upstream predictions in-consistent or un-known are indicated with yellow or gray dotted lines, respectively. The relevance of modulations in these upstream regulators related to cancer/melanoma development and progression are detailed in the discussion section. Overall, these are important observations to demonstrate a crucial connection between SIRT3 and key cancer/melanoma-associated signaling events.

DISCUSSION

The goal of this study was to validate the pro-proliferative function of SIRT3 in melanoma and establish its associated potential mechanisms, especially focusing on metabolic regulation. Our study includes data from BRAF-mutant G361 and Hs294T as well as NRAS-mutant SK-MEL-2 melanoma cells. These two mutations (BRAF and NRAS) are the most common genetic alterations in human melanoma (30). We investigated the tumorigenic behavior of SIRT3 knockdown and overexpression in melanoma cells in Nu/Nu mice. Our data demonstrated that SIRT3 knockdown abrogated tumor growth and/or tumor establishment abilities in BRAF-mutant G361-xenografted mouse model. Also, forced overexpression of SIRT3 in BRAF-mutant Hs294T-xenografted mouse model promoted tumorigenesis in melanoma. These data along with our previous study of SIRT3 knockdown in NRAS-mutant SK-MEL-2-xenografted mouse model (19) support the

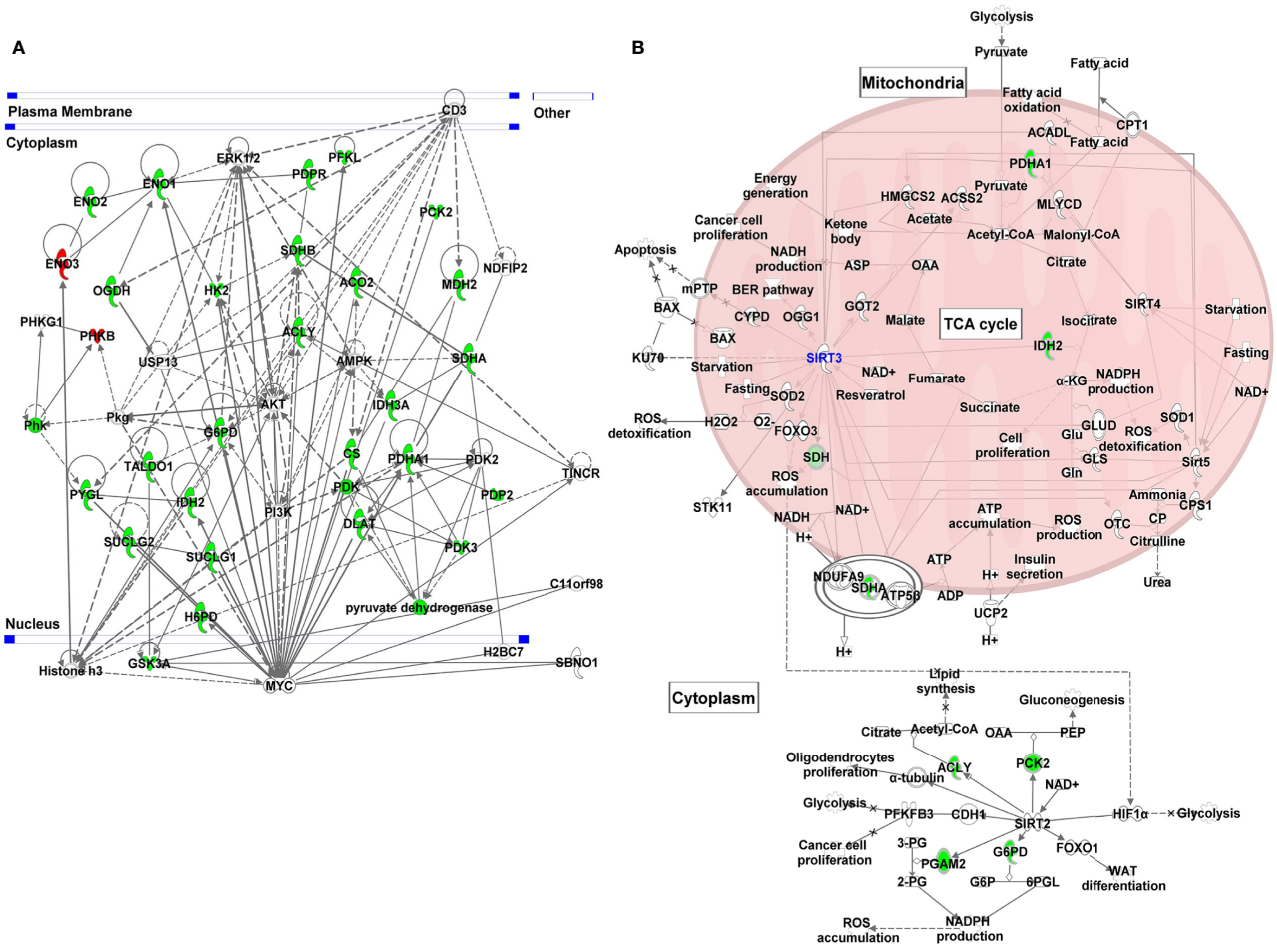

FIGURE 5 | Gene network and canonical pathway analyses of glucose metabolism genes identified in response to SIRT3 knockdown (shSIRT3- SK-MEL-2). Differentially expressed genes from glucose metabolism PCR array with cut-off criteria of ≥1.96-fold change with statistically significant change were analyzed using IPA. **(A)** Gene network indicating complex interactions among SIRT3 modulated genes and with several cancer/melanoma-associated genes. **(B)** Canonical pathway showing the interaction of SIRT3 with some of the SIRT3-modulated genes along with other sirtuins. Genes are represented with green (downregulated) or red (upregulated) or no color (appeared during gene network analysis). Solid lines indicate robust interactions, and dashed lines are significant but less frequent.

pro-proliferative nature of SIRT3. This also suggests that antitumor effects observed in response to SIRT3 inhibition are independent of BRAF or NRAS mutations.

Utilizing RT-qPCR and Wes ProteinSimple analyses, we found modulation in the markers of cell proliferation (PCNA), survival (Survivin) and angiogenesis (VEGF) in response to SIRT3 manipulation, further supporting the pro-proliferative role of SIRT3 in melanoma. These are important observations from the following perspectives too. Cytoplasmic PCNA has recently been shown to control glucose metabolism in hematological cells (31). Survivin has been shown to increase the stability of oxidative phosphorylation Complex II, which enhances mitochondrial respiration, and thereby cancer metabolism (32). Proangiogenic factor VEGF has been reported to be an indicator of angiogenesis in melanoma (33). It is known that the tumor cells undergo metabolic changes during angiogenesis that favor tumor growth and progression. Our data suggest the melanoma promoting potential of SIRT3 may be linked with alteration in the metabolic phenotypes, and thus SIRT3 inhibition may be a potential strategy to inhibit melanoma progression.

As SIRT3 has been implicated in regulating cellular metabolism, we determined the role of SIRT3 in metabolic regulation of melanoma cells. Melanoma cells are known to display metabolic adaptations with deregulated glycolysis that favors tumorigenesis (34). Earlier, we have demonstrated that chemical inhibition of SIRT3 along with SIRT1 decreased aerobic glycolysis (glucose uptake, lactate production and NAD+/NADH ratio) in melanoma cells (35). Importantly, the inhibition of glycolysis in cancer has been suggested as a potential target for cancer therapy. Thus, to analyze the effects of SIRT3 knockdown on metabolic regulators in melanoma cells, we utilized glucose metabolism PCR array. We found that SIRT3 inhibition significantly modulates genes related to glycolysis,

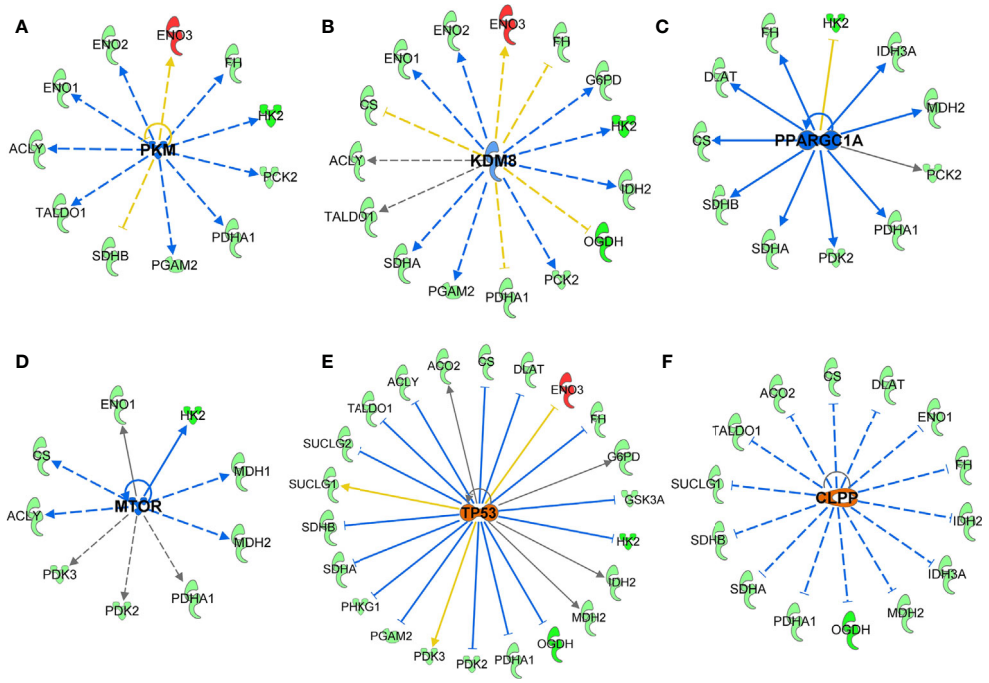

FIGURE 6 | Key upstream signaling pathways predicted in response to SIRT3 knockdown (shSIRT3- SK-MEL-2). Using IPA, upstream regulator analysis identified genes potentially involved in melanoma or cancer. These are **(A)** PKM, **(B)** KDM8, **(C)** PPARGC1A, **(D)** mTOR, **(E)** P53, and **(F)** CLPP signaling. Upstream regulations are denoted with blue (inhibition) **(F)** or orange (activation) color. The interaction lines are indicated as solid (robust interactions), dashed (significant but less frequent), blue (inhibition), orange (activation), yellow (finding inconsistent), and gray (unpredicted).

gluconeogenesis, Krebs cycle and Pentose phosphate pathway, suggesting that inhibition of SIRT3 hampers cellular metabolism, which eventually hinders the proliferative potential of melanoma cells. This can be understood from the fact that tumor cells require not only ATP but also biosynthetic precursors for proliferation. Glycolysis, Pentose phosphate pathway and Krebs cycle are the important source of biosynthetic precursors, in addition to the production of ATP. For example, citrate in mitochondria can be transported into cytoplasm for the conversion of acetyl-CoA and oxaloacetate to fatty acids, which is critical for tumor cell proliferation. This conversion is controlled by the enzyme ATP citrate lyase (ACLY) (36), which was decreased in response to SIRT3 inhibition. The expression levels of glycolytic enzymes, enolase 1 and 2 (ENO1/2) were also lesser in cells having reduced SIRT3, suggesting the metabolic cessation of glycolytic pathway. Enolases are key components of the glycolytic pathway, converting 2-phosphoglycerate into phosphoenolpyruvate. ENO1 knockdown has been shown to result in suppressed glioma cell growth (37). Also, increased ENO2 has been shown to be associated with tumor progression *in vivo* (38). However, ENO3, which is muscle-specific enolase, was increased in response to SIRT3 knockdown. This may be compensatory for the downregulation of its counterpart ENO1 and ENO2, suggesting that the role of enolases needs to be explored in melanoma.

Our data demonstrated that hexokinase (HK2), and oxoglutarate (alpha-ketoglutarate) dehydrogenase (OGDH) were the top two genes that showed maximum changes in the PCR array in response to SIRT3 knockdown. HK2 phosphorylates glucose into glucose-6-phosphate, which serves as the start point for glucose to enter glycolytic pathway and mitochondrial Krebs cycle to produce ATP (39). Aside from being a fundamental component in glycolysis, HK2 is over-expressed in multiple tumors (40). Similarly, in a recent study, cancer cells have been found to display a wide range of sensitivities in response to OGDH knockdown, *in vitro* and *in vivo* (41), suggesting a probable therapeutic target in cancer management. Next, we found that the isoforms of pyruvate dehydrogenase (PDH) complex (PDHA1, PDP2, PDK2 and PDK3), which constitute the link between glycolysis and Krebs cycle (42), were down-regulated upon SIRT3 inhibition, indicating reduced substrate availability for cells to enter the Krebs cycle. Interestingly, SIRT3 is known to deacetylate and increase PDH activity in cancer cells (22). SIRT3 is also known to deacetylate mitochondrial enzyme, isocitrate dehydrogenase (IDH2) that produces NADPH (43); IDH2 was suppressed too upon SIRT3 inhibition. We also found that both glucose-6-phosphate dehydrogenase (G6PD) and hexose-6-phosphate dehydrogenase (H6PD) were significantly down-regulated in SIRT3 knockdown cells, suggesting inhibition of the Pentose phosphate pathway. Overall these results suggest that modulation in these genes in response to SIRT3 inhibition results in metabolic shift in melanoma cells providing lesser fuel for proliferating cells.

Next, upstream analysis of SIRT3 modulated genes predicted the inhibition of HIF1α, PKM, KDM8, PPARGC1A and mTOR,

and activation of P53 and CLPP signaling. The relevance of these observations in melanoma can be understood from the following facts. PKM is known to regulate glycolysis in cells including in malignancies (44, 45). PKM has also been known to be related to the invasiveness of cancers. Indeed, PKM has been identified as one of the major hypoxia-induced HIF1α targets in melanocytes that significantly correlate with reduced melanoma disease-free status (46). Moreover, KDM8 which demethylates H3K36me2 (inhibiting the recruitment of histone deacetylases) and is overexpressed in different types of tumors (47), is known to participate in nuclear translocation of PKM. Similarly, upstream PPARGC1A is used by invasive cancer cells to enhance oxidative phosphorylation, oxygen consumption rate, and mitochondrial biogenesis (48). Oxidative phosphorylation has been shown to promote primary melanoma invasion, suggesting the possible role of PPARGC1A in metabolic rewiring during melanoma progression (49). mTOR, which acts as the target for cell-cycle arrest, is another important signaling predicted to be inhibited in response to SIRT3 inhibition. mTOR deregulation has been observed in many cancer types, including melanoma, and its inhibition has been investigated in clinical treatment (50). Moreover, its association with phosphatidylinositol 3-kinase (PI3K)/protein kinase B (AKT) pathways to regulate cell growth, survival and metabolism make a target of interest in cancer management (50). Interestingly, in our study, we identified the connections of PI3K/AKT and mTOR in response to SIRT3 inhibition (**Figures 5A** and **6D**).

Our analysis of SIRT3-modulated genes further identified upstream activation of tumor suppressor P53. An interaction between SIRT3 and tumor suppressor P53 has been shown in certain cancers. SIRT3 partially abrogates P53 activity to enact growth arrest and senescence in bladder carcinoma (51). Earlier, we have demonstrated that inhibition of SIRT1, another member of sirtuin family, decreased cell proliferation of melanoma cells *via* P53 activation (52, 53). We have also shown a protein network highlighting P53 as key signaling connecting with MYC, and other proteins in response to SIRT1 inhibition (54). SIRT1 and SIRT3 both have been demonstrated to deacetylate P53 protein, and the role of P53 has been implicated in melanoma (reviewed in (55)). Activation of CLPP, which is known to degrade misfolded proteins, was also predicted in our IPA analysis in response to SIRT3 knockdown. Interestingly, it has been found that hyperactivation of CLPP selectively kills cancer cells, without affecting normal cells, and independent of P53 status, by disrupting mitochondrial structure/function *via* the degradation of respiratory chain protein substrates (56).

Overall, our study identified the involvement of SIRT3 in altering the metabolic phenotypes in melanoma. Specifically, our data suggest that modulation of SIRT3 affects the growth of melanoma xenografts as well as various tumor growth markers. Further, our data suggest that inhibition of SIRT3 reverses the glycolytic shift *via* down-regulating key metabolic genes. However, further studies are required to validate SIRT3 as a therapy target in suitable genetically engineered and/or patient-derived xenografts (PDX) models of melanoma. Given the important role of SIRT3 in metabolism, there is always an issue of off-target complications. Therefore the use of SIRT3 as a potential target for melanoma management needs to be carefully investigated.

DATA AVAILABILITY STATEMENT

The original contributions presented in the study are included in the article/supplementary material. Further inquiries can be directed to the corresponding author.

ETHICS STATEMENT

The animal study was reviewed and approved by University of Wisconsin Animal Care and Use Committee.

AUTHOR CONTRIBUTIONS

Conception and design of the study: CS, JG and NA. Methodology: CS, JG, GC, MN. Analysis and interpretation of the data: CS, JG, GC, MN, HC and NA. Writing - original draft preparation: CS. Writing, review and editing: CS, JG, GC, MN, HC and NA. All authors contributed to the article and approved the submitted version.

FUNDING

This work was partially supported by funding from the NIH (R01AR059130 and R01CA176748), and the Department of Veterans Affairs (VA Merit Review Awards I01BX001008 and I01CX001441; and a Research Career Scientist Award IK6BX003780). We also acknowledge the core facilities supported by the Skin Diseases Research Center (SDRC) Core Grant P30AR066524 from NIH/NIAMS.

REFERENCES

1. Siegel RL, Miller KD, Fuchs HE, Jemal A. Cancer Statistics, 2021. *CA Cancer J Clin* (2021) 71(1):7–33. doi: 10.3322/caac.21654
2. Michan S, Sinclair D. Sirtuins in mammals: insights into their biological function. *Biochem J* (2007) 404(1):1–13. doi: 10.1042/BJ20070140
3. Finley LW, Haigis MC. Metabolic regulation by SIRT3: implications for tumorigenesis. *Trends Mol Med* (2012) 18(9):516–23. doi: 10.1016/j.molmed.2012.05.004
4. Wang Q, Zhang Y, Yang C, Xiong H, Lin Y, Yao J, et al. Acetylation of metabolic enzymes coordinates carbon source utilization and metabolic flux. *Science* (2010) 327(5968):1004–7. doi: 10.1126/science.1179687
5. Giralt A, Villarroya F. SIRT3, a pivotal actor in mitochondrial functions: metabolism, cell death and aging. *Biochem J* (2012) 444(1):1–10. doi: 10.1042/BJ20120030
6. Singh CK, Chhabra G, Ndiaye MA, Garcia-Peterson LM, Mack NJ, Ahmad N. The Role of Sirtuins in Antioxidant and Redox Signaling. *Antioxid Redox Signal* (2018) 28(8):643–61. doi: 10.1089/ars.2017.7290

7. Su S, Ndiaye M, Singh CK, Ahmad N. Mitochondrial Sirtuins in Skin and Skin Cancers. *Photochem Photobiol* (2020) 96(5):973–80. doi: 10.1111/php.13254
8. Kwon Y, Kim J, Lee CY, Kim H. Expression of SIRT1 and SIRT3 varies according to age in mice. *Anat Cell Biol* (2015) 48(1):54–61. doi: 10.5115/acb.2015.48.1.54
9. Chen Y, Fu LL, Wen X, Wang XY, Liu J, Cheng Y, et al. Sirtuin-3 (SIRT3), a therapeutic target with oncogenic and tumor-suppressive function in cancer. *Cell Death Dis* (2014) 5:e1047. doi: 10.1038/cddis.2014.14
10. Yang B, Fu X, Shao L, Ding Y, Zeng D. Aberrant expression of SIRT3 is conversely correlated with the progression and prognosis of human gastric cancer. *Biochem Biophys Res Commun* (2014) 443(1):156–60. doi: 10.1016/j.bbrc.2013.11.068
11. Zhang CZ, Liu L, Cai M, Pan Y, Fu J, Cao Y, et al. Low SIRT3 expression correlates with poor differentiation and unfavorable prognosis in primary hepatocellular carcinoma. *PloS One* (2012) 7(12):e51703. doi: 10.1371/journal.pone.0051703
12. Jeong SM, Lee J, Finley LW, Schmidt PJ, Fleming MD, Haigis MC. SIRT3 regulates cellular iron metabolism and cancer growth by repressing iron regulatory protein 1. *Oncogene* (2015) 34(16):2115–24. doi: 10.1038/onc.2014.124
13. Zhao Y, Yang H, Wang X, Zhang R, Wang C, Guo Z. Sirtuin-3 (SIRT3) expression is associated with overall survival in esophageal cancer. *Ann Diagn Pathol* (2013) 17(6):483–5. doi: 10.1016/j.anndiagpath.2013.06.001
14. Ashraf N, Zino S, Macintyre A, Kingsmore D, Payne AP, George WD, et al. Altered sirtuin expression is associated with node-positive breast cancer. *Br J Cancer* (2006) 95(8):1056–61. doi: 10.1038/sj.bjc.6603384
15. Liu C, Huang Z, Jiang H, Shi F. The sirtuin 3 expression profile is associated with pathological and clinical outcomes in colon cancer patients. *BioMed Res Int* (2014) 2014:871263. doi: 10.1155/2014/871263
16. Zhang L, Ren X, Cheng Y, Huber-Keener K, Liu X, Zhang Y, et al. Identification of Sirtuin 3, a mitochondrial protein deacetylase, as a new contributor to tamoxifen resistance in breast cancer cells. *Biochem Pharmacol* (2013) 86(6):726–33. doi: 10.1016/j.bcp.2013.06.032
17. Torrens-Mas M, Pons DG, Sastre-Serra J, Oliver J, Roca P. SIRT3 Silencing Sensitizes Breast Cancer Cells to Cytotoxic Treatments Through an Increment in ROS Production. *J Cell Biochem* (2017) 118(2):397–406. doi: 10.1002/jcb.25653
18. Alhazzazi TY, Kamarajan P, Joo N, Huang JY, Verdin E, D'Silva NJ, et al. Sirtuin-3 (SIRT3), a novel potential therapeutic target for oral cancer. *Cancer* (2011) 117(8):1670–8. doi: 10.1002/cncr.25676
19. George J, Nihal M, Singh CK, Zhong W, Liu X, Ahmad N. Pro-Proliferative Function of Mitochondrial Sirtuin Deacetylase SIRT3 in Human Melanoma. *J Invest Dermatol* (2016) 136(4):809–18. doi: 10.1016/j.jid.2015.12.026
20. Warburg O. On the origin of cancer cells. *Science* (1956) 123(3191):309–14. doi: 10.1126/science.123.3191.309
21. George J, Ahmad N. Mitochondrial Sirtuins in Cancer: Emerging Roles and Therapeutic Potential. *Cancer Res* (2016) 76(9):2500–6. doi: 10.1158/0008-5472.CAN-15-2733
22. Ozden O, Park SH, Wagner BA, Yong Song H, Zhu Y, Vassilopoulos A, et al. SIRT3 deacetylates and increases pyruvate dehydrogenase activity in cancer cells. *Free Radic Biol Med* (2014) 76:163–72. doi: 10.1016/j.freeradbiomed.2014.08.001
23. Gutteridge RE, Singh CK, Ndiaye MA, Ahmad N. Targeted knockdown of polo-like kinase 1 alters metabolic regulation in melanoma. *Cancer Lett* (2017) 394:13–21. doi: 10.1016/j.canlet.2017.02.013
24. Wang X, Spandidos A, Wang H, Seed B. PrimerBank: a PCR primer database for quantitative gene expression analysis, 2012 update. *Nucleic Acids Res* (2012) 40(Database issue):D1144–9. doi: 10.1093/nar/gkr1013
25. Singh CK, Chhabra G, Ndiaye MA, Siddiqui IA, Panackal JE, Mintie CA, et al. Quercetin-Resveratrol Combination for Prostate Cancer Management in TRAMP Mice. *Cancers (Basel)* (2020) 12(8):2141. doi: 10.3390/cancers12082141
26. Cui Y, Qin L, Wu J, Qu X, Hou C, Sun W, et al. SIRT3 Enhances Glycolysis and Proliferation in SIRT3-Expressing Gastric Cancer Cells. *PloS One* (2015) 10(6):e0129834. doi: 10.1371/journal.pone.0129834
27. Liu-Smith F, Dellinger R, Meyskens FL Jr. Updates of reactive oxygen species in melanoma etiology and progression. *Arch Biochem Biophys.* (2014) 563:51–5. doi: 10.1016/j.abb.2014.04.007
28. Finley LW, Carracedo A, Lee J, Souza A, Egia A, Zhang J, et al. SIRT3 opposes reprogramming of cancer cell metabolism through HIF1alpha destabilization. *Cancer Cell* (2011) 19(3):416–28. doi: 10.1016/j.ccr.2011.02.014
29. Wilking-Busch MJ, Ndiaye MA, Huang W, Ahmad N. Expression profile of SIRT2 in human melanoma and implications for sirtuin-based chemotherapy. *Cell Cycle* (2017) 16(6):574–7. doi: 10.1080/15384101.2017.1288323
30. Goldinger SM, Murer C, Stieger P, Dummer R. Targeted therapy in melanoma - the role of BRAF, RAS and KIT mutations. *EJC Suppl* (2013) 11(2):92–6. doi: 10.1016/j.ejcsup.2013.07.011
31. Røst LM, Olaisen C, Sharma A, Nedal A, Petrovic V, Kvitvang HFN, et al. PCNA has specific functions in regulation of metabolism in haematological cells. *bioRxiv* (2020) 104(29):067512. doi: 10.1101/2020.04.29.067512
32. Rivadeneira DB, Caino MC, Seo JH, Angelin A, Wallace DC, Languino LR, et al. Survivin promotes oxidative phosphorylation, subcellular mitochondrial repositioning, and tumor cell invasion. *Sci Signal* (2015) 8(389):ra80. doi: 10.1126/scisignal.aab1624
33. Corrie PG, Basu B, Zaki KA. Targeting angiogenesis in melanoma: prospects for the future. *Ther Adv Med Oncol* (2010) 2(6):367–80. doi: 10.1177/1758834010380101
34. Neagu M. Metabolic Traits in Cutaneous Melanoma. *Front Oncol* (2020) 10:851. doi: 10.3389/fonc.2020.00851
35. George J, Nihal M, Singh CK, Ahmad N. 4'-Bromo-resveratrol, a dual Sirtuin-1 and Sirtuin-3 inhibitor, inhibits melanoma cell growth through mitochondrial metabolic reprogramming. *Mol Carcinog* (2019) 58(10):1876–85. doi: 10.1002/mc.23080
36. Migita T, Okabe S, Ikeda K, Igarashi S, Sugawara S, Tomida A, et al. Inhibition of ATP citrate lyase induces an anticancer effect *via* reactive oxygen species: AMPK as a predictive biomarker for therapeutic impact. *Am J Pathol* (2013) 182(5):1800–10. doi: 10.1016/j.ajpath.2013.01.048
37. Song Y, Luo Q, Long H, Hu Z, Que T, Zhang X, et al. Alpha-enolase as a potential cancer prognostic marker promotes cell growth, migration, and invasion in glioma. *Mol Cancer* (2014) 13:65. doi: 10.1186/1476-4598-13-65
38. Sanzey M, Abdul Rahim SA, Oudin A, Dirkse A, Kaoma T, Vallar L, et al. Comprehensive analysis of glycolytic enzymes as therapeutic targets in the treatment of glioblastoma. *PloS One* (2015) 10(5):e0123544. doi: 10.1371/journal.pone.0123544
39. Mathupala SP, Rempel A, Pedersen PL. Glucose catabolism in cancer cells: identification and characterization of a marked activation response of the type II hexokinase gene to hypoxic conditions. *J Biol Chem* (2001) 276(46):43407–12. doi: 10.1074/jbc.M108181200
40. Pedersen PL, Mathupala S, Rempel A, Geschwind JF, Ko YH. Mitochondrial bound type II hexokinase: a key player in the growth and survival of many cancers and an ideal prospect for therapeutic intervention. *Biochim Biophys Acta* (2002) 1555(1-3):14–20. doi: 10.1016/S0005-2728(02)00248-7
41. Allen EL, Ulanet DB, Pirman D, Mahoney CE, Coco J, Si Y, et al. Differential Aspartate Usage Identifies a Subset of Cancer Cells Particularly Dependent on OGDH. *Cell Rep* (2016) 17(3):876–90. doi: 10.1016/j.celrep.2016.09.052
42. Kaplon J, Zheng L, Meissl K, Chaneton B, Selivanov VA, Mackay G, et al. A key role for mitochondrial gatekeeper pyruvate dehydrogenase in oncogene-induced senescence. *Nature* (2013) 498(7452):109–12. doi: 10.1038/nature12154
43. Schlicker C, Gertz M, Papatheodorou P, Kachholz B, Becker CF, Steegborn C. Substrates and regulation mechanisms for the human mitochondrial sirtuins Sirt3 and Sirt5. *J Mol Biol* (2008) 382(3):790–801. doi: 10.1016/j.jmb.2008.07.048
44. Welinder C, Pawlowski K, Szasz AM, Yakovleva M, Sugihara Y, Malm J, et al. Correlation of histopathologic characteristics to protein expression and function in malignant melanoma. *PloS One* (2017) 12(4):e0176167. doi: 10.1371/journal.pone.0176167
45. Zhao X, Zhu Y, Hu J, Jiang L, Li L, Jia S, et al. Shikonin Inhibits Tumor Growth in Mice by Suppressing Pyruvate Kinase M2-mediated Aerobic Glycolysis. *Sci Rep* (2018) 8(1):14517. doi: 10.1038/s41598-018-31615-y
46. Loftus SK, Baxter LL, Cronin JC, Fufa TD, Program NCS, Pavan WJ. Hypoxia-induced HIF1alpha targets in melanocytes reveal a molecular profile associated with poor melanoma prognosis. *Pigment Cell Melanoma Res* (2017) 30(3):339–52. doi: 10.1111/pcmr.12579
47. Wang HJ, Pochampalli M, Wang LY, Zou JX, Li PS, Hsu SC, et al. KDM8/JMJD5 as a dual coactivator of AR and PKM2 integrates AR/EZH2 network and tumor

metabolism in CRPC. *Oncogene* (2019) 38(1):17–32. doi: 10.1038/s41388-018-0414-x

48. LeBleu VS, O'Connell JT, Gonzalez Herrera KN, Wikman H, Pantel K, Haigis MC, et al. PGC-1alpha mediates mitochondrial biogenesis and oxidative phosphorylation in cancer cells to promote metastasis. *Nat Cell Biol* (2014) 16(10):1–15. doi: 10.1038/ncb3039
49. Salhi A, Jordan AC, Bochaca II, Izsak A, Darvishian F, Houvras Y, et al. Oxidative Phosphorylation Promotes Primary Melanoma Invasion. *Am J Pathol* (2020) 190(5):1108–17. doi: 10.1016/j.ajpath.2020.01.012
50. Chamcheu JC, Roy T, Uddin MB, Banang-Mbeumi S, Chamcheu RN, Walker AL, et al. Role and Therapeutic Targeting of the PI3K/Akt/mTOR Signaling Pathway in Skin Cancer: A Review of Current Status and Future Trends on Natural and Synthetic Agents Therapy. *Cells* (2019) 8(8):803. doi: 10.3390/cells8080803
51. Li S, Banck M, Mujtaba S, Zhou MM, Sugrue MM, Walsh MJ. p53-induced growth arrest is regulated by the mitochondrial SirT3 deacetylase. *PloS One* (2010) 5(5):e10486. doi: 10.1371/journal.pone.0010486
52. Wilking MJ, Singh CK, Nihal M, Ndiaye MA, Ahmad N. Sirtuin deacetylases: a new target for melanoma management. *Cell Cycle* (2014) 13(18):2821–6. doi: 10.4161/15384101.2014.949085
53. Wilking MJ, Singh C, Nihal M, Zhong W, Ahmad N. SIRT1 deacetylase is overexpressed in human melanoma and its small molecule inhibition imparts anti-proliferative response *via* p53 activation. *Arch Biochem Biophys* (2014) 563:94–100. doi: 10.1016/j.abb.2014.04.001
54. Singh CK, George J, Nihal M, Sabat G, Kumar R, Ahmad N. Novel downstream molecular targets of SIRT1 in melanoma: a quantitative proteomics approach. *Oncotarget* (2014) 5(7):1987–99. doi: 10.18632/oncotarget.1898
55. Singh CK, Panackal JE, Siddiqui S, Ahmad N, Nihal M. Combined Inhibition of Specific Sirtuins as a Potential Strategy to Inhibit Melanoma Growth. *Front Oncol* (2020) 10:591972. doi: 10.3389/fonc.2020.591972
56. Ishizawa J, Zarabi SF, Davis RE, Halgas O, Nii T, Jitkova Y, et al. Mitochondrial ClpP-Mediated Proteolysis Induces Selective Cancer Cell Lethality. *Cancer Cell* (2019) 35(5):721–37. doi: 10.1016/j.ccell.2019.03.014

Conflict of Interest: The authors declare that the research was conducted in the absence of any commercial or financial relationships that could be construed as a potential conflict of interest.

frontiers in Oncology

REVIEW
published: 19 July 2021
doi: 10.3389/fonc.2021.702287

Mucosal Melanoma: Pathological Evolution, Pathway Dependency and Targeted Therapy

Yanni Ma[1,2], *Ronghui Xia*[3], *Xuhui Ma*[4], *Robert L. Judson-Torres*[5,6] *and Hanlin Zeng*[1,2*]

[1] Department of Oncology, Ninth People's Hospital, Shanghai Jiaotong University School of Medicine, Shanghai, China, [2] Shanghai Institute of Precision Medicine, Shanghai, China, [3] Department of Oral Pathology, Ninth People's Hospital, Shanghai Jiaotong University School of Medicine, Shanghai, China, [4] Department of Oral & Maxillofacial - Head and Neck Oncology, Ninth People's Hospital, Shanghai Jiao Tong University School of Medicine, Shanghai, China, [5] Department of Dermatology, University of Utah, Salt Lake City, UT, United States, [6] Huntsman Cancer Institute, Salt Lake City, UT, United States

Mucosal melanoma (MM) is a rare melanoma subtype that originates from melanocytes within sun-protected mucous membranes. Compared with cutaneous melanoma (CM), MM has worse prognosis and lacks effective treatment options. Moreover, the endogenous or exogenous risk factors that influence mucosal melanocyte transformation, as well as the identity of MM precursor lesions, are ambiguous. Consequently, there remains a lack of molecular markers that can be used for early diagnosis, and therefore better management, of MM. In this review, we first summarize the main functions of mucosal melanocytes. Then, using oral mucosal melanoma (OMM) as a model, we discuss the distinct pathologic stages from benign mucosal melanocytes to metastatic MM, mapping the possible evolutionary trajectories that correspond to MM initiation and progression. We highlight key areas of ambiguity during the genetic evolution of MM from its benign lesions, and the resolution of which could aid in the discovery of new biomarkers for MM detection and diagnosis. We outline the key pathways that are altered in MM, including the MAPK pathway, the PI3K/AKT pathway, cell cycle regulation, telomere maintenance, and the RNA maturation process, and discuss targeted therapy strategies for MM currently in use or under investigation.

Keywords: mucosal melanoma, mucosal melanocytes, melanocytic lesions, mutations, signaling dependency, targeted therapy

OPEN ACCESS

Edited by:
Vladimir Spiegelman, Penn State Milton S. Hershey Medical Center, United States

Reviewed by:
Moran Amit, University of Texas MD Anderson Cancer Center, United States
Ciro Dantas Soares, Laboratório de Citopatologia, Brazil

***Correspondence:**
Hanlin Zeng
hanlin.zeng@shsmu.edu.cn

Specialty section:
This article was submitted to Skin Cancer, a section of the journal Frontiers in Oncology

Received: *29 April 2021*
Accepted: *02 July 2021*
Published: *19 July 2021*

Citation:
Ma Y, Xia R, Ma X, Judson-Torres RL and Zeng H (2021) Mucosal Melanoma: Pathological Evolution, Pathway Dependency and Targeted Therapy. Front. Oncol. 11:702287. doi: 10.3389/fonc.2021.702287

INTRODUCTION

Melanoma develops due to the unchecked proliferation of melanocytes, which are responsible for the production of pigment. About 90% of melanoma cases are cutaneous melanoma (CM) mainly induced by exposure to ultraviolet (UV) light (1). Non-cutaneous subtypes include uveal melanoma (UM) and mucosal melanoma (MM). MM is a rare type of melanoma that presents on mucosal surfaces of cavities within the body, including the oral, nasal, anorectal, genitourinary, and vulvovaginal region (2). Although MM makes up approximately 1% of all cases of melanoma, it is one of the most aggressive subtypes, and thus exhibits a worse prognosis compared with the

common CM (3, 4). Based on a retrospective study, the 5-year survival rate of MM, considering all stages at the time of diagnosis, is 10-20% when compared to 93% for CM (4–6).

There are several possible reasons for this worse prognosis in MM: 1) Both the biology of mucosal melanocytes as well as the risk factors that are related to MM incidence are poorly understood. Exposure to UV is a well-established risk factor for CM but the mutagens that contribute to the development of MM remain unknown. According to epidemiological studies, smoking, ill-fitting dentures, and ingested/inhaled carcinogens such as tobacco and formaldehyde are regarded as potential causative factors for oral and sinonasal mucosal melanoma (2, 7), while chronic inflammatory disease, viral infections as well as chemical irritants are thought to be implicated in vulvar mucosal melanoma and human immunodeficiency virus (HIV) is associated with anorectal mucosal melanoma (2). However, the contributions and mechanisms of the aforementioned factors to MM initiation or progression are not clearly defined. 2) The evolution of MM from precursor lesions is poorly understood. CM is associated with different types of precursor lesions, including benign melanocytic nevi commonly associated with the *BRAF V600E* mutation and dysplastic nevi associated *NRAS* alterations and *TERT* promoter mutations (8). CM can evolve from these benign lesions following additional mutations that drive tumor invasion and metastasis such as loss of *CDKN2A*, *PTEN*, or *TP53 (*9). Characterization of the morphology and molecular landscape of precursors compared to early melanoma has provided candidate molecular biomarkers for early diagnosis in CM (10–13). However, although several forms of mucosal melanocytic benign lesions are reported, there is still a lack of defined MM precursor lesions, leading to a weak understanding of the evolutionary trajectory of MM despite molecular profiles unveiled by recent whole-genome sequencing data (14–16). 3) MM has more diverse mutation patterns with fewer targetable mutations compared to CM. According to the most frequent and mutually exclusive mutations, CM is mainly classified into 4 genomic subtypes: *BRAF*(52%), *RAS*(31%), *NF1*(14%), and a small portion of triple wild-type (17, 18). Hence, co-targeting BRAF and MEK have been proved to achieve a significant response rate for *BRAF V600* mutated CM patients in clinical management (19, 20). In contrast, MM has more diverse mutation patterns, with less than 20% of *BRAFV600E* mutations (16), followed by the majority of mutations that are scattered and difficult to target, including *NRAS*, *NF1*, *KIT, SF3B1*, and *SPRED1* (21).

Our goals in conducting this review were to: 1) Summarize the types of mucosal melanocytic benign lesions, aiming to find possible genetic and pathological evolutional patterns from benign mucosal melanocytes lesions to malignant tumors; 2) Discuss the main driver mutations and pathways in MM; and 3) Outline the options of targeted treatment for MM in clinical use or under clinical trials.

BIOLOGICAL FUNCTIONS OF MELANOCYTES

Melanocytes are neural crest-derived cells that migrate to specific anatomic locations - including skin, eyes, leptomeninges, and mucous membrane - during development. Cutaneous melanocytes have two final destinations: hair follicles and the basal cell layer of epithelium where they conduct their main biological function of melanin production (22, 23). Melanin is a natural pigment in skin that absorbs UV radiation and scavenges cytotoxic free radicals generated from sunlight exposure (23, 24). Synthesized melanin is secreted to the nearby keratinocytes under solar stimulation and protects the genome of keratinocytes from sun damage (25).

In addition to residing in the skin, melanocytes also dwell in many sun-shielded mucosal tissues like respiratory (oral, nasal, pharynx, larynx, and upper esophagus), intestinal, urogenital, and rectal tracts (2, 24, 26–28). As melanocytes located in mucous membranes are not usually directly exposed to sunlight, it is unlikely that photoprotection is the primary and definitive function of mucosal melanocytes. It was hypothesized that melanocytes localized to mucosal tissues due to errors of migration from the neural crest during embryogenesis (6, 26), but recent evidence suggests that mucosal melanocytes might have biological functions besides pigment production. Specifically, since mucosa plays an important role in the innate immune defense system, it is speculated that mucosal melanocytes are also equipped with immunogenic functions (23, 29).

It is reported that melanin has strong toxin binding properties that can neutralize toxins produced by bacteria (30). Meanwhile, aromatic precursors, including quinone and semiquinone intermediates generated during the melanization cascade, can disrupt the lipid bilayer of cell membranes of microorganisms and mediate an anti-bacterial effect (31, 32). The strong binding capacity of melanin is probably due to its specific graphite-like lamellar structure in which four to eight monomers are covalently bound to form a porphyrin-like system (33). As a result, melanin is able to interact with aromatic metabolites or compositions of microorganisms through hydrogen bonds or π-π interactions (34, 35). Another explanation for the anti-bacterial properties of melanin and its intermediates is that they contain high levels of redox-active catechol groups, which can produce reactive oxygen species under light and water stimulation (36). However, since the mucosal melanocytes are in a dark environment with marginal melanin production, it remains unknown whether the pigment levels in mucosal regions are sufficient for antimicrobial effects.

In addition to the anti-bacterial properties of melanin, melanocytes can also participate in the intrinsic and acquired immune system. On the one hand, melanocytes can participate in innate immunity since they are found to express Toll-like receptors, indicating melanocytes can recognize pathogen-associated molecular patterns present in microbes (37, 38). Once being recognized, bacteria and fungi can be engulfed by melanocytes – a phenomenon that has been observed under the microscope - before undergoing possible degradation pathways by lysosome hydrolytic enzymes contained in melanosomes (39, 40). On the other hand, melanocytes may be a component of acquired immunity. Melanocytes have been reported to express MHC class II loaded with mycobacterial peptides (41), suggesting that melanocytes may function as antigen-

presenting cells and subsequently activate $CD4^+$ T cells proliferation (42). Although the phagocytotic functions of melanocytes have been observed, the activation of T cells through antigen presented by melanocytes, for instance, should be further verified by investigating the expression of CD86, CD80, or other markers of antigen-presenting cells on the surface of melanocytes. Since melanocytes have the capacity to produce a variety of cytokines, including interleukins and interferons which may be involved in the regulation of the activity of neighboring immune cells under stimulations of exogenous nucleic acids (43–47), the hypothesis that melanocytes activate T cells through secreting specific cytokines, instead of acting as antigen-presenting cells, must also be tested. These collective observations suggest melanocytes likely participate to some extent in the immune defense of the body, but their precise immunological roles in the innate or adaptive immune system need to be dissected in further studies.

MUCOSAL MELANOCYTIC BENIGN LESIONS

Studies in the pathologic evolution of CM have shown that invasive melanomas can evolve from a variety of benign and intermediate pathological stages including benign nevus, dysplastic nevus, and malignant tumor in situ (8, 9). Melanocytic nevi are benign lesions requiring no further treatment, while atypical melanocytic hyperplasia or atypical nevi are regarded as either indeterminant or premalignant lesions that warrant careful clinical management and long-term follow-up for patients. In contrast, there is no clear definition and characterization of precursor lesions of MM despite the fact that multiple mucosal melanocytic benign lesions are observed and documented in the clinic (**Figures 1A, B**). Using OMM as the most well-studied example, **Table 1** summarizes several benign pigmented lesions including macule, nevus, and melanocanthoma with their specific pathological characteristics.

Melanotic Macule of the Oral Mucosa

Melanotic macules are one of the most common melanocytic lesions (48, 49) and lentigo simplex is the term used to describe a group of small and round macules (50). The color of macules varies from gray to brown to black. The diversity of pigmentation is thought to be associated with the ratio of eumelanin and pheomelanin (23, 24). Macules are usually regarded as benign lesions since the causative factor of macules is melanin deposition and no Ki-67 positive melanocytes are observed (51, 52). Hence, the diameter of the pigmented lesions is usually less than 1 cm, and their morphology is flat, solitary, and well-circumscribed (**Figure 1A**). From histological examinations, the basal cell layer of benign macules is exhibited with uniform melanin accumulation without an increase in the density of melanocytes or the presence of nevus (**Figures 1E, F**). These lesions are asymptomatic and no malignant transformation is reported at this stage. The most frequently observed site for macules in the oral cavity is the vermillion border of the lip at the rate of 30% followed by the gingiva and alveolar ridge (23%), and the buccal (16%) or labial mucosa (9%) (24). Interestingly, the hard palate, which is one of the most common locations for OMM has less chance for macule occurrence (7%) (24). Although there is no evidence that melanotic macules are directly associated with the eventual diagnosis of MM in oral mucosa, some published case reports have recorded the transformation of benign macules to malignant OMM after years of diagnosis (53–55), suggesting the malignant potential of some macular lesions to be considered as precursor lesions. As Ki-67 staining is not routinely requested in the diagnosis of melanotic macules, it is unclear what percentage of lesions contain proliferating melanocytes and may possess malignancy potentiality.

Oral Mucosal Nevus

Oral nevi are much less common than their counterparts on the skin and their prevalence is about 0.1% in the general population (24). Subepithelial lesions are the most common oral mucosal nevi (55%), followed by blue nevi in submucosal–mucosal junction (**Figures 1I, J**) (36%), and junctional nevi are the least frequent ones (3%) (7, 56). According to the histologic location of melanocytes, oral nevi can be divided into three categories: junctional nevi (**Figures 1K, L**) at the tip of the widened and elongated epithelial spikes; compound nevi arranged in nests and belts in the lamina propria; and subepithelial nevi (**Figures 1B, G, H**) entirely in the subepithelial connective tissue. The formation of nevi in oral mucosa results from the proliferation of melanocytes along with the epithelial basal cell layer, but most are relatively small with a mean diameter of 0.5cm. Similar to macules, nevi harbor clear borders. However, instead of being flat, more than 50% of nevi are elevated pigmented lesions. In addition, about 15% of oral nevi are non-pigmented and the mechanism behind the lack of pigmentation remains unclear (24). From the histopathological point of view, the appearance of nevus cells along epithelial spikes is polygonal and epithelioid. Typical nevus cells have uniformly round or oval nuclei and contain sparse, uniform, and small melanin granules in the cytoplasm. As for nevus cells in the deeper subepithelial tissue, they become smaller with less cytoplasm and dense and deeply stained nucleus-like lymphocytes.

Although there is a lack of case reports unequivocally documenting the transformation of benign nevi to malignant tumors in the oral cavity, the risk of malignancy in some oral nevi cannot be excluded. The deficiency of case reports is partially due to the rare individuals with congenital or acquired nevi and short follow-up periods of objects (57). A clinicopathologic analysis shows that five out of seven OMM patients have junctional nevi, therefore some clinicians recommend a complete excisional biopsy to rule out early OMM for individuals with junctional nevi (58). In addition, nowadays the classification of nevi is mainly based on their histologic positions and lacks criteria based on the degree of malignancy. Only the appearance of dysplastic nevi is considered as an increased risk of melanoma (59–61). Dysplastic nevi are usually larger than normal nevi with macular or popular components and ill-defined borders (62). The current

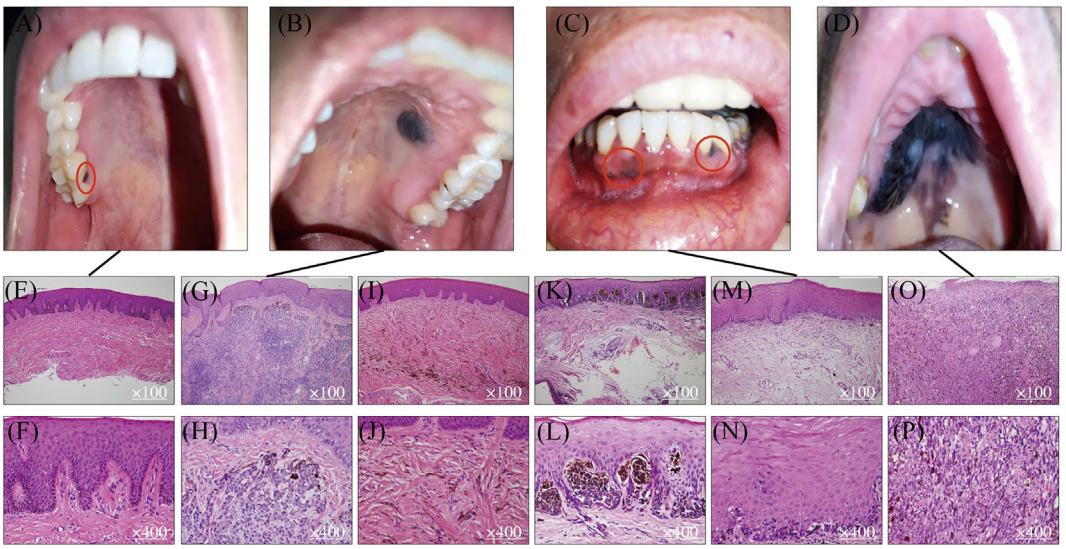

FIGURE 1 | Mucosal melanocytic benign lesions and malignant OMM. Benign hyperpigmented lesions **(A, B)** and malignant OMM in situ **(C, D)**. Benign macule in gingiva **(A)** and its HE staining pictures **(E, F)**. Benign intramucosal nevus on the hard palate **(B)** and its HE staining pictures **(G, H)**. HE staining of blue nevus **(I, J)**. HE staining of junctional nevus **(K, L)**. Lentigo maligma melanoma on mandibular gingiva **(C)** and its HE staining figures **(M, N)**. Ulcerated malignant MM on the hard palate **(D)** and its HE staining pictures **(O, P)**.

diagnosis of dysplastic nevi mainly depends on their architectural disorder rather than specific biomarkers, which heavily relies on the experience of pathologists and causes a relatively high rate of misdiagnosis. Hence, more refined diagnostic criteria and more sensitive biomarkers are needed clinically to find potential precancerous nevi.

Melanoacanthoma

Melanoacanthoma is a rare form of benign melanotic lesion characterized by benign proliferation of both keratinocytes and melanocytes (24, 63). Microscopic examination can detect the hyperplastic keratinocytes, while positive immunostainings of HMB-45 and S-100 prove the presence of melanocytes abnormal accumulation (64). Compared with macule and nevus, this benign entity is much rarer but may mimic OMM due to its rapid increase in size with diameters of several centimeters being reached in just a few weeks. The lesion is usually flat or slightly raised and most commonly occurs on the buccal mucosa. Histopathologic examination shows many dendritic melanocytes and processes containing melanin in all strata of

TABLE 1 | Comparison of benign lesions and malignant oral mucosal melanoma.

	Macule	Nevi	Melanoacanthoma	OMM
Prevalence in melanocytic lesions	62% (48, 49)	15% (48, 49)	0.8% (48, 49)	0.7% (48, 49)
Color	Gray to brown to black	Brown, bluish-gray or black, 15% non-pigmented	Brown or black	Variable
Size (mean diameter)	<1 cm	0.5cm	Several centimeters	4 cm
Shape	Flat, solitary & well-circumscribed	Well-demarcated but elevated	Flat or slightly raised	Asymmetric with irregular outline
Commonly occurred site	Lip & gingiva	Palate	Buccal mucosa	Hard palate & maxillary gingiva
Causative factor	Melanin deposition	Proliferation of melanocytes	Proliferation of keratinocytes & melanocytes	Uncontrolled growth of melanocytes
Histopathologic features	Melanin accumulation without an increase in melanocytes.	Polygonal & epithelioid nevus cells in the superficial. Cytoplasm transparent to light stained.	Many dendritic melanocytes, processes containing melanin & melanophagocytes in all strata of epithelium.	Large, vesicular nucleus & prominent nucleoli. Aggregated into sheets or alveolar groups. Neurotropic or desmoplastic configurations.

epithelium. Besides, melanophagocytes, mild lymphocyte infiltration, as well as vasodilation are seen in the lamina proporia. Similar to other benign lesions, once the melanoacanthoma is diagnosed, the site is usually just monitored, as these lesions are highly likely to regress within 2 to 6 months after biopsy (65, 66). However, if a melanoacanthoma enlarges in a very short period of time, it may indicate a sign of malignancy (67). A more comprehensive understanding of what drives mucosal melanocyte proliferation as well as the regression in melanoacanthoma, and how the fast-growing melanoacanthoma transforms into MM, is needed.

Oral macule, nevus, and melanoacanthoma are usually diagnosed as benign lesions, but periodical physical examinations and biopsies of those melanocytic lesions are still recommended because approximately one-third of OMM patients are found to present benign pigmented lesions prior to the emergence of the malignant state (67–69). Additionally, our collaborating clinicians and pathologists at Shanghai Ninth People's Hospital have observed the development of hyperpigmentations adjacent to OMM in a majority of patients and they suspect that tumors expand through those *de novo* pigmented lesions (**Figures 1D**). Based on the above findings, we propose that a subgroup of benign lesions, especially macules, possess the potential to transform to OMM. If true, identification of biomarkers for those cancer-predisposing lesions coupled with more radical surgical excision may improve the outcome of patients. To achieve this goal, a thorough genetic evolution study sequencing not only malignant MMs but also benign lesions and suspected premalignant lesions is needed. Assessment of the genetic evolution of benign and malignant MM subtypes may reveal markers of increased risk of malignant transformation to aid in early diagnosis and clinical management.

MUCOSAL MELANOMA

OMM is one of the most frequent and well-studied MM subtypes. The preferred site for OMM (**Figure 1D**) is the keratinized mucosa, including the hard palate and maxillary gingiva where the masticatory stress is focused (70). Symptoms include pain, ulceration, bleeding, loose teeth, bone erosion, etc. (71, 72). The MM shows variable color from black to red or white accompanied with asymmetric and irregular morphology (73). Contrasting from CM, which is commonly diagnosed in the radial growth phase, OMM is usually first identified in a vertical growth phase with 30% of lesions at an invasive stage, and 55% of lesions at a combined invasive and *in situ* stage (7). Also different from CM, MM lacks a clear classification system for subtypes of lesions. Based on the histopathologic patterns and levels of solar damage, there are several different categorization methods for CM (74), whereas the subclassification of MM remains controversial. Currently, it is simply divided into MM *in situ*, invasive MM, and MM with a mixed pattern. The observing surface architecture of MM ranges from macular to ulcerated and nodular (75). Lentigo maligna melanoma (**Figure 1C**) is regarded as one form of OMM *in situ* as it shares similar histopathological traits as typical OMM *in situ* (**Figures 1M, N**). From the microscopic perspective, OMM consists of diverse morphological melanocytes including epithelioid, spindle, and plasmacytoid, which typically have a large, vesicular nucleus with prominent nucleoli (**Figures 1O, P**). They are usually aggregated into sheets or alveolar groups and less commonly neurotropic or desmoplastic configurations are observed. Most of the tumors contain melanin, while only a small proportion is amelanotic (76). As for immunohistochemical features of OMM, there is no single immunohistochemical marker that invariantly identifies all OMM. A variable expression of S-100, Melan-A, MITF, tyrosinase, and HMB-45 has been reported (27, 28, 49, 76). SOX 10 is a new marker, showing high sensitivity (positive in 88-100% of OMM cases) but moderate specificity in MM (77, 78). Hence, identification of biomarkers for OMM with better test characteristics of needed to achieve a consistent accurate diagnosis of MM and its initial lesions.

MUTATIONS AND SIGNALING PATHWAY DEPENDENCY IN MM

To date, whole-genome sequencing (WGS) and whole-exome sequencing (WES) has revealed the genomic profile of MM and pinpointed reoccurring aberrant genes that potentially drive the evolution of melanocytes to malignant tumors in the mucosal membrane. In contrast to CM, MM harbors a low single nucleotide mutation burden, but a high number of chromosomal structural variants (16, 79). *BRAF* and *NRAS* mutations, which are widely present in CM, are less frequent in MM (16, 79). Instead, activating mutations in *SF3B1* and *KIT*, loss of *CDKN2A, PTEN*, or *SPRED1*, as well as amplification of *CDK4, TERT, KIT, MDM2*, or *CCND1*, are more common in MM (16). **Table 2** compares the genetic profile between CM and MM. The data for altered genes in CM are average from Akbani's and Hayward's papers (17, 79), while the figures for MM are obtained from Newell's paper (16). **Figure 2** summarizes the frequency of alterations in possible driver genes based upon WGS data of 67 frozen tumors (16). Those mutated genes correspond to specific cellular pathways that are potentially highly dependent on the initiation and progression of MM, providing potentially effective targets for combined treatment in the clinic.

KIT Signaling Pathway

C-KIT is a receptor tyrosine kinase located on the membrane of various cell types. The stimulation of the C-KIT receptor by its extracellular ligand leads to downstream activation of the MAPK and PI3K signaling cascades that play an important role in proliferation, survival, and motility of melanoma cells (80). There is a high prevalence of *KIT* gain-of-function alterations including missense mutation and copy number amplification in patients with MM at rates of 15% and 21% respectively (16), while the corresponding figures in CM are only 3.7% and 4.2% separately (17, 79). MMs with *KIT* mutations presumably affect the function of juxta-membrane autoinhibitory domain (JMD) (W557R, N566D, V559A, V559D, V560D, V569G, P573L,

TABLE 2 | Comparison of genetic profiles MM and CM.

Cellular pathway	Gene	CM	MM
C-KIT pathway	*KIT*	$3.7\%_{mut}$; $4.2\%_{amp}$ (17, 79)	$15\%_{mut}$; $21\%_{amp}$ (16)
MAPK pathway	*NRAS*	$29\%_{mut}$ (17, 79)	$18\%_{mut}$ (16)
	BRAF	$51\%_{mut}$ (17, 79)	$16\%_{mut}$; $13\%_{amp}$ (16)
	NF1	$15\%_{mut}$ (17, 79)	$16\%_{mut}$ (16)
	SPRED1	rare	$7.5\%_{mut}$; $3.0\%_{del}$ (16)
PI3K pathway	*PTEN*	$9.0\%_{mut}$; $12\%_{del}$ (17, 79)	$6.0\%_{del}$ (16)
Splicesome pathway	*SF3B1*	$6.4\%_{mut}$ (17, 79)	$12\%_{mut}$ (16)
Cell cycle pathway	*TP53*	$16\%_{mut}$ (17, 79)	$9.0\%_{mut}$ (16)
	CDK4	$4.0\%_{amp}$ (17, 79)	$28\%_{amp}$ (16)
	CCND1	$5.5\%_{amp}$ (17, 79)	$18\%_{amp}$ (16)
	MDM2	$3.5\%_{amp}$ (17, 79)	$19\%_{amp}$ (16)
	CDKN2A	$16\%_{mut}$;$44\%_{del}$ (17, 79)	$24\%_{del}$ (16)
Telomere maintenance	*TERT* promoter	$72\%_{mut}$ (17, 79)	$9.0\%_{mut}$ (16)
	TERT	$8.2\%_{amp}$ (17, 79)	$22\%_{amp}$ (16)

Mut, mutation; Amp, amplification; Del, deletion.

L576P, K642E) and tyrosine kinase domains (D816H, D820Y, A829P, N822K), causing constitutive activation of C-KIT-regulated pathways (81–84). Among the aforementioned mutations, K642E is the most frequently observed in MM. Although codon 642 is located out of the JMD, amino acid aberrations in this position are thought to destabilize the JMD through amino acid interactions (81). Besides WGS and WES data, immunohistochemistry images show increased protein expression of C-KIT in all *in situ* MMs and nearly 90% of invasive tissues in a cohort of 18 cases (85), indicating the strengthening of the C-KIT signaling pathway. Compared to CM, the gain-of-function alterations of *KIT* are more common not only in MM but also in acral melanoma (AM) (86). Although the mechanism explaining why C-KIT is pathogenetically important in sun-protected melanomas remains poorly understood, it does not prevent the protein from being a potentially effective therapeutic target and a series of C-KIT inhibitors are currently under pre-clinical and clinical investigations (82, 87–89).

RAS-RAF-MEK-ERK MAP Kinases Pathway

Stimulation of C-KIT or other receptor tyrosine kinase on the cellular membrane by extracellular growth factors provokes downstream activation of RAS and RAF kinases followed by phosphorylation of MEK and ERK, leading to activation of the

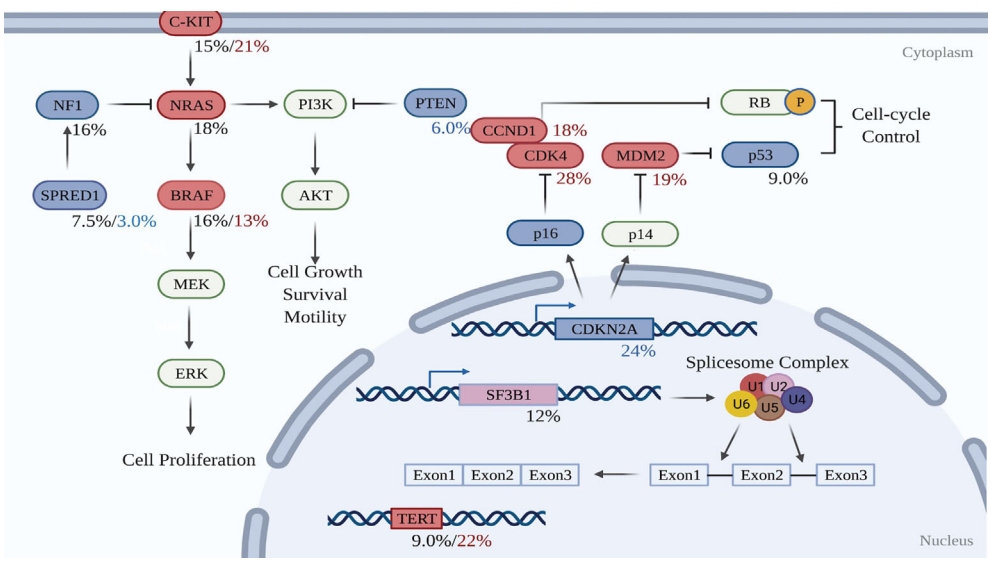

FIGURE 2 | Molecular pathways involved in the development of mucosal melanoma. Red-filled rectangles indicate genes experiencing activating mutation or amplification, while blue-filled rectangles genes undoing suppressing mutation or deletion. Black figures suggest mutation rates, whereas red and blue percentages are respectively amplification and deletion proportions in the test cohort. Created with BioRender.com (2021). *Retrieved from* https://app.biorender.com/biorender-templates.

MAPK pathway implicated in the regulation of cell proliferation, differentiation, and survival (90). NRAS and BRAF both play a part in the MAPK pathway, which are thought to contribute to melanoma development.

NRAS activating mutations are prevalent in CM at 29% (17, 79), while the mutation frequency in MM is only 18% (16). Furthermore, nearly 90% of *NRAS* missense mutations occur at codon 61 in CM, compared to 54% for MM. The remaining 46% of mutations are located at codon 12 and codon 13 (91). Compared with *NRAS* activating mutations at positions 12 and 13, *NRAS* Q61 mutations exert a stronger activating effect on the MAPK pathway since codon 61 is the catalytic residue for GTP hydrolysis and Q61 mutation impedes the return of RAS to an inactive GDP-bound state (92). For both CM and MM, Q61R and Q61K are the most commonly detected amino acid transitions at codon 61. Similarly, the most common mutations for both types of melanoma at codon 13 are G13D and G13R, although G13R is predominant in CM and G13D in MM (93).

BRAF is a serine-threonine kinase involved in the MAPK signaling pathway. Over 50% of CM cases report activating mutation of the *BRAF* gene (17, 79), while merely 16% of MMs experience the same alteration (16). In addition to harboring common active mutations, *BRAF* is distinct from *NRAS* in MM in that the locus undergoes amplification in 13% of cases (16). Mutations in the *BRAF* gene are missense mutations and they most frequently occur at codon 600, the activating loop, where amino acids change from valine to glutamic acid (V600E) (93). Besides the activation loop (A-loop), the second most common site for amino acid substitutions is the GSGSFG phosphate-binding loop (P-loop) at residues 464-469 (94). The activity of BRAF kinase is regulated by the interaction formed between A-loop and P-loop, thus mutations in either A-loop or P-loop disrupt the interaction and cause hyperactivation of the kinase (93, 95). In CM, more than 90% of mutations are present on the V600 codon, whereas in MM only 63% are V600 mutations, with the remainder (37%) on the G469, D594, and K601 codons (91, 93). In other words, MM not only has far less frequent *BRAF* missense mutations but also has more diverse locations for *BRAF* mutations as compared to CM. However, similar to CM there is nearly no coincidence of *NRAS* and *BRAF* missense mutations, suggesting functionally redundant *NRAS* and *BRAF* mutations in MM despite more variable mutational locations.

Although the contribution of mutant *NRAS* and *BRAF* to MM progression appears to be less common than melanoma of the skin, more components in the MAPK pathway of MM tend to undergo mutations or copy number changes, rendering inhibition of MAPK signaling transduction more challenging. The *NF1* gene, for example, encodes neurofibromin 1 protein, a negative regulator of Ras proteins, and can lose its function in both CM and MM. *NF1* mutation rates are 16% in MM (16) and 15% in CM (17, 79), suggesting *NF1* plays a pivotal role in the biology of both types of melanoma. Loss of *NF1* is associated with sustained activation of Ras proteins, leading to hyperactivation of MAPK and PI3K-AKT intracellular signaling pathway that evokes melanogenesis. Similar to CM, *NF1* suppression is significantly enriched in tumors lacking either *BRAF* or *NRAS* mutations (16, 96). However, in melanomas harboring both *BRAF* and *NF1* mutations, it is more likely that tumors can escape from MAPK inhibiting therapy (97, 98). Meanwhile, *NF1* is significantly co-mutated with *KIT* in 32% of MMs, whereas the co-occurrence level in CM is merely 4% (99), which indicates that the MAPK cascade is upregulated in MM not only by the single protein in the cytoplasm but also by the assistance of C-KIT receptor on the cell membrane.

SPRED1 is another potential driver gene for MM. SPRED1, sprout-related, EVH1 domain containing protein 1, is a tumor suppressor. SPRED1 facilitates the localization of NF1 to the plasma membrane where it suppresses RAS signaling (6). Therefore, the loss of SPRED1 function leads to the activation of MAPK pathway signaling transduction. 7.5% of MM have *SPRED1* inactivating mutations and 12% undergo *SPRED1* copy number loss (16), whereas *SPRED1* alterations are insignificant in CM (17, 79). In MM, *SPRED1* loss rarely co-occurs with *BRAF* mutations, *NRAS* mutations, or *NF1* inactivation mutations (6), indicating those alterations play similar roles in activating MAPK pathway signaling in MM. Analogous to *NF1*, around 30% of MM cases with *SPRED1* inactivation simultaneously exhibit *KIT* alterations, suggesting that *SPRED1* inactivation may be in collaboration with other oncogenic events to stimulate tumor development (100). Based on the pattern of mutually exclusive occurrence of *NF1* and *SPRED1* and their respective tendency to alter simultaneously with *KIT*, it is reasonable to speculate that NF1 and SPRED1 loss function similarly in MM. In addition, it has been proposed that the reduced sensitivity and drug resistance to KIT inhibitors partially result from the hyperactivation of MAPK caused by the loss of *SPRED1* – a model verified in human melanoma cell lines and *in vivo* zebrafish model (6, 101), but presently untested in mouse models and patient samples.

PI3K-AKT-mTOR Pathway

The PI3K-AKT-mTOR pathway is another frequently activated oncogenic signaling cascade in MM, which is verified by elevated AKT phosphorylation through immunohistochemical staining (102, 103). The aforementioned abnormal *KIT*, *NRAS*, *NF1*, and *SPRED1* genes are able to not only activate the MAPK signaling cascade but also dysregulate the PI3K-AKT-mTOR pathway. Additionally, the PI3K pathway is stimulated by suppression of a negative regulator, phosphatase and tensin homologue (PTEN) (104). Compared with 12% of *PTEN* loss in CM where deletions and mutations both account for the changes (17, 79), *PTEN* is deeply deleted in merely 6.0% of MM cases and has hardly any mutations (16) Furthermore, there is rare co-occurrence of deleted *PTEN* and amplified *KIT* that possibly implies that loss of *PTEN* or gain of *KIT* are redundant for the activation of the PI3K pathway in MM. This is also supported by the fact that besides *KIT* and *PTEN*, mutations in PI3K and AKT homologous of PI3K-AKT-mTOR are scarce (4.8% *PIK3CA*, 3.8% *PIK3CG*, and 4.8% *AKT3*) (105). It has been reported that silencing of

PTEN cooperates with activated AKT to promote metastasis of melanoma (102, 103, 106, 107), but MM does not show a weaker performance in metastasis than CM in the clinic possibly because there are other gene alterations in the PI3K pathway promoting invasiveness of tumor (108). In a cohort of 91 MM patients, 18% of cases show TSC1 loss-of-function mutations which plays a suppressive role in cellular proliferation initiated by mTOR (109) and a similar result also showed in a recently published meta-analysis review of MM (105). Due to the limited sample size, the alteration levels for TSC need to be further verified. Taking into account the frequency of alterations in known genes involved in PI3K-AKT-mTOR pathway activation, applying PI3K pathway blockers could possibly be an effective target strategy in MM patients.

The Spliceosome Pathway

The spliceosome complex is responsible for the removal of introns from precursor mRNA and the ligation of exons to form mature mRNA. SF3B1 (splicing factor 3b subunit 1) is the largest and core component of the U2 small nuclear ribonucleoprotein (snRNP) and thus *SF3B1* mutations directly cause aberrant gene transcripts which eventually lead to mRNA degradation or abnormal protein function or protein decay (110, 111). *SF3B1* mutations have been reported in 12% of MM (16), while a very small portion of tested CM patients harbor similar alterations (17, 79, 112). Despite their notable absence in CM, alterations in the *SF3B1* gene are not unique to MM - similar mutations have also been detected in uveal melanoma, breast cancer, myelodysplastic syndromes, and chronic lymphocytic leukemia, including mutation hotspots such as codon 700, 622, 625, 662, and 666 (99, 113). To be more specific, *SF3B1* mutations at codon 625 are predominately associated with mucosal and uveal melanoma, while alterations at codon 700 are present across myeloid leukemia and chronic lymphocytic leukemia (6), implying disparate SF3B1 mutational preference that is possibly related to distinct etiology. Although *SF3B1* mutations are widely present in MM, it is poorly understood which genes alternatively spliced by mutant *SF3B1* drive malignant transformation. It has been discovered that *BRD9, PPP2R5A*, and *DVL2*, are candidate genes for alternative splicing in *SF3B1 K700*-mutant chronic lymphocytic leukemia (114–116), while *ABCC5*, *UQCC*, and *CRNDE* are possible targets in three uveal melanoma cases mixed with R625 and K700 mutations (117). Hence, due to the variability of SF3B1 mutations in solid and hematologic cancers, experiments that query the consequence of the *SF3B1 R625* mutation in mucosal melanocytes are needed to understand mis-spliced targets and tumorigenic oncogenic mechanisms related to SF3B1 mutations in MM.

Intriguingly, although SF3B1 does not possess a direct role in MAPK pathway signal transduction, there is little overlap between tumors with MAPK pathway mutations and *SF3B1*-mutated tumors, suggesting that SF3B1 mutations possibly lead to splicing variations of specific genes that can lead to MAPK activation (16). Meanwhile, the MAPK pathway can also regulate splicesome activity. It is reported that activation of the MEK-ERK pathway by Golgi stress enhances the activity of ETS transcriptional factors that have the capacity to regulate the expression of splicesome components, resulting in a switch of MCL1 protein function through different splicing (118). This study indicates that dysregulation of some downstream effectors by the MAPK pathway is able to lead to splicing aberrations. The mechanisms connecting the splicing alternations to signal transduction remain enigmatic. Mutant K700E *SF3B1* causes loss of function of phosphatase PP2A, followed by the phosphorylation changes related to signaling cascade (115), thereby providing a potential link between an alternative splicing and signaling pathways. Further investigations are needed to elucidate the specific mis-spliced genes and proteins directly influenced by *SF3B1* mutations together with the crosstalk between SF3B1 and MAPK pathway in tumorigenesis of MM, and the findings may provide a new perspective for targeted therapy.

Cell Cycle Pathway

The abrogation of cell cycle checkpoint and apoptosis regulators is widely present in melanoma (119), including *CDKN2A* loss and *CDK4/6* or *CCND1* amplification. The *CDKN2A* locus encodes two distinct tumor suppressors, $p16^{INK4A}$ and $p14^{ARF}$. The $p16^{INK4A}$ protein suppresses the forward progression of the cell cycle by inhibiting CDK4 or CDK6. The CDK4/6/CCND1 complex phosphorylates and inhibits the retinoblastoma (Rb), which leads to E2F1 transcription activation and G1-S phase cell cycle transmission (120). The other CDKN2A transcript, $p14^{ARF}$, functions, at least in part, by blocking MDM2 ubiquitylation mediated TP53 degradation, which permits apoptosis escape (121). In MM patients, 24% of tumors exhibit copy number loss of *CDKN2A (*16). Additionally, *CDK4*, *CCND1*, and *MDM2* are amplified in 28%, 18%, and 19% of samples respectively, and *TP53* mutations occur in 9.0% of MMs (16). Most of these cell cycle components are also commonly disrupted in CM. However, although CM has a much higher *CDKN2A* loss than MM, MM tends to show a greater frequency of *CCND1* and *CDK4* amplification (120, 122), implying CDK4 blocking agents may achieve a desired anti-tumor effect on MM. Intriguingly, MM cells without mutations in *BRAF* or *NRAS* mutations tend to exhibit *CCND1* or *CDK4* amplification (122), suggesting that copy number variations of cell cycle regulatory genes act as an alternative driver and can substitute for *BRAF* or *NRAS* mediated proliferation signaling pathway activation.

Telomere Maintenance

Telomerase reverse transcriptase, encoded by the gene *TERT*, is the catalytic subunit of the enzyme telomerase, responsible for lengthening telomeres at the end of chromatin (123, 124). Thus, overexpression of TERT confers the potential of cells to become immortal (125), which is one of the hallmarks of cancer. *TERT* promoter mutations and *TERT* amplifications are common genetic events in the early stages of melanoma of the skin (8). For CM, more than two-thirds of tumors exhibit *TERT* promoter mutation, and only a minority of malignancies present copy number amplification (17, 79). As a comparison, the frequency of *TERT* activating alteration in MM declines to 30%, and most of them are copy number gain rather than promoter mutations

(16). As for why CM and MM present distinct mechanisms of TERT activation, most *TERT* promoter mutations in CM are C>T mutations or CC>TT di-pyrimidine mutations (126, 127), suggesting that *TERT* promoter mutations are induced by UV radiation which partially explains why these mutations are rare in sun-shielded MM. Apart from *TERT*, the gene *ATRX* is also involved in telomere maintenance. *ATRX* is associated with alternative lengthening of telomeres as an additional mechanism for telomere maintenance in tumors lacking *TERT* promoter mutations (128). Despite rare samples associated with *ATRX* alterations in CM, nonsense mutation and frameshift of *ATRX* are detected in 11.9% of MMs (16) implying that *ATRX* is responsible for telomere extension in MM as well. However, the altering level of *ATRX* needs to be further tested in a larger cohort since the gene are not significantly mutated in other sequencing results except for Newell's study.

Although CM exhibits a much higher frequency of TERT activation than MM, there is no statistically significant difference in telomere length among CM and MM, and both of them even undergo telomere shortening (8, 79, 129). Those intriguing findings remind us that aberrant *TERT* might have tumorigenic impacts in melanocytes other than telomere lengthening. It is reported that human TERT (hTERT) is equipped with a telomere protective function independent of its canonical catalytic activity (130). Overexpression of hTERT in melanoma is able to produce a protective complex on DNA damage that leads to the sustained proliferation capacity of cancer cells (130). In addition, phosphorylated TERT at a specific position by CDK1 has an RNA-dependent RNA polymerase (RdRP) activity (131). RdRP generates small interfering RNAs complementary to a tumor suppressor gene *FOXO4*, degrading mRNAs of *FOXO4*, reducing protein expression and consequently leading to tumor formation (131, 132). Taken together, these observations suggest potential differences in telomere maintenance mechanisms among different subtypes of melanoma.

PROGRESS IN MM TARGET THERAPY

When compared with CM, MM is typically detected at advanced stages, which renders the tumor challenging to treat. Surgical excision is predominately the first choice for MM (133–135). However, due to the lentiginous growth pattern, multifocal nature of MM, and limitations of the specific MM anatomic sites, it is extremely difficult for surgery to achieve wide negative margins, which leads to a high local relapse rate at 50%-90% (2). For unresectable and metastatic MM, targeted therapy and immunotherapy are constrained since MM is deficient in dominant MAPK activating mutations that can be targeted and is less responsive to immunotherapy (136). Therefore, to date, the first-line therapeutic modality for advanced MM remains chemotherapy despite limited efficacy (137).

While targeted therapies for MM are limited, multiple clinical trials targeting aberrant genes in MM are ongoing. Similar to CM, the MAPK cascade is hyperactivated by altered genes in MM including *NRAS*, *BRAF*, *NF1*, and *SPRED1*, thereby making inhibition of MAPK signal transduction a promising treatment strategy for MM patients. For the minority of MM patients with *BRAF* mutations, combined inhibition of BRAF and MEK is an attractive strategy because the combination therapy shows an impressive response rate at 76% and has a 5-year survival rate of 33% for *BRAFV600E/K* positive CM patients (138). Although there is no clinical trial underway specifically evaluating the safety and efficacy of combination therapy of BRAF inhibitor plus MEK inhibitor in MM, a retrospective study in Japan showed that MM/AM and CM exhibited similar response rates to combined BRAF and MEK suppression (64.3% vs 76.5%) (139), suggesting the potential efficiency of dual repression of BRAF and MEK in MM. For patients without *BRAF* mutations but with *NRAS*, *NF1*, or *SPRED1* alterations, targeting the downstream protein MEK is another strategy for MM patients. The safety and efficacy of MEK blocking agents in MM have been confirmed in an ongoing phase 2 study where 20% NRAS-mutated melanoma patients showed partial response to MEK inhibitor binimetinib with tolerated and manageable adverse events (140). However, for both monotherapy of MEK inhibitor and combined treatment of BRAF and MEK inhibitors, acquired resistance through reactivation of the MAPK pathway can restrict their therapeutic efficacy (141). To overcome this resistance, it is necessary to inhibit downstream proteins like ERK or develop new molecules targeting aberrant MAPK signaling. Meanwhile, besides independent suppression of MAPK pathway, MEK blockers have also been combined with mTOR1/2, AKT, or CDK4/6 inhibitors in preclinical models or in clinical trials of MM (142–144). Although therapeutic parameters do not significantly improve compared to the single MAPK inhibition, dual signaling pathway blocking still provides a new perspective for MM targeted therapy.

Interestingly, compared to CM, MM patients tend to harbor more activating mutations or amplifications in the receptor tyrosine kinase *KIT*, providing a rationale for targeting C-KIT. Imatinib, sunitinib, dasatinib, nilotinib, and masitinib are approved C-KIT inhibitors in different cancer types and their anti-cancer effects for MM are currently in the clinical research stage (145–148). Imatinib is the most widely investigated C-KIT inhibitor. In a recent trial of 78 melanoma patients harboring *KIT* alterations, the median overall survival for imatinib is 13.1 months and the objective response rate is 21.8% (149). Additionally, it has been discovered that C-KIT inhibitor imatinib harbors high efficacy against melanoma with *KIT* mutations, but not with *KIT* amplification only (54% vs 0% partial response) (148, 150). To be more specific, MMs with *KIT* mutations in exon 11 (L576P) and exon 13 (K642E) tend to have a better and longer response to C-KIT inhibitors than other mutations (84, 151). Despite the strong anti-tumor effect of C-KIT inhibitors, MM patients who respond to the inhibiting agents well at the beginning will frequently experience a brief period of disease response before developing resistance to KIT inhibitors that eventually leads to progressive disease (152, 153). The acquired resistance to KIT inhibitors is possibly conferred from pre-existing concomitant mutations in other oncogenes like

NRAS or secondary *KIT* mutations during the use of drugs. For instance, secondary A829P *KIT* mutation renders melanoma cells resistant to imatinib but has no influence on nilotinib and dasatinib, while the T670I *KIT* mutation exhibits resistance to imatinib, nilotinib as well as dasatinib, but can still be suppressed by sunitinib (154). Considering the promising performance of C-KIT inhibitors in MM, now more efforts have been focused on the understanding of the acquired resistance mechanism and the development of new blocking agents to overcome resistance, offering hope for patients with advanced MM and limited treatment options.

In the future, targeted therapy could offer an alternative adjuvant therapy option for a group of patients based on their gene sequencing results. If actionable driver mutations are identified in an individual MM, targeted therapies for the driver genes or proteins could be utilized on a patient-by-patient basis. Until now there are only a few available targeted therapies for MM clinical trials: BRAF, MEK, CDK4/6 and, C-KIT inhibitors, with limited clinical use and efficacy. Therefore, it requires more efforts on developing other alternative targeting strategies based on mutated genes in MM such as splicesome complex components, telomerase, and DNA repair pathway. H3B-8800, for instance, is the blocker for splicing modulator of SF3B complex and it at present is in phase I study of myeloid cancers (155). Considering the MM specific SF3B1 hotspot mutation in R625, developing strategies that can specifically target R625 mutant SF3B1 might may achieve benefit MM patients with low side effects.

DISCUSSION

MM is a rare but aggressive malignancy. Due at least in part to delayed diagnosis at the advanced stage and the lack of efficient therapeutic strategies, this subtype of melanoma is associated with a worse prognosis than melanoma arising from the skin. In contrast to CM, the etiology, risk factors, and pathogenesis of MM are poorly understood, partially explaining the deficiency of effective treatment options and extremely poor prognosis. This review takes OMM as a model and attempts to identify commonalities in etiology, pathogenesis, mutation patterns, and corresponding pathway dependency. Besides cigarette smoking, denture irritation, and alcohol, chronic infections caused by microorganisms and mechanical stress generated by routine activities may have an impact on tumorigenesis in the mucosal membrane. However, the oral microflora is in a dynamic process of change and is influenced by many internal and external factors, including the host's physical conditions, diet, and hygiene habits. A more comprehensive study investigating the relationship between flora and cancer, the selection of patients, sampling locations, and control settings will be needed.

Since there is limited knowledge about pre-MM lesions and a lack of corresponding molecular pathological biomarkers, early diagnosis, as well as early intervention becomes extremely challenging, leading to the short life expectancy in MM patients. Due to the unclear relationships between benign lesions and precursor lesions, histopathological information alone cannot thoroughly define and accurately discriminate them. It is reported that one patient died of OMM after 63 months of misdiagnosed premalignant atypical melanocytic hyperplasia as a benign lentigo simplex (50). Therefore, it is an urgent need to discover biomarkers for lesions with a greater tendency of malignant transformation. To achieve this goal, a thorough genomic and transcriptomic profiling of the evolutionary trajectories of MM starting from benign lesions and potential intermediate lesions is worth pursuit. Another strategy for studying cancer evolution is to establish transgenic mice that capture the evolution process of MM. However, unlike CM, there is a lack of animal models that can recapitulate the oncogenesis process accompanied with the accumulation of genetic alterations in MM. By stepwise introduction of *BRAF V600E* mutation, *CDKN2A* loss, *PTEN* loss and *mTOR* activation, CM precursor lesions followed by CM formation was observed in mice (156–159). Likewise, decoding the accumulative mutation pattern based on MM patient samples will pave the path to the generation of MM transgenic mice model, which not only contribute to understanding the pathogenesis of MM but also serve as functional tools to evaluate the efficacy of novel therapeutic modalities.

Recent sequencing studies have identified significant alterations in *NRAS, BRAF, NF1, KIT, SF3B1, TP53*, and *SPRED1*, informing potential targeted therapeutic strategies for MM (14–16, 160, 161). Firstly, MM patients have shown similar pathway dependency although with divergent mutation patterns. Compared to CM, fewer *NRAS*, *BRAF* mutations are seen in MM, but more *SF3B1* mutation and *KIT* alterations are found. Since targetable *BRAF* mutations are far less frequent in MM, target validation of other alterations in the MAPK pathway is needed. The sequencing results of 67 MMs show that mutations of *NRAS*, *BRAF*, *KIT*, and *SF3B1* are mutually exclusive, implying those mutations may converge on activating the MAPK pathways (16). Further studies about how *SF3B1* mutations are involved in MAPK pathway activation are needed. Secondly, MM has gained fewer genetic mutations for cell cycle regulators but more copy number changes than CM. While *CDKN2A* copy number loss is a frequently observed event in both CM and MM, MM presents more CDK4 and CCND1 amplifications, which makes targeting CDK4 promising in MM.

It is worth mentioning that MM has a much higher level of structure variation and chromosomal instability compared to CM. As a result, specific attention should be paid to targeting the chromosomal rearrangements. Targeting genes involved in DNA damage repair response including PARP, DNA-PKcs, ATR, ATM, CHK1, WEE1 might achieve unexpected clinical response in MM patients (162–164). Olaparib, for instance, is an FDA-approved inhibitor of the enzyme poly ADP ribose polymerase (PARP) which can efficiently kill BRCA mutant tumor cells, a successful synthetic lethality based targeting strategy used in breast cancers and ovarian cancers (165). Although MM rarely shows BRCA mutations, the significantly high level of structure variation indicates the deficiency of

homologous recombination repair (HRR) capacity, which makes MM potentially responsive to PARP inhibition. Nevertheless, a more comprehensive understanding about the mutation signatures as well as signatures of chromosome structure variation in MM are needed. A more stringent validation of PARP inhibitor response in MM cell lines, PDX, and early clinical trials are supposed to conduct to better understand the pharmacological mechanism of drug response in MM.

Other than targeted therapy, immune checkpoint blocker (ICB) based immunotherapy has shown a strong anti-tumor effect on metastatic CM. Ipilimumab against cytotoxic T-lymphocyte antigen 4 (CTLA4), nivolumab and pembrolizumab against programmed death 1 (PD1) as well as atezolizumab against programmed death-ligand 1 (PD-L1) are approved by the FDA for the treatment for advanced melanoma either as monotherapy or combination therapy (166). The overall response rate (ORR) for CM patients to ipilimumab, nivolumab, pembrolizumab and atezolizumab is 12%, 40%, 33% and 30% respectively (167–169), while the combined treatment of ipilimumab with nivolumab significantly improves the ORR to 61% with median progression-free survival (PFS) of 11.5 months (170, 171). However, those ICBs do not exert a satisfactorily inhibitory impact on MM as they do on CM, showing the ORR to anti-CTLA4 or anti-PD1/PDL1 as the single agent from 7% to 35% (136, 172–174). Even the combination regimen of anti-CTLA4 (ipilimumab) and anti-PD1 (nivolumab) agents merely witness a slight increased ORR to 37% with PFS at 5.9 month (136, 175). The limited response to ICBs in MM is mainly because of low mutation burden and limited immune cell infiltration compared to CM (3, 176, 177). To further overcome unsatisfactory performance of ICBs in MM, combination of ICBs with different targeted therapy strategies has been tested in clinical trials. For example, a phase Ib trial using PD-1 antibody toripalimab and vascular endothelial growth factor receptors (VEGFR) inhibitor axitinib showed a dramatical improvement in ORR and PFS to 61% and 9.1 months separately (178, 179), although the safety and efficacy of this combination strategy needs to be further validated. Meanwhile, the combination of toripalimab and vorolanib which targets and inhibits multi-tyrosine kinase including VEGF and C-KIT are ongoing in MM trial (180).

In summary, both basic research and drug discoveries in CM have achieved enormous progress, whereas little is known about either how MM initiates or how to target MM. As a result, patients of MM are suffering from limited treatment options and undesirable response rates that lead to extremely poor prognoses. Here we summarize the current state of knowledge regarding initiation and progression of MM and the risk factors and treatment options for MM. In doing so, we highlight current gaps in our knowledge regarding MM progression, and propose important future research directions, includes studying the genetic evolution trajectory of MM from benign precursor lesions and evaluating new targeting strategies specifically for MM, such as targeting CDK4, SF3B1 or PARP, either as single agent or in combinations with ICBs. We hope these efforts will give more comprehensive knowledge about how MM initiates and progresses, provide more specific biomarkers for MM early diagnosis, offer more potentially effective treatment options for MM and, in the end, improve the life expectancy and quality for MM patients.

AUTHOR CONTRIBUTIONS

YM wrote the main body of the paper. HZ and RLJ revised the review. RX and XM provided significant intellectual contribution on clinical observations and pathological description of melanocytic lesions. HZ conceived and directed the idea of the manuscript. All authors contributed to the article and approved the submitted version.

REFERENCES

1. D'Orazio J, Jarrett S, Amaro-Ortiz A, Scott T. UV Radiation and the Skin. *Int J Mol Sci* (2013) 14(6):12222–48. doi: 10.3390/ijms140612222
2. Carvajal RD, Spencer SA, Lydiatt W. Mucosal Melanoma: A Clinically and Biologically Unique Disease Entity. *J Natl Compr Canc Netw* (2012) 10 (3):345–56. doi: 10.6004/jnccn.2012.0034
3. Tyrrell H, Payne M. Combatting Mucosal Melanoma: Recent Advances and Future Perspectives. *Melanoma Manag* (2018) 5(3):MMT11. doi: 10.2217/mmt-2018-0003
4. Hahn HM, Lee KG, Choi W, Cheong SH, Myung KB, Hahn HJ. An Updated Review of Mucosal Melanoma: Survival Meta-Analysis. *Mol Clin Oncol* (2019) 11(2):116–26. doi: 10.3892/mco.2019.1870
5. Gershenwald JE, Scolyer RA, Hess KR, Sondak VK, Long GV, Ross MI, et al. Melanoma Staging: Evidence-Based Changes in the American Joint Committee on Cancer Eighth Edition Cancer Staging Manual. *CA Cancer J Clin* (2017) 67(6):472–92. doi: 10.3322/caac.21409
6. Nassar KW, Tan AC. The Mutational Landscape of Mucosal Melanoma. *Semin Cancer Biol* (2020) 61:139–48. doi: 10.1016/j.semcancer.2019.09.013
7. Femiano F, Lanza A, Buonaiuto C, Gombos F, Di Spirito F, Cirillo N. Oral Malignant Melanoma: A Review of the Literature. *J Oral Pathol Med* (2008) 37(7):383–8. doi: 10.1111/j.1600-0714.2008.00660.x
8. Shain AH, Yeh I, Kovalyshyn I, Sriharan A, Talevich E, Gagnon A, et al. The Genetic Evolution of Melanoma From Precursor Lesions. *N Engl J Med* (2015) 373(20):1926–36. doi: 10.1056/NEJMoa1502583
9. Shain AH, Bastian BC. From Melanocytes to Melanomas. *Nat Rev Cancer* (2016) 16(6):345–58. doi: 10.1038/nrc.2016.37
10. Bastian BC, Olshen AB, LeBoit PE, Pinkel D. Classifying Melanocytic Tumors Based on DNA Copy Number Changes. *Am J Pathol* (2003) 163 (5):1765–70. doi: 10.1016/S0002-9440(10)63536-5
11. Clarke LE, Flake DD2nd, Busam K, Cockerell C, Helm K, McNiff J, et al. An Independent Validation of a Gene Expression Signature to Differentiate Malignant Melanoma From Benign Melanocytic Nevi. *Cancer* (2017) 123 (4):617–28. doi: 10.1002/cncr.30385
12. Hilliard NJ, Krahl D, Sellheyer K. P16 Expression Differentiates Between Desmoplastic Spitz Nevus and Desmoplastic Melanoma. *J Cutan Pathol* (2009) 36(7):753–9. doi: 10.1111/j.1600-0560.2008.01154.x
13. Lezcano C, Jungbluth AA, Nehal KS, Hollmann TJ, Busam KJ. PRAME Expression in Melanocytic Tumors. *Am J Surg Pathol* (2018) 42(11):1456–65. doi: 10.1097/PAS.0000000000001134
14. Lyu J, Song Z, Chen J, Shepard MJ, Song H, Ren G, et al. Whole-Exome Sequencing of Oral Mucosal Melanoma Reveals Mutational Profile and Therapeutic Targets. *J Pathol* (2018) 244(3):358–66. doi: 10.1002/path.5017

15. Mikkelsen LH, Maag E, Andersen MK, Kruhoffer M, Larsen AC, Melchior LC, et al. The Molecular Profile of Mucosal Melanoma. *Melanoma Res* (2020) 30(6):533–42. doi: 10.1097/CMR.0000000000000686
16. Newell F, Kong Y, Wilmott JS, Johansson PA, Ferguson PM, Cui C, et al. Whole-Genome Landscape of Mucosal Melanoma Reveals Diverse Drivers and Therapeutic Targets. *Nat Commun* (2019) 10(1):3163. doi: 10.1038/s41467-019-11107-x
17. Cancer Genome Atlas N. Genomic Classification of Cutaneous Melanoma. *Cell* (2015) 161(7):1681–96. doi: 10.1016/j.cell.2015.05.044
18. Conway JR, Dietlein F, Taylor-Weiner A, AlDubayan S, Vokes N, Keenan T, et al. Integrated Molecular Drivers Coordinate Biological and Clinical States in Melanoma. *Nat Genet* (2020) 52(12):1373–83. doi: 10.1038/s41588-020-00739-1
19. Larkin J, Ascierto PA, Dreno B, Atkinson V, Liszkay G, Maio M, et al. Combined Vemurafenib and Cobimetinib in BRAF-Mutated Melanoma. *N Engl J Med* (2014) 371(20):1867–76. doi: 10.1056/NEJMoa1408868
20. Bollag G, Hirth P, Tsai J, Zhang J, Ibrahim PN, Cho H, et al. Clinical Efficacy of a RAF Inhibitor Needs Broad Target Blockade in BRAF-Mutant Melanoma. *Nature* (2010) 467(7315):596–9. doi: 10.1038/nature09454
21. Rabbie R, Ferguson P, Molina-Aguilar C, Adams DJ, Robles-Espinoza CD. Melanoma Subtypes: Genomic Profiles, Prognostic Molecular Markers and Therapeutic Possibilities. *J Pathol* (2019) 247(5):539–51. doi: 10.1002/path.5213
22. Cichorek M, Wachulska M, Stasiewicz A, Tyminska A. Skin Melanocytes: Biology and Development. *Postepy Dermatol Alergol* (2013) 30(1):30–41. doi: 10.5114/pdia.2013.33376
23. Feller L, Masilana A, Khammissa RA, Altini M, Jadwat Y, Lemmer J. Melanin: The Biophysiology of Oral Melanocytes and Physiological Oral Pigmentation. *Head Face Med* (2014) 10:8. doi: 10.1186/1746-160X-10-8
24. Hicks MJ, Flaitz CM. Oral Mucosal Melanoma: Epidemiology and Pathobiology. *Oral Oncol* (2000) 36(2):152–69. doi: 10.1016/s1368-8375(99)00085-8
25. Lin JY, Fisher DE. Melanocyte Biology and Skin Pigmentation. *Nature* (2007) 445(7130):843–50. doi: 10.1038/nature05660
26. Mihajlovic M, Vlajkovic S, Jovanovic P, Stefanovic V. Primary Mucosal Melanomas: A Comprehensive Review. *Int J Clin Exp Pathol* (2012) 5(8):739–53. doi: 10.3109/15513815.2012.659410
27. Pontes FSC, de Souza LL, de Abreu MC, Fernandes LA, Rodrigues ALM, do Nascimento DM, et al. Sinonasal Melanoma: A Systematic Review of the Prognostic Factors. *Int J Oral Maxillofac Surg* (2020) 49(5):549–57. doi: 10.1016/j.ijom.2019.11.001
28. Santos RS, Andrade MF, Alves Fde A, Kowalski LP, Perez DE. Metastases of Melanoma to Head and Neck Mucosa: A Report of Short Series. *Clin Exp Otorhinolaryngol* (2016) 9(1):80–4. doi: 10.21053/ceo.2016.9.1.80
29. Feller L, Chandran R, Kramer B, Khammissa RA, Altini M, Lemmer J. Melanocyte Biology and Function With Reference to Oral Melanin Hyperpigmentation in HIV-Seropositive Subjects. *AIDS Res Hum Retroviruses* (2014) 30(9):837–43. doi: 10.1089/AID.2014.0062
30. Plonka PM, Picardo M, Slominski AT. Does Melanin Matter in the Dark? *Exp Dermatol* (2017) 26(7):595–7. doi: 10.1111/exd.13171
31. Urabe K, Aroca P, Tsukamoto K, Mascagna D, Palumbo A, Prota G, et al. The Inherent Cytotoxicity of Melanin Precursors: A Revision. *Biochim Biophys Acta* (1994) 1221(3):272–8. doi: 10.1016/0167-4889(94)90250-x
32. Man MQ, Lin TK, Santiago JL, Celli A, Zhong L, Huang ZM, et al. Basis for Enhanced Barrier Function of Pigmented Skin. *J Invest Dermatol* (2014) 134(9):2399–407. doi: 10.1038/jid.2014.187
33. Tolleson WH. Human Melanocyte Biology, Toxicology, and Pathology. *J Environ Sci Health C Environ Carcinog Ecotoxicol Rev* (2005) 23(2):105–61. doi: 10.1080/10590500500234970
34. Hong L, Simon JD. Current Understanding of the Binding Sites, Capacity, Affinity, and Biological Significance of Metals in Melanin. *J Phys Chem B* (2007) 111(28):7938–47. doi: 10.1021/jp071439h
35. Jakubiak P, Lack F, Thun J, Urtti A, Alvarez-Sanchez R. Influence of Melanin Characteristics on Drug Binding Properties. *Mol Pharm* (2019) 16(6):2549–56. doi: 10.1021/acs.molpharmaceut.9b00157
36. Rahmani Eliato T, Smith JT, Tian Z, Kim ES, Hwang W, Andam CP, et al. Melanin Pigments Extracted From Horsehair as Antibacterial Agents. *J Mater Chem B* (2021) 9(6):1536–45. doi: 10.1039/d0tb02475a
37. Ahn JH, Park TJ, Jin SH, Kang HY. Human Melanocytes Express Functional Toll-Like Receptor 4. *Exp Dermatol* (2008) 17(5):412–7. doi: 10.1111/j.1600-0625.2008.00701.x
38. Yu N, Zhang S, Zuo F, Kang K, Guan M, Xiang L. Cultured Human Melanocytes Express Functional Toll-Like Receptors 2-4, 7 and 9. *J Dermatol Sci* (2009) 56(2):113–20. doi: 10.1016/j.jdermsci.2009.08.003
39. Le Poole IC, van den Wijngaard RM, Westerhof W, Verkruisen RP, Dutrieux RP, Dingemans KP, et al. Phagocytosis by Normal Human Melanocytes In Vitro. *Exp Cell Res* (1993) 205(2):388–95. doi: 10.1006/excr.1993.1102
40. Dell'Angelica EC, Mullins C, Caplan S, Bonifacino JS. Lysosome-Related Organelles. *FASEB J* (2000) 14(10):1265–78. doi: 10.1096/fj.14.10.1265
41. Le Poole IC, Mutis T, van den Wijngaard RM, Westerhof W, Ottenhoff T, de Vries RR, et al. A Novel, Antigen-Presenting Function of Melanocytes and its Possible Relationship to Hypopigmentary Disorders. *J Immunol* (1993) 151(12):7284–92.
42. van Tuyn J, Jaber-Hijazi F, MacKenzie D, Cole JJ, Mann E, Pawlikowski JS, et al. Oncogene-Expressing Senescent Melanocytes Up-Regulate MHC Class II, a Candidate Melanoma Suppressor Function. *J Invest Dermatol* (2017) 137(10):2197–207. doi: 10.1016/j.jid.2017.05.030
43. Swope VB, Sauder DN, McKenzie RC, Sramkoski RM, Krug KA, Babcock GF, et al. Synthesis of Interleukin-1 Alpha and Beta by Normal Human Melanocytes. *J Invest Dermatol* (1994) 102(5):749–53. doi: 10.1111/1523-1747.ep12376970
44. Mattei S, Colombo MP, Melani C, Silvani A, Parmiani G, Herlyn M. Expression of Cytokine/Growth Factors and Their Receptors in Human Melanoma and Melanocytes. *Int J Cancer* (1994) 56(6):853–7. doi: 10.1002/ijc.2910560617
45. Wang S, Liu D, Ning W, Xu A. Cytosolic dsDNA Triggers Apoptosis and Pro-Inflammatory Cytokine Production in Normal Human Melanocytes. *Exp Dermatol* (2015) 24(4):298–300. doi: 10.1111/exd.12621
46. Besch R, Poeck H, Hohenauer T, Senft D, Hacker G, Berking C, et al. Proapoptotic Signaling Induced by RIG-I and MDA-5 Results in Type I Interferon-Independent Apoptosis in Human Melanoma Cells. *J Clin Invest* (2009) 119(8):2399–411. doi: 10.1172/JCI37155
47. Satomi H, Wang B, Fujisawa H, Otsuka F. Interferon-Beta From Melanoma Cells Suppresses the Proliferations of Melanoma Cells in an Autocrine Manner. *Cytokine* (2002) 18(2):108–15. doi: 10.1006/cyto.2002.1028
48. Buchner A, Merrell PW, Carpenter WM. Relative Frequency of Solitary Melanocytic Lesions of the Oral Mucosa. *J Oral Pathol Med* (2004) 33(9):550–7. doi: 10.1111/j.1600-0714.2004.00238.x
49. Tavares TS, Meirelles DP, de Aguiar MCF, Caldeira PC. Pigmented Lesions of the Oral Mucosa: A Cross-Sectional Study of 458 Histopathological Specimens. *Oral Dis* (2018) 24(8):1484–91. doi: 10.1111/odi.12924
50. Umeda M, Komatsubara H, Shibuya Y, Yokoo S, Komori T. Premalignant Melanocytic Dysplasia and Malignant Melanoma of the Oral Mucosa. *Oral Oncol* (2002) 38(7):714–22. doi: 10.1016/s1368-8375(02)00008-8
51. Rivera RS, Nagatsuka H, Siar CH, Gunduz M, Tsujigiwa H, Han PP, et al. Heparanase and Vascular Endothelial Growth Factor Expression in the Progression of Oral Mucosal Melanoma. *Oncol Rep* (2008) 19(3):657–61. doi: 10.3892/or.19.3.657
52. Buery RR, Siar CH, Katase N, Fujii M, Liu H, Kubota M, et al. Clinico-Pathological Evaluation of Oral Melanotic Macule, Oral Pigmented Nevus and Oral Mucosal Melanoma. *J Hard Tissue Biol* (2010) 19(1):57–64. doi: 10.2485/jhtb.19.57
53. Garzino-Demo P, Fasolis M, Maggiore GM, Pagano M, Berrone S. Oral Mucosal Melanoma: A Series of Case Reports. *J Craniomaxillofac Surg* (2004) 32(4):251–7. doi: 10.1016/j.jcms.2003.12.007
54. Kahn MA, Weathers DR, Hoffman JG. Transformation of a Benign Oral Pigmentation to Primary Oral Melanoma. *Oral Surg Oral Med Oral Pathol Oral Radiol Endod* (2005) 100(4):454–9. doi: 10.1016/j.tripleo.2005.01.018
55. Lu S-Y, Lin C-F, Huang S-C. Metastatic Oral Malignant Melanoma Transformed From Pre-Existing Pigmented Lesions in Mandibular Gingiva: Report of an Unusual Case. *J Dental Sci* (2013) 8(3):328–32. doi: 10.1016/j.jds.2012.11.005
56. Patrick RJ, Fenske NA, Messina JL. Primary Mucosal Melanoma. *J Am Acad Dermatol* (2007) 56(5):828–34. doi: 10.1016/j.jaad.2006.06.017
57. Meleti M, Mooi WJ, Casparie MK, van der Waal I. Melanocytic Nevi of the Oral Mucosa - No Evidence of Increased Risk for Oral Malignant Melanoma:

An Analysis of 119 Cases. *Oral Oncol* (2007) 43(10):976–81. doi: 10.1016/j.oraloncology.2006.11.013
58. Liu W, Wang Y, Du G, Zhou Z, Yang X, Shi L. Potential Association Between Oral Mucosal Nevus and Melanoma: A Preliminary Clinicopathologic Study. *Oral Dis* (2020) 26(6):1240–5. doi: 10.1111/odi.13335
59. Ferreira L, Jham B, Assi R, Readinger A, Kessler HP. Oral Melanocytic Nevi: A Clinicopathologic Study of 100 Cases. *Oral Surg Oral Med Oral Pathol Oral Radiol* (2015) 120(3):358–67. doi: 10.1016/j.oooo.2015.05.008
60. Psaty EL, Scope A, Halpern AC, Marghoob AA. Defining the Patient at High Risk for Melanoma. *Int J Dermatol* (2010) 49(4):362–76. doi: 10.1111/j.1365-4632.2010.04381.x
61. Kim CC, Berry EG, Marchetti MA, Swetter SM, Lim G, Grossman D, et al. Risk of Subsequent Cutaneous Melanoma in Moderately Dysplastic Nevi Excisionally Biopsied But With Positive Histologic Margins. *JAMA Dermatol* (2018) 154(12):1401–8. doi: 10.1001/jamadermatol.2018.3359
62. Clark WHJr., Reimer RR, Greene M, Ainsworth AM, Mastrangelo MJ. Origin of Familial Malignant Melanomas From Heritable Melanocytic Lesions. 'The B-K Mole Syndrome'. *Arch Dermatol* (1978) 114(5):732–8. doi: 10.1001/archderm.114.5.732
63. Rosebush MS, Briody AN, Cordell KG. Black and Brown: Non-Neoplastic Pigmentation of the Oral Mucosa. *Head Neck Pathol* (2019) 13(1):47–55. doi: 10.1007/s12105-018-0980-9
64. Datta A, Lamba AK, Tandon S, Urs A, Lnu M. A Unique Presentation of Gingival Melanoacanthoma: Case Report and Review of Literature. *Cureus* (2020) 12(3):e7315. doi: 10.7759/cureus.7315
65. Lakshminarayanan V, Ranganathan K. Oral Melanoacanthoma: A Case Report and Review of the Literature. *J Med Case Rep* (2009) 3:11. doi: 10.1186/1752-1947-3-11
66. Rohilla K, Ramesh V, Balamurali P, Singh N. Oral Melanoacanthoma of a Rare Intraoral Site: Case Report and Review of Literature. *Int J Clin Pediatr Dent* (2013) 6(1):40–3. doi: 10.5005/jp-journals-10005-1185
67. Olszewska M, Banka A, Gorska R, Warszawik O. Dermoscopy of Pigmented Oral Lesions. *J Dermatol Case Rep* (2008) 2(3):43–8. doi: 10.3315/jdcr.2008.1015
68. Magremanne M, Vervaet C. [Melanoma of the Oral Mucosa]. *Rev Stomatol Chir Maxillofac* (2008) 109(3):175–7. doi: 10.1016/j.stomax.2008.02.003
69. Hashemi Pour MS. Malignant Melanoma of the Oral Cavity: A Review of Literature. *Indian J Dent Res* (2008) 19(1):47–51. doi: 10.4103/0970-9290.38932
70. Rambhia PH, Stojanov IJ, Arbesman J. Predominance of Oral Mucosal Melanoma in Areas of High Mechanical Stress. *J Am Acad Dermatol* (2019) 80(4):1133–5. doi: 10.1016/j.jaad.2018.07.064
71. Tacastacas JD, Bray J, Cohen YK, Arbesman J, Kim J, Koon HB, et al. Update on Primary Mucosal Melanoma. *J Am Acad Dermatol* (2014) 71(2):366–75. doi: 10.1016/j.jaad.2014.03.031
72. Lopez F, Rodrigo JP, Cardesa A, Triantafyllou A, Devaney KO, Mendenhall WM, et al. Update on Primary Head and Neck Mucosal Melanoma. *Head Neck* (2016) 38(1):147–55. doi: 10.1002/hed.23872
73. Warszawik-Hendzel O, Slowinska M, Olszewska M, Rudnicka L. Melanoma of the Oral Cavity: Pathogenesis, Dermoscopy, Clinical Features, Staging and Management. *J Dermatol Case Rep* (2014) 8(3):60–6. doi: 10.3315/jdcr.2014.1175
74. Elder DE, Bastian BC, Cree IA, Massi D, Scolyer RA. The 2018 World Health Organization Classification of Cutaneous, Mucosal, and Uveal Melanoma: Detailed Analysis of 9 Distinct Subtypes Defined by Their Evolutionary Pathway. *Arch Pathol Lab Med* (2020) 144(4):500–22. doi: 10.5858/arpa.2019-0561-RA
75. Wu Y, Zhong Y, Li C, Song H, Guo W, Ren G. Neck Dissection for Oral Mucosal Melanoma: Caution of Nodular Lesion. *Oral Oncol* (2014) 50(4):319–24. doi: 10.1016/j.oraloncology.2014.01.008
76. de-Andrade BA, Toral-Rizo VH, Leon JE, Contreras E, Carlos R, Delgado-Azanero W, et al. Primary Oral Melanoma: A Histopathological and Immunohistochemical Study of 22 Cases of Latin America. *Med Oral Patol Oral Cir Bucal* (2012) 17(3):e383–8. doi: 10.4317/medoral.17588
77. Williams MD. Update From the 4th Edition of the World Health Organization Classification of Head and Neck Tumours: Mucosal Melanomas. *Head Neck Pathol* (2017) 11(1):110–7. doi: 10.1007/s12105-017-0789-y
78. Miettinen M, McCue PA, Sarlomo-Rikala M, Biernat W, Czapiewski P, Kopczynski J, et al. Sox10–a Marker for Not Only Schwannian and Melanocytic Neoplasms But Also Myoepithelial Cell Tumors of Soft Tissue: A Systematic Analysis of 5134 Tumors. *Am J Surg Pathol* (2015) 39(6):826–35. doi: 10.1097/PAS.0000000000000398
79. Hayward NK, Wilmott JS, Waddell N, Johansson PA, Field MA, Nones K, et al. Whole-Genome Landscapes of Major Melanoma Subtypes. *Nature* (2017) 545(7653):175–80. doi: 10.1038/nature22071
80. Ronnstrand L. Signal Transduction via the Stem Cell Factor Receptor/C-Kit. *Cell Mol Life Sci* (2004) 61(19-20):2535–48. doi: 10.1007/s00018-004-4189-6
81. Curtin JA, Busam K, Pinkel D, Bastian BC. Somatic Activation of KIT in Distinct Subtypes of Melanoma. *J Clin Oncol* (2006) 24(26):4340–6. doi: 10.1200/JCO.2006.06.2984
82. Satzger I, Schaefer T, Kuettler U, Broecker V, Voelker B, Ostertag H, et al. Analysis of C-KIT Expression and KIT Gene Mutation in Human Mucosal Melanomas. *Br J Cancer* (2008) 99(12):2065–9. doi: 10.1038/sj.bjc.6604791
83. Omholt K, Grafstrom E, Kanter-Lewensohn L, Hansson J, Ragnarsson-Olding BK. KIT Pathway Alterations in Mucosal Melanomas of the Vulva and Other Sites. *Clin Cancer Res* (2011) 17(12):3933–42. doi: 10.1158/1078-0432.CCR-10-2917
84. Carvajal RD, Antonescu CR, Wolchok JD, Chapman PB, Roman RA, Teitcher J, et al. KIT as a Therapeutic Target in Metastatic Melanoma. *JAMA* (2011) 305(22):2327–34. doi: 10.1001/jama.2011.746
85. Rivera RS, Nagatsuka H, Gunduz M, Cengiz B, Gunduz E, Siar CH, et al. C-Kit Protein Expression Correlated With Activating Mutations in KIT Gene in Oral Mucosal Melanoma. *Virchows Arch* (2008) 452(1):27–32. doi: 10.1007/s00428-007-0524-2
86. Yun J, Lee J, Jang J, Lee EJ, Jang KT, Kim JH, et al. KIT Amplification and Gene Mutations in Acral/Mucosal Melanoma in Korea. *APMIS* (2011) 119(6):330–5. doi: 10.1111/j.1600-0463.2011.02737.x
87. Meng D, Carvajal RD. KIT as an Oncogenic Driver in Melanoma: An Update on Clinical Development. *Am J Clin Dermatol* (2019) 20(3):315–23. doi: 10.1007/s40257-018-0414-1
88. Boichuk S, Galembikova A, Dunaev P, Valeeva E, Shagimardanova E, Gusev O, et al. A Novel Receptor Tyrosine Kinase Switch Promotes Gastrointestinal Stromal Tumor Drug Resistance. *Molecules* (2017) 22(12):2152. doi: 10.3390/molecules22122152
89. Martorana A, Lauria A. Design of Antitumor Drugs Targeting C-Kit Receptor by a New Mixed Ligand-Structure Based Method. *J Mol Graph Model* (2020) 100:107666. doi: 10.1016/j.jmgm.2020.107666
90. Reddy BY, Miller DM, Tsao H. Somatic Driver Mutations in Melanoma. *Cancer* (2017) 123(S11):2104–17. doi: 10.1002/cncr.30593
91. Alicea GM, Rebecca VW. Emerging Strategies to Treat Rare and Intractable Subtypes of Melanoma. *Pigment Cell Melanoma Res* (2021) 34(1):44–58. doi: 10.1111/pcmr.12880
92. Burd CE, Liu W, Huynh MV, Waqas MA, Gillahan JE, Clark KS, et al. Mutation-Specific RAS Oncogenicity Explains NRAS Codon 61 Selection in Melanoma. *Cancer Discov* (2014) 4(12):1418–29. doi: 10.1158/2159-8290.CD-14-0729
93. Dumaz N, Jouenne F, Delyon J, Mourah S, Bensussan A, Lebbe C. Atypical BRAF and NRAS Mutations in Mucosal Melanoma. *Cancers (Basel)* (2019) 11(8):1133. doi: 10.3390/cancers11081133
94. Karoulia Z, Gavathiotis E, Poulikakos PI. New Perspectives for Targeting RAF Kinase in Human Cancer. *Nat Rev Cancer* (2017) 17(11):676–91. doi: 10.1038/nrc.2017.79
95. Lavoie H, Therrien M. Regulation of RAF Protein Kinases in ERK Signalling. *Nat Rev Mol Cell Biol* (2015) 16(5):281–98. doi: 10.1038/nrm3979
96. Hodis E, Watson IR, Kryukov GV, Arold ST, Imielinski M, Theurillat JP, et al. A Landscape of Driver Mutations in Melanoma. *Cell* (2012) 150(2):251–63. doi: 10.1016/j.cell.2012.06.024
97. Whittaker SR, Theurillat JP, Van Allen E, Wagle N, Hsiao J, Cowley GS, et al. A Genome-Scale RNA Interference Screen Implicates NF1 Loss in Resistance to RAF Inhibition. *Cancer Discov* (2013) 3(3):350–62. doi: 10.1158/2159-8290.CD-12-0470
98. Gibney GT, Smalley KS. An Unholy Alliance: Cooperation Between BRAF and NF1 in Melanoma Development and BRAF Inhibitor Resistance. *Cancer Discov* (2013) 3(3):260–3. doi: 10.1158/2159-8290.CD-13-0017
99. Hintzsche JD, Gorden NT, Amato CM, Kim J, Wuensch KE, Robinson SE, et al. Whole-Exome Sequencing Identifies Recurrent SF3B1 R625 Mutation

and Comutation of NF1 and KIT in Mucosal Melanoma. *Melanoma Res* (2017) 27(3):189–99. doi: 10.1097/CMR.0000000000000345
100. Ablain J, Xu M, Rothschild H, Jordan RC, Mito JK, Daniels BH, et al. Human Tumor Genomics and Zebrafish Modeling Identify SPRED1 Loss as a Driver of Mucosal Melanoma. *Science* (2018) 362(6418):1055–60. doi: 10.1126/science.aau6509
101. Ablain J, Liu S, Moriceau G, Lo RS, Zon LI. SPRED1 Deletion Confers Resistance to MAPK Inhibition in Melanoma. *J Exp Med* (2021) 218(3): e20201097. doi: 10.1084/jem.20201097
102. Soares CD, Borges CF, Sena-Filho M, Almeida OP, Stelini RF, Cintra ML, et al. Prognostic Significance of Cyclooxygenase 2 and Phosphorylated Akt1 Overexpression in Primary Nonmetastatic and Metastatic Cutaneous Melanomas. *Melanoma Res* (2017) 27(5):448–56. doi: 10.1097/CMR.0000000000000368
103. Soares C, Melo de Lima Morais T, Carlos R, Mariano FV, Altemani A, Freire de Carvalho MG, et al. Phosphorylated Akt1 Expression is Associated With Poor Prognosis in Cutaneous, Oral and Sinonasal Melanomas. *Oncotarget* (2018) 9(99):37291–304. doi: 10.18632/oncotarget.26458
104. Wu H, Goel V, Haluska FG. PTEN Signaling Pathways in Melanoma. *Oncogene* (2003) 22(20):3113–22. doi: 10.1038/sj.onc.1206451
105. Broit N, Johansson PA, Rodgers CB, Walpole ST, Newell F, Hayward NK, et al. Meta-Analysis and Systematic Review of the Genomics of Mucosal Melanoma. *Mol Cancer Res* (2021) 19(6):991–1004. doi: 10.1158/1541-7786.MCR-20-0839
106. Damsky WE, Curley DP, Santhanakrishnan M, Rosenbaum LE, Platt JT, Gould Rothberg BE, et al. Beta-Catenin Signaling Controls Metastasis in Braf-Activated Pten-Deficient Melanomas. *Cancer Cell* (2011) 20(6):741–54. doi: 10.1016/j.ccr.2011.10.030
107. Cho JH, Robinson JP, Arave RA, Burnett WJ, Kircher DA, Chen G, et al. AKT1 Activation Promotes Development of Melanoma Metastases. *Cell Rep* (2015) 13(5):898–905. doi: 10.1016/j.celrep.2015.09.057
108. Tas F, Keskin S, Karadeniz A, Dagoglu N, Sen F, Kilic L, et al. Noncutaneous Melanoma Have Distinct Features From Each Other and Cutaneous Melanoma. *Oncology* (2011) 81(5-6):353–8. doi: 10.1159/000334863
109. Ma M, Dai J, Xu T, Yu S, Yu H, Tang H, et al. Analysis of TSC1 Mutation Spectrum in Mucosal Melanoma. *J Cancer Res Clin Oncol* (2018) 144(2):257–67. doi: 10.1007/s00432-017-2550-z
110. Darman RB, Seiler M, Agrawal AA, Lim KH, Peng S, Aird D, et al. Cancer-Associated SF3B1 Hotspot Mutations Induce Cryptic 3' Splice Site Selection Through Use of a Different Branch Point. *Cell Rep* (2015) 13(5):1033–45. doi: 10.1016/j.celrep.2015.09.053
111. Zhou Z, Gong Q, Wang Y, Li M, Wang L, Ding H, et al. The Biological Function and Clinical Significance of SF3B1 Mutations in Cancer. *Biomark Res* (2020) 8:38. doi: 10.1186/s40364-020-00220-5
112. Kong Y, Krauthammer M, Halaban R. Rare SF3B1 R625 Mutations in Cutaneous Melanoma. *Melanoma Res* (2014) 24(4):332–4. doi: 10.1097/CMR.0000000000000071
113. Alsafadi S, Houy A, Battistella A, Popova T, Wassef M, Henry E, et al. Cancer-Associated SF3B1 Mutations Affect Alternative Splicing by Promoting Alternative Branchpoint Usage. *Nat Commun* (2016) 7:10615. doi: 10.1038/ncomms10615
114. Inoue D, Chew GL, Liu B, Michel BC, Pangallo J, D'Avino AR, et al. Spliceosomal Disruption of the non-Canonical BAF Complex in Cancer. *Nature* (2019) 574(7778):432–6. doi: 10.1038/s41586-019-1646-9
115. Liu Z, Yoshimi A, Wang J, Cho H, Chun-Wei Lee S, Ki M, et al. Mutations in the RNA Splicing Factor SF3B1 Promote Tumorigenesis Through MYC Stabilization. *Cancer Discov* (2020) 10(6):806–21. doi: 10.1158/2159-8290.CD-19-1330
116. Wang L, Brooks AN, Fan J, Wan Y, Gambe R, Li S, et al. Transcriptomic Characterization of SF3B1 Mutation Reveals Its Pleiotropic Effects in Chronic Lymphocytic Leukemia. *Cancer Cell* (2016) 30(5):750–63. doi: 10.1016/j.ccell.2016.10.005
117. Furney SJ, Pedersen M, Gentien D, Dumont AG, Rapinat A, Desjardins L, et al. SF3B1 Mutations are Associated With Alternative Splicing in Uveal Melanoma. *Cancer Discov* (2013) 3(10):1122–9. doi: 10.1158/2159-8290.CD-13-0330
118. Baumann J, Ignashkova TI, Chirasani SR, Ramirez-Peinado S, Alborzinia H, Gendarme M, et al. Golgi Stress-Induced Transcriptional Changes Mediated by MAPK Signaling and Three ETS Transcription Factors Regulate MCL1 Splicing. *Mol Biol Cell* (2018) 29(1):42–52. doi: 10.1091/mbc.E17-06-0418
119. Si L, Wang X, Guo J. Genotyping of Mucosal Melanoma. *Chin Clin Oncol* (2014) 3(3):34. doi: 10.3978/j.issn.2304-3865.2014.07.03
120. Xu L, Cheng Z, Cui C, Wu X, Yu H, Guo J, et al. Frequent Genetic Aberrations in the Cell Cycle Related Genes in Mucosal Melanoma Indicate the Potential for Targeted Therapy. *J Transl Med* (2019) 17 (1):245. doi: 10.1186/s12967-019-1987-z
121. Williams GH, Stoeber K. The Cell Cycle and Cancer. *J Pathol* (2012) 226 (2):352–64. doi: 10.1002/path.3022
122. Curtin JA, Fridlyand J, Kageshita T, Patel HN, Busam KJ, Kutzner H, et al. Distinct Sets of Genetic Alterations in Melanoma. *N Engl J Med* (2005) 353 (20):2135–47. doi: 10.1056/NEJMoa050092
123. Huang FW, Hodis E, Xu MJ, Kryukov GV, Chin L, Garraway LA. Highly Recurrent TERT Promoter Mutations in Human Melanoma. *Science* (2013) 339(6122):957–9. doi: 10.1126/science.1229259
124. Vinagre J, Almeida A, Populo H, Batista R, Lyra J, Pinto V, et al. Frequency of TERT Promoter Mutations in Human Cancers. *Nat Commun* (2013) 4:2185. doi: 10.1038/ncomms3185
125. Bell RJ, Rube HT, Xavier-Magalhaes A, Costa BM, Mancini A, Song JS, et al. Understanding TERT Promoter Mutations: A Common Path to Immortality. *Mol Cancer Res* (2016) 14(4):315–23. doi: 10.1158/1541-7786.MCR-16-0003
126. Pleasance ED, Cheetham RK, Stephens PJ, McBride DJ, Humphray SJ, Greenman CD, et al. A Comprehensive Catalogue of Somatic Mutations From a Human Cancer Genome. *Nature* (2010) 463(7278):191–6. doi: 10.1038/nature08658
127. Griewank KG, Murali R, Puig-Butille JA, Schilling B, Livingstone E, Potrony M, et al. TERT Promoter Mutation Status as an Independent Prognostic Factor in Cutaneous Melanoma. *J Natl Cancer Inst* (2014) 106(9):dju246. doi: 10.1093/jnci/dju246
128. Clynes D, Jelinska C, Xella B, Ayyub H, Scott C, Mitson M, et al. Suppression of the Alternative Lengthening of Telomere Pathway by the Chromatin Remodelling Factor ATRX. *Nat Commun* (2015) 6:7538. doi: 10.1038/ncomms8538
129. Chiba K, Lorbeer FK, Shain AH, McSwiggen DT, Schruf E, Oh A, et al. Mutations in the Promoter of the Telomerase Gene TERT Contribute to Tumorigenesis by a Two-Step Mechanism. *Science* (2017) 357(6358):1416–20. doi: 10.1126/science.aao0535
130. Perera ON, Sobinoff AP, Teber ET, Harman A, Maritz MF, Yang SF, et al. Telomerase Promotes Formation of a Telomere Protective Complex in Cancer Cells. *Sci Adv* (2019) 5(10):eaav4409. doi: 10.1126/sciadv.aav4409
131. Yasukawa M, Ando Y, Yamashita T, Matsuda Y, Shoji S, Morioka MS, et al. CDK1 Dependent Phosphorylation of hTERT Contributes to Cancer Progression. *Nat Commun* (2020) 11(1):1557. doi: 10.1038/s41467-020-15289-7
132. Maida Y, Yasukawa M, Masutomi K. De Novo RNA Synthesis by RNA-Dependent RNA Polymerase Activity of Telomerase Reverse Transcriptase. *Mol Cell Biol* (2016) 36(8):1248–59. doi: 10.1128/MCB.01021-15
133. Khan S, Carvajal RD. Mucosal Melanoma: Current Strategies and Future Directions. *Expert Opin Orphan Drugs* (2019) 7(10):427–34. doi: 10.1080/21678707.2019.1672534
134. Seifried S, Haydu LE, Quinn MJ, Scolyer RA, Stretch JR, Thompson JF. Melanoma of the Vulva and Vagina: Principles of Staging and Their Relevance to Management Based on a Clinicopathologic Analysis of 85 Cases. *Ann Surg Oncol* (2015) 22(6):1959–66. doi: 10.1245/s10434-014-4215-3
135. Lazarev S, Gupta V, Hu K, Harrison LB, Bakst R. Mucosal Melanoma of the Head and Neck: A Systematic Review of the Literature. *Int J Radiat Oncol Biol Phys* (2014) 90(5):1108–18. doi: 10.1016/j.ijrobp.2014.03.042
136. D'Angelo SP, Larkin J, Sosman JA, Lebbe C, Brady B, Neyns B, et al. Efficacy and Safety of Nivolumab Alone or in Combination With Ipilimumab in Patients With Mucosal Melanoma: A Pooled Analysis. *J Clin Oncol* (2017) 35 (2):226–35. doi: 10.1200/JCO.2016.67.9258
137. Postow MA, Hamid O, Carvajal RD. Mucosal Melanoma: Pathogenesis, Clinical Behavior, and Management. *Curr Oncol Rep* (2012) 14(5):441–8. doi: 10.1007/s11912-012-0244-x
138. Long GV, Eroglu Z, Infante J, Patel S, Daud A, Johnson DB, et al. Long-Term Outcomes in Patients With BRAF V600-Mutant Metastatic Melanoma Who

Received Dabrafenib Combined With Trametinib. *J Clin Oncol* (2018) 36 (7):667–73. doi: 10.1200/JCO.2017.74.1025
139. Fujisawa Y, Ito T, Kato H, Irie H, Kaji T, Maekawa T, et al. Outcome of Combination Therapy Using BRAF and MEK Inhibitors Among Asian Patients With Advanced Melanoma: An Analysis of 112 Cases. *Eur J Cancer* (2021) 145:210–20. doi: 10.1016/j.ejca.2020.12.021
140. Ascierto PA, Schadendorf D, Berking C, Agarwala SS, van Herpen CM, Queirolo P, et al. MEK162 for Patients With Advanced Melanoma Harbouring NRAS or Val600 BRAF Mutations: A non-Randomised, Open-Label Phase 2 Study. *Lancet Oncol* (2013) 14(3):249–56. doi: 10.1016/S1470-2045(13)70024-X
141. Trunzer K, Pavlick AC, Schuchter L, Gonzalez R, McArthur GA, Hutson TE, et al. Pharmacodynamic Effects and Mechanisms of Resistance to Vemurafenib in Patients With Metastatic Melanoma. *J Clin Oncol* (2013) 31(14):1767–74. doi: 10.1200/JCO.2012.44.7888
142. Algazi AP, Muthukumar AH, O'Brien K, Lencioni A, Tsai KK, Kadafour M, et al. Phase II Trial of Trametinib in Combination With the AKT Inhibitor GSK 2141795 in BRAF Wild-Type Melanoma. *Am Soc Clin Oncol* (2015) 33 (15):suppl 9068–9068. doi: 10.1200/jco.2015.33.15_suppl.9068
143. Sosman JA, Kittaneh M, Lolkema MP, Postow MA, Schwartz G, Franklin C, et al. A Phase 1b/2 Study of LEE011 in Combination With Binimetinib (MEK162) in Patients With NRAS-Mutant Melanoma: Early Encouraging Clinical Activity. *Am Soc Clin Oncol* (2014) 32(15):suppl 9068–9068. doi: 10.1200/jco.2015.33.15_suppl.9068
144. Wei BR, Hoover SB, Peer CJ, Dwyer JE, Adissu HA, Shankarappa P, et al. Efficacy, Tolerability and Pharmacokinetics of Combined Targeted MEK and Dual Mtorc1/2 Inhibition in a Preclinical Model of Mucosal Melanoma. *Mol Cancer Ther* (2020) 19(11):2308–18. doi: 10.1158/1535-7163.MCT-19-0858
145. Minor DR, Kashani-Sabet M, Garrido M, O'Day SJ, Hamid O, Bastian BC. Sunitinib Therapy for Melanoma Patients With KIT Mutations. *Clin Cancer Res* (2012) 18(5):1457–63. doi: 10.1158/1078-0432.CCR-11-1987
146. Kluger HM, Dudek AZ, McCann C, Ritacco J, Southard N, Jilaveanu LB, et al. A Phase 2 Trial of Dasatinib in Advanced Melanoma. *Cancer* (2011) 117(10):2202–8. doi: 10.1002/cncr.25766
147. Cho JH, Kim KM, Kwon M, Kim JH, Lee J. Nilotinib in Patients With Metastatic Melanoma Harboring KIT Gene Aberration. *Invest New Drugs* (2012) 30(5):2008–14. doi: 10.1007/s10637-011-9763-9
148. Carvajal RD, Lawrence DP, Weber JS, Gajewski TF, Gonzalez R, Lutzky J, et al. Phase II Study of Nilotinib in Melanoma Harboring KIT Alterations Following Progression to Prior KIT Inhibition. *Clin Cancer Res* (2015) 21 (10):2289–96. doi: 10.1158/1078-0432.CCR-14-1630
149. Wei X, Mao L, Chi Z, Sheng X, Cui C, Kong Y, et al. Efficacy Evaluation of Imatinib for the Treatment of Melanoma: Evidence From a Retrospective Study. *Oncol Res* (2019) 27(4):495–501. doi: 10.3727/096504018X15331163433914
150. Hodi FS, Corless CL, Giobbie-Hurder A, Fletcher JA, Zhu M, Marino-Enriquez A, et al. Imatinib for Melanomas Harboring Mutationally Activated or Amplified KIT Arising on Mucosal, Acral, and Chronically Sun-Damaged Skin. *J Clin Oncol* (2013) 31(26):3182–90. doi: 10.1200/JCO.2012.47.7836
151. Guo J, Carvajal RD, Dummer R, Hauschild A, Daud A, Bastian BC, et al. Efficacy and Safety of Nilotinib in Patients With KIT-Mutated Metastatic or Inoperable Melanoma: Final Results From the Global, Single-Arm, Phase II TEAM Trial. *Ann Oncol* (2017) 28(6):1380–7. doi: 10.1093/annonc/mdx079
152. Woodman SE, Davies MA. Targeting KIT in Melanoma: A Paradigm of Molecular Medicine and Targeted Therapeutics. *Biochem Pharmacol* (2010) 80(5):568–74. doi: 10.1016/j.bcp.2010.04.032
153. Spencer KR, Mehnert JM. Mucosal Melanoma: Epidemiology, Biology and Treatment. *Cancer Treat Res* (2016) 167:295–320. doi: 10.1007/978-3-319-22539-5_13
154. Todd JR, Becker TM, Kefford RF, Rizos H. Secondary C-Kit Mutations Confer Acquired Resistance to RTK Inhibitors in C-Kit Mutant Melanoma Cells. *Pigment Cell Melanoma Res* (2013) 26(4):518–26. doi: 10.1111/pcmr.12107
155. Steensma DP, Wermke M, Klimek VM, Greenberg PL, Font P, Komrokji RS, et al. Results of a Clinical Trial of H3B-8800, a Splicing Modulator, in Patients With Myelodysplastic Syndromes (MDS), Acute Myeloid Leukemia (AML) or Chronic Myelomonocytic Leukemia (CMML). *Am Soc Hematol Washington DC* (2019) 134(Supplement_1):673. doi: 10.1182/blood-2019-123854
156. Damsky WE, Bosenberg M. Melanocytic Nevi and Melanoma: Unraveling a Complex Relationship. *Oncogene* (2017) 36(42):5771–92. doi: 10.1038/onc.2017.189
157. Dhomen N, Reis-Filho JS, da Rocha Dias S, Hayward R, Savage K, Delmas V, et al. Oncogenic Braf Induces Melanocyte Senescence and Melanoma in Mice. *Cancer Cell* (2009) 15(4):294–303. doi: 10.1016/j.ccr.2009.02.022
158. Damsky W, Micevic G, Meeth K, Muthusamy V, Curley DP, Santhanakrishnan M, et al. Mtorc1 Activation Blocks BrafV600E-Induced Growth Arrest But is Insufficient for Melanoma Formation. *Cancer Cell* (2015) 27(1):41–56. doi: 10.1016/j.ccell.2014.11.014
159. Patton EE, Mueller KL, Adams DJ, Anandasabapathy N, Aplin AE, Bertolotto C, et al. Melanoma Models for the Next Generation of Therapies. *Cancer Cell* (2021) 39(5):610–31. doi: 10.1016/j.ccell.2021.01.011
160. Furney SJ, Turajlic S, Stamp G, Nohadani M, Carlisle A, Thomas JM, et al. Genome Sequencing of Mucosal Melanomas Reveals That They are Driven by Distinct Mechanisms From Cutaneous Melanoma. *J Pathol* (2013) 230 (3):261–9. doi: 10.1002/path.4204
161. Wroblewska JP, Mull J, Wu CL, Fujimoto M, Ogawa T, Marszalek A, et al. SF3B1, NRAS, KIT, and BRAF Mutation; CD117 and cMYC Expression; and Tumoral Pigmentation in Sinonasal Melanomas: An Analysis With Newly Found Molecular Alterations and Some Population-Based Molecular Differences. *Am J Surg Pathol* (2019) 43(2):168–77. doi: 10.1097/PAS.0000000000001166
162. Ronco C, Martin AR, Demange L, Benhida R. ATM, ATR, CHK1, CHK2 and WEE1 Inhibitors in Cancer and Cancer Stem Cells. *Medchemcomm* (2017) 8 (2):295–319. doi: 10.1039/c6md00439c
163. Brown JS, O'Carrigan B, Jackson SP, Yap TA. Targeting DNA Repair in Cancer: Beyond PARP Inhibitors. *Cancer Discov* (2017) 7(1):20–37. doi: 10.1158/2159-8290.CD-16-0860
164. Rundle S, Bradbury A, Drew Y, Curtin NJ. Targeting the ATR-CHK1 Axis in Cancer Therapy. *Cancers (Basel)* (2017) 9(5):41. doi: 10.3390/cancers9050041
165. Lord CJ, Ashworth A. PARP Inhibitors: Synthetic Lethality in the Clinic. *Science* (2017) 355(6330):1152–8. doi: 10.1126/science.aam7344
166. Vaddepally RK, Kharel P, Pandey R, Garje R, Chandra AB. Review of Indications of FDA-Approved Immune Checkpoint Inhibitors Per NCCN Guidelines With the Level of Evidence. *Cancers (Basel)* (2020) 12(3):738. doi: 10.3390/cancers12030738
167. Robert C, Schachter J, Long GV, Arance A, Grob JJ, Mortier L, et al. Pembrolizumab Versus Ipilimumab in Advanced Melanoma. *N Engl J Med* (2015) 372(26):2521–32. doi: 10.1056/NEJMoa1503093
168. Robert C, Long GV, Brady B, Dutriaux C, Maio M, Mortier L, et al. Nivolumab in Previously Untreated Melanoma Without BRAF Mutation. *N Engl J Med* (2015) 372(4):320–30. doi: 10.1056/NEJMoa1412082
169. Hamid O, Molinero L, Bolen CR, Sosman JA, Munoz-Couselo E, Kluger HM, et al. Safety, Clinical Activity, and Biological Correlates of Response in Patients With Metastatic Melanoma: Results From a Phase I Trial of Atezolizumab. *Clin Cancer Res* (2019) 25(20):6061–72. doi: 10.1158/1078-0432.CCR-18-3488
170. Postow MA, Chesney J, Pavlick AC, Robert C, Grossmann K, McDermott D, et al. Nivolumab and Ipilimumab Versus Ipilimumab in Untreated Melanoma. *N Engl J Med* (2015) 372(21):2006–17. doi: 10.1056/NEJMoa1414428
171. Larkin J, Chiarion-Sileni V, Gonzalez R, Grob JJ, Rutkowski P, Lao CD, et al. Five-Year Survival With Combined Nivolumab and Ipilimumab in Advanced Melanoma. *N Engl J Med* (2019) 381(16):1535–46. doi: 10.1056/NEJMoa1910836
172. Del Vecchio M, Di Guardo L, Ascierto PA, Grimaldi AM, Sileni VC, Pigozzo J, et al. Efficacy and Safety of Ipilimumab 3mg/Kg in Patients With Pretreated, Metastatic, Mucosal Melanoma. *Eur J Cancer* (2014) 50 (1):121–7. doi: 10.1016/j.ejca.2013.09.007
173. Shoushtari AN, Wagstaff J, Ascierto PA, Butler MO, Lao CD, Marquez-Rodas I, et al. CheckMate 067: Long-Term Outcomes in Patients With Mucosal Melanoma. *J Clin Oncol* (2020) 38(15_suppl):10019–. doi: 10.1200/JCO.2020.38.15_suppl.10019
174. Moya-Plana A, Herrera Gomez RG, Rossoni C, Dercle L, Ammari S, Girault I, et al. Evaluation of the Efficacy of Immunotherapy for non-Resectable Mucosal Melanoma. *Cancer Immunol Immunother* (2019) 68(7):1171–8. doi: 10.1007/s00262-019-02351-7

175. Wolchok JD, Kluger H, Callahan MK, Postow MA, Rizvi NA, Lesokhin AM, et al. Nivolumab Plus Ipilimumab in Advanced Melanoma. *N Engl J Med* (2013) 369(2):122–33. doi: 10.1056/NEJMoa1302369
176. Johnson DB, Carlson JA, Elvin JA, Vergilio J-A, Suh J, Ramkissoon S, et al. Landscape of Genomic Alterations (GA) and Tumor Mutational Burden (TMB) in Different Metastatic Melanoma (MM) Subtypes. *J Clin Oncol* (2017) 35(15_suppl):9536–. doi: 10.1200/JCO.2017.35.15_suppl.9536
177. Klemen ND, Wang M, Rubinstein JC, Olino K, Clune J, Ariyan S, et al. Survival After Checkpoint Inhibitors for Metastatic Acral, Mucosal and Uveal Melanoma. *J Immunother Cancer* (2020) 8(1):e000341. doi: 10.1136/jitc-2019-000341
178. Taylor MH, Vogelzang NJ, Cohn AL, Stepan DE, Shumaker RC, Dutcus CE, et al. Phase Ib/II Trial of Lenvatinib Plus Pembrolizumab in Advanced Melanoma. *J Clin Oncol* (2019) 37(8_suppl):15–. doi: 10.1200/JCO.2019.37.8_suppl.15
179. Guo J, Sheng X, Si L, Kong Y, Chi Z, Cui C, et al. A Phase Ib Study of JS001, a Humanized IgG4 mAb Against Programmed Death-1 (PD-1) Combination With Axitinib in Patients With Metastatic Mucosal Melanoma. *J Clin Oncol* (2018) 36(15_suppl):9528–. doi: 10.1200/JCO.2018.36.15_suppl.9528
180. Si L, Sheng X, Mao L, Li C, Wang X, Bai X, et al. A Phase II Study of Vorolanib (CM082) in Combination With Toripalimab (JS001) in Patients With Advanced Mucosal Melanoma. *J Clin Oncol* (2020) 38 (15_suppl):10040–. doi: 10.1200/JCO.2020.38.15_suppl.10040

Conflict of Interest: The authors declare that the research was conducted in the absence of any commercial or financial relationships that could be construed as a potential conflict of interest.

frontiers in Oncology

ORIGINAL RESEARCH
published: 30 July 2021
doi: 10.3389/fonc.2021.704543

N^6-Methyladenosine Regulators and Related LncRNAs Are Potential to be Prognostic Markers for Uveal Melanoma and Indicators of Tumor Microenvironment Remodeling

Zhicheng Liu[1,2], *Shanshan Li*[1,2], *Shan Huang*[1,2], *Tao Wang*[1,2] *and Zhicheng Liu*[1,2*]

[1] School of Biomedical Engineering, Capital Medical University, Beijing, China, [2] Beijing Key Laboratory of Fundamental Research on Biomechanics in Clinical Application, Capital Medical University, Beijing, China

OPEN ACCESS

Edited by:
Vijayasaradhi Setaluri, University of Wisconsin-Madison, United States

Reviewed by:
Chandra K. Singh, University of Wisconsin-Madison, United States
Sandhya Annamaneni, Osmania University, India

***Correspondence:**
Zhicheng Liu
zcliu@ccmu.edu.cn

Specialty section:
This article was submitted to Skin Cancer, a section of the journal Frontiers in Oncology

Received: *03 May 2021*
Accepted: *14 July 2021*
Published: *30 July 2021*

Citation:
Liu Z, Li S, Huang S, Wang T and Liu Z (2021) N^6-Methyladenosine Regulators and Related LncRNAs Are Potential to be Prognostic Markers for Uveal Melanoma and Indicators of Tumor Microenvironment Remodeling. Front. Oncol. 11:704543. doi: 10.3389/fonc.2021.704543

Uveal melanoma (UM) is one of the most common malignant intraocular tumors in adults. Few studies have investigated the effect of N^6-methyladenosine (m^6A) RNA methylation regulators and related long noncoding RNAs (lncRNAs) on the tumor microenvironment (TME) and survival time of patients with UM. Based on the transcriptome and clinical data from The Cancer Genome Atlas, we systematically identified m^6A regulators. Then, we constructed an m^6A regulators-based signature to predict the prognostic risk using univariate and LASSO Cox analyses. The signature was then validated by performing Kaplan-Meier, and receiver operating characteristic analyses. Through the correlation analysis, m^6A regulators-related lncRNAs were identified, and they were divided into different clustering subtypes according to their expression. We further assessed differences in TME scores, the survival time of patients, and immune cell infiltration levels between different clustering subtypes. Finally, we screened out the common immune genes shared by m^6A-related lncRNAs and determined their expression in different risk groups and clustering subtypes. For further validation, we used single-cell sequencing data from the GSE139829 dataset to explore the expression distribution of immune genes in the TME of UM. We constructed a prognostic risk signature representing an independent prognostic factor for UM using 3 m^6A regulators. Patients in the low-risk group exhibited a more favorable prognosis and lower immune cell infiltration levels than patients in the high-risk group. Two subtypes (cluster 1/2) were identified based on m^6A regulators-related lncRNAs. The TME scores, prognosis, and immune cell infiltration have a marked difference between cluster 1 and cluster 2. Additionally, 13 common immune genes shared by 5 lncRNAs were screened out. We found that these immune genes were differentially expressed in different risk groups and clustering subtypes and were widely distributed in 3 cell types of TME. In conclusion, our study demonstrated the important

role of m6A regulators and related lncRNAs in TME remodeling. The signature developed using m6A regulators might serve as a promising parameter for the clinical prediction of UM.

Keywords: m6A RNA methylation regulators, long noncoding RNAs, tumor microenvironment, immune cell infiltration, uveal melanoma

INTRODUCTION

Uveal melanoma (UM), which is the second most common type of melanoma, originates from melanocytes in the intraocular uvea (1). Currently, surgery and radiotherapy are the most effective methods to treat local tumors (2). However, the overall mortality in patients with UM is more than 50%, because it is highly susceptible to early metastasis (3, 4). Therefore, new treatments such as immunotherapy or targeted therapy (5, 6) are being developed, which requires the identification of several potential prognostic biomarkers and therapeutic targets for UM.

The most prevalent RNA modification is N^6-methyladenosine (m^6A), which involves methylation of the sixth N atom of adenine (7). m^6A methylation is a dynamic process regulated by methyltransferases (writers) and demethylases (erasers), whereas binding proteins (readers) bind to m^6A methylation sites (8, 9). Methyltransferases such as METTL3/14/16, WTAP, RBM15, and VIRMA promote m^6A methylation (9–11). On the other hand, demethylases, which include FTO and ALKBH5, inhibit m^6A methylation (9, 11). Binding proteins, such as YTHDC1/2, YTHDF1-3, IGF2BP1-3, and HNRNPC, bind to the m^6A modified site to form a complex that mediates its biological function (12). These m^6A methylases are primarily involved in mammalian development, immune response, tumorigenesis, and metastasis, and stem cell differentiation (13–16). However, the prognostic role of m^6A methylases in UM development has not been sufficiently investigated. Besides, the involvement of m^6A methylases in the tumor microenvironment (TME) remains to be thoroughly explored.

Long noncoding RNAs (lncRNAs) are frequently defined as RNAs that have a transcript length exceeding 200 nucleotides and do not encode proteins (17). They can regulate gene expression at epigenetic, transcriptional, and post-transcriptional levels (18). A recent study has reported that lncRNAs promote tumor development by altering the immune microenvironment (19). Increasing evidence has demonstrated the TME, which mainly consists of stromal and immune cells, plays an important role in tumor progression (20). Stromal cells may contribute to tumor angiogenesis and extracellular matrix reorganization, whereas immune cells may contribute to TME *via* dysregulation of immune-mediated responses (21). Therefore, immune cell infiltration in the TME may serve as a potential target for immunotherapy. However, the involvement of lncRNAs in immune cell infiltration in UM remains unclear.

This study aimed to systematically explore m^6A regulators and related lncRNAs involved in the TME in UM and developed an m^6A regulators-based signature for improving the accuracy of prognosis in patients with UM. We also established clustering subtypes based on m^6A regulators-related lncRNAs to determine the relationships between the clustering subtypes, TME scores, prognosis, and immune cell infiltration, and further explained the mechanism of action of m^6A regulators. Finally, we explored the expression of 13 immune genes shared by 5 lncRNAs in different risk groups and clustering subtypes.

MATERIALS AND METHODS

Data Collection and Preparation

The RNA-sequencing transcriptome data of 80 patients with UM and corresponding clinical data were downloaded from The Cancer Genome Atlas (TCGA) data portal (https://portal.gdc.cancer.gov/). GTF files were downloaded from Ensembl (https://asia.ensembl.org) to distinguish between lncRNAs and mRNAs for subsequent analyses. The list of immune genes was downloaded from the ImmPort database (https://www.immport.org).

Generation of TME Scores and Tumor-Infiltrating Immune Cells

The ESTIMATE algorithm in the R "estimate" package was used to calculate the TME scores of 80 UM patients. The Kaplan-Meier survival analysis was conducted to compare the difference in survival time using R "survMiner" and "survival" packages. The fraction of 22 immune cell types in each sample was estimated using CIBERSORT. The association between TME scores and tumor-infiltrating immune cells (TICs) was established using correlation analysis.

Construction and Validation of m^6A Regulators-Based Signature

The m^6A regulators were identified from the published literature (9–12). The m^6A regulators contain 8 writers (METTL3, METTL14, METTL16, WTAP, VIRMA, ZC3H13, RBM15, and RBM15B), 13 readers (YTHDC1, YTHDC2, YTHDF1, YTHDF2, YTHDF3, HNRNPC, FMR1, LRPPRC, HNRNPA2B1, IGF2BP1, IGF2BP2, IGF2BP3, and RBMX), and 2 erasers (FTO and ALKBH5). The expression data of m^6A regulators were extracted from the mRNA expression data of TCGA. The m^6A regulators, which were previously identified using the univariate Cox regression analysis, were further subjected to the LASSO Cox regression analysis using the "glmnet" package. The minimum 10-fold cross-validation was used to select the best penalty parameter λ. Then, the risk score of each patient was calculated

using a linear combination of m^{6}A regulators expression weighted by the multivariate Cox regression analysis. According to the median risk score, the samples were divided into high-risk and low-risk groups. Subsequently, the Kaplan-Meier survival analysis was performed to compare the survival difference. Receiver operating characteristic (ROC) analysis was performed to evaluate the prognostic value of the signature using the "timeROC" package.

Generation and Validation of Clustering Subtypes From m^{6}A Regulators-Related LncRNAs

We screened m^{6}A regulators-related lncRNAs by Pearson's correlation analysis. The process used the criteria of |correlation coefficient| > 0.4 and $p < 0.001$. The expression data of m^{6}A regulators-related lncRNAs were extracted from the lncRNA expression data of TCGA. To clarify the biological characteristics of m^{6}A regulators-related lncRNAs, the R "ConsensusClusterPlus" package was used to divide the samples into different clustering subtypes according to the expression of lncRNAs. Principal component analysis (PCA), Kaplan-Meier survival analysis, TME scores, and TICs profiles were performed for different clustering subtypes.

Identification and Validation of Immune Genes Shared by 5 LncRNAs

The Pearson's correlation analysis was performed to screen common immune genes shared by 5 lncRNAs. The Kaplan-Meier survival analysis was used to compare the survival difference between high- and low-expression of immune genes. The differential expression analysis of immune genes was performed using the R "limma" package in different risk groups and clustering subtypes. A p-value < 0.05 indicated statistical significance. At present, single-cell sequencing technology has been widely used to explore the heterogeneity of TME. To characterize immune genes expression distribution in TME of UM, we search for single-cell sequencing data of UM from Tumor Immune Single-cell Hub (TISCH) (22). The GSE139829 dataset including 59,915 cell sequencing data from 11 samples was collected to perform gene expression distribution (23).

RESULTS

The Correlation Between TME Scores With the Survival of UM Patients and Immune Cell Infiltration

To establish the correlation of ImmuneScore and StromalScore with the survival time, we performed the Kaplan-Meier survival analysis. A high score of immune and stromal cells signified large numbers of these cells in the TME. As shown in **Figure 1A**, the overall survival (OS) in the low ImmuneScore group was longer than that in the high ImmuneScore group. Similarly, StromalScore and ESTIMATEScore showed a negative correlation with the OS (**Figures 1B, C**). To confirm exact changes in the genetic profiles in the TME about immune and stromal cell components, variance analysis of high and low scores was performed. As shown in **Figures 1D, E**, 700 common differentially expressed genes (DEGs) were upregulated, and 74 common DEGs were downregulated. To further explore the interaction between TME scores and the 22 immune cell types, we first estimated the 22 types of TICs with abundance distribution in all the tumor samples and then calculated the correlation index between the TME scores and TICs. The results showed that ImmuneScore is correlated with $CD8^+$ T cells, resting memory $CD4^+$ T cells, activated memory $CD4^+$ T cells, helper T cells (follicular), Tregs, resting NK cells, monocytes, M0 macrophages, M1 macrophages, resting mast cells, and eosinophils (**Figure 1F**).

Construction and Validation of m^{6}A Regulators-Based Signature

To clarify the biological function of m^{6}A regulators in the prognosis of patients with UM, we comprehensively investigated the prognostic value of m^{6}A regulators based on the expression and clinical data (**Table S1**). Of these m^{6}A regulators, seven exhibited a prognostic value based on OS (**Figure 2A**), while nine displayed a prognostic value based on progression-free survival (PFS) (**Figure 2B**). The Venn plot results indicated that 6 m^{6}A regulators (RBM15B, IGF2BP2, YTHDF1, METTL16, VIRMA, and YTHDF3) were identified based on OS and PFS (**Figure 2C**). To avoid overfitting, we performed the LASSO Cox analysis and selected 3 of the 6 m^{6}A regulators were to establish a risk signature (**Figures 2D, E**). Thus, we established a predictive model: risk score = (RBM15B * −0.14284) + (YTHDF3 * 0.02121) + (IGF2BP2 * −0.11533). The distribution of risk score (Upper), patients' survival time (Middle), and heat map analysis (Bottom) of the 3 prognostic m^{6}A regulators were shown based on the OS (**Figures 2F**) and PFS (**Figure 2G**). Results of the heat maps (**Figures 2F, G**) was survival curves (**Figures 3A–C**) suggested that YTHDF3 was likely to be a high-risk factor because it was upregulated in the high-risk group. However, the highly expressed RBM15B and IGF2BP2 in the low-risk group might be protective factors. As shown in **Figures 3D, E**, the OS and PFS of patients in the low-risk group were longer than in the high-risk group. To evaluate the prognostic accuracy of the 3 m^{6}A regulators-based signature, we performed the ROC analysis based on OS and PFS. Areas under the ROC curves of 1, 2, and 3 years were 0.774, 0.811, and 0.843, respectively (**Figure 4A**). The PFS prediction of 3 m^{6}A regulators-based signature was also accurate (**Figure 4B**). These results suggested that the 3 m^{6}A regulators-based signature might serve as a promising parameter for prognostic prediction of UM.

The Association Between Risk Score With Immune Cell Infiltration and TME Scores

The correlation between the risk score and the immune cell infiltration levels was calculated to establish the association

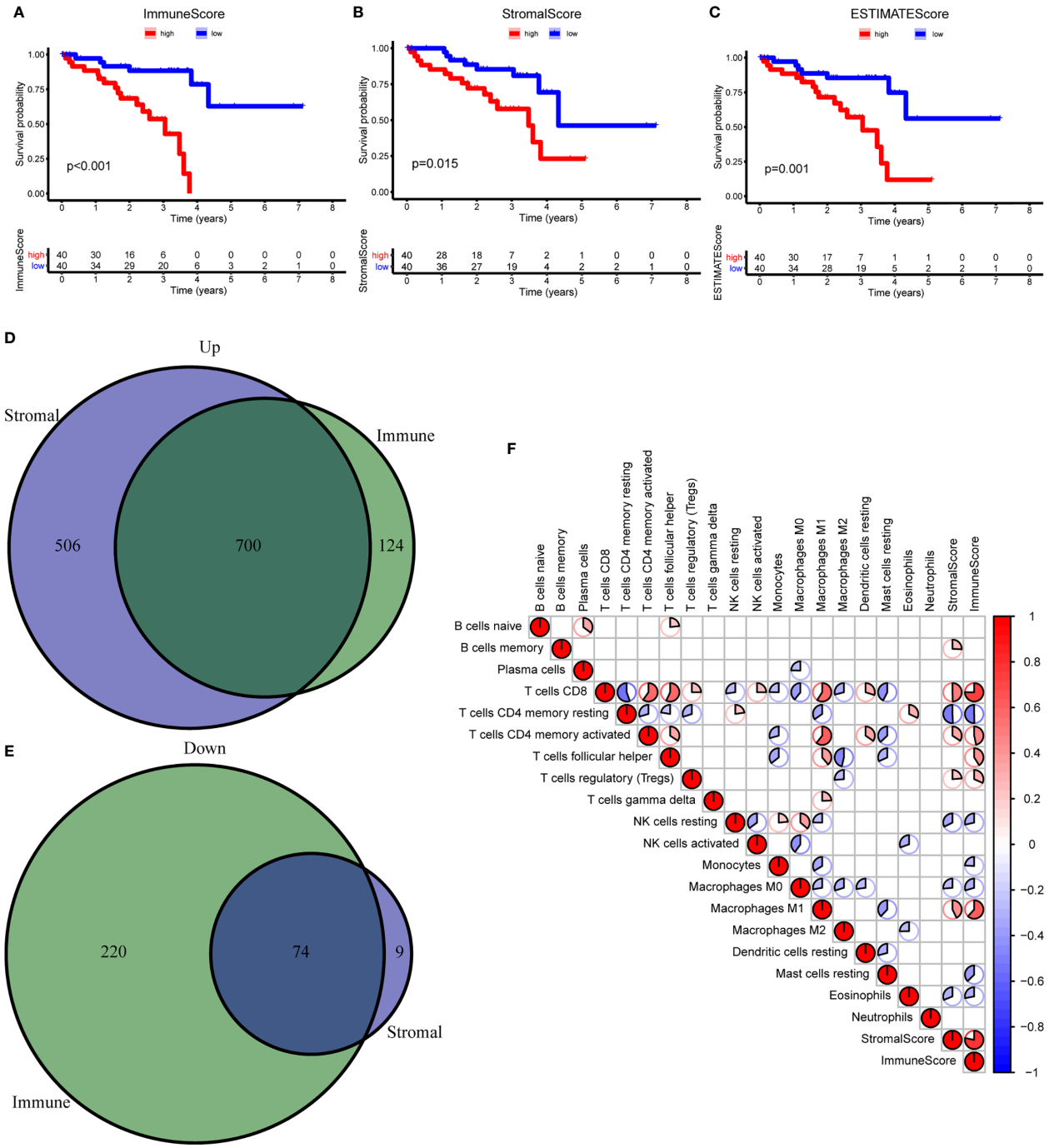

FIGURE 1 | Correlation between the TME scores and survival of UM patients. **(A–C)** Kaplan-Meier survival analysis between high and low ImmuneScore **(A)**, StromalScore **(B)**, and ESTIMATEScore **(C)**. **(D, E)** The Venn diagram showed the common upregulated **(D)** and downregulated **(E)** DEGs shared by ImmuneScore and StromalScore. **(F)** The relationship between 19 immune cell types and score of immune and stromal. DEGs, differentially expressed genes.

between the 3 m^{6}A regulators-based signature with the TME. ImmuneScore, StromalScore, and ESTIMATEScore in the high-risk group were significantly higher than in the low-risk group (**Figures 5A–C**). The results showed that the risk score was significantly negatively correlated with the infiltration levels of naive B cells (**Figure 5D**), eosinophils (**Figure 5F**), monocytes (**Figure 5G**), and plasma cells (**Figure 5H**). Only the infiltration level of resting dendritic cells was positively correlated with the risk score (**Figure 5E**). These results indicated that the 3 m^{6}A regulators were involved in the immune cell infiltration of UM.

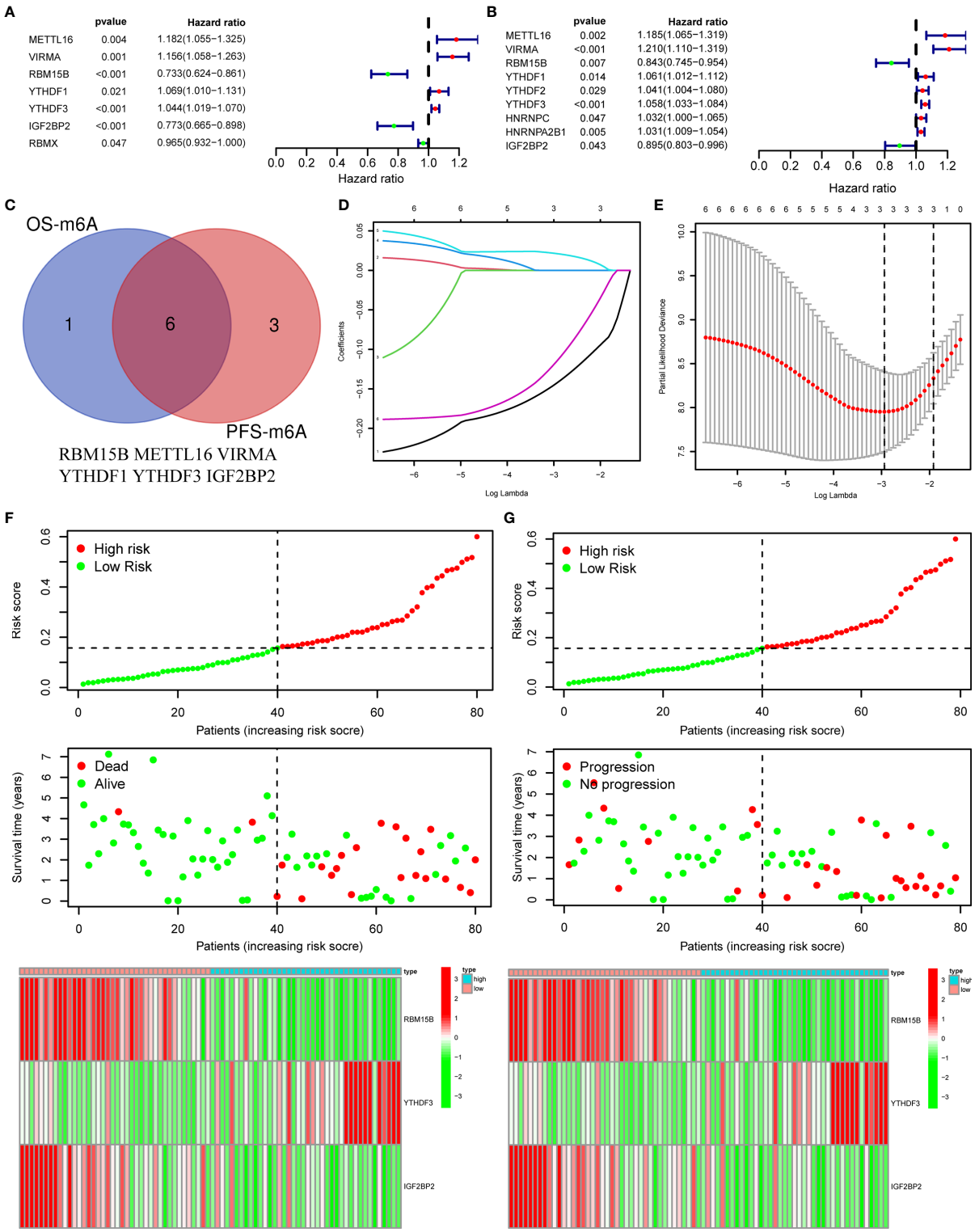

FIGURE 2 | Construction of a prognostic signature based on m^{6}A regulators. **(A, B)** Forest plots for the univariate Cox analysis of prognosis based on OS **(A)** and PFS **(B)**. Colored dots represent hazard ratio, and the horizontal lines across the hazard ratio represent 95% confidence interval. **(C)** The Venn plot showed 6 common m^{6}A regulators based on both OS and PFS. **(D)** LASSO coefficient profiles of the 6 m^{6}A regulators. **(E)** The minimum 10-fold cross-validation was used to select the best penalty parameter λ in the LASSO model. **(F, G)** The distribution of the risk score (Upper), pattern of survival time and survival status (Middle), and the heat map (Bottom) of the 3 prognostic m^{6}A regulators levels based on OS **(F)** and PFS **(G)**. OS, overall survival; PFS, progression free survival.

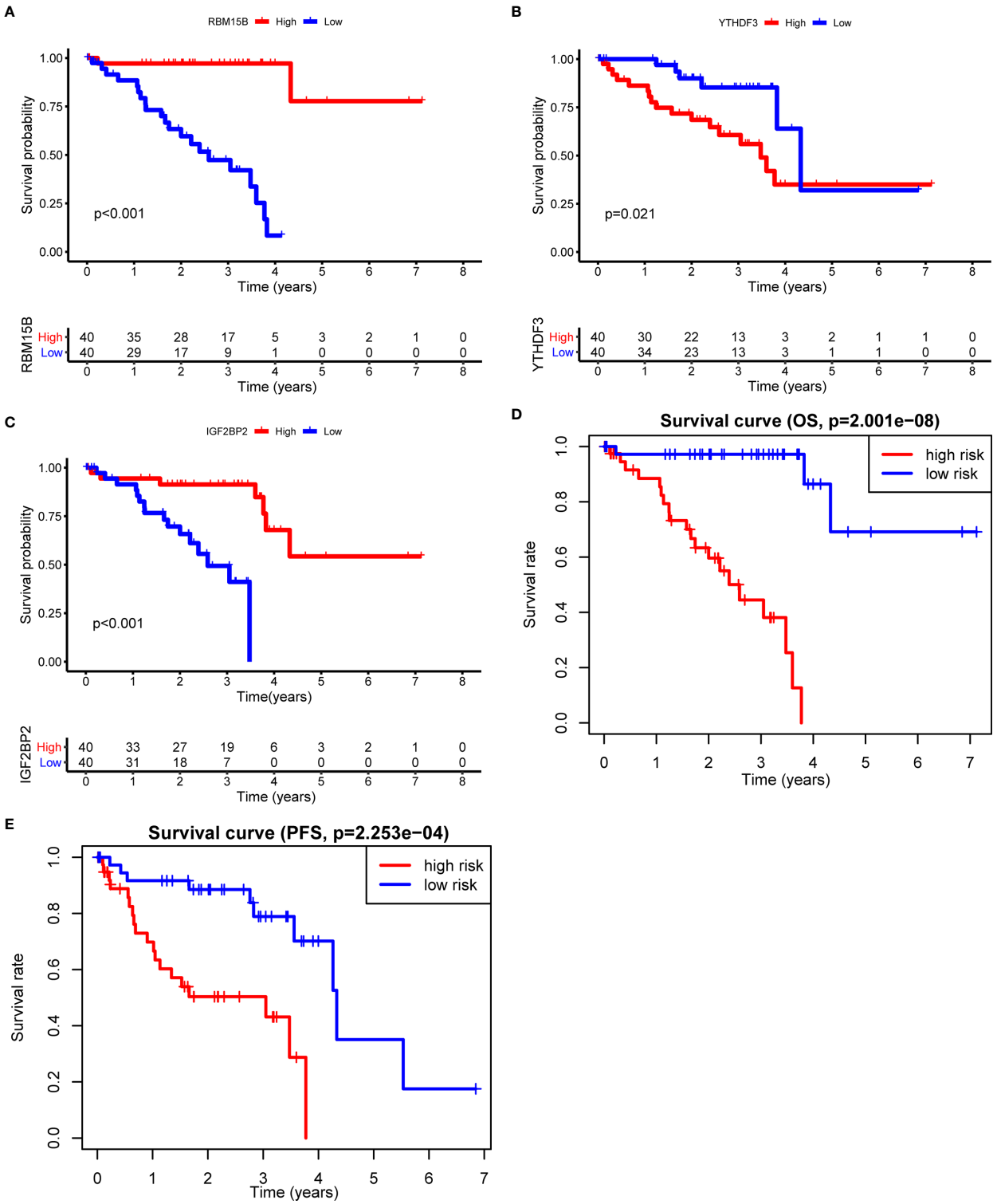

FIGURE 3 | Kaplan-Meier survival analysis of the 3 m^{6}A regulators and the risk signature. **(A–C)** Survival curves between the high- and low-expression of RBM15B **(A)**, YTHDF3 **(B)**, and IGF2BP2 **(C)**. **(D, E)** Survival curves of the 3 m^{6}A regulators-based signature based on OS **(D)** and PFS **(E)**. OS, overall survival; PFS, progression free survival.

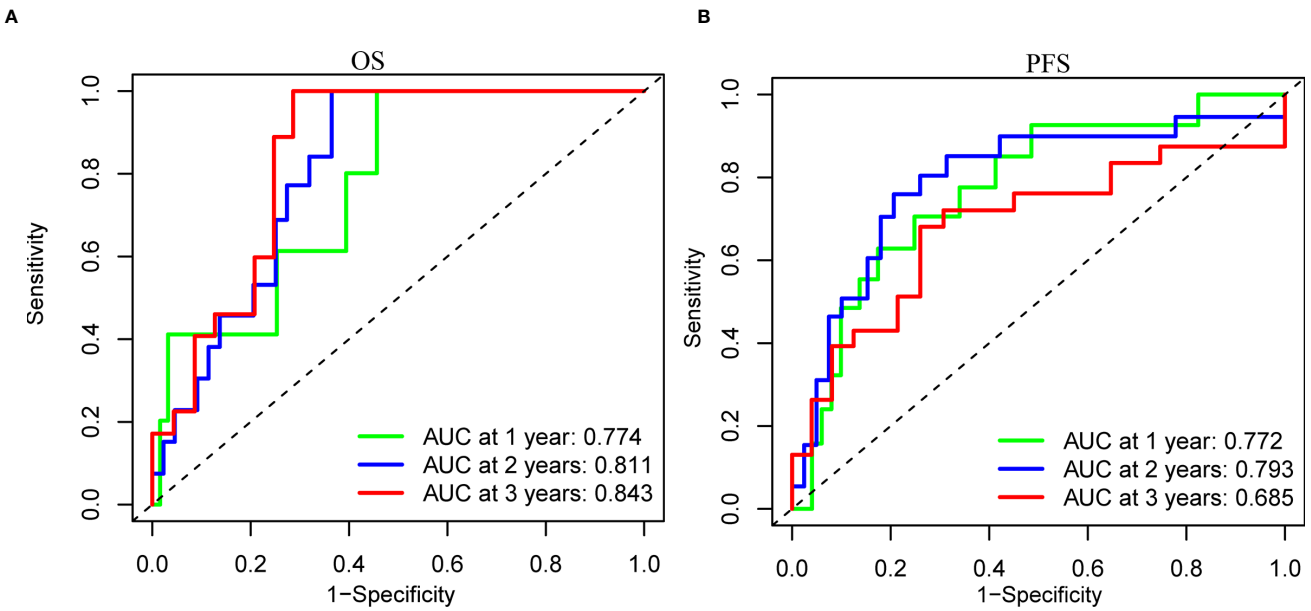

FIGURE 4 | ROC analysis of the 3 m^{6}A regulators-based signature. **(A, B)** The 1-, 2-, and 3-years ROC analysis of the prognostic prediction based on the 3 m^{6}A regulators according to OS **(A)** and PFS **(B)**. OS, overall survival; PFS, progression free survival; AUC, area under the ROC curve.

The Correlation Between Consensus Clustering of m^{6}A Regulators-Related LncRNAs and TME Scores, Survival Time, and Immune Cell Infiltration

Using the correlation analysis, we identified 514 lncRNAs based on RNA-Seq data and constructed a network between m^{6}A regulators and lncRNAs (**Figure 6A**). A total of 66 of the 514 lncRNAs had a prognostic value based on the OS (**Figure S1A**), while 70 of the 514 lncRNAs had a prognostic value based on the PFS (**Figure S1B**). The Venn plot results showed that 38 lncRNAs were common according to OS and PFS (**Figure 6B**). Based on the similarity identified by consensus clustering using the 'ConsensusClusterPlus' package, we found that k = 2 was the optimal clustering stability value (**Figures 6C, D**). The 80 UM samples were well-differentiated into two subtypes according to the expression of 38 lncRNAs (**Figure 6E**).

The TME scores of cluster 1 were lower than those of cluster 2 (**Figures 7A–C**), while the OS (**Figure 7D**) and PFS (**Figure 7E**) of cluster 1 were notably longer than those of cluster 2. Subsequently, the 22 immune cell levels for the two subtypes were calculated. The results showed that cluster 1 had higher immune infiltration levels of plasma cells, and monocytes while there were higher immune cell infiltration levels of activated memory CD4$^+$ T cells, follicular helper T cells, M1 macrophages, and resting dendritic cells (**Figure 7F**).

Identification and Validation of Immune Genes Shared by 5 LncRNAs

First, we identified the common lncRNAs from 5 lists that were DEGs in ImmuneScore (Immune-DEGs) and StromalScore (Stromal-DEGs), m^{6}A regulators-related lncRNAs (m^{6}A-lncRNAs), and immune gene-specific lncRNAs based on OS (OS-immune) and PFS (PFS-immune). A total of 5 lncRNAs, namely AC008555.4, AC018529.1, AC104129.1, CYTOR, and MIR4435-2HG, were found to be common across the 5 lists (**Figure 8A**). High expression of AC018529.1 (**Figure 8B**), MIR4435-2HG (**Figure 8C**), AC104129.1 (**Figure 8D**), and CYTOR (**Figure 8F**) was related to the poor prognosis of patients, while high expression of AC008555.4 was associated with good prognosis (**Figure 8E**). Next, 13 immune genes having 5 common lncRNAs were screened using the correlation analysis (**Figure 9A**). The 13 immune genes were ADGRE5, C2, CD79B, CTSC, GEM, JAG2, LYN, MAFB, MBP, MR1, PREX1, RUNX1, and TCF12. Except for C2, the other 12 immune genes were associated with a poor prognosis (**Figures 9B–M**). To further verify whether the immune genes were differentially expressed in different groups based on m^{6}A regulators and lncRNAs, we extracted the expression data from RNA-Seq data and performed the differential expression analysis. The expression levels of 13 immune genes in the high-risk group were upregulated than those in the low-risk group (**Figure 10**). Similarly, the 13 immune genes levels in cluster 2 were upregulated compared with cluster 1 (**Figure 11**). For further validation, we used TISCH to depict the expression distribution of 13 immune genes in the TME of UM. The overall distribution of the 3 cell types in the GSE139829 dataset was shown in **Figure 12A**. Through analysis, we found that the expression distribution of ADGRE5 (**Figure 12B**), CTSC (**Figure 12E**), LYN (**Figure 12H**), MAFB (**Figure 12I**), PREX1 (**Figure 12L**), and RUNX1 (**Figure 12M**) were abundant in immune cells. CD79B (**Figure 12D**), GEM (**Figure 12F**), and JAG2 (**Figure 12G**)

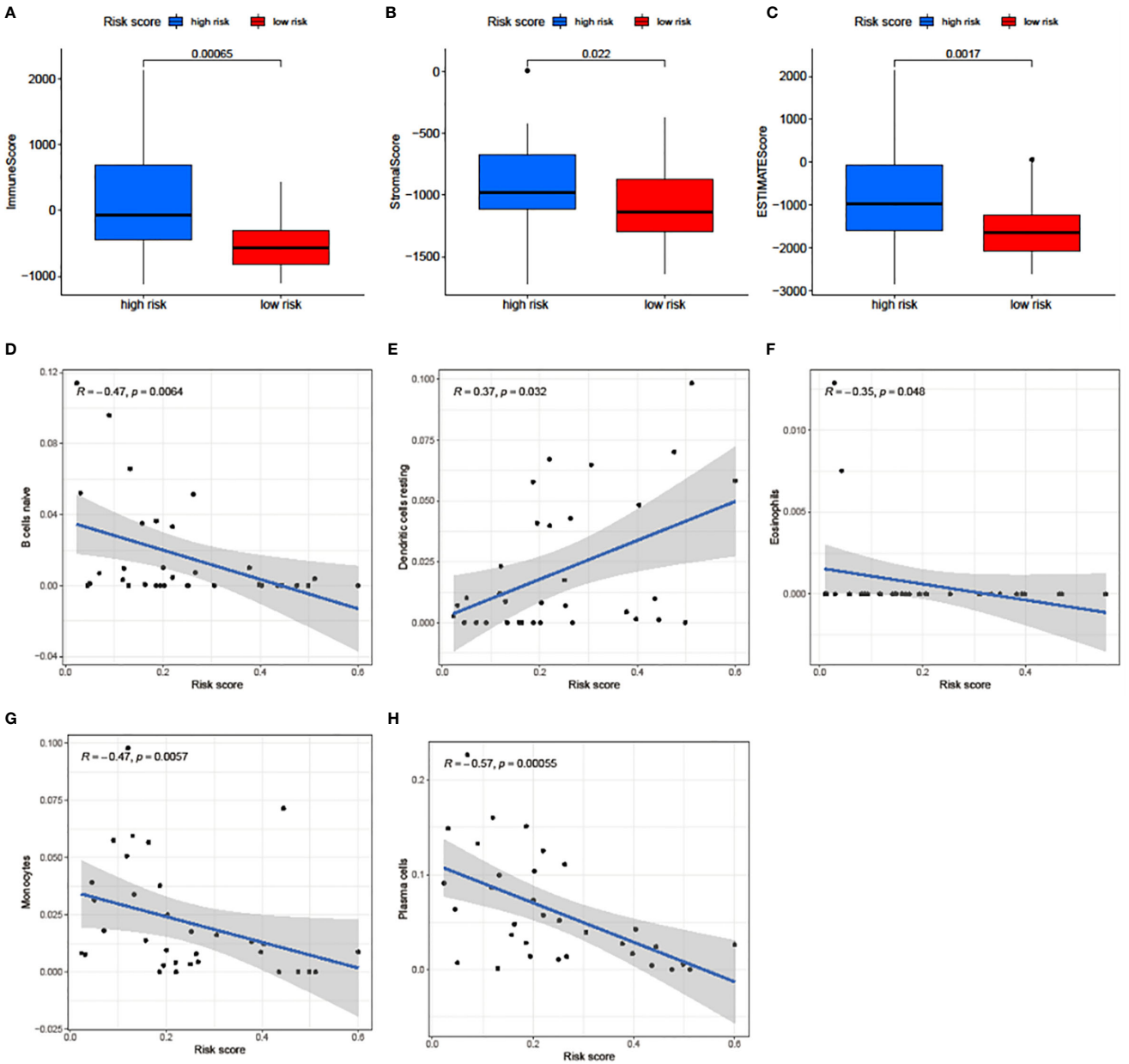

FIGURE 5 | Relationships among the risk score, TME scores, and immune cell infiltration of 5 immune cell types. **(A–C)** The variance analysis of ImmuneScore **(A)**, StromalScore **(B)**, and ESTIMATEScore **(C)** in the high- and low-risk groups. **(D–H)** The correlation between risk score and naive B cells **(D)**, resting dendritic cells **(E)**, eosinophils **(F)**, monocytes **(G)**, and plasma cells **(H)**. The blue line in each plot was fitted linear model indicating the proportion tropism of immune cell along with risk score. The shade around the blue line represents the 95% confidence interval.

expression distribution were concentrated in malignant cells. The gene expression of C2 (**Figure 12C**), MBP (**Figure 12J**), MR1 (**Figure 12K**), and TCF12 (**Figure 12N**) were evenly distributed in immune cells and malignant cells. These results suggested that these immune genes may be the downstream regulators of m^{6}A regulators and related lncRNAs participated in TME remodeling.

DISCUSSION

The TME plays a key role in different stages of tumorigenesis. Eyes are an immune-privileged site but inflammation can develop in an ocular tumor TME (24). UM is homogeneous without much stromal tissue, and therefore, it may be affected by immune cells (25). Compared with other malignancies, the presence of infiltrating

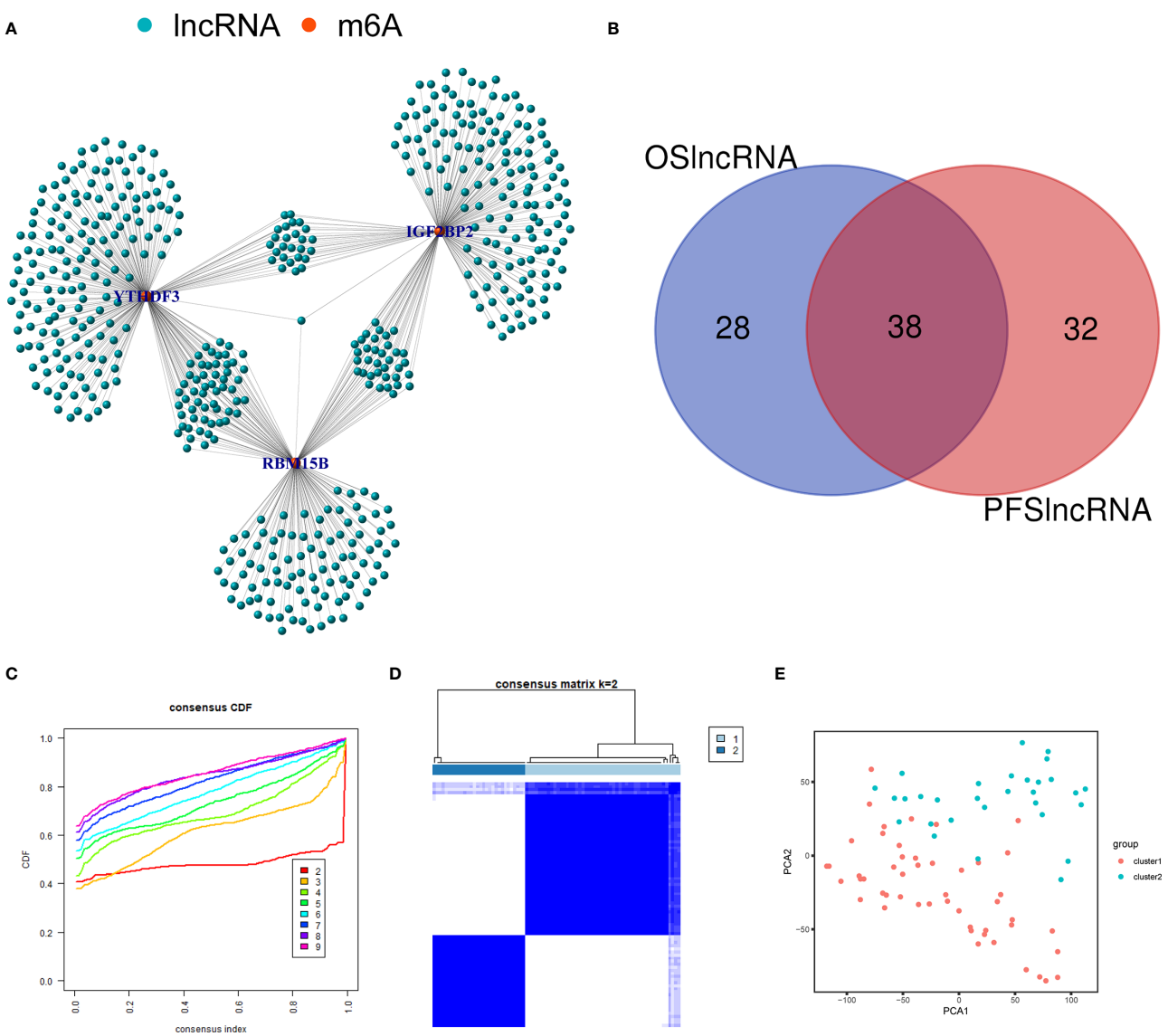

FIGURE 6 | Identification of m^{6}A regulators-related lncRNAs. **(A)** The network between the 3 m^{6}A regulators (red dots) and lncRNAs (green dots). **(B)** The Venn plot showed 38 common lncRNAs shared by OS-related lncRNAs and PFS-related lncRNAs. **(C)** Consensus clustering cumulative distribution function (CDF) for k = 2 to 9. **(D)** Consensus clustering matrix for k = 2. **(E)** Principal component analysis (PCA) of 2 subtypes based on 38 lncRNAs for each sample. OS, overall survival; PFS, progression free survival.

macrophages and T cells in UM is associated with a poorer rather than a better prognosis (25), which was consistent with our findings. Moreover, previous studies have suggested that tumor-infiltrating macrophages and T cells are independent predictors for the prognosis of patients with UM (26, 27). In this study, results of the transcriptome analysis of UM data indicated that UM patients with high ImmuneScore had a poor prognosis. Besides, ImmuneScore was found to be significantly associated with many TICs such as T cells and macrophages. These results suggested that the TME played an important role in UM. Clarifying the mechanisms of the TME will provide novel insight into the development of highly effective immunotherapeutic strategies.

Post-transcriptional regulation is important for regulating the gene expression processes, which determine cellular function. Decades of research have identified more than 100 types of ribonucleosides that are post-transcriptionally modified (28). m^{6}A methylation is one of the most prevalent post-transcriptional modifications found in eukaryotic mRNAs and lncRNAs (28, 29). More studies have reported that m^{6}A regulators extensively participate in diverse biological processes and prognoses in different cancers (13, 14, 30, 31). A recent study has suggested that METTL3-mediated m^{6}A methylation modulates UM cell proliferation, migration, and invasion by targeting c-Met (32). As far as we know, the role of m^{6}A

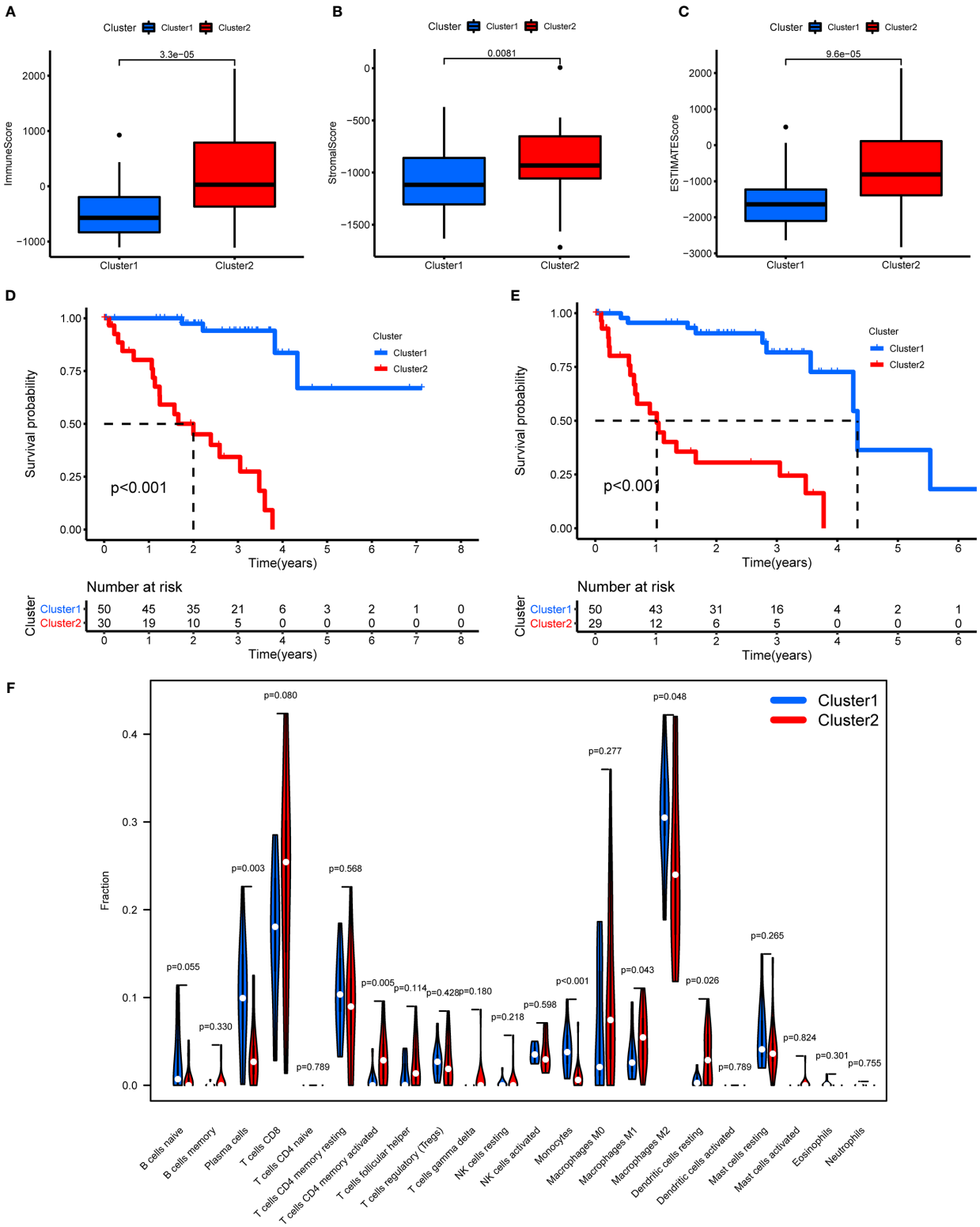

FIGURE 7 | TME scores, survival analysis for UM, and TICs in cluster 1/2 subtypes constructed by 38 m^{6}A regulators-related lncRNAs. **(A–C)** The variance analysis of ImmuneScore **(A)**, StromalScore **(B)**, and ESTIMATEScore **(C)** in cluster 1/2 subtypes. **(D, E)** Kaplan-Meier survival analysis of OS **(D)** and PFS **(E)** for patients with UM in cluster 1/2 subtypes. **(F)** The violin plot showed the fraction differentiation of 22 kinds of immune cells in cluster 1/2 subtypes. TICs, tumor-infiltrating immune cells; OS, overall survival; PFS, progression free survival.

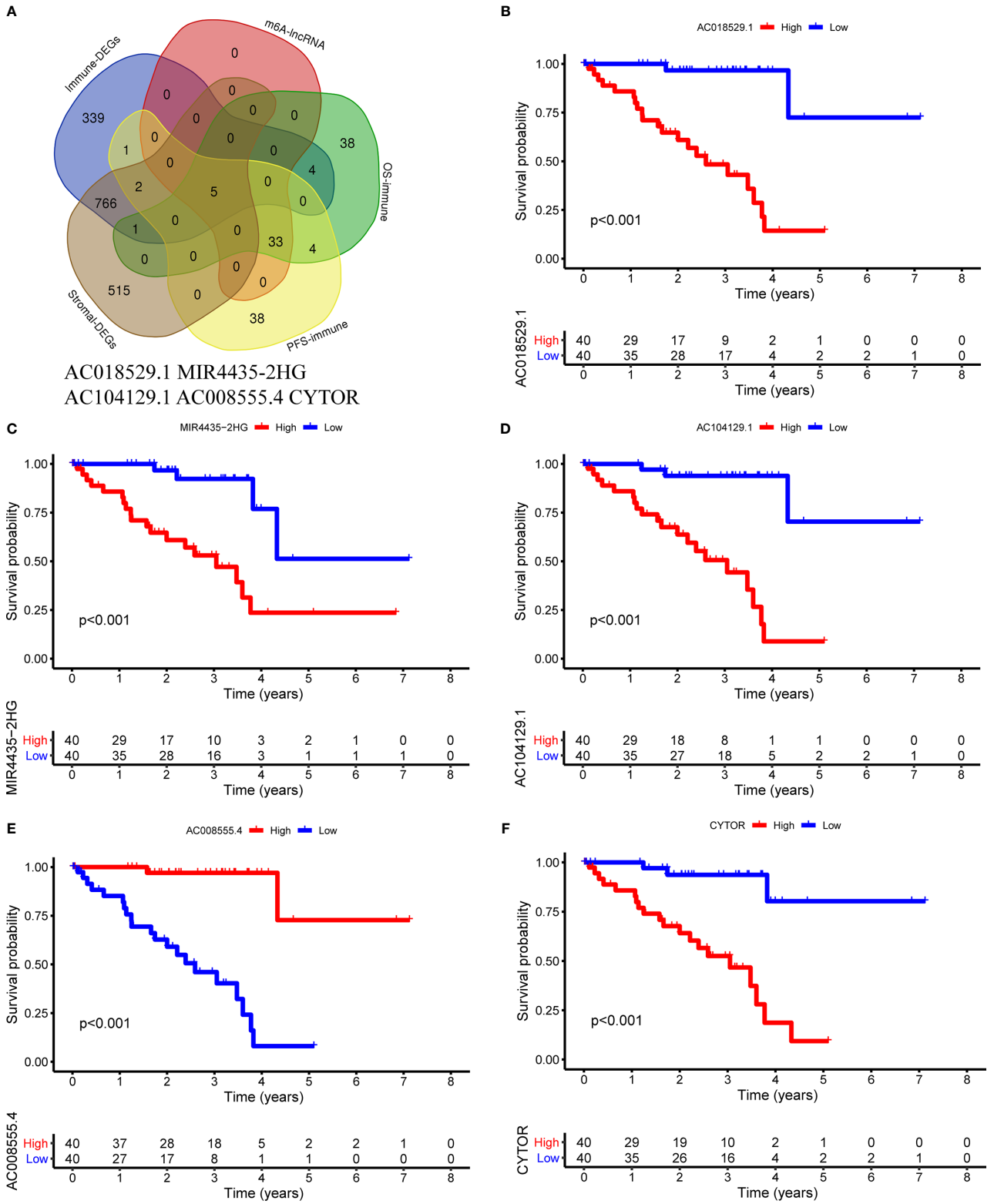

FIGURE 8 | Identification of common lncRNAs from 5 lists. **(A)** The Venn plot showed 5 common lncRNAs in 5 lists. They were ImmuneScore (Immune-DEGs) and StromalScore (Stromal-DEGs), m^{6}A regulators-related lncRNAs (m^{6}A-lncRNAs), and immune gene-specific lncRNAs based on OS (OS-immune) and PFS (PFS-immune). **(B–F)** Survival curves based on the high or low expression of AC018529.1 **(B)**, MIR4435-2HG **(C)**, AC104129.1 **(D)**, AC008555.4 **(E)**, and CYTOR **(F)**. DEGs, differentially expressed genes.

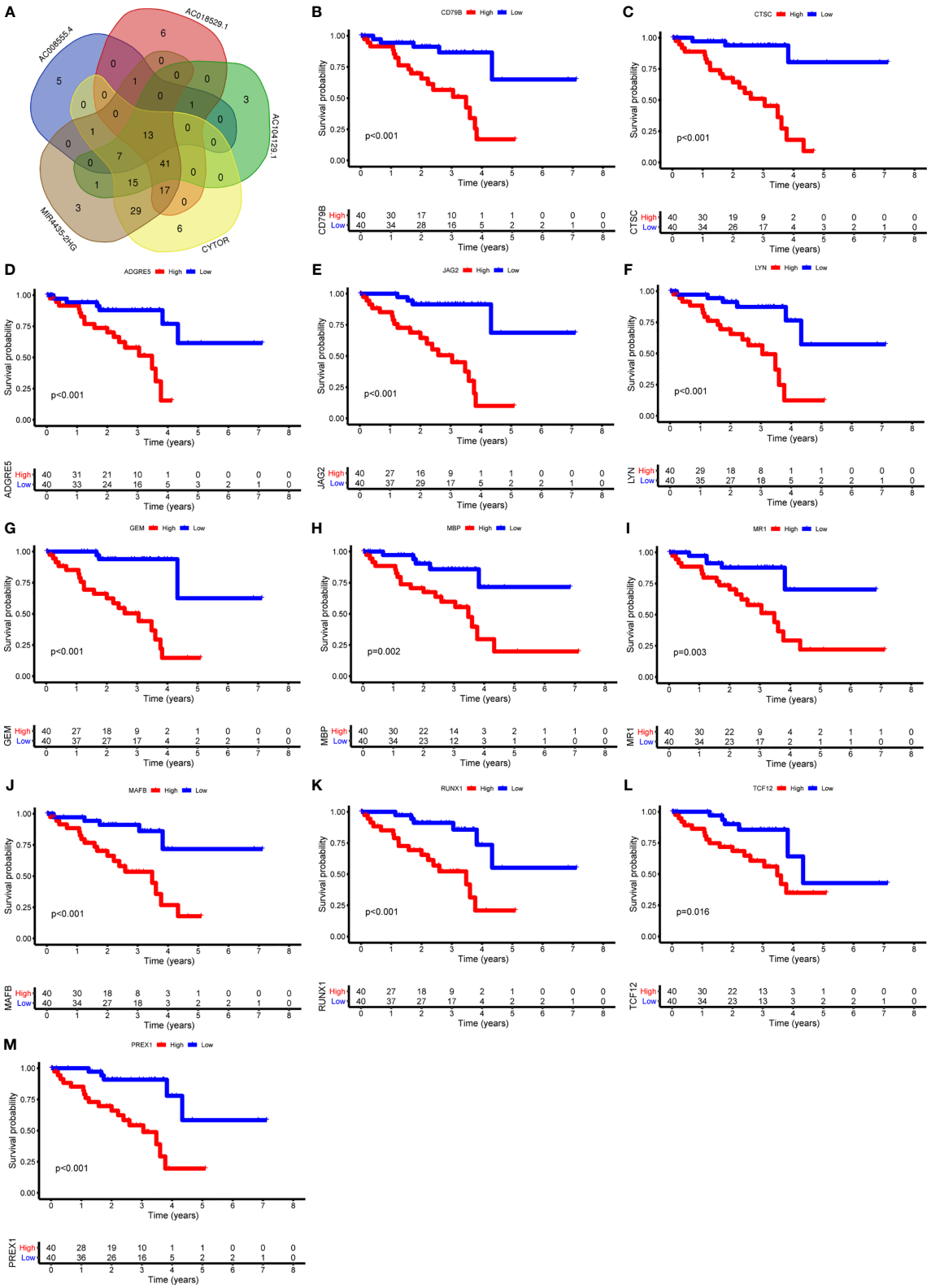

FIGURE 9 | Identification of immune genes targeted by lncRNAs. **(A)** 13 immune genes shared by 5 lncRNAs were identified. (B-M) Survival curves based on the high or low expression of CD79B **(B)**, CTSC **(C)**, ADGRE5 **(D)**, JAG2 **(E)**, LYN **(F)**, GEM **(G)**, MBP **(H)**, MR1 **(I)**, MAFB **(J)**, RUNX1 **(K)**, TCF12 **(L)**, and PREX1 **(M)**. High expression of these immune genes was associated with a poor prognosis.

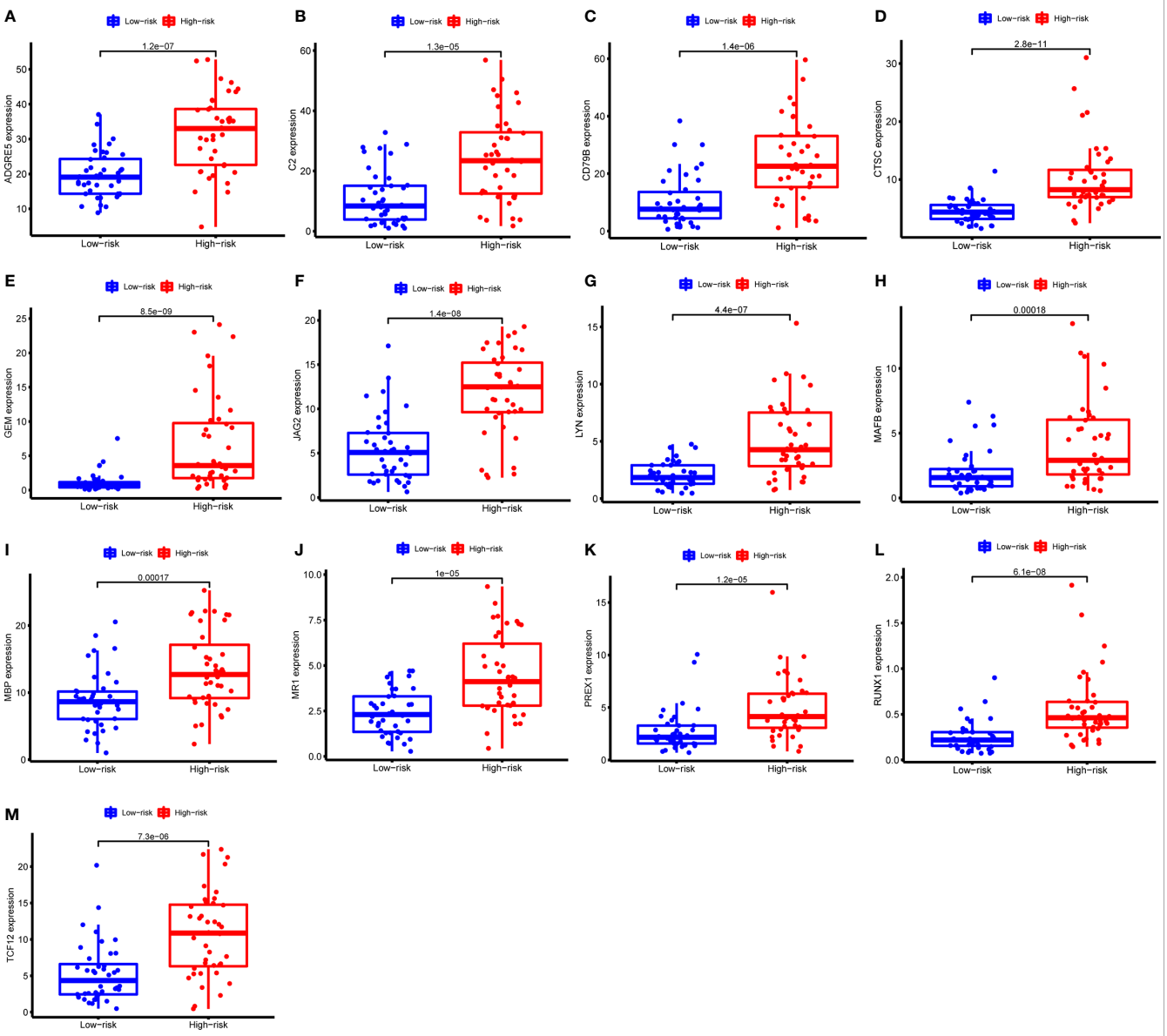

FIGURE 10 | Expression of the 13 immune genes in the high- or low-risk groups based on 3 m^{6}A regulators. (A-M) The differential expression analysis of ADGRE5 **(A)**, C2 **(B)**, CD79B **(C)**, CTSC **(D)**, GEM **(E)**, JAG2 **(F)**, LYN **(G)**, MAFB **(H)**, MBP **(I)**, MR1 **(J)**, PREX1 **(K)**, RUNX1 **(L)**, and TCF12 **(M)** between the high- and low-risk groups. The expression levels of 13 immune genes were all upregulated in the high-risk group than those in the low-risk group.

methylation in UM has less been studied, and the effect of m^{6}A methylation on the TME of UM has not been fully understood.

In this study, we found that m^{6}A regulators were related to the prognosis and TME of patients with UM. We established a prognostic risk signature using 3 m^{6}A regulators based on OS. The signature helped differentiate UM patients into high- and low-risk groups and could serve as an independent risk factor for UM prognosis. The high-risk group was positively correlated with immune cell infiltration levels. Among the 3 m^{6}A regulators, IGF2BP2 acts as m^{6}A readers to enhance mRNA stability and translation and plays an important role in tumors (33). YTHDF3 functions as oncogenes in breast cancer (34). A recent study has investigated that ocular melanoma samples show decreased m^{6}A levels, indicating a poor prognosis (35). In our study, patients with high RBM15B expression had a good prognosis. RBM15B acts as a methyltransferase and thus promotes the level of m^{6}A RNA methylation. Therefore, it is reasonable to speculate that high levels of m^{6}A methylation are beneficial to patients' survival, which is consistent with the current study. These findings indicated that m^{6}A regulators played an important role in the development and progression of cancer. However, the underlying mechanisms of m^{6}A in tumor development still need to be further clarified.

Currently, some studies have clarified the role of lncRNAs in UM. Among these lncRNAs, lncRNA PVT1 and R2RX7-V3

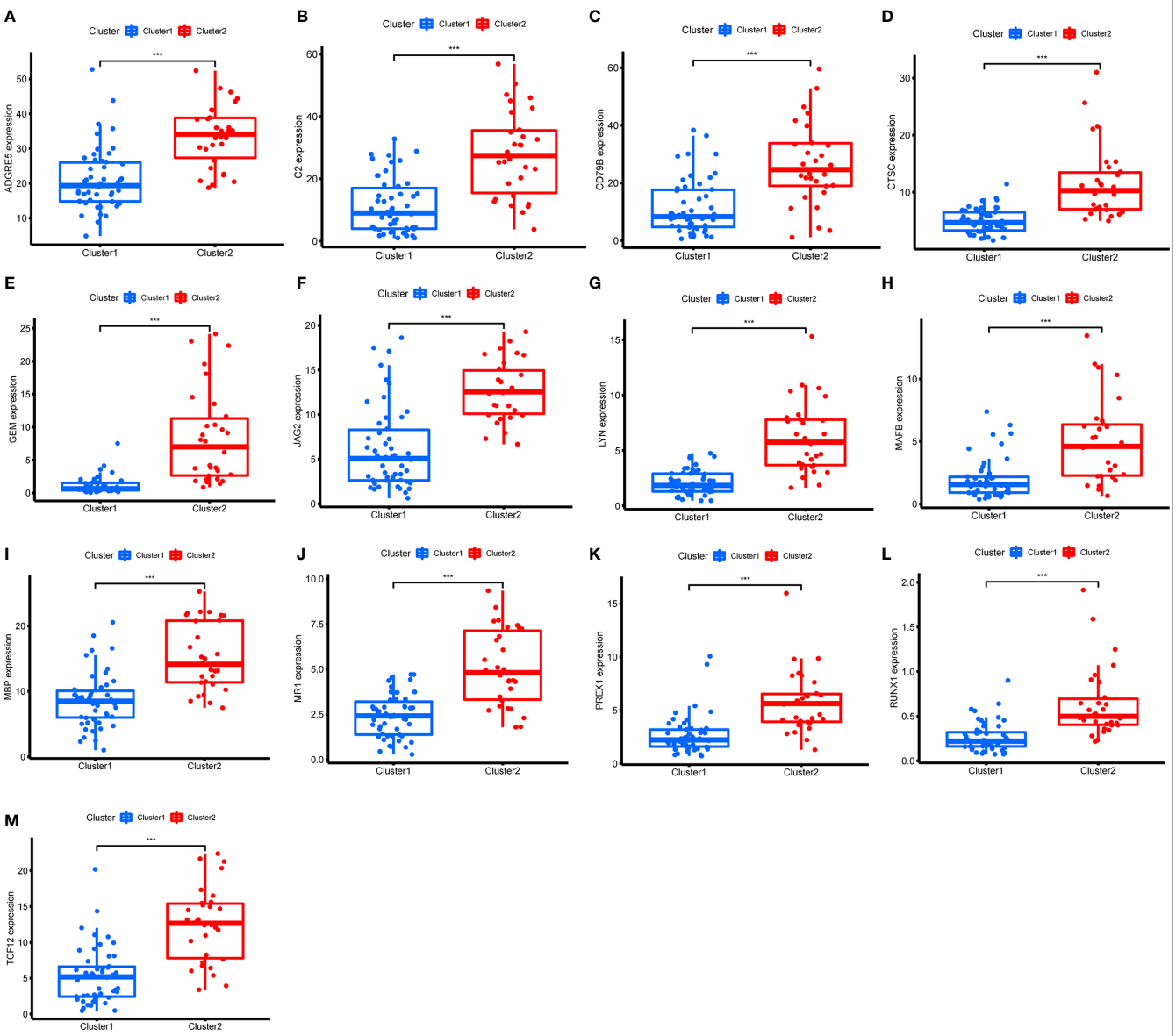

FIGURE 11 | Expression of the 13 immune genes in cluster 1/2 based on m^{6}A-related lncRNAs. **(A–M)** The differential expression analysis of ADGRE5 **(A)**, C2 **(B)**, CD79B **(C)**, CTSC **(D)**, GEM **(E)**, JAG2 **(F)**, LYN **(G)**, MAFB **(H)**, MBP **(I)**, MR1 **(J)**, PREX1 **(K)**, RUNX1 **(L)**, and TCF12 **(M)** between cluster 1 and cluster 2. The expression levels of 13 immune genes in cluster 2 were significantly increased compared with those in cluster 1. ***P < 0.001.

function as novel oncogenes and promote tumorigenesis (36, 37), whereas lncRNAs CANT1 and PAUPAR suppress tumorigenesis in malignant UM (38, 39). However, no study has analyzed the effect of m^{6}A regulators-related lncRNAs on the TME and prognosis in UM. Here we identified m^{6}A regulators-related lncRNAs by performing the correlation analysis and further screened lncRNAs based on OS and PFS. The cluster 1/2 subtypes identified through consensus clustering based on the expression of m^{6}A regulators-related lncRNAs were also related to ImmuneScore, the prognosis of patients, and immune cell infiltration levels. Finally, 5 m^{6}A regulators-related lncRNAs were found to be associated with the OS of UM patients. Among the 5 lncRNAs, lncRNA MIR4435-2HG targets desmoplakin and promotes growth and metastasis of gastric cancer by activating Wnt/β-catenin signaling (40). LncRNA-CYTOR and Wnt/β-Catenin signaling form a positive feed-forward loop to promote the metastasis of colon cancer (41). Through the correlation analysis, we screened 13 downstream immune genes targeted by 5 lncRNAs. They were all found to be upregulated in the high-risk group and cluster 2. At present, RUNX1, MR1, and PREX1 have been reported to be associated with T cells (42–44). CD79B is an important driver of immune-privileged site-associated diffuse large B cell lymphoma (45). JAG2 has been found to be overexpressed

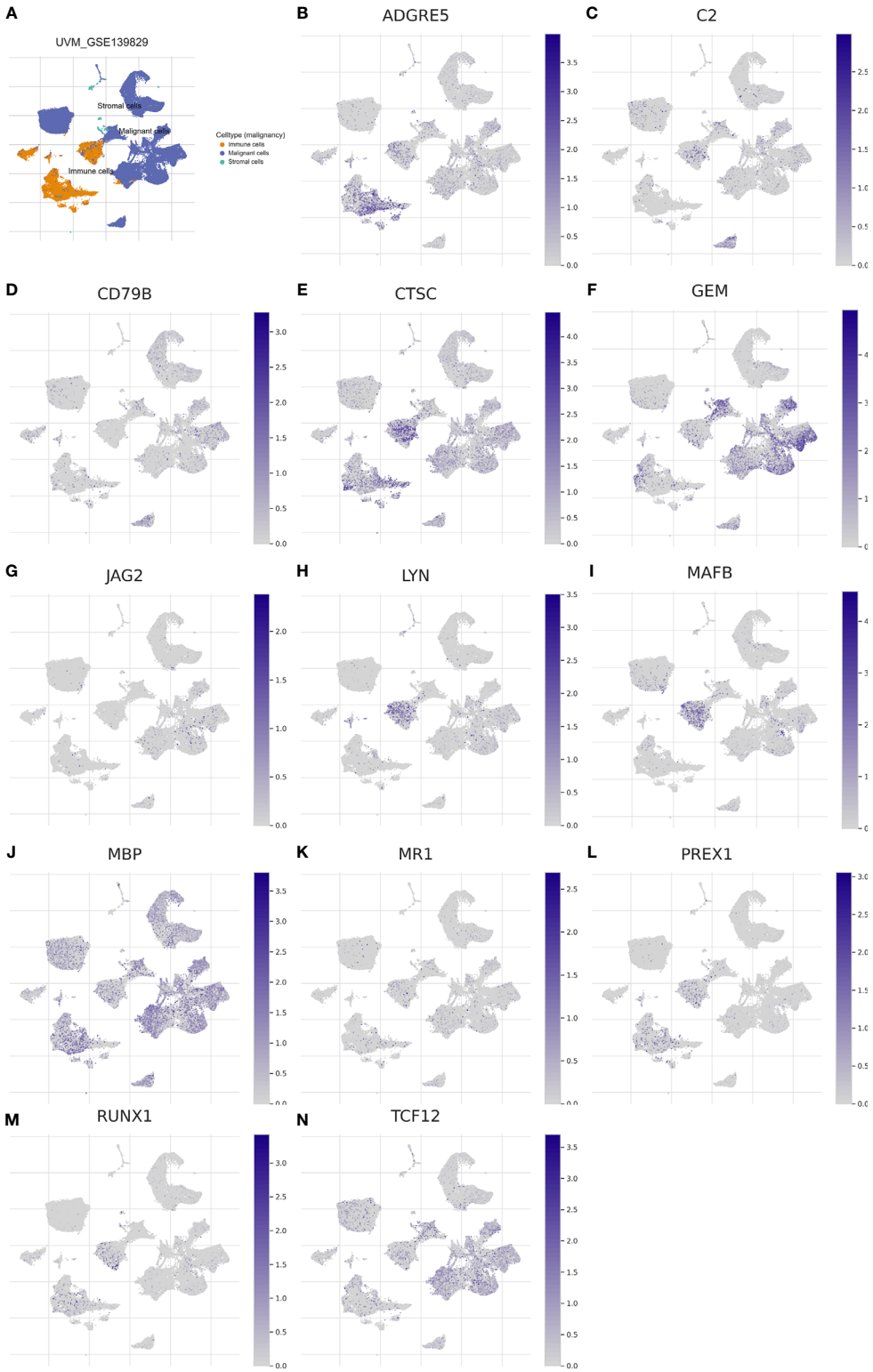

FIGURE 12 | Expression distribution of the 13 immune genes in TME of UM. **(A)** The overview tab of 3 cell types from the GSE139829 dataset. The colored shapes (left) showed the cell distribution and the cell type annotations were displayed on the right side. orange dot: immune cells; blue dot: malignant cells; green dot: stromal cells. **(B–N)** The expression distribution of ADGRE5 **(B)**, C2 **(C)**, CD79B **(D)**, CTSC **(E)**, GEM **(F)**, JAG2 **(G)**, LYN **(H)**, MAFB **(I)**, MBP **(J)**, MR1 **(K)**, PREX1 **(L)**, RUNX1 **(M)**, and TCF12 **(N)** in 3 cell types. The colored dots indicate the distribution of immune genes in the corresponding cell type.

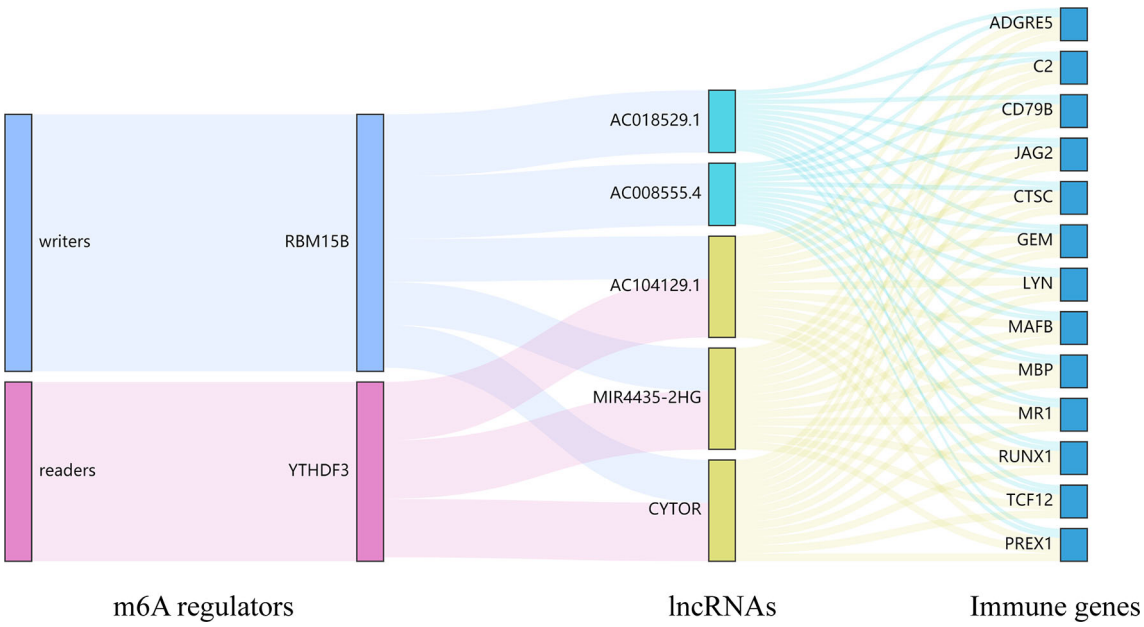

FIGURE 13 | The Sankey diagram depicted the relationship between 2 m^{6}A regulators, 5 lncRNAs, and 13 immune genes. m^{6}A readers: YTHDF3; m^{6}A writers: RBM15B; lncRNAs: AC008555.4, AC018529.1, AC104129.1, CYTOR, and MIR4435-2HG; immune genes: ADGRE5, C2, CD79B, CTSC, GEM, JAG2, LYN, MAFB, MBP, MR1, PREX1, RUNX1, and TCF12.

in malignant plasma cells from multiple myeloma patients and cell lines (46). These results suggested that lncRNAs may affect the immune cell infiltration through 13 common immune genes. Finally, we constructed a Sankey diagram that depicted the relationship between m^{6}A methylation regulators, lncRNAs, and immune genes (**Figure 13**). These findings require further validation and may provide invaluable insights into the future treatment of patients with UM.

m^{6}A methylation is a prevalent form of RNA modification that may provide a novel approach for tumor treatment. However, many key aspects, such as the regulatory mechanisms of m^{6}A regulators and the unidentified relationship between m^{6}A regulators and TME, remain to be explored. Therefore, in this study, we systematically explored the relationship between m^{6}A regulators with the prognosis and TME in UM, further identified the potential lncRNAs and immune genes. However, further validation based on more clinical samples is required, and thus clinical samples will be collected to determine the level of m^{6}A methylation and the association between the expression of m^{6}A regulators and patients' survival in the future. Furthermore, the downstream regulatory mechanisms of m^{6}A regulators will be investigated to screen possible targets by methylated RNA immunoprecipitation sequencing (MeRIP-seq) and RNA-binding protein immunoprecipitation-quantitative polymerase chain reaction (RIP-qPCR). Tumorigenesis in animals and phenotypes of cell lines are necessary to explore the function of m^{6}A regulators in this process.

In conclusion, our study provided an m^{6}A regulators-based signature for prognostic prediction of UM and confirmed that m^{6}A regulators and related lncRNAs played an important role in TME remodeling. These findings might provide promising targets for improving the survival of UM patients.

DATA AVAILABILITY STATEMENT

The datasets analysed for this study can be found in The Cancer Genome Atlas (https://portal.gdc.cancer.gov/).

AUTHOR CONTRIBUTIONS

ZL (1st author) and ZL (5th author) conceived the project. ZL (1st author) performed the computational analyses and wrote the manuscript. SL designed and produced the figures. SH and TW contributed to the literature search for the manuscript. SL and ZL (5th author) revised the manuscript. All authors contributed to the article and approved the submitted version.

SUPPLEMENTARY MATERIAL

The Supplementary Material for this article can be found online at: https://www.frontiersin.org/articles/10.3389/fonc.2021.704543/full#supplementary-material

Supplementary Figure 1 | Identification of m^{6}A regulators-related lncRNAs related to OS and PFS. **(A, B)** Forest plots for the univariate Cox analysis of prognosis based on OS **(A)** and PFS **(B)**. Colored dots represent hazard ratio, and the horizontal lines across the hazard ratio represent 95% confidence interval. OS, overall survival; PFS, progression free survival.

REFERENCES

1. McLaughlin CC, Wu XC, Jemal A, Martin HJ, Roche LM, Chen VW. Incidence of Noncutaneous Melanomas in the U.S. *Cancer* (2005) 103 (5):1000–7. doi: 10.1002/cncr.20866
2. Kaliki S, Shields CL. Uveal Melanoma: Relatively Rare But Deadly Cancer. *Eye (Lond)* (2017) 31(2):241–57. doi: 10.1038/eye.2016.275
3. Kujala E, Makitie T, Kivela T. Very Long-Term Prognosis of Patients With Malignant Uveal Melanoma. *Invest Ophthalmol Vis Sci* (2003) 44(11):4651–9. doi: 10.1167/iovs.03-0538
4. Singh AD, Turell ME, Topham AK. Uveal Melanoma: Trends in Incidence, Treatment, and Survival. *Ophthalmology* (2011) 118(9):1881–5. doi: 10.1016/j.ophtha.2011.01.040
5. Weber JS, D'Angelo SP, Minor D, Hodi FS, Gutzmer R, Neyns B, et al. Nivolumab Versus Chemotherapy in Patients With Advanced Melanoma Who Progressed After Anti-CTLA-4 Treatment (CheckMate 037): A Randomised, Controlled, Open-Label, Phase 3 Trial. *Lancet Oncol* (2015) 16(4):375–84. doi: 10.1016/s1470-2045(15)70076-8
6. Verdegaal EM. Adoptive Cell Therapy: A Highly Successful Individualized Therapy for Melanoma With Great Potential for Other Malignancies. *Curr Opin Immunol* (2016) 39:90–5. doi: 10.1016/j.coi.2016.01.004
7. Wang S, Sun C, Li J, Zhang E, Ma Z, Xu W, et al. Roles of RNA Methylation by Means of N^6-methyladenosine (m^{6}A) in Human Cancers. *Cancer Lett* (2017) 408:112–20. doi: 10.1016/j.canlet.2017.08.030
8. Niu Y, Zhao X, Wu Y, Li M, Wang X, Yang Y. N^6-Methyl-Adenosine (m^{6}A) in RNA: An Old Modification With a Novel Epigenetic Function. *Genomics Proteomics Bioinf* (2013) 11(1):8–17. doi: 10.1016/j.gpb.2012.12.002
9. Sun T, Wu R, Ming L. The Role of m^{6}A RNA Methylation in Cancer. *BioMed Pharmacother* (2019) 112:108613. doi: 10.1016/j.biopha.2019.108613
10. Ping X, Sun B, Wang L, Xiao W, Yang X, Wang W, et al. Mammalian WTAP is a Regulatory Subunit of the RNA N6-Methyladenosine Methyltransferase. *Cell Res* (2014) 24(2):177–89. doi: 10.1038/cr.2014.3
11. Yang Y, Hsu PJ, Chen Y, Yang Y. Dynamic Transcriptomic m^{6}A Decoration: Writers, Erasers, Readers and Functions in RNA Metabolism. *Cell Res* (2018) 28(6):616–24. doi: 10.1038/s41422-018-0040-8
12. Meyer KD, Jaffrey SR. Rethinking m^{6}A Readers, Writers, and Erasers. *Annu Rev Cell Dev Biol* (2017) 33:319–42. doi: 10.1146/annurev-cellbio-100616-060758
13. Li H, Tong J, Zhu S, Batista PJ, Duffy EE, Zhao J, et al. m^{6}A mRNA Methylation Controls T Cell Homeostasis by Targeting the IL-7/STAT5/SOCS Pathways. *Nature* (2017) 548(7667):338–42. doi: 10.1038/nature23450
14. Chen R, Chen X, Xia L, Zhang J, Pan Z, Ma X, et al. N^6-Methyladenosine Modification of circNSUN2 Facilitates Cytoplasmic Export and Stabilizes HMGA2 to Promote Colorectal Liver Metastasis. *Nat Commun* (2019) 10 (1):4695. doi: 10.1038/s41467-019-12651-2
15. Chokkalla AK, Mehta SL, Vemuganti R. Epitranscriptomic Regulation by m^{6}A RNA Methylation in Brain Development and Diseases. *J Cereb Blood Flow Metab* (2020) 40(12):2331–49. doi: 10.1177/0271678X20960033
16. Lasman L, Hanna JH, Novershtern N. Role of m^{6}A in Embryonic Stem Cell Differentiation and in Gametogenesis. *Epigenomes* (2020) 4(1):5. doi: 10.3390/epigenomes4010005
17. Ponting CP, Oliver PL, Reik W. Evolution and Functions of Long Noncoding RNAs. *Cell* (2009) 136(4):629–41. doi: 10.1016/j.cell.2009.02.006
18. Yang G, Lu X, Yuan L. LncRNA: A Link Between LncRNA and Cancer. *Biochim Biophys Acta* (2014) 1839(11):1097–109. doi: 10.1016/j.bbagrm.2014.08.012
19. Sang L, Ju H, Liu G, Tian T, Ma G, Lu Y, et al. LncRNA CamK-A Regulates Ca^{2+}-Signaling-Mediated Tumor Microenvironment Remodeling. *Mol Cell* (2018) 72(1):71–83.e7. doi: 10.1016/j.molcel.2018.08.014
20. Nicholas NS, Apollonio B, Ramsay AG. Tumor Microenvironment (TME)-Driven Immune Suppression in B Cell Malignancy. *Biochim Biophys Acta* (2016) 1863(3):471–82. doi: 10.1016/j.bbamcr.2015.11.003
21. Bussard KM, Mutkus L, Stumpf K, Gomez-Manzano C, Marini FC. Tumor-Associated Stromal Cells as Key Contributors to the Tumor Microenvironment. *Breast Cancer Res* (2016) 18(1):84. doi: 10.1186/s13058-016-0740-2
22. Sun D, Wang J, Han Y, Dong X, Ge J, Zheng R, et al. TISCH: A Comprehensive Web Resource Enabling Interactive Single-Cell Transcriptome Visualization of Tumor Microenvironment. *Nucleic Acids Res* (2021) 49(D1):D1420–30. doi: 10.1093/nar/gkaa1020
23. Durante MA, Rodriguez DA, Kurtenbach S, Kuznetsov JN, Sanchez MI, Decatur CL, et al. Single-Cell Analysis Reveals New Evolutionary Complexity in Uveal Melanoma. *Nat Commun* (2020) 11:496. doi: 10.1038/s41467-019-14256-1
24. McKenna KC, Chen PW. Influence of Immune Privilege on Ocular Tumor Development. *Ocul Immunol Inflammation* (2010) 18(2):80–90. doi: 10.3109/09273941003669950
25. Bronkhorst IH, Jager MJ. Uveal Melanoma: The Inflammatory Microenvironment. *J Innate Immun* (2012) 4(5-6):454–62. doi: 10.1159/000334576
26. DelaCruz JR, Ian W, Mclean. Lymphocytic Infiltration in Weal Malignant Melanoma. *Cancer* (1990) 65:112–5. doi: 10.1002/1097-0142(19900101)65:1<112::aid-cncr2820650123>3.0.co;2-x. Panfilo 0.
27. Teemu Ma kitie PS, Tarkkanen A, Kivel T. Tumor-Infiltrating Macrophages (CD68$^+$ Cells) and Prognosis in Malignant Uveal Melanoma. *Invest Ophthalmol Visual Sci* (2001) 42(7):1414–21. doi: 10.1097/00004397-200107000-00014
28. Yi C, Pan T. Cellular Dynamics of RNA Modification. *Acc Chem Res* (2011) 44 (12):1380–8. doi: 10.1021/ar200057m
29. Zheng G, Dahl JA, Niu Y, Fu Y, Klungland A, Yang YG, et al. Sprouts of RNA Epigenetics: The Discovery of Mammalian RNA Demethylases. *RNA Biol* (2013) 10(6):915–8. doi: 10.4161/rna.24711
30. Chen X, Zhang J, Zhu J. The Role of m^{6}A RNA Methylation in Human Cancer. *Mol Cancer* (2019) 18(1):103. doi: 10.1186/s12943-019-1033-z
31. Yue B, Song C, Yang L, Cui R, Cheng X, Zhang Z, et al. METTL3-Mediated N6-methyladenosine Modification Is Critical for Epithelial-Mesenchymal Transition and Metastasis of Gastric Cancer. *Mol Cancer* (2019) 18(1):142. doi: 10.1186/s12943-019-1065-4
32. Luo G, Xu W, Zhao Y, Jin S, Wang S, Liu Q, et al. RNA m^{6}A Methylation Regulates Uveal Melanoma Cell Proliferation, Migration, and Invasion by Targeting c-Met. *J Cell Physiol* (2020) 235(10):7107–19. doi: 10.1002/jcp.29608
33. Huang H, Wang H, Sun W, Qin X, Shi H, Wu H, et al. Recognition of RNA N^6-Methyladenosine by IGF2BP Proteins Enhances mRNA Stability and Translation. *Nat Cell Biol* (2018) 20:285–95. doi: 10.1038/s41556-018-0045-z
34. Chang G, Shi L, Ye Y, Shi H, Zeng L, Tiwary S, et al. YTHDF3 Induces the Translation of m^{6}A-Enriched Gene Transcripts to Promote Breast Cancer Brain Metastasis. *Cancer Cell* (2020) 38(6):857–71.e7. doi: 10.1016/j.ccell.2020.10.004
35. Jia R, Chai P, Wang S, Sun B, Xu Y, Yang Y, et al. m^{6}A Modification Suppresses Ocular Melanoma Through Modulating HINT2 mRNA Translation. *Mol Cancer* (2019) 18:161. doi: 10.1186/s12943-019-1088-x
36. Pan H, Ni H, Zhang L, Xing Y, Fan J, Li P, et al. P2RX7-V3 Is a Novel Oncogene That Promotes Tumorigenesis in Uveal Melanoma. *Tumour Biol* (2016) 37(10):13533–43. doi: 10.1007/s13277-016-5141-8
37. Wu S, Chen H, Han N, Zhang C, Yan H. Long Noncoding RNA PVT1 Silencing Prevents the Development of Uveal Melanoma by Impairing MicroRNA-17-3p-Dependent MDM2 Upregulation. *Invest Ophthalmol Vis Sci* (2019) 60(14):4904–14. doi: 10.1167/iovs.19-27704
38. Ding X, Wang X, Lin M, Xing Y, Ge S, Jia R, et al. PAUPAR lncRNA Suppresses Tumourigenesis by H3K4 Demethylation in Uveal Melanoma. *FEBS Lett* (2016) 590(12):1729–38. doi: 10.1002/1873-3468.12220
39. Xing Y, Wen X, Ding X, Fan J, Chai P, Jia R, et al. CANT1 lncRNA Triggers Efficient Therapeutic Efficacy by Correcting Aberrant Lncing Cascade in Malignant Uveal Melanoma. *Mol Ther* (2017) 25(5):1209–21. doi: 10.1016/j.ymthe.2017.02.016
40. Wang H, Wu M, Lu Y, He K, Cai X, Yu X, et al. LncRNA MIR4435-2HG Targets Desmoplakin and Promotes Growth and Metastasis of Gastric Cancer by Activating Wnt/β-Catenin Signaling. *Aging-US* (2019) 11(17):6657–73. doi: 10.18632/aging.102164
41. Yue B, Liu C, Sun H, Liu M, Song C, Cui R, et al. A Positive Feed-Forward Loop Between LncRNA-CYTOR and Wnt/beta-Catenin Signaling Promotes Metastasis of Colon Cancer. *Mol Ther* (2018) 26(5):1287–98. doi: 10.1016/j.ymthe.2018.02.024
42. Wong WF, Kohu K, Nakamura A, Ebina M, Kikuchi T, Tazawa R, et al. Runx1 Deficiency in CD4$^+$ T Cells Causes Fatal Autoimmune Inflammatory Lung

Disease Due to Spontaneous Hyperactivation of Cells. *J Immunol* (2012) 188:5408–20. doi: 10.4049/jimmunol.1102991
43. Gold MC, Napier RJ, Lewinsohn DM. MR1-Restricted Mucosal Associated Invariant T (MAIT) Cells in the Immune Response to Mycobacterium Tuberculosis. *Immunol Rev* (2015) 264:154–66. doi: 10.1111/imr.12271
44. Dinkel BA, Kremer KN, Rollins MR, Medlyn MJ, Hedin KE. GRK2 Mediates TCR-induced Transactivation of CXCR4 and TCR-CXCR4 Complex Formation That Drives PI3Kgamma/PREX1 Signaling and T Cell Cytokine Secretion. *J Biol Chem* (2018) 293:14022–39. doi: 10.1074/jbc.RA118.003097
45. Kraan W, Horlings HM, van Keimpema M, Schilder-Tol EJ, Oud ME, Scheepstra C, et al. High Prevalence of Oncogenic MYD88 and CD79B Mutations in Diffuse Large B-cell Lymphomas Presenting at Immune-Privileged Sites. *Blood Cancer J* (2013) 3:e139. doi: 10.1038/bcj.2013.28
46. Houde C, Li Y, Song L, Barton K, Zhang Q, Godwin J, et al. Overexpression of the NOTCH Ligand JAG2 in Malignant Plasma Cells From Multiple Myeloma Patients and Cell Lines. *Blood* (2004) 104:3697–704. doi: 10.1182/blood-2003-12-4114

Conflict of Interest: The authors declare that the research was conducted in the absence of any commercial or financial relationships that could be construed as a potential conflict of interest.

Publisher's Note: All claims expressed in this article are solely those of the authors and do not necessarily represent those of their affiliated organizations, or those of the publisher, the editors and the reviewers. Any product that may be evaluated in this article, or claim that may be made by its manufacturer, is not guaranteed or endorsed by the publisher.

frontiers in Oncology

MINI REVIEW
published: 06 October 2021
doi: 10.3389/fonc.2021.743667

The Role of the Vitamin D Receptor in the Pathogenesis, Prognosis, and Treatment of Cutaneous Melanoma

Alyssa L. Becker[1,2], *Evan L. Carpenter*[1], *Andrzej T. Slominski*[3,4] *and Arup K. Indra*[1,5,6,7,8*]

[1] Department of Pharmaceutical Sciences, College of Pharmacy, OSU, Corvallis, OR, United States, [2] John A. Burns School of Medicine at the University of Hawai'i at Mānoa, Honolulu, HI, United States, [3] Department of Dermatology, University of Alabama at Birmingham, Birmingham, AL, United States, [4] Cancer Chemoprevention Program, Comprehensive Cancer Center, University of Alabama at Birmingham, Birmingham, AL, United States, [5] Knight Cancer Institute, Oregon Health & Science University (OHSU), Portland, OR, United States, [6] Department of Biochemistry and Biophysics, Oregon State University (OSU), Corvallis, OR, United States, [7] Linus Pauling Science Center, Oregon State University (OSU), Corvallis, OR, United States, [8] Department of Dermatology, Oregon Health & Science University (OHSU), Portland, OR, United States

OPEN ACCESS

Edited by:
Vijayasaradhi Setaluri, University of Wisconsin-Madison, United States

Reviewed by:
Sanjay Premi, Moffitt Cancer Center & Research Institute, United States
Chandra K. Singh, University of Wisconsin-Madison, United States

***Correspondence:**
Arup K. Indra
arup.indra@oregonstate.edu

Specialty section:
This article was submitted to Skin Cancer, a section of the journal Frontiers in Oncology

Received: *19 July 2021*
Accepted: *15 September 2021*
Published: *06 October 2021*

Citation:
Becker AL, Carpenter EL, Slominski AT and Indra AK (2021) The Role of the Vitamin D Receptor in the Pathogenesis, Prognosis, and Treatment of Cutaneous Melanoma. Front. Oncol. 11:743667. doi: 10.3389/fonc.2021.743667

Melanoma is the malignant transformation of melanocytes and represents the most lethal form of skin cancer. While early-stage melanoma localized to the skin can be cured with surgical excision, metastatic melanoma often requires a multi-pronged approach and even then can exhibit treatment resistance. Understanding the molecular mechanisms involved in the pathogenesis of melanoma could lead to novel diagnostic, prognostic, and therapeutic strategies to ultimately decrease morbidity and mortality. One emerging candidate that may have value as both a prognostic marker and in a therapeutic context is the vitamin D receptor (VDR). VDR is a nuclear steroid hormone receptor activated by 1,25 dihydroxy-vitamin D3 [calcitriol, 1,25$(OH)_2$D3]. While 1,25 dihydroxy-vitamin D3 is typically thought of in relation to calcium metabolism, it also plays an important role in cell proliferation, differentiation, programmed-cell death as well as photoprotection. This review discusses the role of VDR in the crosstalk between keratinocytes and melanocytes during melanomagenesis and summarizes the clinical data regarding VDR polymorphisms, VDR as a prognostic marker, and potential uses of vitamin D and its analogs as an adjuvant treatment for melanoma.

Keywords: melanoma, vitamin D receptor (VDR), vitamin D3 metabolite, therapy, pathogenesis, tumor microenvironment, polymorphisms, heterodimers

INTRODUCTION

The worldwide incidence of melanoma has steadily increased over the past several decades with the annual incidence rising as rapidly as 4-6% in certain regions (1). In 2021, it is estimated that approximately 106,110 new melanomas will be diagnosed in the United States alone (2). While the incidence of melanoma is greatest in older adult populations, peaking at the sixth decade of life in the United States, it is also one of the most common malignancies found in adolescent and young adult populations (1, 3, 4). In addition to being a relatively ubiquitous cancer, melanoma is the most lethal skin cancer resulting in 9,008 deaths per year in the United States between the years of 2012-2016 (1).

Cutaneous melanoma results from the malignant transformation of predominantly melanocytes (5). Since these pigment producing cells are generally confined to the epidermis of the skin the appearance of vertical growth or Breslow thickness play key roles in determining the aggressiveness of the tumor and its likelihood of metastasis (6). For instance, a stage 0 melanoma is confined only to the epidermis and does not involve nearby dermis or spread to lymph nodes and distant organs. Whereas any melanoma that involves distant metastases is classified as a stage IV tumor.

In early-stage melanoma surgical excision is often curative when the tumor is localized to the skin (1). However, following progression to metastatic melanoma treatment becomes more complex and may include inhibition of metastasis, immunotherapy, targeted inhibition of the mitogen-activated protein kinase (MAPK) pathway, and/or radiation therapy (7, 8). Despite initial improvements these treatments are not fully effective and the cancer is terminal in many cases (9). Reversing this trend is the challenge ahead of melanoma investigators and clinicians, where a more thorough understanding of the molecular mechanisms involved in the pathogenesis of melanoma could lead to novel diagnostic, prognostic, and therapeutic strategies, ultimately resulting in a decreased mortality rate.

One emerging candidate for both targeted therapy and prediction of prognosis is the vitamin-D-receptor (VDR) (10–13). VDR is a nuclear steroid hormone receptor that is found in several organs, including the skin (14). VDR is activated by 1,25 dihydroxy-vitamin D3 (calcitriol, 1,25$(OH)_2$D3) which, in addition of regulating body calcium metabolism, is involved in many pleiotropic activities including regulation of cell proliferation, differentiation, and programmed cell death as well as in photoprotection (12, 13, 15–21).

ACTIVATION OF VITAMIN D

In the canonical pathway of the activation of vitamin D to 1,25$(OH)_2$D3 involves sequential hydroxylations at C25 by CYP2R1 and CYP27A1 and at C1α by CYP27B1 occurring, respectively, in the liver and kidney (22, 23) and in peripheral organs including skin (24). In alternative pathway (non-canonical) vitamin D is activated by CYP11A1 through sequential hydroxylations of it side chain with additional metabolism by other CYP enzymes (23, 25–28). In addition, CYP11A1 is expressed in immune cells, raising a possibility that CYP11A1-derived vitamin D metabolites can be produced in immune cells to regulate their function in a cell autonomous manner (29). While 1,25(OH)2D3 exerts its phenotypic activity through activation of the VDR (30–35) and to some degree through non-genomic action on 1,25D3-MARRS receptor (36, 37), the CYP11A1-derived vitamin D metabolites, in addition on acting on the VDR (13, 38–41), can also interact with alternative nuclear receptors including retinoic acid receptors (RORs) (41, 42), aryl hydrocarbon receptor (AhR) (43) and liver X receptors (LXR) (44). It should be noted that 1,25(OH)2D3 can also act as an agonist on the AhR and LXRs (see **Figures 1** and **2** for details).

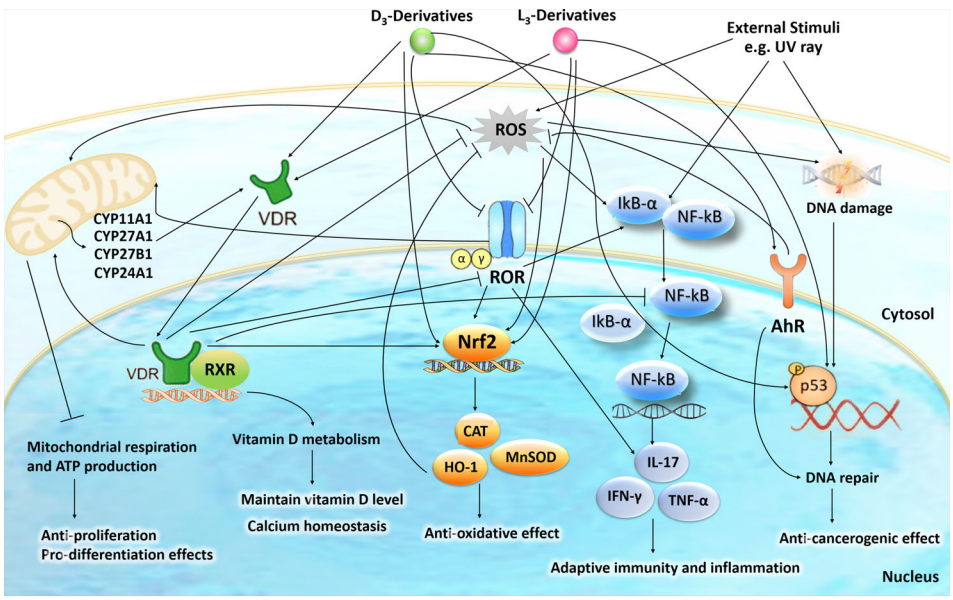

FIGURE 1 | The intracellular action of vitamin D3 (D3)- and lumisterol (L3)-hydroxyderivatives in photoprotection against UVR. Signal transduction includes the activation of nuclear receptors such as vitamin D receptor (VDR), retinoic acid orphan receptor (ROR)α/γ, and aryl hydrocarbon receptor (AhR) and the direct action of D3- and L3-hydroxyderivatives on mitochondrial processes. The nuclear receptors activities are linked with the transcriptional master regulators NRF2 (nuclear factor erythroid-derived 2-like 2), p53 and NFκB (nuclear factor kappa-light-chain-enhancer of activated B cells) to coordinate anti-oxidative, DNA repair, anti-inflammatory, and antiproliferative as well as anti-carcinogenesis mechanisms. The figure is reprinted from (45) with a permission from the publisher.

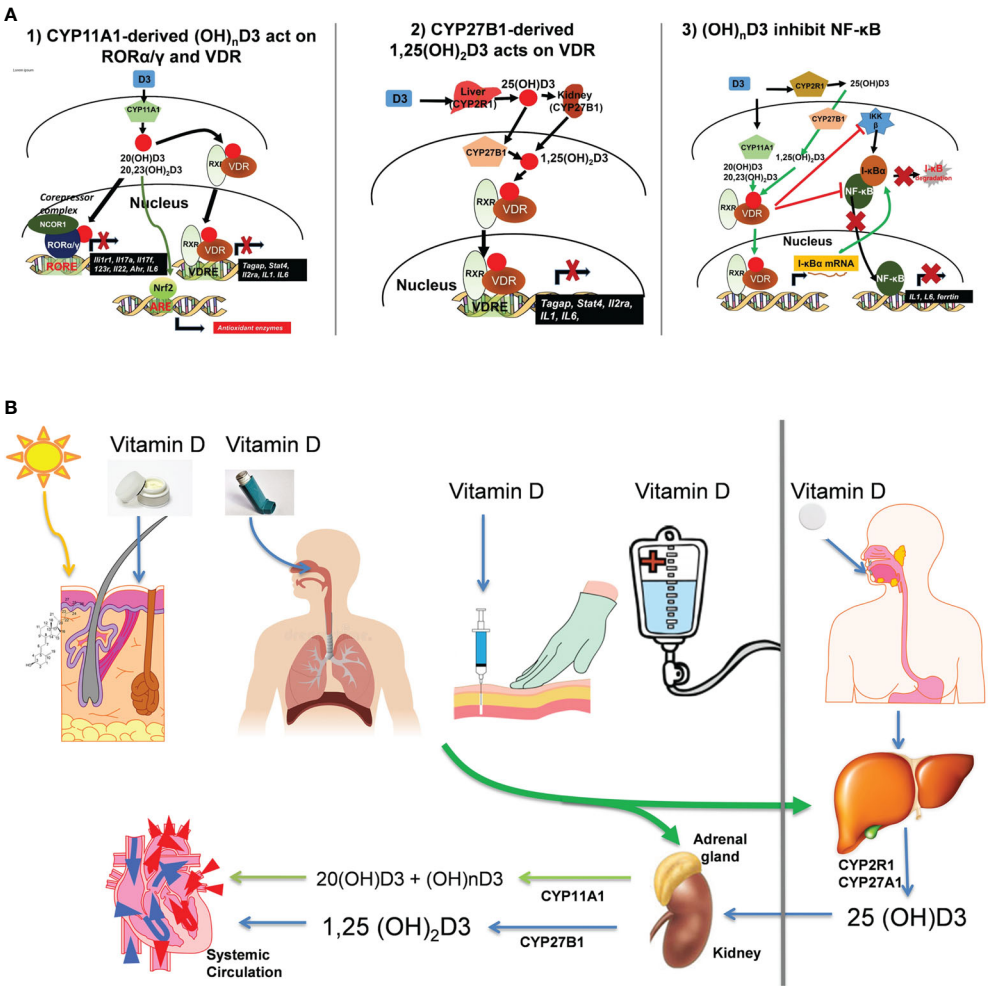

FIGURE 2 | **(A)** Mechanism of action of canonical and non-canonical vitamin D-hydroxyderivatives. Vitamin D signaling in mononuclear cells downregulates inflammatory genes and suppresses oxidative stress. VDR, vitamin D receptor; RXR, retinoid X receptor; ROR, retinoic acid orphan receptor, ROR, ROR response element; ARE, antioxidant response element; VDRE, vitamin D response element; NRF2, nuclear factor erythroid-derived 2-like 2. **(B)** Different routes of vitamin D delivery will impact vitamin D activation pattern. The figure is reprinted from (46) with a permission from the publisher.

VDR IN THE CROSSTALK BETWEEN KERATINOCYTES AND MELANOCYTES IN MELANOMAGENESIS

Under normal physiological conditions, melanocyte homeostasis is maintained by paracrine, autocrine, and direct cell-cell communication between melanocytes and adjacent keratinocytes that comprise epidermal melanin units (47, 48). During melanomagenesis, melanocytes begin to downregulate expression of adhesion molecules, such as E-cadherin, enabling an epithelial-mesenchymal transition that severs transforming melanoma cells from the regulatory activity of adjacent keratinocytes. This process then enables the tumor to take control of its epidermal microenvironment (49). It is known that Wnt/β-catenin signaling is a key regulator of melanocyte-keratinocyte adhesion and interactions; however, the exact role it plays is complicated. Some studies indicate activation of Wnt/β-catenin signaling is associated with decreased melanoma cell proliferation and that loss of this signaling pathway might induce melanomegenesis (50). Indeed, Wnt/β-catenin signaling is important for melanocyte differentiation *via* activation of MITF expression and posttranslational processing (51). On the other hand, others have shown that Wnt/β-catenin signaling is essential for metastatic melanoma cell survival and its inhibition leads to reduced proliferation, migration, and invasion (52). These differing observations could result from differing influences of canonical (β-catenin dependent) or non-canonical Wnt signaling on melanomas during disease progression (53). Of note, active forms of vitamin D inhibit Wnt/β-catenin signaling in squamous cell carcinoma (54). Recently, there is evidence that points towards an inverse relationship with VDR expression and Wnt/β-catenin signaling

in primary melanomas which yields reduced proliferation and immune response evasion (11). It could be that differences in VDR expression contribute to how Wnt/β-catenin signaling influences melanomas. The complex changes in vitamin D signaling and their roles in melanoma development, progression, and therapy have been also discussed recently (12, 55).

Also important in the crosstalk within the epidermal melanin unit is that VDR heterodimerizes with other nuclear receptors including retinoid X receptors (RXRs). We have previously shown that in a VDR null ($VDR^{-/-}$) mouse model topically treated with the carcinogen 12-dimethyl-benz[a]anthracene (DMBA)-12-O-tetradecanoylphorbol-13 acetate (TPA) resulted in numerous melanocytic growths. In that same study, a separate mouse model harboring a conditional tissue-specific keratin 14 promoter-driven cre-mediated epidermal RXRα knockout ($RXR\alpha^{ep-/-}$ mice) also exhibited melanocytic growths (10). These data indicated that both absence of VDR and keratinocytic RXRα knockout stimulated melanocytic growth following tumor promoting treatment. This observation was further explored in additional mouse models in which keratinocytic RXRα knockout was combined with two melanomagenic mutational backgrounds ($RXR\alpha^{ep-/-}|CDk4^{R24C/R24C}$ and $RXR\alpha^{ep-/-}|Tyr\text{-}NRAS^{Q61K}$) and exposed to acute neonatal UVB irradiation in combination with adult chronic UVB doses. These mice exhibited increased melanocytic growth as had been seen previously. They also had elevated malignant melanocytic tumors and increased metastasis to the draining lymph nodes concurrent with a loss in skin expression of PTEN and P53 tumor suppressors (29). To further explore the contribution of keratinocytic RXRα towards melanomagenesis we generated a mouse model that combined the previous background mutations to generate a highly conducive mutational landscape ($RXR\alpha^{ep-/-}|Tyr\text{-}NRAS^{Q61K}|CDk4^{R24C/R24C}$). With this mouse model we observed the formation of spontaneous melanomas in the absence of UVB when keratinocytic RXRα was ablated. Following acute neonatal UVB irradiation, melanomas in adult keratinocytic RXRα ablated mice had increased radial and vertical growth phases, increased proliferation, increased angiogenesis, reduced apoptosis, and increased metastasis to the draining lymph nodes. We also noted in the tumor adjacent normal skin irradiated with UVB that there was increased expression of activated AKT, p21, and cyclin D1 with reduced expression of pro-apoptotic marker BAX (30).

A significantly higher percent of cells from benign human nevi samples exhibited nuclear localization and strong expression of RXRα ($P < 0.0001$) compared to melanomas (with or without metastasis) (31). In the same report, primary human melanoma samples exhibited significantly higher cytoplasmic expression of RXRα compared to the nevi ($P = 0.018$) or the melanomas with metastasis and in metastasis samples ($P = 0.004$). The nuclear *vs* cytoplasmic expression of transcription factor such as RXRα could be critical for regulating their target gene expression by limiting its interaction with their heterodimeric partners and cytoplasmic localization could be essential to mediate the non-genomic actions of RXRα. A previous study by Boehm et al. also showed decreased expression of RXRα in human melanocytic tumors (32). Above results argue for its anticancerogenic role and suggest a cell-autonomous role of melanocytic RXRα in melanoma suppression.

Interestingly, strong nuclear expression of RXRα is also reported in epidermal keratinocytes of normal human skin and we reported for the first time that its expression is reduced or lost in skin keratinocytes adjacent to melanocytic tumors during melanoma progression in humans (33) suggesting a non-cell autonomous role of keratinocytic RXRα in suppressing melanoma progression. In contrast, cytoplasmic intensity of RXRβ did not differ significantly between groups of nevi and melanoma. Although, cytoplasmic expression of RXRβ was significantly reduced in human metastasis samples compared to the human melanoma samples (31) indicating a role of RXRβ in mediating melanoma metastasis.

We have also shown that both VDR and keratinocytic RXRα contribute towards photoprotection of melanocytes against UVB radiation *in vivo* using preclinical studies in mice models. Using the $RXR\alpha^{ep-/-}$ mouse model subjected to acute neonatal UVB irradiation, we demonstrated that the absence of keratinocytic RXRα resulted in increased DNA damage, proliferation, and migration of melanocytes *in vivo*. We then confirmed these results *ex vivo* using primary melanocytes which exhibited increased growth in conditioned media generated from culturing isolated RXRα knockout keratinocytes. This was explained by increased expression of keratinocyte secreted growth factors ET-1, FGF2, and SCF in the skin of $RXR\alpha^{ep-/-}$ *mice* following UVB irradiation (34) underscoring a "non-cell autonomous" role of keratinocytic RXRα in UV-induced melanocyte homeostasis.

Interestingly, mice with melanocyte-specific ablation of RXRα and RXRβ ($RXR\alpha^{mel-/-}$ | $RXR\beta^{mel-/-}$) attract a reduced number of IFN-γ secreting immune cells than in wild-type mice following acute UVR, *via* altered expression of chemoattractive and chemorepulsive chemokines/cytokines. Reduced IFN-γ in the microenvironment modifies UVR-induced apoptosis, and due to this, the survival of dermal fibroblasts is significantly decreased in mice lacking RXRα/β (35). Results demonstrate that melanocytic-RXRs in a "non-cell autonomous" manner modulate post-UVR survival of dermal fibroblasts highlighting a role in immune surveillance, while independently in a "cell autonomous" manner regulate post-UVR melanocyte survival (35).

We have also demonstrated that melanocytic VDR also affords photoprotective properties in a different mouse model in which melanocytic VDR was ablated ($VDR^{mel-/-}$). When knockout mice were subjected to acute neonatal UVB irradiation they exhibited fewer differentiated melanocytes with reduced proliferation, reduced apoptosis, and increased DNA damage (36).

Interestingly active forms of vitamin D3 show photoprotective activities in both melanocytes and keratinocytes (37–43) through various mechanisms also including the VDR (40, 44, 56, 57).

Altogether, above data highlight the importance of nuclear receptor signaling in melanocytes driven by VDR and its

principal heterodimer partners RXRα and RXRβ in the regulation of melanocyte homeostasis and melanomagenesis in the skin and tumor microenvironment. Our data further underscores a non-cell autonomous role of RXRα both in keratinocytes and melanocytes of the skin in controlling melanocyte homeostasis and melanomagenesis.

VITAMIN D RECEPTOR POLYMORPHISMS IN MELANOMA

The VDR gene is located on chromosome 12q13.11 and has 11 exons (58). Over 600 single nucleotide polymorphisms have been identified in the VDR gene including FokI (C/T-rs2228570, previously named rs10735810), TaqI (rs731236), BsmI (rs1544410), and ApaI (rs7975232) which are the most commonly analyzed in relation to melanoma (5). Cdx2 (rs11568820), EcoRV (rs4516035), BglI (rs739837) have also been studied in this context, but to a lesser extent.

The FokI polymorphism (C/T-rs2228570, previously named rs10735810) is located on exon 2 of the VDR gene (5). This polymorphism creates a new start codon 10 base pairs upstream from the usual start codon, leading to a longer VDR protein that is less active compared to the shorter protein variant. The shorter protein variant is 424 amino acids and corresponds to the C nucleotide allele or F allele, and the longer 427 amino acid variant corresponds to the F allele (59, 60). The TaqI polymorphism (rs731236) is located at codon 352 of exon 9 of the VDR gene, and functions as a restriction fragment length polymorphism (5). It creates a silent codon change of ATT to ATC, which both code for isoleucine (5, 61).

The BsmI polymorphism (rs1544410) also acts as a restriction fragment length polymorphism that results in a silent mutation (5, 61). It is located in intron 8 at the 3rd end of the VDR gene, thus it may affect VDR gene expression and mRNA stability (60). The ApaI polymorphism is located near the BsmI polymorphism, and thus, may have similar effects (5, 61). The Cdx2 (rs11568820) polymorphism is located in the promoter region of the VDR gene, and results in an adenine replacing a guanine (5, 61). The EcoRV polymorphism (rs4516035) is also located in the promoter region of the VDR gene, and is thought to play a role in the anticancer immune response (5, 62). Lastly, the BglI polymorphism (rs739837) is located near the stop codon in exon 9 (5).

A 2020 meta-analysis calculated the odds ratios and 95% confidence intervals for the dominant and recessive models for 7 VDR gene polymorphisms (63). The dominant model (Bb + BB *vs*. bb) of Bsml (rs1544410) showed a statistically significant 15% risk reduction in malignant melanoma incidence for carriers of the rarer allele B. Carriers of the rarer allele f (Ff + ff *vs*. FF) of FokI (rs2228570) were shown to be 22% more likely to develop malignant melanoma. Additionally, for ApaI (rs7975232), there is a 20% higher risk of melanoma for carriers of the rarer a allele (Aa + aa *vs*. AA). No significant association between melanoma risk and the other investigated VDR polymorphisms, which included TaqI (rs731236), A-1012G (rs4516035), Cdx2 (rs11568820), and BglI (rs739837), was found.

VDR EXPRESSION AS A PROGNOSTIC BIOMARKER

One cohort-study assessed the relationship between VDR expression and prognostic factors in Central European cohort of melanoma patients (64, 65). VDR expression was quantified immunohistochemically in 69 cutaneous melanomas and compared to the tumors' pTNM (pathological tumor, node, metastasis) stage, ulceration, and tumor-infiltrating lymphocytes. pTNM staging is based on the tumor (i.e., Breslow thickness, ulceration), spread to nearby lymph nodes, and distant metastases. The higher the tumor's stage, the worse the prognosis.

Strongest and highest VDR expression was detected in the nuclei of epidermal keratinocytes for normal uninvolved skin compared to melanocytic lesions. For "nuclear localization", VDR expression decreased in the following order: *normal skin* > *melanocytic nevi* > *primary melanomas* = *metastases* (64). For "cytoplasmic localization", VDR expression decreased in the order: *normal skin* = *melanocytic nevi* > *primary melanomas* = *metastases*. Reduction in VDR expression with the development of the pigmented lesions was more evident in the nuclei than in the cell-cytoplasm suggesting a cell-autonomous role of canonical VDR signaling in the melanocytes during melanoma progression and metastasis (64).

Interestingly, VDR expression in the basal and supra-basal keratinocytes of the skin epidermis surrounding the melanocytic tumors was markedly lower in comparison to normal skin without any skin lesions, which also suggests a non-cell autonomous role of keratinocytic VDR in melanomagenesis (64). Further, high VDR expression both in primary and metastatic melanomas was a factor that favorably influenced the OS in melanoma cohort.

In melanoma, ulceration contributes to the tumor of pTNM staging, and is a hallmark of more aggressive tumors. Whereas, the presence of tumor-infiltrating lymphocytes in melanoma is associated with a favorable prognosis. Less advanced melanomas, like those with fewer than three lymph node metastases and those without distant metastases, had the strongest VDR expression (64, 65). Whereas tumors with indicators of poor prognosis like ulceration or non-brisk or absence of tumor-infiltrating lymphocytes, showed significantly lower VDR expression. Most importantly patients with metastatic disease and *VDR*$^{-/-}$ melanomas had the poorest probability of survival (64, 65). Interestingly, the expression of activating vitamin D enzyme CYP27B1 was inversely correlated with melanoma progression and overall and disease-free survival times and such correlation was amplified by a concomitant decrease in the VDR expression (55, 65, 66). While CYP24A1 levels were high in nevi and early-stage melanomas in comparison to normal epidermis, its level decreased during melanoma progression similarly to CYP27B1 and VDR (67). These findings indicate that vitamin D signaling system including VDR expression plays an important role in melanoma prognosis and may also be used as an additional prognostic biomarker. Similar trend was reported for ocular melanoma (68). Importantly, recent experimental studies have shown that knocking out of the VDR in melanoma cells increase their malignant behavior and decreases responsiveness to active form of vitamin D indicating that the VDR can serve as the

melanoma tumor suppressor gene (69), which is consistent with the role of the VDR as the tumor suppressor gene in the skin as originally proposed by Bikle (44). Of note, defects in VDR lead to increased malignant behavior in other tumors including bladder, ovarian, lung and breast cancers, lymphomas (70–75).

There was a reverse correlation between melanin content and expression of the VDR and CYP27B1 as well as of RORα and γ in human melanoma samples (64, 66, 76). RORα and γ, alternative receptors for vitamin D-hydroxyderivatives, are expressed at lower levels in melanomas than in nevi and their expression decreases during melanoma progression, with lowest expression found in stage III and IV melanomas and in metastases (76). Interestingly, the expression of VDR as wells as of RORs was related to the HIF1α activity, which also affected FoxP3 expression in metastatic melanoma (77). Of note, melanogenesis can stimulate HIF1α expression and anaerobic glycolysis in melanoma cells (78) explaining in part the correlation between defects in VDR expression and signaling and defective responses to vitamin D in pigmented melanoma cells (64, 79, 80).

A separate study conducted by Muralidhar et al. analyzed 703 primary melanoma transcriptomes to better understand the role of vitamin D-VDR signaling (11). They found that VDR expression was independently protective against melanoma-related death in both primary and metastatic disease. VDR expression was shown to be inversely related to Wnt/β-catenin signaling, suggesting a mechanism for the anti-proliferative effects of vitamin D-VDR signaling. Additionally, increased VDR expression was associated with the upregulation of pathways involving the antitumor immune response as demonstrated by a greater abundance of tumor-infiltrating lymphocytes. This study further supports VDR's utility as a prognostic biomarker, especially in those patients considering immunotherapy. It also establishes a causal relationship between vitamin D-VDR signaling and melanoma survival, suggesting that this mechanism could serve as a target for pharmacologic agents.

In addition to its generalized expression, the subcellular localization of VDR to the nucleus also could be beneficial as a biomarker for melanoma progression. Hutchinson et al. studied 34 benign nevi, 149 metastatic melanomas, and 44 matched metastases *via* immunohistology for the subcellular localization of VDR and phosphorylated ERK (p-ERK) as an indicator of MAPK activation (81). They found that as melanomas progressed, they exhibited reduced nuclear localization of VDR and increased cytoplasmic localization. Overall, expression of VDR decreased from benign nevi to metastatic melanoma and further decreased in metastasizing primary tumors. When they observed VDR localization in malignant melanomas known to have metastasized and compared them to those known to not have metastasized within five years, they saw nuclear VDR was reduced while there was no difference in cytoplasmic localization. They also found increased p-ERK consistent with cytoplasmic localization of VDR likely a result of the known mechanism of MAPK inhibition of VDR signaling when it is heterodimerized to RXRα *via* phosphorylation of serine 260 (82). These observations highlight the need for more research on the usefulness of VDR nuclear localization as a prognosticator for metastasizing melanomas.

SERUM VITAMIN D LEVELS AND PROGNOSIS

As part of the Leeds Melanoma Cohort, Newton-Bishop et al. reported an association between higher 25-hydroxyvitamin D3 serum levels at time of melanoma diagnosis and lower Breslow thickness (p value= .002) (83). Higher 25-hydroxyvitamin D3 levels were also found to be associated with increased survival independent of Breslow thickness. Several other studies have confirmed an association between higher serum vitamin D levels at diagnosis and better prognosis in melanoma (84–86). However, a more recent study asserts that rather than high levels of vitamin D being protective a deficiency in vitamin D (<25 nmol/L) actually shortens patient survival time from melanoma in a VDR-dependent manner (11).

Additionally, an observational single center study with estimated study completion date of January 2021, not yet published, is investigating the response to treatment with anti-programmed death 1 (PD-1) therapy in relation to serum vitamin D levels in 40 advanced melanoma patients (ClinicalTrials.gov Identifier: NCT03197636) (87). Serum levels of vitamin D will be measured at baseline, 3, and 6 weeks after initiation of treatment with anti-PD1 therapy followed by three years of observational follow-up. Response to treatment will be assessed at each visit within the study period and at follow-up.

VITAMIN D, VDR AND IMMUNOTHERAPY

The issue of interference of active forms of vitamin D on immunotherapy deserves special attention, especially that immunotherapy represents the promising therapeutic approach against melanoma (88–95). In this context, inhibitory role of vitamin D in the adaptive immune responses (96, 97) requires explanation. Although it inhibits T cell responses in autoimmune responses (98), the evidence that it acts as an immunosuppressor is missing. On the opposite, it is inhibiting proinflammatory responses through VDR mediated inhibition of NFκβ and inverse agonism on RORγ and inhibition of oxidative stress through activation of NRF2-dependent pathways (45, 46, 57, 99). However, it is unclear to which degree, how, and whether it will inhibit anti-tumor T-cell responses. On the other hand, vitamin D activates the innate immune system (96, 97), which plays an important role in anti-tumor activity (100–106). Therefore, the actions of active forms of vitamin D can be defined as immunoregulatory, with their full definitions requiring future careful studies.

VITAMIN D AND ITS ANALOGS IN THE TREATMENT OF MELANOMA

Several studies are investigating the use of vitamin D or its analogs as adjuvant treatment in melanoma patients with an understanding that different delivery routes will influence vit D activation (**Figures 2B** and see below).

One report that utilized data from the Women's Health initiative (WHI) calcium/vitamin D randomized controlled trial, studied the effects of calcium and low-dose vitamin D on the risk of non-melanoma and melanoma skin cancers in post-menopausal women (107). Women ages 50-79 years (N=36,282) were randomly assigned to receive 1,000 mg of elemental calcium plus 400 IU of vitamin D3 daily or placebo for a mean follow-up period of seven years. Non-melanoma and melanoma skin cancer diagnoses were self-reported annually. The study concluded that the treatment group and control group showed no significant difference in the incidence of melanoma or non-melanoma skin cancers. However, women on the calcium/vitamin D regiment with a history of non-melanoma skin cancer had a reduced risk of melanoma as opposed to those receiving placebo (hazard ratio 0.43; 95% confidence interval: 0.21 to 0.90: P(interaction) =.038). It was also noted that this difference was not seen in women that did not have a history of non-melanoma skin cancer.

In 2010, the Australia and New Zealand Melanoma Trials Group conducted a pilot randomized placebo-controlled phase II trial, Mel-D, to investigate the safety and efficacy of adjuvant high-dose vitamin D administration in patients with cutaneous melanoma that had initially been treated with wide excision (Australian New Zealand Clinical Trials Registry #ACTRN12609000351213) (108, 109). The adjuvant treatment included an oral loading dose of 500,000 IU Vitamin D followed by a once monthly oral dose of 50,000 IU Vitamin D for two years. Patients in this study reportedly experienced an improvement in progression-free survival and overall survival.

The ongoing study, VidMe, is a multicenter randomized placebo-controlled phase III trial intended to examine the efficacy and long-term safety of high-dose vitamin D supplementation in 500 patients with melanoma (ClinicalTrials.gov Identifier: NCT01748448) (110, 111). Once a month, participants will either receive 100,000 IU of vitamin D or placebo (Arachidis oleum raffinatum). This study's primary endpoint is relapse-free survival. They also plan to assess the expression of VDR in the primary tumor and its possible correlation with relapse. Secondarily, vitamin D levels at diagnosis will be correlated with melanoma site, subtype, and stage at diagnosis. Vitamin D levels will continue to be monitored after supplementation to determine if serum levels depend on the genetic variability of the vitamin D pathway. Additionally, they plan to investigate whether VDR immunoreactivity correlates with stage at diagnosis.

Vitamin D analogs have also exhibited promising photoprotective and anticancer properties (13, 57, 112) indicating their possible application to counteracting skin cancer, including melanomas. The anti-melanoma activity of the non-calcemic analog, 20(OH)D3, was shown in a preclinical *in vivo* model (113). 20(OH)D3 is non-calcemic but possesses similar antiproliferative activity *in vitro* when compared to 1,25 (OH)2D3. Skobowiat et al. demonstrated decreased colony formation both in the monolayer and soft agar conditions when cells were treated with 20(OH)D3. 20(OH)D3 was also shown to inhibit melanoma cells in transwell migration and spheroid toxicity. Additionally, 20(OH)D3 decreased melanoma tumor growth in immunocompromised mice without obvious signs of toxicity. These results suggest that 20(OH)D3 is likely effective and safe, and thus, should undergo further preclinical testing as an antimelanoma therapy.

Therefore, cellular expression of RXRs and VDR in addition to their sub-cellular localization could be used as a prognostic biomarker for melanoma progression in humans. While vitamin D3 and its analogs are currently being explored in pre-clinical and clinical settings as a possible adjuvant therapy in the treatment of melanoma (107, 108, 110, 111, 113), in those individuals with decreased or dysfunctional VDR and RXR expression, vitamin D supplementation is unlikely to be beneficial. Thus, there is a need for a novel therapy that increases and/or restores functional VDR and RXR expression in conjunction with the supplementation of vit D or its analogs. Similarly, the *in vivo* anti-melanoma effects of the novel vit D analogs need to be established and the underlying mechanisms of action need to be deciphered.

AUTHOR CONTRIBUTIONS

All authors have contributed intellectually for the preparation of the manuscript. All authors contributed to the article and approved the submitted version.

FUNDING

Research reported in this publication was supported in part by National Institute of Environmental Health Sciences (NIEHS) of the National Institutes of Health (NIH) under the award number 1R01ES016629-01A1 (PI :AI), the OSU/OHSU College of Pharmacy Pilot Project Grant (PI :AI), NIH grants to ATS including 1R01AR073004-01A1, R01AR071189-01A1, and a VA merit grant [no. 1I01BX004293-01A1 (PI ATS)], and a Training grant from the National Center for Complementary and Integrative Health (NCCIH) of the National Institutes of Health under award number T32AT010131.

REFERENCES

1. Matthews NH, Li W-Q, Qureshi AA, Weinstock MA, Cho E. "Epidemiology of Melanoma", In: *Cutaneous Melanoma: Etiology and Therapy*. Brisbane (AU: Codon Publications. Available at: http://www.ncbi.nlm.nih.gov/books/NBK481862/ (Accessed February 17, 2021).
2. Siegel RL, Miller KD, Fuchs HE, Jemal A. Cancer Statistics, 2021. *CA Cancer J Clin* (2021) 71:7–33. doi: 10.3322/caac.21654
3. Watson M, Geller AC, Tucker MA, Guy GP, Weinstock MA. Melanoma Burden and Recent Trends Among Non-Hispanic Whites Aged 15–49 Years, United States. *Prev Med* (2016) 91:294–8. doi: 10.1016/j.ypmed.2016.08.032
4. Ballantine KR, Watson H, Macfarlane S, Winstanley M, Corbett RP, Spearing R, et al. Small Numbers, Big Challenges: Adolescent and Young Adult Cancer Incidence and Survival in New Zealand. *J Adolesc Young Adult Oncol* (2017) 6:277–85. doi: 10.1089/jayao.2016.0074

5. Vasilovici AF, Grigore LE, Ungureanu L, Fechete O, Candrea E, Trifa AP, et al. Vitamin D Receptor Polymorphisms and Melanoma. *Oncol Lett* (2019) 17:4162–9. doi: 10.3892/ol.2018.9733
6. Uong A, Zon LI. Melanocytes in Development and Cancer. *J Cell Physiol* (2010) 222:38–41. doi: 10.1002/jcp.21935
7. Davis LE, Shalin SC, Tackett AJ. Current State of Melanoma Diagnosis and Treatment. *Cancer Biol Ther* (2019) 20:1366–79. doi: 10.1080/15384047.2019.1640032
8. Domingues B, Lopes JM, Soares P, Pópulo H. Melanoma Treatment in Review. *ImmunoTargets Ther* (2018) 7:35–49. doi: 10.2147/ITT.S134842
9. Slominski AT, Carlson JA. Melanoma Resistance: A Bright Future for Academicians and a Challenge for Patient Advocates. *Mayo Clin Proc* (2014) 89:429–33. doi: 10.1016/j.mayocp.2014.02.009
10. Indra AK, Castaneda E, Antal MC, Jiang M, Messaddeq N, Meng X, et al. Malignant Transformation of DMBA/TPA-Induced Papillomas and Nevi in the Skin of Mice Selectively Lacking Retinoid-X-Receptor Alpha in Epidermal Keratinocytes. *J Invest Dermatol* (2007) 127:1250–60. doi: 10.1038/sj.jid.5700672
11. Muralidhar S, Filia A, Nsengimana J, Poźniak J, O'Shea SJ, Diaz JM, et al. Vitamin D-VDR Signaling Inhibits Wnt/β-Catenin-Mediated Melanoma Progression and Promotes Antitumor Immunity. *Cancer Res* (2019) 79:5986–98. doi: 10.1158/0008-5472.CAN-18-3927
12. Slominski AT, Brozyna AA, Zmijewski MA, Jozwicki W, Jetten AM, Mason RS, et al. Vitamin D Signaling and Melanoma: Role of Vitamin D and Its Receptors in Melanoma Progression and Management. *Lab Invest* (2017) 97:706–24. doi: 10.1038/labinvest.2017.3
13. Brozyna AA, Hoffman RM, Slominski AT. Relevance of Vitamin D in Melanoma Development, Progression and Therapy. *Anticancer Res* (2020) 40:473–89. doi: 10.21873/anticanres.13976
14. Stumpf WE, Sar M, Reid FA, Tanaka Y, DeLuca HF. Target Cells for 1,25-Dihydroxyvitamin D3 in Intestinal Tract, Stomach, Kidney, Skin, Pituitary, and Parathyroid. *Science* (1979) 206:1188–90. doi: 10.1126/science.505004
15. Orlow I, Roy P, Reiner AS, Yoo S, Patel H, Paine S, et al. Vitamin D Receptor Polymorphisms in Patients With Cutaneous Melanoma. *Int J Cancer J Int Cancer* (2012) 130:405–18. doi: 10.1002/ijc.26023
16. Colston K, Colston MJ, Feldman D. 1,25-Dihydroxyvitamin D3 and Malignant Melanoma: The Presence of Receptors and Inhibition of Cell Growth in Culture. *Endocrinology* (1981) 108:1083–6. doi: 10.1210/endo-108-3-1083
17. Evans SR, Houghton AM, Schumaker L, Brenner RV, Buras RR, Davoodi F, et al. Vitamin D Receptor and Growth Inhibition by 1,25-Dihydroxyvitamin D3 in Human Malignant Melanoma Cell Lines. *J Surg Res* (1996) 61:127–33. doi: 10.1006/jsre.1996.0092
18. Ranson M, Posen S, Mason RS. Human Melanocytes as a Target Tissue for Hormones: In Vitro Studies With 1 Alpha-25, Dihydroxyvitamin D3, Alpha-Melanocyte Stimulating Hormone, and Beta-Estradiol. *J Invest Dermatol* (1988) 91:593–8. doi: 10.1111/1523-1747.ep12477126
19. Holick MF. Vitamin D Deficiency. *N Engl J Med* (2007) 357:266–81. doi: 10.1056/NEJMra070553
20. Bouillon R, Marcocci C, Carmeliet G, Bikle D, White JH, Dawson-Hughes B, et al. Skeletal and Extraskeletal Actions of Vitamin D: Current Evidence and Outstanding Questions. *Endocr Rev* (2018) 40:1109–51. doi: 10.1210/er.2018-00126
21. Bikle DD. The Vitamin D Receptor as Tumor Suppressor in Skin. *Adv Exp Med Biol* (2020) 1268:285–306. doi: 10.1007/978-3-030-46227-7_14
22. Jenkinson C. The Vitamin D Metabolome: An Update on Analysis and Function. *Cell Biochem Funct* (2019) 37:408–23. doi: 10.1002/cbf.3421
23. Tuckey RC, Cheng CYS, Slominski AT. The Serum Vitamin D Metabolome: What We Know and What Is Still to Discover. *J Steroid Biochem Mol Biol* (2019) 186:4–21. doi: 10.1016/j.jsbmb.2018.09.003
24. Bikle D, Christakos S. New Aspects of Vitamin D Metabolism and Action - Addressing the Skin as Source and Target. *Nat Rev Endocrinol* (2020) 16:234–52. doi: 10.1038/s41574-019-0312-5
25. Guryev O, Carvalho RA, Usanov S, Gilep A, Estabrook RW. A Pathway for the Metabolism of Vitamin D3: Unique Hydroxylated Metabolites Formed During Catalysis With Cytochrome P450scc (Cyp11a1. *Proc Natl Acad Sci USA* (2003) 100:14754–9. doi: 10.1073/pnas.2336107100
26. Slominski A, Semak I, Zjawiony J, Wortsman J, Li W, Szczesniewski A, et al. The Cytochrome P450scc System Opens an Alternate Pathway of Vitamin D3 Metabolism. *FEBS J* (2005) 272:4080–90. doi: 10.1111/j.1742-4658.2005.04819.x
27. Slominski AT, Kim TK, Li W, Postlethwaite A, Tieu EW, Tang EK, et al. Detection of Novel CYP11A1-Derived Secosteroids in the Human Epidermis and Serum and Pig Adrenal Gland. *Sci Rep* (2015) 5:14875. doi: 10.1038/srep14875
28. Slominski AT, Li W, Kim TK, Semak I, Wang J, Zjawiony JK, et al. Novel Activities of CYP11A1 and Their Potential Physiological Significance. *J Steroid Biochem Mol Biol* (2015) 151:25–37. doi: 10.1016/j.jsbmb.2014.11.010
29. Coleman DJ, Chagani S, Hyter S, Sherman AM, Löhr CV, Liang X, et al. Loss of Keratinocytic Rxrα Combined With Activated CDK4 or Oncogenic NRAS Generates UVB-Induced Melanomas via Loss of P53 and PTEN in the Tumor Microenvironment. *Mol Cancer Res MCR* (2015) 13:186–96. doi: 10.1158/1541-7786.MCR-14-0164
30. Chagani S, Wang R, Carpenter EL, Löhr CV, Ganguli-Indra G, Indra AK. Ablation of Epidermal Rxrα in Cooperation With Activated CDK4 and Oncogenic NRAS Generates Spontaneous and Acute Neonatal UVB Induced Malignant Metastatic Melanomas. *BMC Cancer* (2017) 17:736. doi: 10.1186/s12885-017-3714-6
31. Chakravarti N, Lotan R, Diwan AH, Warneke CL, Johnson MM, Prieto VG. Decreased Expression of Retinoid Receptors in Melanoma: Entailment in Tumorigenesis and Prognosis. *Clin Cancer Res* (2007) 13:4817–24. doi: 10.1158/1078-0432.ccr-06-3026
32. Boehm N, Samama B, Cribier B, Rochette-Egly C. Retinoic-Acid Receptor Beta Expression in Melanocytes. *Eur J Dermatol EJD* (2004) 14:19–23.
33. Hyter S, Bajaj G, Liang X, Barbacid M, Ganguli-Indra G, Indra AK. Loss of Nuclear Receptor Rxrα in Epidermal Keratinocytes Promotes the Formation of Cdk4-Activated Invasive Melanomas. *Pigment Cell Melanoma Res* (2010) 23:635–48. doi: 10.1111/j.1755-148X.2010.00732.x
34. Wang Z, Coleman DJ, Bajaj G, Liang X, Ganguli-Indra G, Indra AK. Rxrα Ablation in Epidermal Keratinocytes Enhances UVR-Induced DNA Damage, Apoptosis, and Proliferation of Keratinocytes and Melanocytes. *J Invest Dermatol* (2011) 131:177–87. doi: 10.1038/jid.2010.290
35. Coleman DJ, Garcia G, Hyter S, Jang HS, Chagani S, Liang X, et al. Retinoid-X-Receptors (α/β) in Melanocytes Modulate Innate Immune Responses and Differentially Regulate Cell Survival Following UV Irradiation. *PloS Genet* (2014) 10:e1004321. doi: 10.1371/journal.pgen.1004321
36. Chagani S, Kyryachenko S, Yamamoto Y, Kato S, Ganguli-Indra G, Indra AK. In Vivo Role of Vitamin D Receptor Signaling in UVB-Induced DNA Damage and Melanocyte Homeostasis. *J Invest Dermatol* (2016) 136:2108–11. doi: 10.1016/j.jid.2016.06.004
37. Gordon-Thomson C, Tongkao-On W, Song EJ, Carter SE, Dixon KM, Mason RS. Protection From Ultraviolet Damage and Photocarcinogenesis by Vitamin D Compounds. *Adv Exp Med Biol* (2014) 810:303–28. doi: 10.1007/978-1-4939-0437-2_17
38. Slominski AT, Janjetovic Z, Kim TK, Wasilewski P, Rosas S, Hanna S, et al. Novel Non-Calcemic Secosteroids That Are Produced by Human Epidermal Keratinocytes Protect Against Solar Radiation. *J Steroid Biochem Mol Biol* (2015) 148:52–63. doi: 10.1016/j.jsbmb.2015.01.014
39. Tongkao-On W, Carter S, Reeve VE, Dixon KM, Gordon-Thomson C, Halliday GM, et al. CYP11A1 in Skin: An Alternative Route to Photoprotection by Vitamin D Compounds. *J Steroid Biochem Mol Biol* (2015) 148:72–8. doi: 10.1016/j.jsbmb.2014.11.015
40. Rybchyn MS, De Silva WGM, Sequeira VB, Mccarthy BY, Dilley AV, Dixon KM, et al. Enhanced Repair of UV-Induced DNA Damage by 1,25-Dihydroxyvitamin D3 in Skin Is Linked to Pathways That Control Cellular Energy. *J Invest Dermatol* (2018) 138:1146–56. doi: 10.1016/j.jid.2017.11.037
41. Chaiprasongsuk A, Janjetovic Z, Kim TK, Jarrett SG, D'orazio JA, Holick MF, et al. Protective Effects of Novel Derivatives of Vitamin D3 and Lumisterol Against UVB-Induced Damage in Human Keratinocytes Involve Activation of Nrf2 and P53 Defense Mechanisms. *Redox Biol* (2019) 24:101206. doi: 10.1016/j.redox.2019.101206
42. Chaiprasongsuk A, Janjetovic Z, Kim TK, Schwartz CJ, Tuckey RC, Tang EKY, et al. Hydroxylumisterols, Photoproducts of Pre-Vitamin D3, Protect

Human Keratinocytes Against UVB-Induced Damage. *Int J Mol Sci* (2020) 21:9374. doi: 10.3390/ijms21249374
43. Chaiprasongsuk A, Janjetovic Z, Kim TK, Tuckey RC, Li W, Raman C, et al. CYP11A1-Derived Vitamin D3 Products Protect Against UVB-Induced Inflammation and Promote Keratinocytes Differentiation. *Free Radic Biol Med* (2020) 155:87–98. doi: 10.1016/j.freeradbiomed.2020.05.016
44. Bikle DD. Vitamin D Receptor, a Tumor Suppressor in Skin. *Can J Physiol Pharmacol* (2015) 93:349–54. doi: 10.1139/cjpp-2014-0367
45. Slominski AT, Chaiprasongsuk A, Janjetovic Z, Kim TK, Stefan J, Slominski RM, et al. Photoprotective Properties of Vitamin D and Lumisterol Hydroxyderivatives. *Cell Biochem Biophys* (2020) 78(2):165–80. doi: 10.1007/s12013-020-00913-6
46. Slominski RM, Stefan J, Athar M, Holick MF, Jetten AM, Raman C, et al. COVID-19 and Vitamin D: A Lesson From the Skin. *Exp Dermatol* (2020) 29(9):885–90. doi: 10.1111/exd.14170
47. Slominski A, Tobin DJ, Shibahara S, Wortsman J. Melanin Pigmentation in Mammalian Skin and Its Hormonal Regulation. *Physiol Rev* (2004) 84:1155–228. doi: 10.1152/physrev.00044.2003
48. Brandner JM, Haass NK. Melanoma's Connections to the Tumour Microenvironment. *Pathol (Phila)* (2013) 45:443–52. doi: 10.1097/PAT.0b013e328363b3bd
49. Gurzu S, Beleaua MA, Jung I. The Role of Tumor Microenvironment in Development and Progression of Malignant Melanomas - a Systematic Review. *Romanian J Morphol Embryol Rev Roum Morphol Embryol* (2018) 59:23–8.
50. Chien AJ, Moore EC, Lonsdorf AS, Kulikauskas RM, Rothberg BG, Berger AJ, et al. Activated Wnt/beta-Catenin Signaling in Melanoma Is Associated With Decreased Proliferation in Patient Tumors and a Murine Melanoma Model. *Proc Natl Acad Sci USA* (2009) 106:1193–8. doi: 10.1073/pnas.0811902106
51. Vance KW, Goding CR. The Transcription Network Regulating Melanocyte Development and Melanoma. *Pigment Cell Res* (2004) 17:318–25. doi: 10.1111/j.1600-0749.2004.00164.x
52. Sinnberg T, Menzel M, Ewerth D, Sauer B, Schwarz M, Schaller M, et al. β-Catenin Signaling Increases During Melanoma Progression and Promotes Tumor Cell Survival and Chemoresistance. *PloS One* (2011) 6:e23429. doi: 10.1371/journal.pone.0023429
53. Gajos-Michniewicz A, Czyz M. WNT Signaling in Melanoma. *Int J Mol Sci* (2020) 21:E4852. doi: 10.3390/ijms21144852
54. Oak ASW, Bocheva G, Kim T-K, Brożyna AA, Janjetovic Z, Athar M, et al. Noncalcemic Vitamin D Hydroxyderivatives Inhibit Human Oral Squamous Cell Carcinoma and Down-Regulate Hedgehog and WNT/β-Catenin Pathways. *Anticancer Res* (2020) 40:2467–74. doi: 10.21873/anticanres.14216
55. Slominski AT, Brozyna AA, Skobowiat C, Zmijewski MA, Kim TK, Janjetovic Z, et al. On the Role of Classical and Novel Forms of Vitamin D in Melanoma Progression and Management. *J Steroid Biochem Mol Biol* (2018) 177:159–70. doi: 10.1016/j.jsbmb.2017.06.013
56. Bikle DD, Oda Y, Tu CL, Jiang Y. Novel Mechanisms for the Vitamin D Receptor (VDR) in the Skin and in Skin Cancer. *J Steroid Biochem Mol Biol* (2015) 148:47–51. doi: 10.1016/j.jsbmb.2014.10.017
57. Slominski AT, Brozyna AA, Zmijewski MA, Janjetovic Z, Kim TK, Slominski RM, et al. The Role of Classical and Novel Forms of Vitamin D in the Pathogenesis and Progression of Non-Melanoma Skin Cancers. (2020) 1268:257–83. doi: 10.1007/978-3-030-46227-7_13
58. Miyamoto K, Kesterson RA, Yamamoto H, Taketani Y, Nishiwaki E, Tatsumi S, et al. Structural Organization of the Human Vitamin D Receptor Chromosomal Gene and Its Promoter. *Mol Endocrinol Baltim Md* (1997) 11:1165–79. doi: 10.1210/mend.11.8.9951
59. Saijo T, Ito M, Takeda E, Huq AH, Naito E, Yokota I, et al. A Unique Mutation in the Vitamin D Receptor Gene in Three Japanese Patients With Vitamin D-Dependent Rickets Type II: Utility of Single-Strand Conformation Polymorphism Analysis for Heterozygous Carrier Detection. *Am J Hum Genet* (1991) 49:668–73.
60. Uitterlinden AG, Fang Y, Van Meurs JBJ, Pols HAP, Van Leeuwen JPTM. Genetics and Biology of Vitamin D Receptor Polymorphisms. *Gene* (2004) 338:143–56. doi: 10.1016/j.gene.2004.05.014
61. Hustmyer FG, DeLuca HF, Peacock M. ApaI, BsmI, EcoRV and TaqI Polymorphisms at the Human Vitamin D Receptor Gene Locus in Caucasians, Blacks and Asians. *Hum Mol Genet* (1993) 2:487. doi: 10.1093/hmg/2.4.487
62. Halsall JA, Osborne JE, Potter L, Pringle JH, Hutchinson PE. A Novel Polymorphism in the 1A Promoter Region of the Vitamin D Receptor Is Associated With Altered Susceptibilty and Prognosis in Malignant Melanoma. *Br J Cancer* (2004) 91:765–70. doi: 10.1038/sj.bjc.6602006
63. Birke M, Schöpe J, Wagenpfeil S, Vogt T, Reichrath J. Association of Vitamin D Receptor Gene Polymorphisms With Melanoma Risk: A Meta-Analysis and Systematic Review. *Anticancer Res* (2020) 40:583–95. doi: 10.21873/anticanres.13988
64. Brozyna AA, Jozwicki W, Janjetovic Z, Slominski AT. Expression of Vitamin D Receptor Decreases During Progression of Pigmented Skin Lesions. *Hum Pathol* (2011) 42:618–31. doi: 10.1016/j.humpath.2010.09.014
65. Brozyna AA, Jozwicki W, Slominski AT. Decreased VDR Expression in Cutaneous Melanomas as Marker of Tumor Progression: New Data and Analyses. *Anticancer Res* (2014) 34:2735–43.
66. Brozyna AA, Jozwicki W, Janjetovic Z, Slominski AT. Expression of the Vitamin D-Activating Enzyme 1alpha-Hydroxylase (CYP27B1) Decreases During Melanoma Progression. *Hum Pathol* (2013) 44:374–87. doi: 10.1016/j.humpath.2012.03.031
67. Brozyna AA, Jochymski C, Janjetovic Z, Jozwicki W, Tuckey RC, Slominski AT. CYP24A1 Expression Inversely Correlates With Melanoma Progression: Clinic-Pathological Studies. *Int J Mol Sci* (2014) 15:19000–17. doi: 10.3390/ijms151019000
68. Markiewicz A, Brozyna AA, Podgorska E, Elas M, Urbanska K, Jetten AM, et al. Vitamin D Receptors (VDR), Hydroxylases CYP27B1 and CYP24A1 and Retinoid-Related Orphan Receptors (ROR) Level in Human Uveal Tract and Ocular Melanoma With Different Melanization Levels. *Sci Rep* (2019) 9:9142. doi: 10.1038/s41598-019-45161-8
69. Podgorska E, Kim TK, Janjetovic Z, Urbanska K, Tuckey RC, Bae S, et al. Knocking Out the Vitamin D Receptor Enhances Malignancy and Decreases Responsiveness to Vitamin D3 Hydroxyderivatives in Human Melanoma Cells. *Cancers Basel* (2021) 13:3111. doi: 10.3390/cancers13133111
70. Srinivasan M, Parwani AV, Hershberger PA, Lenzner DE, Weissfeld JL. Nuclear Vitamin D Receptor Expression Is Associated With Improved Survival in Non-Small Cell Lung Cancer. *J Steroid Biochem Mol Biol* (2011) 123:30–6. doi: 10.1016/j.jsbmb.2010.10.002
71. Jozwicki W, Brozyna AA, Siekiera J, Slominski AT. Expression of Vitamin D Receptor (VDR) Positively Correlates With Survival of Urothelial Bladder Cancer Patients. *Int J Mol Sci* (2015) 16:24369–86. doi: 10.3390/ijms161024369
72. Al-Azhri J, Zhang Y, Bshara W, Zirpoli G, Mccann SE, Khoury T, et al. Tumor Expression of Vitamin D Receptor and Breast Cancer Histopathological Characteristics and Prognosis. *Clin Cancer Res* (2017) 23:97–103. doi: 10.1158/1078-0432.CCR-16-0075
73. Atoum M, Alzoughool F. Vitamin D and Breast Cancer: Latest Evidence and Future Steps. *Breast Cancer Auckl* (2017) 11:1178223417749816. doi: 10.1177/1178223417749816
74. Gascoyne DM, Lyne L, Spearman H, Buffa FM, Soilleux EJ, Banham AH. Vitamin D Receptor Expression in Plasmablastic Lymphoma and Myeloma Cells Confers Susceptibility to Vitamin D. *Endocrinology* (2017) 158:503–15. doi: 10.1210/en.2016-1802
75. Brozyna AA, Kim TK, Zablocka M, Jozwicki W, Yue J, Tuckey RC, et al. Association Among Vitamin D, Retinoic Acid-Related Orphan Receptors, and Vitamin D Hydroxyderivatives in Ovarian Cancer. *Nutrients* (2020) 12:3541. doi: 10.3390/nu12113541
76. Brozyna AA, Jozwicki W, Skobowiat C, Jetten A, Slominski AT. RORalpha and RORgamma Expression Inversely Correlates With Human Melanoma Progression. *Oncotarget* (2016) 7:63261–82. doi: 10.18632/oncotarget.11211
77. Brozyna AA, Jozwicki W, Jetten AM, Slominski AT. On the Relationship Between VDR, RORalpha and RORgamma Receptors Expression and HIF1-Alpha Levels in Human Melanomas. *Exp Dermatol* (2019) 28:1036–43. doi: 10.1111/exd.14002
78. Slominski A, Kim TK, Brozyna AA, Janjetovic Z, Brooks DL, Schwab LP, et al. The Role of Melanogenesis in Regulation of Melanoma Behavior: Melanogenesis Leads to Stimulation of HIF-1alpha Expression and HIF-Dependent Attendant Pathways. *Arch Biochem Biophys* (2014) 563:79–93. doi: 10.1016/j.abb.2014.06.030
79. Janjetovic Z, Brozyna AA, Tuckey RC, Kim TK, Nguyen MN, Jozwicki W, et al. High Basal NF-kappaB Activity in Nonpigmented Melanoma Cells Is

Associated With an Enhanced Sensitivity to Vitamin D3 Derivatives. *Br J Cancer* (2011) 105:1874–84. doi: 10.1038/bjc.2011.458
80. Brozyna AA, Jozwicki W, Carlson JA, Slominski AT. Melanogenesis Affects Overall and Disease-Free Survival in Patients With Stage III and IV Melanoma. *Hum Pathol* (2013) 44:2071–4. doi: 10.1016/j.humpath.2013.02.022
81. Hutchinson PE, Halsall JA, Popovici S, Papadogeorgakis E, Osborne JE, Powley IR, et al. Compromised Vitamin D Receptor Signalling in Malignant Melanoma Is Associated With Tumour Progression and Mitogen-Activated Protein Kinase Activity. *Melanoma Res* (2018) 28:410–22. doi: 10.1097/CMR.0000000000000475
82. Solomon C, White JH, Kremer R. Mitogen-Activated Protein Kinase Inhibits 1,25-Dihydroxyvitamin D3-Dependent Signal Transduction by Phosphorylating Human Retinoid X Receptor Alpha. *J Clin Invest* (1999) 103:1729–35. doi: 10.1172/JCI6871
83. Newton-Bishop JA, Beswick S, Randerson-Moor J, Chang Y-M, Affleck P, Elliott F, et al. Serum 25-Hydroxyvitamin D3 Levels Are Associated With Breslow Thickness at Presentation and Survival From Melanoma. *J Clin Oncol Off J Am Soc Clin Oncol* (2009) 27:5439–44. doi: 10.1200/JCO.2009.22.1135
84. Fang S, Sui D, Wang Y, Liu H, Chiang Y-J, Ross MI, et al. Association of Vitamin D Levels With Outcome in Patients With Melanoma After Adjustment For C-Reactive Protein. *J Clin Oncol Off J Am Soc Clin Oncol* (2016) 34:1741–7. doi: 10.1200/JCO.2015.64.1357
85. Saiag P, Aegerter P, Vitoux D, Lebbé C, Wolkenstein P, Dupin N, et al. Prognostic Value of 25-Hydroxyvitamin D3 Levels at Diagnosis and During Follow-Up in Melanoma Patients. *JNCI J Natl Cancer Inst* (2015) 107: djv264. doi: 10.1093/jnci/djv264
86. Gambichler T, Bindsteiner M, Höxtermann S, Kreuter A. Serum 25-Hydroxyvitamin D Serum Levels in a Large German Cohort of Patients With Melanoma. *Br J Dermatol* (2013) 168:625–8. doi: 10.1111/j.1365-2133.2012.11212.x
87. Schmidt H. *An Observational Study Design to Detect If Co-Stimulatory Markers and Vitamin D Status in Anti-PD-1 Treated Advanced Melanoma Patients Can Predict Treatment Outcome* (2020). clinicaltrials.gov. Available at: https://clinicaltrials.gov/ct2/show/results/NCT03197636 (Accessed July 1, 2021).
88. Fillon M. Fecal Microbiota Transplants may Aid Melanoma Immunotherapy Resistance. *CA Cancer J Clin* (2021) 71:285–6. doi: 10.3322/caac.21676
89. Trojaniello C, Luke JJ, Ascierto PA. Therapeutic Advancements Across Clinical Stages in Melanoma, With a Focus on Targeted Immunotherapy. *Front Oncol* (2021) 11:670726. doi: 10.3389/fonc.2021.670726
90. Puglisi R, Bellenghi M, Pontecorvi G, Pallante G, Carè A, Mattia G. Biomarkers for Diagnosis, Prognosis and Response to Immunotherapy in Melanoma. *Cancers* (2021) 13:2875. doi: 10.3390/cancers13122875
91. Burzi L, Alessandrini AM, Quaglino P, Piraccini BM, Dika E, Ribero S. Cutaneous Events Associated With Immunotherapy of Melanoma: A Review. *J Clin Med* (2021) 10:3047. doi: 10.3390/jcm10143047
92. Naik PP. Current Trends of Immunotherapy in the Treatment of Cutaneous Melanoma: A Review. *Dermatol Ther* (2021). doi: 10.1007/s13555-021-00583-z
93. Rohatgi A, Kirkwood JM. Beyond PD-1: The Next Frontier for Immunotherapy in Melanoma. *Front Oncol* (2021) 11:640314. doi: 10.3389/fonc.2021.640314
94. Buchanan T, Amouzegar A, Luke JJ. Next-Generation Immunotherapy Approaches in Melanoma. *Curr Oncol Rep* (2021) 23:116. doi: 10.1007/s11912-021-01104-z
95. Moreira A, Heinzerling L, Bhardwaj N, Friedlander P. Current Melanoma Treatments: Where Do We Stand? *Cancers* (2021) 13:E221. doi: 10.3390/cancers13020221
96. Chun RF, Liu PT, Modlin RL, Adams JS, Hewison M. Impact of Vitamin D on Immune Function: Lessons Learned From Genome-Wide Analysis. *Front Physiol* (2014) 5:151. doi: 10.3389/fphys.2014.00151
97. Hewison M. An Update on Vitamin D and Human Immunity. *Clin Endocrinol (Oxf)* (2012) 76:315–25. doi: 10.1111/j.1365-2265.2011.04261.x
98. Postlethwaite AE, Tuckey RC, Kim T-K, Li W, Bhattacharya SK, Myers LK, et al. 20s-Hydroxyvitamin D3, a Secosteroid Produced in Humans, Is Anti-Inflammatory and Inhibits Murine Autoimmune Arthritis. *Front Immunol* (2021) 12:678487. doi: 10.3389/fimmu.2021.678487
99. Slominski RM, Raman C, Elmets C, Jetten AM, Slominski A, Tuckey RC. The Significance of CYP11A1 Expression in Skin Physiology and Pathology. *Mol Cell Endocrinol* (2021) 530:111238. doi: 10.1016/j.mce.2021.111238
100. Jacquelot N, Belz GT. Type 2 Innate Lymphoid Cells: A Novel Actor in Anti-Melanoma Immunity. *Oncoimmunology* (2021) 10:1943168. doi: 10.1080/2162402X.2021.1943168
101. Wang H, Zhang L, Yang L, Liu C, Zhang Q, Zhang L. Targeting Macrophage Anti-Tumor Activity to Suppress Melanoma Progression. *Oncotarget* (2017) 8:18486–96. doi: 10.18632/oncotarget.14474
102. Marzagalli M, Ebelt ND, Manuel ER. Unraveling the Crosstalk Between Melanoma and Immune Cells in the Tumor Microenvironment. *Semin Cancer Biol* (2019) 59:236–50. doi: 10.1016/j.semcancer.2019.08.002
103. Vacca P, Pietra G, Tumino N, Munari E, Mingari MC, Moretta L. Exploiting Human NK Cells in Tumor Therapy. *Front Immunol* (2019) 10:3013. doi: 10.3389/fimmu.2019.03013
104. Gonzalez-Gugel E, Saxena M, Bhardwaj N. Modulation of Innate Immunity in the Tumor Microenvironment. *Cancer Immunol Immunother CII* (2016) 65:1261–8. doi: 10.1007/s00262-016-1859-9
105. Atherton MJ, Morris JS, McDermott MR, Lichty BD. Cancer Immunology and Canine Malignant Melanoma: A Comparative Review. *Vet Immunol Immunopathol* (2016) 169:15–26. doi: 10.1016/j.vetimm.2015.11.003
106. Navarini-Meury AA, Conrad C. Melanoma and Innate Immunity–Aactive Inflammation or Just Erroneous Attraction? Melanoma as the Source of Leukocyte-Attracting Chemokines. *Semin Cancer Biol* (2009) 19:84–91. doi: 10.1016/j.semcancer.2008.10.012
107. Tang JY, Fu T, Leblanc E, Manson JE, Feldman D, Linos E, et al. Calcium Plus Vitamin D Supplementation and the Risk of Nonmelanoma and Melanoma Skin Cancer: Post Hoc Analyses of the Women's Health Initiative Randomized Controlled Trial. *J Clin Oncol Off J Am Soc Clin Oncol* (2011) 29:3078–84. doi: 10.1200/JCO.2011.34.5967
108. Saw RP, Armstrong BK, Mason RS, Morton RL, Shannon KF, Spillane AJ, et al. Adjuvant Therapy With High Dose Vitamin D Following Primary Treatment of Melanoma at High Risk of Recurrence: A Placebo Controlled Randomised Phase II Trial (ANZMTG 02.09 Mel-D). *BMC Cancer* (2014) 14:780. doi: 10.1186/1471-2407-14-780
109. Stucci LS, D'Oronzo S, Tucci M, Macerollo A, Ribero S, Spagnolo F, et al. Vitamin D in Melanoma: Controversies and Potential Role in Combination With Immune Check-Point Inhibitors. *Cancer Treat Rev* (2018) 69:21–8. doi: 10.1016/j.ctrv.2018.05.016
110. De Smedt J, Van Kelst S, Boecxstaens V, Stas M, Bogaerts K, Vanderschueren D, et al. Vitamin D Supplementation in Cutaneous Malignant Melanoma Outcome (ViDMe): A Randomized Controlled Trial. *BMC Cancer* (2017) 17:562. doi: 10.1186/s12885-017-3538-4
111. Universitaire Ziekenhuizen Leuven. *Vitamin D Supplementation in Cutaneous Malignant Melanoma Outcome* (2020). clinicaltrials.gov. Available at: https://clinicaltrials.gov/ct2/show/NCT01748448 (Accessed July 1, 2021).
112. Slominski AT, Kim TK, Janjetovic Z, Brozyna AA, Zmijewski MA, Xu H, et al. *Differ Overlapping Eff Of* (2018) 19:E3072. doi: 10.3390/ijms19103072
113. Skobowiat C, Oak AS, Kim TK, Yang CH, Pfeffer LM, Tuckey RC, et al. Noncalcemic 20-Hydroxyvitamin D3 Inhibits Human Melanoma Growth in In Vitro and In Vivo Models. *Oncotarget* (2017) 8:9823–34. doi: 10.18632/oncotarget.14193

Conflict of Interest: The authors declare that the research was conducted in the absence of any commercial or financial relationships that could be construed as a potential conflict of interest.

Publisher's Note: All claims expressed in this article are solely those of the authors and do not necessarily represent those of their affiliated organizations, or those of the publisher, the editors and the reviewers. Any product that may be evaluated in this article, or claim that may be made by its manufacturer, is not guaranteed or endorsed by the publisher.

Advantages of publishing in Frontiers

OPEN ACCESS
Articles are free to read for greatest visibility and readership

FAST PUBLICATION
Around 90 days from submission to decision

HIGH QUALITY PEER-REVIEW
Rigorous, collaborative, and constructive peer-review

TRANSPARENT PEER-REVIEW
Editors and reviewers acknowledged by name on published articles

Frontiers
Avenue du Tribunal-Fédéral 34
1005 Lausanne | Switzerland

Visit us: www.frontiersin.org
Contact us: frontiersin.org/about/contact

REPRODUCIBILITY OF RESEARCH
Support open data and methods to enhance research reproducibility

DIGITAL PUBLISHING
Articles designed for optimal readership across devices

FOLLOW US
@frontiersin

IMPACT METRICS
Advanced article metrics track visibility across digital media

EXTENSIVE PROMOTION
Marketing and promotion of impactful research

LOOP RESEARCH NETWORK
Our network increases your article's readership